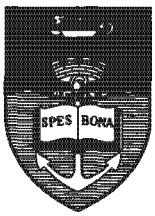

Variations in Modeling and Algorithmic Factors Impacting on Small-signal Stability Results: Assessment of Five Industrial-grade Power System Simulation Tools

by

Keren Kanuthu Kaberere

Thesis presented in fulfillment of the requirements for the degree of

Doctor of Philosophy

in the

Department of Electrical Engineering

University of Cape Town

Supervised by

Prof. K.A. Folly

Prof. A.I. Petroianu

August 2006

Declaration

I declare that the work presented in this thesis is my original work. I also affirm that this work has not been presented in this, or any other university for examination, or for any other purposes.

Signed: signature removed

Keren Kanuthu Kaberere

August 2006

Acknowledgement

A *Gĩkũyũ* proverb on co-operation, *kĩara kĩmwe gĩtiũragaga ndaa*, quite appropriately expresses my feelings after the Ph.D. journey, which has been quite long. I could not have made it without the help, words of wisdom, and emotional support by a number of people whom I would like to thank.

My sincere gratitude goes to my supervisors Prof. Komla Folly and Prof. Alexander Petroianu for their guidance and dedication throughout the research period. They showed a lot of patience and understanding as I was grappling with the research, particularly at the initial stages when all was so new to me. Prof. Petroianu I shall forever be grateful to you for giving me unlimited access to your office (read: library with a very rich collection of books and publications). I have learnt a lot from you and I look forward to passing it on to the young, up-coming power engineers.

I am indebted to the following specialists for the technical support and advice that I received from them. They responded to my numerous queries promptly and tirelessly: Leonardo Lima, PTI; Markus Pöller, Jochen Alber, and Holger Müller, DIgSILENT Powerfactory; Peter Van Meirhaeghe, Tractebel; Lei Wang, Powertech Labs Inc.; Graham Rogers, Cherry Tree Scientific Software. Mpumelelo Ntombela, thank you for the simulations you ran using MatNetEig the results of which are reported in this thesis. Chris

Wozniak, thanks for setting up my workstation and for maintaining the software licenses thereafter. Members of the power engineering group at UCT, I appreciate what we shared during the seminars. Sally Burt, I am grateful to you for taking your time to edit this thesis.

I would like to thank my sponsors profusely, University Science, Humanities, and Engineering Partnerships in Africa (USHEPiA), for the financial support. It went a long way in facilitating the smooth running of the research and dissemination of the findings. I presented papers at four international conferences on four continents, courtesy of USHEPiA funding. Thank you also for all the social occasions that you organize to spice up our life in Cape Town. They make fellows feel important amidst the humbling academic experiences. Lesley Rossouw and Marlene Joubert, thanks for efficiently handling my research fund. My gratitude to my employer, Jomo Kenyatta University of Agriculture & Technology (JKUAT), for granting me leave to pursue my studies.

Miss. Khayakazi Mngxuma, I do not know what life in Cape Town would have been without you around. Thanks a lot for taking your time to orientate me. Your kindness and the times we shared will forever be treasured. Luisa Petroianu, your stamina inspired me a lot. Every time I came to your office, you spared a few minutes for laughter and you had kind words for me. Karanja Kibicho, Siphila Mumenya, and Purity Macheru, the Friday sessions of *gĩũthi* ensured that we kept our sanity. We shared a lot on the ups and downs of the life of a Ph.D. candidate during these sessions.

Finally, I would like to thank some people with whom I have a relationship that is not in any way linked to this thesis but is rooted much deeper. To my good old friend Kaberere Ndũng'ũ, who also happens to be my husband, and

my children Mũthoni and Dush, thank you very much for being so understanding to allow me leave you for so long without a wife and a mother. Your love and encouragement during stormy "weather" kept me going. Mũthoni and Dush you might not understand why an old *mama* had to be on the academic receiving end, but I hope one day you will understand. Ann Msacky made sure my family kept running smoothly in my absence and played the role of a mother before she actually became one. *Mungu akubariki sana.* All the friends and relatives who kept my family company while I was away, God bless you all.

Abstract

There are several industrial-grade simulation tools, used for small-signal stability studies, that are commercially available on the market. However, these tools differ in their components modeling and solution methodology. Therefore, different simulation tools can give different results for the same power system model. In this thesis, five industrial-grade simulation tools – PSS/E, PowerFactory, EUROSTAG, SSAT, and MatNetEig – are investigated. The features and capabilities of the five tools are compared based on components modeling, numerical methodology, and tool flexibility in terms of data input and output.

Variations among the five tools in the modeling of generator saturation, speed voltage terms, turbine output, and the techniques used by the tools for the construction of the state matrix have been identified in this thesis, as possible causes of the discrepancies in results obtained with these tools. It has been found that the five tools represent saturation using total saturation (PowerFactory, EUROSTAG, SSAT, and MatNetEig), incremental saturation (SSAT), and effective excitation (PSS/E) methods. In addition, some tools, such as PowerFactory and EUROSTAG, consider speed deviation in speed voltage terms, whereas others neglect it. Furthermore, some tools (PSS/E, PowerFactory, and SSAT) model the turbine output as mechanical power and others as mechanical torque. It has also been found that some

tools employ numerical differentiation, whereas others employ analytical differentiation for constructing the state matrix.

The effect of the variation in each of the above factors on local and inter-area modes was investigated using the single machine infinite bus system and the multi-machine, two-area four-generator system. The generators in the two systems were represented using 6^{th} order models. The complexity of the models was progressively increased from simple, manual excitation control and constant prime mover output, to full model with excitation system controlled by automatic voltage regulator (AVR) with power system stabilizer (PSS), and speed governor control.

The investigations were carried out with three excitation control configurations:

- Manual excitation control
- Excitation controlled by AVR without PSS
- Excitation controlled by AVR with PSS.

For all the investigations, it has been found that variations in the factors listed above affect the damping of both local and inter-area modes but they have a negligible effect on the frequency. It has also been found that the three methods of representing saturation have different effects on the damping, for different excitation control configurations. The results obtained from the investigations carried out in this research are inconclusive, regarding the effect of saturation on damping. Thus, further work in this area is recommended.

It has also been found that the damping of both the local and the inter-area modes obtained with the speed deviation considered in speed voltage terms is lower than that obtained with speed deviation neglected. This is due to the

fact that inclusion of speed deviation in speed voltage terms "adds" negative damping if the system is heavily loaded. The "added" damping depends on the parameters of the machine, the external network, and the operating condition.

The effect of variation in the modeling of turbine output has also been investigated. It has been found that the damping of both the local and the inter-area modes obtained with mechanical power turbine output is higher than that obtained with mechanical torque turbine output. This is due to the "additional" positive damping associated with the mechanical power-torque relationship of the turbine. The "additional" damping is directly proportional to the generator loading and inversely proportional to its inertia constant. Thus, with heavy loading, the "additional" damping is higher for a small generator than for a large one.

The comparison of the results obtained using the five tools shows that the effect of saturation on the damping of both the local and the inter-area modes is erratic, for the three excitation control configurations. Indeed, for the same excitation control configuration, different effects of saturation are observed for tools that employ the same method of representing saturation. There is therefore a need for further investigation into the modeling of saturation by the simulation tools.

For some of the simulated cases, the five tools gave contradictory results. The discrepancies in the results are caused by variations among the tools in the modeling of generator saturation, speed voltage terms, and turbine output. It is shown in this thesis that variations in the methods used for constructing the state matrix do not introduce significant discrepancies in results.

Contents

List of Tables

List of Figures

Notation

This section gives the most commonly used notation in this thesis. All inductances are in per unit.

Roman symbols

$\boldsymbol{A}$	State matrix
a_{ij}	Element of the $\boldsymbol{A}$ matrix for $i, j = 1, \ldots, n$
E_t	Stator terminal voltage
e_d, e_q	d-axis, q-axis terminal voltage component
i_d, i_q	d-axis, q-axis terminal current component
H	Inertia constant (s)
K_D	Damping torque coefficient
L_{1d}	d-axis amortisseur leakage inductance
L_{1q}, L_{2q}	q-axis amortisseur leakage inductance
L_{ad}, L_{aq}	d-axis, q-axis stator to rotor mutual inductance
L_{fd}	Field winding leakage inductance
L_l	Stator leakage inductance
$L_{\rho l}$	Differential leakage inductance proportional to flux that links both the field winding and the amortisseur, but does not link the stator
L_d, L_q	d-axis, q-axis synchronous inductance
L'_d, L'_q	d-axis, q-axis transient inductance

L''_d, L''_q	d-axis, q-axis subtransient inductance
n	System order
P_e	Electrical power
P_m	Mechanical power
R_a	Stator resistance
R_{fd}	Field resistance
R_{1d}	d-axis amortisseur resistance
R_{1q}, R_{2q}	q-axis amortisseur resistance
T'_{do}, T'_{qo}	d-axis, q-axis transient open-circuit time constants in seconds
T''_{do}, T''_{qo}	d-axis, q-axis subtransient open-circuit time constants in seconds
T_e	Electrical torque
T_m	Mechanical torque

Greek symbols

δ	Rotor angle
Δ	Small perturbation
λ	Eigenvalue
σ	Damping
ω_r	Rotor angular velocity
ω_0	Base angular velocity
ψ_d, ψ_q	d-axis, q-axis stator flux linkage
ψ_{1d}	d-axis amortisseur flux linkage
ψ_{1q}, ψ_{2q}	q-axis amortisseur flux linkage
ψ_{fd}	Field flux linkage
ζ	Damping ratio

Abbreviations

2A4G	Two-area four-generator
AC	Alternating current
AESOPS	Analysis of essentially spontaneous oscillations in power systems
AVR	Automatic voltage regulator
DAE	Differential algebraic equation
DSA	Dynamic security assessment
FACTS	Flexible AC transmission system
GUI	Graphical user interface
HVDC	High voltage direct current
IEEE	Institute of Electrical and Electronics Engineers
OCC	Open circuit characteristic
pu	Per unit
PSS	Power system stabilizer
PSS/E	Power systems simulator for engineering
SMIB	Single machine infinite bus
SSAT	Small signal analysis tool
SVC	Static VAr compensator
TSAT	Transient security assessment tool

Units

°	degrees
km	Kilometers
kV	Kilovolts
MW	Megawatts
MVA	Megavolt-amperes
MVAr	Megavolt-amperes-reactive
s	Seconds

Chapter 1

Introduction

Under real-time operating conditions, it is difficult to perform field experiments in a power system without jeopardizing its security. Thus, digital simulation of the power system response to changes in operating conditions plays a very important role in control and security assessment. Decision makers increasingly rely on digital simulations for planning and operation. The advancement of computer technology has led to the emergence of several industrial-grade power system simulation tools. One important function of some of these tools is eigenvalue calculation. Small-signal system stability is deduced from the analysis of eigenvalue results.

1.1 Comparison of simulation tools – Background

All over the world, more and more power systems are being interconnected, resulting in large, complex systems that cover very large geographical areas. The interconnections have been made to realize benefits such as shared generation reserves, diversity in sources of power, and improved security of

supply. Stability is one of the main challenges in large interconnected power systems. In these systems, the full effect of a disturbance in some parts of the system far from the location of the disturbance is felt some time after its occurrence. This time lag causes different parts of the system to respond to the same disturbance at different times. The initial disturbance may sometimes cause other disturbances in neighboring areas, which may result in widespread system instability. This cascade of events may eventually culminate in a blackout, like the ones that occurred in North America and Europe in 2003 [1,2].

Power systems around the world are at different stages of restructuring from regulated, vertically integrated structure, where the three sub-sectors – generation, transmission, and distribution – are operated by a monopoly, to a horizontal structure, where the three sub-sectors are separate private entities. The primary goal of restructuring is to introduce market competition, and thus reduce the cost of electricity and improve the efficiency of electricity supply [3].

One of the expected consequences of restructuring is the increase in the transfer of power in interconnected systems, from low-cost to high-cost generation areas. With the increase in power transfer and loading on the system, dynamic phenomena could increase in complexity e.g. inter-area oscillations could become more common [3]. Another expected consequence of restructuring is the need to guarantee sufficient transmission capability to conduct a transaction without jeopardizing system reliability [1]. The entity responsible for maintaining system reliability will have to analyze the system to evaluate limiting conditions such as available transfer capability and stability limits. To investigate power system stability we rely increasingly on the new multi-

[1] Adequacy and security

disciplinary, computational approach and on simulation tools. The tools play a critical role in decision-making in both planning and real-time operation. Electric power systems are expected to be highly reliable. Therefore, the simulation tools should accurately and reliably replicate the actual power system.

The advancement of computer technology has led to the emergence of several industrial-grade power system design and analysis tools. These tools have transformed power system analysis, from one where a lot of time was spent learning advanced programming skills to one where the user spends more time working on power system aspects [4]. However, the tools are expensive to acquire and mastering a new tool is a time consuming exercise. In most cases the input data cannot be transferred from one tool to another tool and the user has to learn anew how to introduce the input data. Hence, most users rely on results obtained with only one tool; these results are seldom validated by field measurements and, in most of the cases, they are not compared with results obtained with similar industrial-grade tools. Therefore, users cannot easily detect inaccuracies in the results, which may be caused by inaccurate components' modeling and algorithmic factors. At the inception of this research, little had been reported in literature on the comparison of simulation tools used for power system stability analysis [4–6].

In [4], Ibrahim compares thirteen software packages used for power engineering education and research. The comparison criteria are the softwares' capabilities with regard to available modules e.g. AC load flow, short-circuit analysis, dynamic simulation etc. In this reference, no simulation results are presented.

Persson *et al.* [5] compare eigenvalue results obtained with two simulation

tools – PSS/E and Simpow. For their investigation, the authors use the single machine infinite bus (SMIB) system with the generator represented using a 6^{th} order model, equipped with an automatic voltage regulator (AVR) and a speed governor. Some discrepancies are observed in the results obtained with the two tools. The authors attribute the discrepancies to differences in the machine models and linearization methods used by the two tools. However, the authors do not point out the differences in the machine models that are possible causes of the discrepancies in results. The authors also neglect the effect of saturation in their study.

In [6], Slootweg *et al.* report the eigenvalue analysis capabilities of two simulation tools – PSS/E and Simpow. For their investigation, the authors use both the SMIB system and the two-area four-generator (2A4G) system, with system data given in [7]. For both power systems, the generators are represented using the 6^{th} order model. However, turbo-generator controllers such as AVR and speed governor are not modeled. The authors attribute the discrepancies in results obtained with the two tools to differences in methods used for constructing the $\boldsymbol{A}$ matrix, the modeling of magnetic saturation, and modeling of the synchronous generator. They highlight the modeling of turbine output and speed voltage terms as factors that influence the damping of the electromechanical modes of the SMIB system. The authors do not draw any conclusions on whether the influence of these two factors enhances or impairs damping. In addition, the effect of speed voltage terms on the inter-area modes is not investigated.

Slootweg *et al.* [6] have found that, for the electromechanical modes, the results obtained with different tools differ in damping but agree on frequency of oscillation. Damping, however, is a crucial aspect of stability. Inaccurate

modeling of damping could result in erroneous conclusions being drawn from stability studies e.g. the calculated stability margin may be higher or lower than the actual limit. An over estimation of the stability margin may be catastrophic whereas an underestimation is opportunity lost to take advantage of the full capability of the system. Kyriakides and Farmer [8] recognize the need for carrying out studies to determine the modeling aspects that result in "damping errors".

The above studies have one or the other of the following limitations:

(i) Only two tools are compared.

(ii) Simplified generator models have been used for the studies.

(iii) The studies do not cover multi-machine systems.

(iv) The generator controllers are not modeled.

Currently, there are no industry-accepted standards for comparing the power system simulation tools available on the market. Therefore, there is need for comparison of the tools in a systematic and comprehensible manner to understand the causes of the discrepancies in results. The motivation of this research was the need to bridge this gap.

In this thesis, five industrial-grade tools – PSS/E, PowerFactory, EUROSTAG, SSAT[2], and MatNetEig – are investigated. The variations among the five tools in components modeling and algorithmic factors impacting on small-signal stability results are identified. The effect of these variations on the electromechanical modes is investigated using two power systems – the SMIB

[2]Module for small-signal stability analysis in DSA PowerTools

system and the multi-machine, 2A4G system. For the two power systems, all the generators are modeled using the 6^{th} order model with different excitation and prime mover control configurations.

The main objectives of this thesis are summarized as:

(i) Identify the variations[3] among five industrial-grade simulation tools – PSS/E, PowerFactory, EUROSTAG, SSAT, and MatNetEig – that cause discrepancies in eigenvalue results obtained with the tools.

(ii) Investigate the impact of the variations on electromechanical modes with an aim to come up with a basis or standard for comparison of simulation tools used for small-signal stability analysis.

(iii) Simulate benchmark networks using the five industrial-grade tools, compare the eigenvalue results, and assess the impact of the variations on the results.

(iv) Compare the features and capabilities of the five industrial-grade tools in their application for small-signal stability analysis.

The details of the objectives are discussed in the next section.

1.2 Objectives of the thesis

The first objective of this thesis is to identify the variations among five industrial-grade simulations tools – PSS/E, PowerFactory, EUROSTAG, SSAT, and MatNetEig – that cause discrepancies in eigenvalue results obtained with

[3]Differences in components modeling and numerical methodology

the tools. This is the first step towards setting standards for the comparison of simulation tools used for small-signal stability analysis.

To achieve the first objective, a thorough understanding of the tools' components modeling and numerical methodology is necessary. The information was obtained from the software users manuals [9–13]. However, in some cases the manuals were inadequate and thus direct enquiry was made from the vendors. Hence, some of the information presented in this thesis is not documented in the software manuals.

We have found [14–16] variations among the five tools in:

(i) the modeling of turbo-generator

  (a) generator saturation – the methods used by the five tools to represent the effects of saturation are total saturation, incremental saturation, and effective excitation.

  (b) speed voltage terms – some tools consider rotor speed deviation in speed voltage terms whereas other tools neglect it.

  (c) turbine output – some tools model the turbine output as mechanical power P_m, and other tools as mechanical torque T_m.

(ii) methods used for constructing the state matrix – some tools employ numerical differentiation and other tools employ analytical differentiation.

The second objective is to investigate the impact on the eigenvalue results of variations in (i) modeling of generator saturation, speed voltage terms, and turbine output, and (ii) methods used for constructing the state matrix. Two power systems are used for the investigations. The single machine infinite

bus (SMIB) system is used to study the impact of each factor on the local modes, with the generator heavily loaded. The impact of the above factors on inter-area modes is studied using the multi-machine, two-area four-generator (2A4G) system. The 6^{th} order generator model is used for the two power systems. Each power system is simulated with manual excitation control, automatic excitation control without power system stabilizer (PSS) and with PSS.

For both the local and the inter-area modes, we have found the impact of generator saturation to be erratic and thus difficult to characterize from the simulation results. Our results [14] show that for the three excitation control configurations, the damping ratio obtained with speed deviation neglected in speed voltage terms, is higher than that obtained with speed deviation included. The impact of variations in modeling of speed voltage terms on electromechanical modes is more significant, with excitation controlled by AVR, than with manual excitation control. The damping ratio obtained with P_m turbine output is higher than that obtained with T_m turbine output [14, 16]. This observation is true for both constant prime mover output and speed governor control. The variations in the three modeling aspects have little effect on the frequency of the electromechanical modes. We have found [16] that differences in the methods used for constructing the state matrix do not introduce significant discrepancies in results, provided that the perturbation size used in numerical differentiation is well chosen. Too small a perturbation size results in numerical instability whereas a large perturbation size does not approximate the linear model correctly.

The third objective is to compare the results obtained with the five industrial-grade tools for the two power systems and to draw quantitative conclusions

with respect to the impact of the variations among the tools on the electromechanical modes. To achieve this objective, each power system was simulated with three excitation control configurations; manual excitation control, automatic excitation control without PSS and with PSS. To investigate the impact of the generator saturation representation used by each tool, for each excitation control configuration, each power system was simulated both with saturation included and with saturation neglected. The effect of speed governor on the electromechanical modes was also investigated. Each simulation was run using the five tools, except the cases with speed governor control for which four tools were used. MatNetEig does not have in its standard library, the IEEEG1 turbine-governor model used in the study. Hence this tool was excluded from these investigations. For each simulated case, the results obtained with different tools are compared.

We have found that [14, 16] for the electromechanical modes, the results obtained with different tools differ in damping but agree on frequency of oscillation. The discrepancies are largest with manual excitation control and smallest with excitation controlled by AVR with PSS. For the same model of speed voltage terms ($\omega_r = 1$ or $\omega_r \neq 1$), the damping ratio obtained with tools that model the turbine output as P_m is higher than that obtained with tools that model the turbine output as T_m. In addition, for the same model of turbine output (P_m or T_m), the damping ratio obtained with tools that neglect speed deviation in the speed voltage terms is higher than that obtained with tools that consider the speed deviation. For the 2A4G system with excitation controlled by AVR without PSS and constant prime mover output, some tools give results that predict the inter-area modes are stable whereas others predict instability. These contradictory results emphasize the fact that different tools can give different results; users of the tools can

draw different conclusions on the stability of same power system. Thus, it is important that the impact of variations among simulation tools on damping is well understood. For all the tools, the results obtained with speed governor control are more conservative than those obtained with constant prime mover output. This is due to the negative damping added by the speed governor.

The fourth objective is to compare the features and capabilities of the five simulation tools in a systematic and comprehensible manner. The tools are compared with regard to their application for small-signal stability analysis. The comparison criteria are components modeling, numerical methodology, and tools flexibility in terms of data input and output.

PSS/E has the widest variety of generator models ranging from 2^{nd} (classical) to 8^{th} order. PSS/E, PowerFactory, and SSAT model the turbine output as P_m whereas EUROSTAG and MatNetEig model it as T_m. In addition, SSAT also models the turbine output as T_m. EUROSTAG and PowerFactory consider speed deviation in the speed voltage terms whereas PSS/E, SSAT, and MatNetEig neglect it. Both PSS/E and PowerFactory use numerical differentiation for constructing the $\boldsymbol{A}$ matrix whereas EUROSTAG, SSAT, and MatNetEig use analytical differentiation. A PSS/E user has to specify the perturbation size whereas in PowerFactory, the perturbation size is fixed by the vendor at 10^{-3}. All the five tools have graphical user interface and data entry is by data input windows. MatNetEig gives the most data output.

As explained above, all the four objectives of the thesis have been met.

1.3 Power system modeling

To study power system behavior using digital simulation, the system is represented using a mathematical model. The model includes the components of the power system that influence the electrical and mechanical torques of the machines e.g. generators and their controls, loads etc.

Figure 1.1 illustrates the concept relating to system modeling. The circle labeled *actual power system* represents the behavior of the real power system. The circle labeled *power system model* represents the system behavior as predicted by the mathematical model.

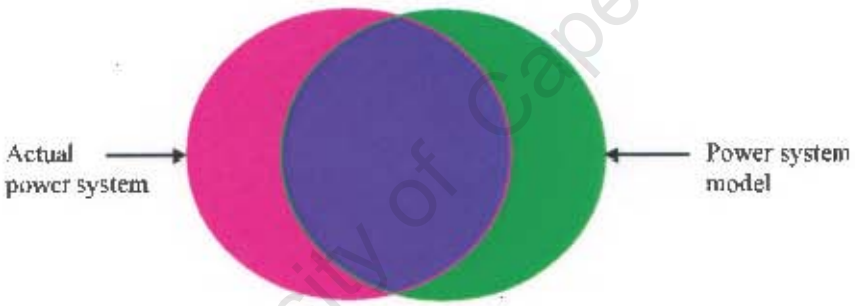

Figure 1.1: Concept of comparing actual power system behavior to power system model performance (Source: [17])

The intersection of the two circles represents the system behavior which is correctly predicted by the model. The part of the *actual power system* circle outside the intersection represents the system behavior that cannot be predicted by the model. The part of the *power system model* circle outside the intersection represents erroneous results i.e. the system does not behave as predicted by the model. The ideal situation would be to have a complete overlap of the two circles, meaning that the model is able to predict the system behavior for all operating conditions.

There is always a discrepancy between the actual power system behavior and the model prediction due to: firstly, measuring devices have restricted accuracy and thus the actual system cannot be identified exactly. Secondly, the behavior of the actual system changes with time, often in an unpredictable manner, due to changes in material properties, environmental or operating conditions. Thirdly, the mathematical models are often simplified or idealized to simplify the mathematical problem or to make it solvable. The accuracy of a simulation mainly depends on (i) components modeling, (ii) numerical methodology, and (iii) system input data. Some research effort has gone into the improvement of system modeling and the acquisition of accurate system data [18–24].

Reference [8] emphasizes the need for accurate modeling of damping effects for full utilization of the transmission capacity of power networks. Power systems are increasingly operating under stressed conditions, with very narrow stability margins. The heavy loading exposes the system to oscillations that can severely restrict system operations by requiring the curtailment of power transfer from one area to another as an operational measure. Alternatively, power system stabilizers (PSS) or other expensive devices such as Flexible AC Transmission System (FACTS) devices, have to be installed to provide additional damping. Correct modeling of damping may in some cases indicate that these expensive devices are not needed. It is suggested in [8] that there is a need for studies to be carried out to determine the modeling aspects that result in "damping errors". This issue is the main task of this thesis.

1.4 Definitions and classification of power system stability

Power system *stability* is that property of a power system that enables it to remain in a state of equilibrium under normal operating conditions and to regain an acceptable state of equilibrium after being subjected to a disturbance [7, 25]. The stability of the system depends on the initial operating condition and the nature of the disturbance, among other factors.

Figure 1.2 shows an example of a classification of power system stability [7, 25, 26]. This research concentrates on the aspects of rotor angle stability shown as shaded in the figure.

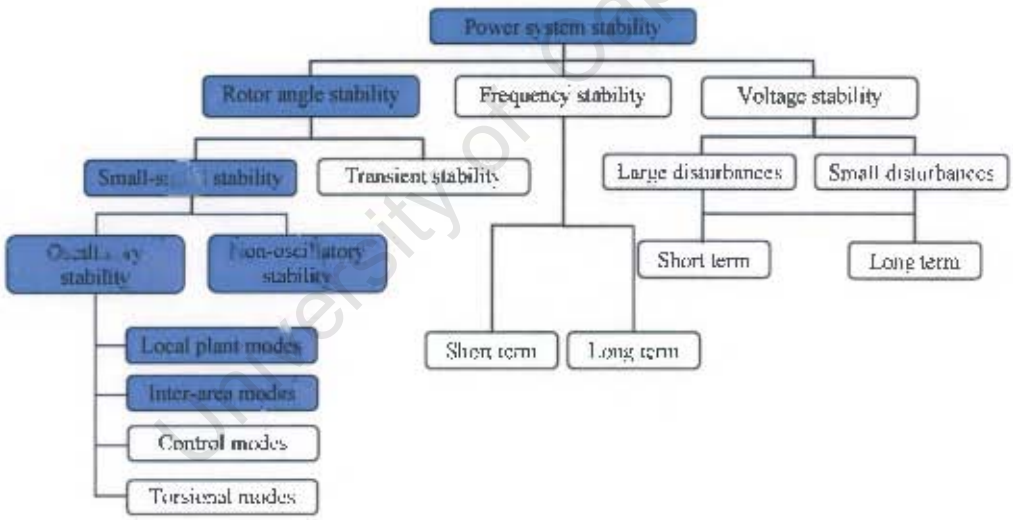

Figure 1.2: Classification of power system stability

Under steady-state conditions, the mechanical torque input and the electromagnetic torque output of each generator connected in the power system are balanced. This balance is offset if a disturbance occurs in the system. The change in electromagnetic torque following a disturbance can be resolved

into two components; the synchronizing torque component in phase with the rotor angle deviation and the damping torque component in phase with the speed deviation. Both components must exist and be positive for stability to be maintained [7, 25]. *Rotor angle stability* is the ability of synchronous machines in an interconnected power system to remain in synchronism after a disturbance [25]. Insufficient synchronizing torque results in *non-oscillatory* instability characterized by steady increase in generator rotor angle, whereas insufficient damping torque results in *oscillatory* instability characterized by rotor oscillations of increasing amplitude.

Rotor angle stability is further classified as *transient stability* and *small-signal stability*. Transient stability is the ability of the power system to maintain synchronism after a large disturbance e.g. system fault, loss of a generator or major load. Small-signal stability is the ability of the system to maintain synchronism after a small disturbance caused by small variations in load and generation. The disturbance is considered to be small enough to allow the linearization of the system differential algebraic equations (DAE), for purposes of analysis [7, 17, 25]. Hence, small-signal stability is commonly studied using eigenvalue techniques applied to linearized system models. In present day power systems, continually acting, high gain, fast acting voltage regulators are commonly used, thus reducing the small-signal stability problem to oscillatory type i.e. the problem involves damping of oscillations.

The oscillatory stability problem can be either local or global in nature. *Local plant modes* problems involve the oscillation of a single generator or a single plant against the rest of the power system. The oscillations are caused by the action of the automatic voltage regulators (AVR) of generating units operating at high output and feeding into weak transmission networks [17].

The frequency of these oscillations is in the range of 0.7 to 2.0 Hz [7]. Their characteristics are well understood and adequate damping can be readily achieved using PSS.

Global problems involve oscillation of a group of generators in one area swinging against a group of generators in another area. The oscillations are known as *inter-area modes* oscillations and their frequency is in the range of 0.1 to 0.7 Hz [7, 27]. Low frequency oscillations occur when two power system generation/load areas are connected by a weak transmission line. The characteristics of inter-area modes are complex and they differ from those of the local modes.

Inter-area oscillations have been observed in many power systems around the world [17, 18, 28–35]. The oscillations can severely restrict system operations by requiring the curtailment of power transfer from one area to another as an operational measure. High voltage DC (HVDC) links, PSS, and FACTS devices have been used to damp the oscillations [7, 29, 36–44].

1.5 Contributions of the thesis

The main contributions of this thesis are summarized as follows.

- The findings of this work lay a foundation for setting standards for comparison of power system simulation tools. With the increasing number of simulation tools available in the market, and the changing power system environment, it is evident that engineers need to understand the causes of discrepancies in results obtained using different tools.

  This thesis has identified variations among five industrial-grade simula-

tion tools – PSS/E, PowerFactory, EUROSTAG, SSAT, and MatNetEig – that cause discrepancies in results. We found variations in the modeling of generator saturation, speed voltage terms, turbine output, and the methods used for constructing the state matrix. Therefore, in case of disagreements on the results obtained with different tools for the same power system, this work would be useful for arbitration purposes. The tools in question should be checked for variations in the above listed turbo-generator modeling and algorithmic factors.

- One of the recommendations of the Power System Damping Ad Hoc Task Force [45] is that research should be carried out to establish the effect of neglecting stator transients and considering rotor speed deviation in speed voltage terms, on system damping. This modeling aspect has been addressed in this thesis. It has been found that with stator transients neglected, the damping ratio of the electromechanical modes obtained with rotor speed deviation considered in speed voltage terms is lower than that obtained with speed deviation neglected. The impact of rotor speed deviation is more significant with the excitation controlled by AVR than with manual excitation control. However, for all excitation control configurations, the effect on frequency is marginal.

- From the comparison of the tools' features and capabilities, users will be able to make informed choices of the most appropriate tool for a particular task.

1.6 Thesis outline

In Chapter 2, the analytical techniques used for small-signal stability studies are presented. The linearization of system equations is given and the methods used by simulation tools for constructing the state matrix are discussed. A brief description of the method used for computing system eigenvalues is given.

In Chapter 3, a theoretical investigation of turbo-generator modeling is presented. The modeling aspects that are investigated include generator saturation, speed voltage terms, and turbine output.

In Chapter 4, the features and capabilities of PSS/E, PowerFactory, EUROSTAG, SSAT, and MatNetEig are compared. The main criteria for comparison are components modeling, numerical methodology, and tool flexibility in terms of data input and output.

In Chapter 5, a description of the two power systems is given. The methods used and the procedure for investigating the five tools are outlined.

In Chapter 6, the simulation results are presented and discussed. The chapter is divided into two main sections according to the two power systems studied. For each power system, the impact of the variations in components modeling and numerical methodology, on the electromechanical modes is investigated. The results obtained with the five tools for different controller configurations are compared.

In Chapter 7, the impact of variations in modeling of speed voltage terms and turbine output on the electromechanical modes is quantified.

In Chapter 8, the conclusions and recommendations of the study are given.

Chapter 2

Analytical techniques

Eigenvalue techniques are widely used for small-signal stability analysis as they give a global view of the system stability at a glance. Eigenvalue analysis provides information on damping ratios, mode shapes (eigenvectors), and participation factors.

In this chapter, the analytical techniques employed by the five simulation tools for small-signal stability are presented. Linearization of system differential algebraic equations (DAE) is reviewed and the methods used by the simulation tools for constructing the state matrix are presented. There are many methods available for computing eigenvalues. However, the five tools employed the QR algorithm to compute the eigenvalues of the two systems studied in this research. The basic formulation of the algorithm is given in Section 2.4. A review of eigenvalue sensitivity is given in Section 2.6.

2.1 State-space representation

The dynamic behavior of the power system is expressed through a system of first order non-linear differential equations of the form

$$\dot{\mathbf{x}} = \mathbf{f}(\mathbf{x}, \mathbf{u}, t) \tag{2.1}$$

where:

$\mathbf{x}$ - nx1 vector of state variables

$\dot{\mathbf{x}}$ - derivative of $\mathbf{x}$ with respect to time

$\mathbf{f}$ - nx1 vector of non-linear functions

$\mathbf{u}$ - mx1 vector of inputs

t - time

n - order of the system

m - number of inputs

The choice of state variables is not unique; any set of n linearly independent system variables may be used. A common choice of the set of state variables used to represent the 6^{th} order generator model is rotor angle, speed, field flux linkage, d and q axes amortisseur flux linkages (δ, ω_r, ψ_{fd}, ψ_{1d}, ψ_{1q}, and ψ_{2q} respectively).

Equation (2.1) simplifies to (2.2) if the system is time invariant i.e. the time derivatives of the state variables are not explicit functions of time. This equation represents the system in an n-dimensional state-space.

$$\dot{\mathbf{x}} = \mathbf{f}(\mathbf{x}, \mathbf{u}) \tag{2.2}$$

The output variables that can be observed on the system may be expressed in terms of state variables and the input variables as:

$$\mathbf{y} = \mathbf{g}(\mathbf{x}, \mathbf{u}) \tag{2.3}$$

where:

$\mathbf{y}$ - px1 vector of outputs

$\mathbf{g}$ - px1 vector of non-linear functions

To allow for linear techniques to be applied for the solution of the system equations, the system is linearized about an equilibrium point.

2.2 Linearization of system equations

As discussed in Chapter 1, a disturbance is considered small if the DAE that describe the system response to the disturbance may be linearized for the purpose of analysis. The equations are linearized in the vicinity of an equilibrium point with state variables $\mathbf{x_0}$ and inputs $\mathbf{u_0}$, that satisfy (2.2). Since the system is at equilibrium,

$$\dot{\mathbf{x_0}} = \mathbf{f}(\mathbf{x_0}, \mathbf{u_0}) = 0 \tag{2.4}$$

If the system is perturbed, both the state variables and the inputs deviate from the equilibrium point by an amount $\mathbf{\Delta x}$ and $\mathbf{\Delta u}$ respectively. The new state must satisfy (2.2). Hence

$$\dot{\mathbf{x}} = \dot{\mathbf{x}}_\mathbf{0} + \mathbf{\Delta}\dot{\mathbf{x}} = \mathbf{f}[(\mathbf{x_0} + \mathbf{\Delta x}), (\mathbf{u_0} + \mathbf{\Delta u})] \tag{2.5}$$

Equation (2.5) can be expressed as a Taylor's series expansion with second and higher order terms of the partial derivatives neglected. Thus, using the first order terms only, the approximation for the i^{th} state variable x_i is given by

$$\begin{aligned}
\dot{x}_i =& \dot{x}_{i0} + \Delta\dot{x}_i \\
\dot{x}_i =& f_i(x_{i0}, u_{i0}) + \frac{\partial f_i}{\partial x_1}.\Delta x_1 + \ldots + \frac{\partial f_i}{\partial x_n}.\Delta x_n + \\
& \frac{\partial f_i}{\partial u_1}.\Delta u_1 + \ldots + \frac{\partial f_i}{\partial u_m}.\Delta u_m
\end{aligned} \tag{2.6}$$

Since $\dot{x}_{i0} = f_i(x_{i0}, u_{i0})$, it can be seen from (2.6) that

$$\Delta\dot{x}_i = \frac{\partial f_i}{\partial x_1}.\Delta x_1 + \ldots + \frac{\partial f_i}{\partial x_n}.\Delta x_n + \frac{\partial f_i}{\partial u_1}.\Delta u_1 + \ldots + \frac{\partial f_i}{\partial u_m}.\Delta u_m \quad (2.7)$$

Similar linearization of the system outputs $\boldsymbol{y}$ expressed as (2.3) yields

$$\Delta y_j = \frac{\partial g_j}{\partial x_1}.\Delta x_1 + \ldots + \frac{\partial g_j}{\partial x_n}.\Delta x_n + \frac{\partial g_j}{\partial u_1}.\Delta u_1 + \ldots + \frac{\partial g_j}{\partial u_m}.\Delta u_m \quad (2.8)$$

After linearizing all components of the vectors $\boldsymbol{x}$ and $\boldsymbol{y}$, the following set of equations is obtained.

$$\begin{aligned} \Delta\dot{\mathbf{x}} &= \mathbf{A}\Delta\mathbf{x} + \mathbf{B}\Delta\mathbf{u} \\ \Delta\mathbf{y} &= \mathbf{C}\Delta\mathbf{x} + \mathbf{D}\Delta\mathbf{u} \end{aligned} \quad (2.9)$$

where:

A - n x n state matrix

B - n x m input matrix

C - p x n output matrix

D - p x m feed-forward matrix

The elements of the $\boldsymbol{A}$, $\boldsymbol{B}$, $\boldsymbol{C}$, and $\boldsymbol{D}$ matrices are partial derivatives of the DAE expressed as (2.10), evaluated at the equilibrium point.

$$\mathbf{A} = \begin{pmatrix} \frac{\partial f_1}{\partial x_1} & \cdots & \frac{\partial f_1}{\partial x_n} \\ \vdots & \ddots & \vdots \\ \frac{\partial f_n}{\partial x_1} & \cdots & \frac{\partial f_n}{\partial x_n} \end{pmatrix} \qquad \mathbf{B} = \begin{pmatrix} \frac{\partial f_1}{\partial u_1} & \cdots & \frac{\partial f_1}{\partial u_m} \\ \vdots & \ddots & \vdots \\ \frac{\partial f_n}{\partial u_1} & \cdots & \frac{\partial f_n}{\partial u_m} \end{pmatrix}$$

$$\mathbf{C} = \begin{pmatrix} \frac{\partial g_1}{\partial x_1} & \cdots & \frac{\partial g_1}{\partial x_n} \\ \vdots & \ddots & \vdots \\ \frac{\partial g_p}{\partial x_1} & \cdots & \frac{\partial g_p}{\partial x_n} \end{pmatrix} \qquad \mathbf{D} = \begin{pmatrix} \frac{\partial g_1}{\partial u_1} & \cdots & \frac{\partial g_1}{\partial u_m} \\ \vdots & \ddots & \vdots \\ \frac{\partial g_p}{\partial u_1} & \cdots & \frac{\partial g_p}{\partial u_m} \end{pmatrix} \quad (2.10)$$

System stability is deduced from the eigenvalues of the state matrix, $\boldsymbol{A}$. The $\boldsymbol{B}$ and $\boldsymbol{C}$ matrices are of interest in the formulation of the mode controllability and observability matrices.

2.3 Techniques for constructing the A matrix

There are two methods that are commonly used for constructing the system matrices: numerical differentiation and analytical differentiation. Since this thesis is concerned with system eigenvalues, the following discussion only deals with the construction of the $\boldsymbol{A}$ matrix. However the same techniques are used for the other system matrices, $\boldsymbol{B}$, $\boldsymbol{C}$, and $\boldsymbol{D}$.

2.3.1 Numerical differentiation

Using this method, the derivatives of the DAE at an equilibrium point with state variables $\mathbf{x_0}$ and inputs $\mathbf{u_0}$ are computed numerically. The finite difference method is used to approximate the values of $f(x_o \pm h^1, u_0)$ at points $(x_o \pm h, u_0)$ in the neighborhood of the equilibrium point (x_0, u_0). Expanding the functions $f(x_o \pm h, u_0)$ in a Taylor series around (x_0, u_0) yields

$$f(x_0 - h, u_0) = f(x_0, u_0) - f'(x_0, u_0)h + \frac{f''(x_0, u_0)h^2}{2!} - \frac{f'''(x_0, u_0)h^3}{3!} + - \dots \tag{2.11}$$

$$f(x_0 + h, u_0) = f(x_0, u_0) + f'(x_0, u_0)h + \frac{f''(x_0, u_0)h^2}{2!} + \frac{f'''(x_0, u_0)h^3}{3!} + \dots \tag{2.12}$$

The derivative $f'(x_0, u_0)$ may be approximated using either (2.11) or (2.12) by neglecting terms in h^2 and higher. The derivatives may thus be expressed

[1] $h = \Delta$ (small perturbation) used elsewhere in this thesis

as

$$f'(x_0, u_0) \approx \frac{f(x_0, u_0) - f(x_0 - h, u_0)}{h} \tag{2.13}$$

$$f'(x_0, u_0) \approx \frac{f(x_0 + h, u_0) - f(x_0, u_0)}{h} \tag{2.14}$$

Equation (2.13) is a *backward difference* approximation of the derivative and (2.14) is a *forward difference* approximation. The two differentiation schemes are termed *one-sided difference* approximations.

The derivative may also be approximated by subtracting (2.11) from (2.12) and neglecting terms in h^2 and higher to give

$$f'(x_0, u_0) \approx \frac{f(x_0 + h, u_0) - f(x_0 - h, u_0)}{2h} \tag{2.15}$$

Equation (2.15) is known as the *central difference* approximation since it uses one point on either side of the equilibrium point.

The elements of the $\boldsymbol{A}$ matrix can thus be obtained by sequentially perturbing the elements of $\mathbf{x_0}$ by an amount h for each of the non-linear functions.

Errors in numerical differentiation

Truncation of the Taylor series expansion introduces errors in the computation of derivatives. Moreover, the DAE are only evaluated up to a relative accuracy thereby introducing a round-off error. The truncation error can be derived for each approximation by retaining the first neglected term in the derivations of the derivatives [46]. If the round-off error is of magnitude ϵ, with signs that accumulate errors, equations (2.13)-(2.15) may be re-written including the truncation and round-off errors as

$$f'(x_0, u_0) = \frac{f(x_0, u_0) - f(x_0 - h, u_0)}{h} + \left(f''(x_0, u_0)\frac{h}{2} + \frac{2\epsilon}{h} \right) \tag{2.16}$$

$$f'(x_0, u_0) = \frac{f(x_0 + h, u_0) - f(x_0, u_0)}{h} - \left(f''(x_0, u_0)\frac{h}{2} + \frac{2\epsilon}{h} \right) \quad (2.17)$$

$$f'(x_0, u_0) = \frac{f(x_0 + h, u_0) - f(x_0 - h, u_0)}{2h} - \left(f'''(x_0, u_0)\frac{h^2}{3!} + \frac{\epsilon}{h} \right) \quad (2.18)$$

It can be observed from (2.16)-(2.18) that the order[2] of accuracy of the central difference approximation is 2, making it more accurate than the one-sided difference approximation with order of accuracy 1 [47]. It can also be observed that the round-off error is inversely proportional to the perturbation size, h; the truncation error is directly proportional to h.

2.3.2 Analytical differentiation

The DAE are expressed as functions of differential state variables x and algebraic state variables u. The elements of the $\boldsymbol{A}$ matrix are obtained by applying standard rules of differentiation on the system equations. The partial derivatives are evaluated at the equilibrium point x_0. This method is more accurate than numerical differentiation as the derivatives are not approximated i.e. there are no truncation errors.

2.3.3 State equations for multi-machine systems

The analysis of a multi-machine system involves the solution of equations representing the generators and their controls (excitation system and prime mover controls), interconnecting transmission network, loads, and other devices such as FACTS and HVDC links. For small-signal stability analysis,

[2]Power of h

these equations are linearized about an equilibrium point and all variables other than the state variables are eliminated.

The general approach involves expressing the linearized model of each device in the form [7, 17, 48]:

$$\Delta\dot{\mathbf{x}}_d = \mathbf{A}_d\Delta\mathbf{x}_d + \mathbf{B}_d\Delta\mathbf{v} \tag{2.19a}$$

$$\Delta\mathbf{i}_d = \mathbf{C}_d\Delta\mathbf{x}_d - \mathbf{Y}_d\Delta\mathbf{v} \tag{2.19b}$$

where:

$\mathbf{x}_d$ - vector of the individual device state variables

$\mathbf{i}_d$ - vector of d and q axes current injection into the network from the device

$\mathbf{v}$ - vector of d and q axes network bus voltages

In (2.19), $\mathbf{B}_d$ and $\mathbf{Y}_d$ have non-zero elements corresponding only to the terminal voltage of the device and any remote bus voltages used to control the device. The state equations for all the dynamic devices in the system are expressed as

$$\Delta\dot{\mathbf{x}} = \mathbf{A}_D\Delta\mathbf{x} + \mathbf{B}_D\Delta\mathbf{v} \tag{2.20a}$$

$$\Delta\mathbf{i} = \mathbf{C}_D\Delta\mathbf{x} - \mathbf{Y}_D\Delta\mathbf{v} \tag{2.20b}$$

where $\mathbf{x}$ is a vector of state variables of the complete system, and $\mathbf{A}_D$ and $\mathbf{C}_D$ are block diagonal matrices composed of $\mathbf{A}_d$ and $\mathbf{C}_d$ associated with the individual devices.

The interconnecting transmission network is represented by node equation (2.21).

$$\Delta\mathbf{i} = \mathbf{Y}_N\Delta\mathbf{v} \tag{2.21}$$

where Y_N is the network admittance matrix.

Equating (2.20b) and (2.21) yields

$$\mathbf{C}_D\Delta\mathbf{x} - \mathbf{Y}_D\Delta\mathbf{v} = \mathbf{Y}_N\Delta\mathbf{v}$$

Re-arranging,

$$\Delta\mathbf{v} = (\mathbf{Y}_N + \mathbf{Y}_D)^{-1}\mathbf{C}_D\Delta\mathbf{x} \tag{2.22}$$

Substituting (2.22) for $\Delta\mathbf{v}$ in (2.20a) gives the overall state equation as

$$\begin{aligned}\Delta\dot{\mathbf{x}} &= \mathbf{A}_D\Delta\mathbf{x} + \mathbf{B}_D(\mathbf{Y}_N + \mathbf{Y}_D)^{-1}\mathbf{C}_D\Delta\mathbf{x} \\ &= \mathbf{A}\Delta\mathbf{x}\end{aligned} \tag{2.23}$$

where the state matrix $\boldsymbol{A}$ for the complete system is given by

$$\mathbf{A} = \mathbf{A}_D + \mathbf{B}_D(\mathbf{Y}_N + \mathbf{Y}_D)^{-1}\mathbf{C}_D \tag{2.24}$$

2.4 Computation of eigenvalues

The eigenvalues λ, of the state matrix $\boldsymbol{A}$ can be computed by solving the equation

$$\mathbf{Au} = \lambda\mathbf{u} \quad \text{for} \quad \mathbf{u} \neq 0 \tag{2.25}$$

where $\mathbf{u}$ is a column vector. Equation (2.25) may be re-written as

$$(\mathbf{A} - \lambda\mathbf{I})\mathbf{u} = 0 \tag{2.26}$$

For a non-trivial solution, $\mathbf{A} - \lambda\mathbf{I}$ must be singular. Hence, the eigenvalues of the $\boldsymbol{A}$ matrix are computed by solving for the roots of the characteristic equation (2.27).

$$\det(\mathbf{A} - \lambda\mathbf{I}) = 0 \tag{2.27}$$

The eigenvalues may be real or complex. A real eigenvalue corresponds to a non-oscillatory mode and a complex eigenvalue corresponds to an oscillatory mode. Complex eigenvalues occur in conjugate pairs $\lambda = \sigma \pm j\omega$, where the real part gives the damping in *1/s* (reciprocal of time constant of amplitude decay) and the imaginary part gives the frequency of oscillation in *rad/s*. The damping ratio ζ, determines the rate of decay of the amplitude of the oscillations and is given by

$$\zeta = \frac{-\sigma}{\sqrt{\sigma^2 + \omega^2}} \tag{2.28}$$

Damping is often considered adequate if all electromechanical modes have a damping ratio in the range 3 to 5% [17, 32, 49, 50]. The low values are admissible if the damping ratio is not too sensitive to variations in operating conditions and system parameters.

For both non-oscillatory and oscillatory modes, the system is stable if the real part is negative. A positive real mode signifies aperiodic instability and the magnitude of the monitored signal increases with time. If a complex mode has a positive real part, the amplitude of the oscillations increases with time.

For large order systems with eigenvalues of widely varying magnitudes, computation of eigenvalues using the characteristic equation fails [7]. Thus, other methods of computing eigenvalues are used for such systems. One of the commonly used methods is the *QR* algorithm. This algorithm uses a decomposition method. The $\boldsymbol{A}$ matrix is factored into two matrices such that

$$\mathbf{A} = \mathbf{QR} \tag{2.29}$$

where $\boldsymbol{Q}$ is orthogonal i.e. $\mathbf{Q}^T = \mathbf{Q}^{-1}$, and $\boldsymbol{R}$ is an upper triangular matrix.

Let $\mathbf{A}_1 = \boldsymbol{A}$ and define a sequence

$$\mathbf{A}_m = \mathbf{Q}_m \mathbf{R}_m \tag{2.30a}$$

$$\mathbf{A}_{m+1} = \mathbf{R}_m \mathbf{Q}_m \tag{2.30b}$$

for $m = 1, 2, \ldots$.

Since $\mathbf{Q}_m$ is orthogonal, it can be seen from (2.30a) that

$$\mathbf{R}_m = \mathbf{Q}_m^T \mathbf{A}_m \tag{2.31}$$

Substituting (2.31) in (2.30b) gives

$$\mathbf{A}_{m+1} = \mathbf{Q}_m^T \mathbf{A}_m \mathbf{Q}_m \tag{2.32}$$

The matrix $\boldsymbol{A}_{m+1}$ is orthogonally similar to $\boldsymbol{A}_m$, $\boldsymbol{A}_{m-1}$, $\ldots$, $\boldsymbol{A}_1$. The sequence $\{\boldsymbol{A}_m\}$ converges either to a triangular matrix with the eigenvalues of $\boldsymbol{A}$ on its diagonal, or to a near-triangular matrix from which the eigenvalues can easily be calculated [46, 51].

All the investigated tools use the QR algorithm for calculating the eigenvalues of the $\boldsymbol{A}$ matrix [9, 52].

2.5 Eigenvectors

For every eigenvalue λ_i, there is a corresponding *right eigenvector* $\mathbf{u}_i$ that satisfies (2.25). Thus

$$\mathbf{A}\mathbf{u}_i = \lambda_i \mathbf{u}_i \quad \text{for} \quad i = 1, 2, \ldots, n \tag{2.33}$$

Each right eigenvector is a column vector with a length equal to the number of state variables and it has the form

$$\mathbf{u}_i = \begin{bmatrix} u_{1i} & u_{2i} & \dots & u_{ni} \end{bmatrix}^T \tag{2.34}$$

The eigenvectors are not unique and each remains a valid eigenvector when multiplied by a scalar.

The right eigenvector describes the activity of the state variables in a mode.

Similarly, *left eigenvectors* are row vectors that satisfy

$$\mathbf{v}_i\mathbf{A} = \lambda_i\mathbf{v}_i \quad \text{for} \quad i = 1, 2, \dots, n. \tag{2.35}$$

The left eigenvector describes the contribution of the activity of a state variable to the mode.

The left and right eigenvectors corresponding to different eigenvalues are orthogonal i.e.

$$\mathbf{v}_i\mathbf{u}_j = 0 \tag{2.36}$$

However, for eigenvectors corresponding to the same eigenvalue,

$$\mathbf{v}_i\mathbf{u}_i = C_i \tag{2.37}$$

where C_i is a non-zero constant. The eigenvectors are usually normalized so that $C_i = 1$.

2.6 Eigenvalue sensitivity

The eigenvalues, and thus the qualitative behavior, of the linearized system depend upon the equilibrium point at which the system is linearized. There-

fore, each eigenvalue is a function of the power system parameters. Sensitivity analysis involves the study of the effect of parameter changes on the dynamics of the system. The parameter changes may be due to errors and tolerances of the underlying mathematical model e.g. parameter measurement errors, model approximations etc. There is a need to guarantee that system eigenvalues are robust in relation to the system parameters [53–55].

Each element a_{kj} of the $\boldsymbol{A}$ matrix is a function of system parameters. Therefore, if an eigenvalue has high sensitivity to changes in any of the elements a_{kj}, it is also likely that the eigenvalue has high sensitivity in relation to some system parameter(s). Thus, if large sensitivity in relation to any a_{kj} is detected, the symbolic expression of the $\boldsymbol{A}$ matrix is necessary to establish which system parameters are involved.

Eigenvalue sensitivity can be determined empirically by repeatedly computing the eigenvalues for different equilibrium points i.e. varying the system parameters. Although accurate, empirical sensitivity analysis is computationally burdensome. An alternative method requires analytical evaluation of formulas for the sensitivities of interest as described below.

In Section 2.5 the relationship between the eigenvalues and eigenvectors of the $\boldsymbol{A}$ matrix was given by equation (2.33) and is repeated here for reference.

$$\mathbf{A}\mathbf{u}_i = \lambda_i \mathbf{u}_i \tag{2.33}$$

Differentiating (2.33) with respect to element a_{kj} gives

$$\frac{\partial \mathbf{A}}{\partial a_{kj}}\mathbf{u}_i + \mathbf{A}\frac{\partial \mathbf{u}_i}{\partial a_{kj}} = \frac{\partial \lambda_i}{\partial a_{kj}}\mathbf{u}_i + \lambda_i \frac{\partial \mathbf{u}_i}{\partial a_{kj}} \tag{2.38}$$

Pre-multiplying both sides of (2.38) by the i^{th} left eigenvector $\mathbf{v}_i$, and re-

arranging yields

$$\mathbf{v}_i \frac{\partial \mathbf{A}}{\partial a_{kj}} \mathbf{u}_i + \mathbf{v}_i (\mathbf{A} - \lambda_i \mathbf{I}) \frac{\partial \mathbf{u}_i}{\partial a_{kj}} = \mathbf{v}_i \frac{\partial \lambda_i}{\partial a_{kj}} \mathbf{u}_i \tag{2.39}$$

From (2.35), $\mathbf{v}_i(\mathbf{A} - \lambda_i \mathbf{I}) = 0$ and (2.37), $\mathbf{v}_i \mathbf{u}_i = 1$. Thus, the sensitivity of eigenvalue λ_i to element a_{kj} is given by

$$S_{a_{kj}}^{\lambda_i} = \frac{\partial \lambda_i}{\partial a_{kj}} = \mathbf{v}_i \frac{\partial \mathbf{A}}{\partial a_{kj}} \mathbf{u}_i \tag{2.40}$$

All the elements of $\partial \mathbf{A} / \partial a_{kj}$ are zero, except for the element in the k^{th} row and j^{th} column which is equal to 1. Hence $S_{a_{kj}}^{\lambda_i}$ reduces to

$$S_{a_{kj}}^{\lambda_i} = \frac{\partial \lambda_i}{\partial a_{kj}} = v_{ik} u_{ji} \tag{2.41}$$

where v_{ik} and u_{ji} are elements of the left and right eigenvectors respectively. Equation (2.41) gives the absolute eigenvalue sensitivity [53, 55].

The sensitivity of the eigenvalue λ_i to a diagonal element a_{kk} of the $\boldsymbol{A}$ matrix is termed the *participation factor* [7, 49] and it is given by

$$S_{a_{kk}}^{\lambda_i} = \frac{\partial \lambda_i}{\partial a_{kk}} = v_{ik} u_{ki} \tag{2.42}$$

The *relative sensitivity* may be obtained by the logarithmic sensitivity (LS) of the eigenvalue [53–56], given by

$$\bar{S}_{a_{kj}}^{\lambda_i} = \left. \frac{\partial \ln \lambda_i}{\partial \ln a_{kj}} \right|_{a_{kj0}} = \left. \frac{\partial \lambda_i / \lambda_i}{\partial a_{kj} / a_{kj}} \right|_{a_{kj0}} = \left. \frac{a_{kj0}}{\lambda_{i0}} \frac{\partial \lambda_i}{\partial a_{kj}} \right|_{a_{kj0}} \tag{2.43}$$

where subscript *0* denotes values evaluated at the equilibrium point.

When the element a_{kj} of the $\boldsymbol{A}$ matrix changes by a certain percentage, $\bar{S}_{a_{kj}}^{\lambda_i}$ magnifies this percentage in λ_i change. Relative sensitivity is ideal for comparing sensitivity to different parameters because they are dimensionless and normalized. Sensitivity values greater than 1 indicate increasing relative errors.

2.7 Summary

In this chapter, the formulation of state-space representation by power system simulation tools has been discussed. The methods used by the tools for constructing the $\boldsymbol{A}$ matrix are analytical differentiation and numerical differentiation and they have been presented. Numerical differentiation is further classified into one-sided and central difference approximation. For the two approximation schemes, the accuracy to which the $\boldsymbol{A}$ matrix is computed depends on the perturbation size, which should be kept small but not so small as to cause numerical instability. It has been shown that the accuracy of the central difference approximation is an order higher than that of the one-sided difference approximation. The importance of establishing the robustness of the eigenvalues in relation to the system parameters has been highlighted.

Chapter 3

Turbo-generator modeling

In Chapter 1, it was highlighted that analytical tools differ in their components modeling and their numerical methodology. Thus, for the same benchmark network, different tools give different results. We have found that the discrepancies in results obtained using different tools are mainly due to variations among the tools in components modeling [15, 16]. The results we obtained with different tools differ in damping but agree on frequency of oscillation.

In references [15] and [16], we highlight variations in the following modeling aspects of the turbo-generator set as possible causes of discrepancies in eigenvalue results obtained using different tools:

i) Generator saturation

ii) Speed voltage terms

iii) Turbine output.

In this chapter, the three modeling aspects listed above are discussed. For the purpose of illustration, the single machine infinite bus (SMIB) system

with the generator on manual control is used.

3.1 Saturation representation

The main factors that affect the dynamic behavior of synchronous machines in the 0–10 Hz frequency range are rotor flux transients and magnetic saturation [11]. Magnetic saturation in a synchronous machine is a phenomenon of great complexity. Various methods of accounting for saturation are available [7, 17, 20, 27, 57–73]. Although saturation representation has been recognized as one of the most important factors in the improvement of synchronous generator models [20, 65], there is no generally accepted method of representing saturation in small-signal stability studies [17]. Finite element analysis provides an accurate method of representing saturation. However, the computational intensity of this method makes it impractical for computing the performance of large power systems. Moreover, the benefit of using the representation appears to be only marginal and the effort may thus not be justified for stability studies [7].

For round rotor machines, the q-axis saturates appreciably more than the d-axis due to the presence of rotor teeth in the magnetic path of the q-axis [7, 17, 62, 70, 71, 73]. Therefore, different d and q axes saturation characteristics should be allowed. However, q-axis saturation data is usually not available. Thus, saturation characteristics represented by the open circuit saturation curve (OCC) are often assumed to be the same for both axes.

For salient pole machines, saturation is assumed to occur only in the d-axis [7, 20, 27, 60, 62, 71]. The path for q-axis flux is largely in air and hence the q-axis mutual inductance does not vary significantly with saturation of the

iron portion of the path. The d-axis saturation characteristic is represented by the OCC.

For machine models represented using coupled-circuit method[1] (see methods of model representation Chapter 4), only the mutual inductances L_{ad} and L_{aq} are assumed to be affected by saturation. The level of saturation of these inductances is determined by the air-gap flux linkages [7, 17]. The leakage inductances are assumed not to saturate since leakage fluxes are in the air for a significant portion of their path so that they are not considerably affected by saturation of the iron portion. For machine models represented using operational impedance method[2] (see methods of model representation Chapter 4), saturation is assumed to affect the various mutual and leakage inductances of the machine.

Some of the methods used to model the effects of saturation by power system simulation tools include total saturation, incremental saturation, and effective excitation. In literature, the incremental saturation method is recommended for small-signal stability studies [7,17,68,73]. The three methods are discussed in the following sub-sections.

3.1.1 Total saturation

In this method, the degree of saturation in the d-axis is represented by a saturation factor K_{sd}. The value of K_{sd} depends on the machine's operating point on the OCC and it is determined from the total air-gap flux linkage.

[1]Uses data specified in form of resistances and inductances

[2]Uses data specified in form of transient and sub-transient inductances, and time constants

The saturated mutual inductance is given by

$$L_{mls} = K_{sd} L_{mlu} \tag{3.1}$$

The subscripts u and s refer to the unsaturated and saturated values, respectively. This method is applicable to machine models represented using the coupled-circuit method.

3.1.1.1 Calculation of saturation factor K_{sd}

Figure 3.1 shows a typical open-circuit saturation curve used to represent the saturation characteristic of a loaded generator. The air-gap line depicts the open circuit characteristic (OCC) if magnetic saturation is neglected. If the machine's operating point lies on the linear part of the OCC that coincides with the air-gap line, then $K_{sd} = 1$ i.e. there is no saturation.

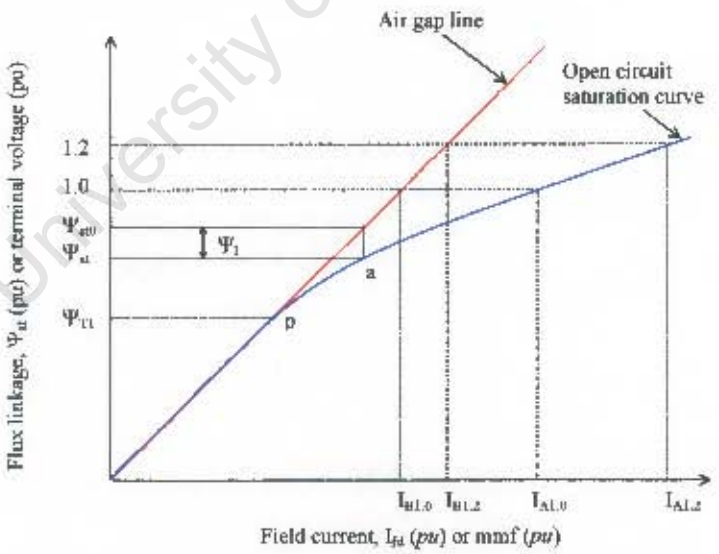

Figure 3.1: Typical open-circuit saturation curve

The flux linkage ψ_{at}, at an operating point 'a' defined on the non-linear part

of the OCC is given by

$$\psi_{at} = \sqrt{\psi_{ad}^2 + \psi_{aq}^2} \tag{3.2}$$

where ψ_{ad} and ψ_{aq} are the d-axis and q-axis components of the air-gap flux linkages and are given by

$$\psi_{ad} = \psi_d + L_l i_d = (e_q + R_a i_q) + L_l i_d \tag{3.3a}$$

$$\psi_{aq} = \psi_q + L_l i_q = (-e_d - R_a i_d) + L_l i_q \tag{3.3b}$$

The saturation factor K_{sd} is calculated as [7, 20, 71]

$$K_{sd} = \frac{\psi_{at}}{\psi_{at} + \psi_I} \tag{3.4}$$

where ψ_I is the drop in flux linkage due to saturation.

Similarly, the degree of saturation in the q-axis is represented by a saturation factor K_{sq}. For a round rotor machine, assuming same saturation characteristic for both d and q axes, K_{sq}=K_{sd}. However, if q-axis data is available and different from d-axis data, K_{sq} is computed using equations similar to those used for computing K_{sd}. For a salient pole machine $K_{sq} = 1.0$ for all loading conditions and thus L_{aq} is considered to be constant.

Several functions can be used to represent the effect of saturation ψ_I e.g. exponential, quadratic functions. It has been found that the choice of function has little effect on the accuracy of the model [17]. For the purpose of this discussion, the exponential function given by (3.5) will be used.

$$\psi_I = \begin{cases} 0, & \psi_{at} \leq \psi_{T1} \\ A_{sat} e^{B_{sat}(\psi_{at} - \psi_{T1})}, & \psi_{at} > \psi_{T1} \end{cases} \tag{3.5}$$

where A_{sat} and B_{sat} are constants and ψ_{T1} is the linear characteristic threshold flux linkage defined as point 'p' in Fig. 3.1.

Substituting (3.5) for ψ_I – non-linear characteristic – in (3.4), yields

$$K_{sd} = \frac{1}{1 + \frac{A_{sat}}{\psi_{at}} e^{B_{sat}(\psi_{at} - \psi_{T1})}} \tag{3.6}$$

The saturation constants, A_{sat} and B_{sat} are determined as described in the following sub-section.

3.1.1.2 Calculation of A_{sat} and B_{sat}

The constants A_{sat} and B_{sat} can be determined if the co-ordinates of two points on the non-linear curve are specified. These saturation constants can be expressed as

$$A_{sat} = \frac{(S_{1.0})^{1+5(1-\psi_{T1})}}{(1.2S_{1.2})^{5(1-\psi_{T1})}} \quad \text{and} \quad B_{sat} = 5 \ln\left(\frac{1.2S_{1.2}}{S_{1.0}}\right) \tag{3.7}$$

The derivations of (3.7) can be found in Appendix E, Section A.1.

In most power system simulation tools, saturation is defined by the parameters $S_{1.0}$ and $S_{1.2}$ corresponding to 1.0 per unit (pu) and 1.2 pu flux linkage (terminal voltage) respectively. These saturation parameters are given by

$$S_{1.0} = \frac{I_{A1.0} - I_{B1.0}}{I_{B1.0}} \tag{3.8a}$$

$$S_{1.2} = \frac{I_{A1.2} - I_{B1.2}}{I_{B1.2}} = \frac{I_{A1.2} - 1.2I_{B1.0}}{1.2I_{B1.0}} \tag{3.8b}$$

The field currents $I_{A1.0}$, $I_{B1.0}$, $I_{A1.2}$, and $I_{B1.2}$ are shown in Fig. 3.1.

Thus for any operating point on the OCC, the saturation factors and hence the saturated values of d and q axes mutual inductances can be determined.

3.1.2 Incremental saturation

In small-signal stability studies, the perturbed values of flux linkages are related to the perturbed values of current using incremental saturation factors. Incremental saturation representation is recommended for small-signal stability studies [7, 17, 68, 73].

Referring to Fig. 3.2, the slopes of the lines ob (air-gap line), oa, and yy′ (tangent to the OCC at point A) are the unsaturated (L_{adu}), total-saturated (L_{ads}), and incremental-saturated ($L_{ads(incr)}$) mutual inductances respectively.

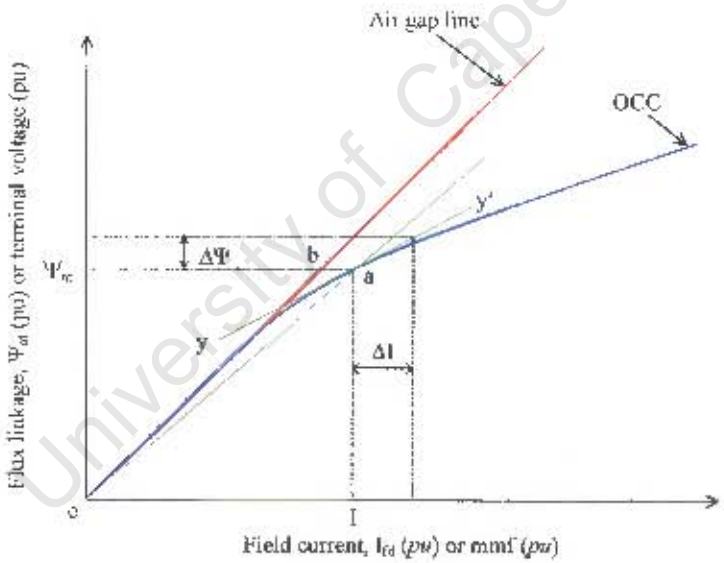

Figure 3.2: Distinction between total and incremental saturation

Incremental-saturated mutual inductance is given by

$$L_{ads(incr)} = K_{sd(incr)} L_{adu} \tag{3.9}$$

The incremental saturation factor $K_{sd(incr)}$ is expressed as [7]

$$K_{sd(incr)} = \frac{1}{1 + B_{sat} A_{sat} e^{B_{sat}(\psi_{at} - \psi_{T1})}} \tag{3.10}$$

The constants A_{sat} and B_{sat} are computed using (3.7). The total-saturated mutual inductances are used to determine the operating point (I, ψ_{at}) on the OCC. The incremental-saturated mutual inductances are used in the machine equations when considering perturbations in the flux linkages and excitation.

Comparing (3.10) and (3.6), it can be seen that $K_{sd(incr)} = K_{sd}$ if $B_{sat} = 1/\psi_{at}$, $K_{sd(incr)} < K_{sd}$ if $B_{sat} > 1/\psi_{at}$ and vice versa.

Previous investigations have indicated that $L_{ads(incr)}$ could be equal to or less than 50% of L_{adu} [68]. This method of representing saturation is applicable to machine models represented using the coupled-circuit method.

3.1.3 Effective excitation

The effective excitation is applicable to machine models represented using operational impedance method [17]. The machine's operating point on the OCC is determined using the voltage behind subtransient reactance. In the other methods described earlier, the machine's operating point is defined by the total air-gap flux linkage or, equivalently, the voltage behind leakage reactance [17]. The effect of saturation is accounted for by adding an incremental term ($L_{ad}\Delta i_{fd}$ which is the difference between the saturated and the air-gap excitation at the operating point) to the effective excitation in both d and q axes. For a round rotor machine, the incremental term (saturation excitation) is divided between the d and q axes in proportion to the subtransient fluxes, ψ''_d and ψ''_q.

A summary of the methods used to model the effects of saturation by the five tools is given in Chapter 4.

3.2 Speed voltage terms

Based on the dq-axis machine representation, assuming the q-axis lags the d-axis and adopting generating sign convention, the per unit (pu) stator terminal voltage, E_t is given by

$$E_t = e_d + je_q \tag{3.11a}$$

$$e_d = \frac{d\psi_d}{dt} + \omega_r\psi_q - R_a i_d \tag{3.11b}$$

$$e_q = \frac{d\psi_q}{dt} - \omega_r\psi_d - R_a i_q \tag{3.11c}$$

where:

e_d, e_q	- d-, q-axis components of terminal voltage
ψ_d, ψ_q	- d-, q-axis components of stator flux linkage
i_d, i_q	- d-, q-axis components of stator current
R_a	- stator resistance

Other notation is as defined earlier.

In (3.11b) and (3.11c), the terms $d\psi_d/dt$ and $d\psi_q/dt$ represent the voltages due to flux change in time and are known as transformer voltages. These terms represent stator transients. The terms $\omega_r\psi_d$ and $\omega_r\psi_q$ are the speed voltages. The speed voltage terms represent the fact that after the transformation from stationary (abc) to rotating (dq) reference frame, a rotating flux wave will create speed voltages in the stationary armature [7, 74].

In stability studies, network transients are neglected because they decay very fast. Therefore, for modeling consistency, the stator transients are also neglected.

Several studies have found that for the analysis of low frequency oscillations, neglecting rotor speed deviation in speed voltage terms counterbalances the effect of neglecting the stator transients [7,27,73,75]. A mathematical proof is given in [7]. By making the simplifying assumption $\omega_r = 1$, it is assumed that speed deviation is small and that it does not have a significant effect on the stator voltage; this is different from assuming that the speed is constant. The Power System Damping Ad Hoc Task Force [45] reports that significant error in the excitation system output could result if the speed effect is neglected.

Various authors [7, 27, 73, 75] agree that it is necessary to neglect stator transients in stator voltage calculation. The authors also concur that if stator transients are neglected, rotor speed deviation should also be neglected.

One of the recommendations of the Power System Damping Ad Hoc Task Force [45] is that research should be carried out to establish the effect of neglecting stator transients and considering rotor speed deviation in speed voltage terms, on system damping. From the available literature, it appears that little has been done in this respect. This modeling aspect is addressed in this research.

Johansson, *et al.* [76] report that if rotor speed deviation is considered in stator voltage calculation, the damping of the electromechanical modes in a SMIB system decreases. The authors used a 2^{nd} order (classical) generator model in their investigation. A study by Slootweg, *et al.* [6] shows that the real part of the electromechanical modes is influenced by the modeling of speed voltage terms. In the reported study, the authors used a 6^{th} or-

der generator model but no controllers were modeled. This reference does not conclude whether the influence of speed voltage terms on damping is beneficial or detrimental.

In [14], we investigate the effect of speed voltage terms on the electromechanical modes. For the investigation, we used the SMIB system with the generator represented by the 6^{th} order model and excitation controlled manually, automatically by AVR without PSS, and with PSS. We found that for the three excitation control configurations, inclusion of rotor speed deviation reduces damping and the effect on frequency of oscillation is marginal. We also noted that the impact of rotor speed deviation is more dominant if an AVR is modeled than with manual excitation control. However, for simplicity we neglected saturation in our study.

The impact of speed voltage terms on inter-area modes has not been reported in the available literature. This aspect was investigated in this research.

The effect of field excitation on damping is discussed in detail in literature [7, 60, 77]. It is shown that small changes in field flux result in a positive damping torque component and a negative synchronizing torque component. However, the discussion is limited to the case with rotor speed deviation neglected in speed voltage terms. Following is a theoretical investigation of the impact of speed voltage terms on the damping of the electromechanical modes.

Consider a single machine connected to an infinite bus through a transmission line with resistance R_E and reactance X_E. Suppose the generator is represented using the 6^{th} order model of Fig. 3.3. For simplicity, saturation is neglected and the generator is on manual excitation control.

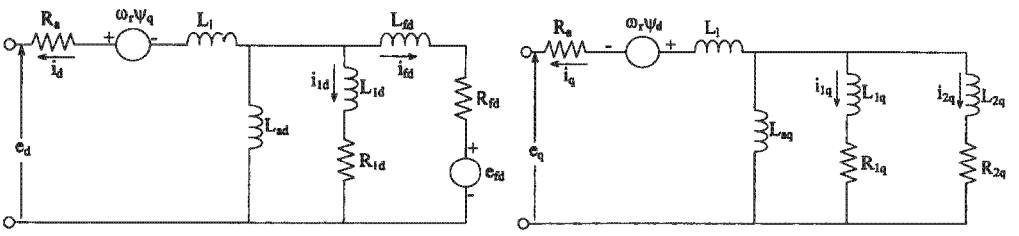

(a) d-axis (b) q-axis

Figure 3.3: Equivalent circuit of 6^{th} order generator

where :

L_l - leakage inductance

L_{fd}, R_{fd} - field winding inductance and resistance

L_{1d}, R_{1d} - d-axis amortisseur inductance and resistance

L_{1q}, R_{1q} - q-axis 1^{st} amortisseur inductance and resistance

L_{2q}, R_{2q} - q-axis 2^{nd} amortisseur inductance and resistance

e_{fd} - field voltage

Other notation is as defined earlier.

The flux linkages are given by

$$\begin{pmatrix} \psi_d \\ \psi_{fd} \\ \psi_{1d} \\ \psi_q \\ \psi_{1q} \\ \psi_{2q} \end{pmatrix} = \begin{pmatrix} L_{ad}+L_l & L_{ad} & L_{ad} & 0 & 0 & 0 \\ L_{ad} & L_{ad}+L_{fd} & L_{ad} & 0 & 0 & 0 \\ L_{ad} & L_{ad} & L_{ad}+L_{1d} & 0 & 0 & 0 \\ 0 & 0 & 0 & L_{aq}+L_l & L_{aq} & L_{aq} \\ 0 & 0 & 0 & L_{aq} & L_{aq}+L_{1q} & L_{aq} \\ 0 & 0 & 0 & L_{aq} & L_{aq} & L_{aq}+L_{2q} \end{pmatrix} \begin{pmatrix} i_d \\ i_{fd} \\ i_{1d} \\ i_q \\ i_{1q} \\ i_{2q} \end{pmatrix} \quad (3.12)$$

where ψ_{fd}, ψ_{1d}, ψ_{1q}, and ψ_{2q} are the field flux linkage, d-axis, 1^{st} q-axis, and 2^{nd} q-axis amortisseur flux linkages, respectively. The rotor currents are as shown in Fig. 3.3.

The rotor currents can be determined as follows:

$$\begin{aligned}
\psi_{fd} = \psi_{ad} + L_{fd} i_{fd} \quad &\Rightarrow \quad i_{fd} = \frac{\psi_{fd} - \psi_{ad}}{L_{fd}} \\
\psi_{1d} = \psi_{ad} + L_{1d} i_{1d} \quad &\Rightarrow \quad i_{1d} = \frac{\psi_{1d} - \psi_{ad}}{L_{1d}} \\
\psi_{1q} = \psi_{aq} + L_{1q} i_{1q} \quad &\Rightarrow \quad i_{1q} = \frac{\psi_{1q} - \psi_{aq}}{L_{1q}} \\
\psi_{2q} = \psi_{aq} + L_{2q} i_{2q} \quad &\Rightarrow \quad i_{2q} = \frac{\psi_{2q} - \psi_{aq}}{L_{2q}}
\end{aligned} \tag{3.13}$$

The voltage equations are

$$\begin{aligned}
e_d &= -R_a i_d + \omega_r \psi_q & e_q &= -R_a i_q - \omega_r \psi_d \\
e_{fd} &= R_{fd} i_{fd} + \dot{\psi}_{fd} & 0 &= R_{1q} i_{1q} + \dot{\psi}_{1q} \\
0 &= R_{1d} i_{1d} + \dot{\psi}_{1d} & 0 &= R_{2q} i_{2q} + \dot{\psi}_{2q}
\end{aligned} \tag{3.14}$$

where $\dot{\psi}$ represent the time derivatives of the flux linkages.

The mutual flux linkages in the d and q axes are given by

$$\begin{aligned}
\psi_{ad} &= L_{ad}(i_d + i_{fd} + i_{1d}) \\
\psi_{aq} &= L_{aq}(i_q + i_{1q} + i_{2q})
\end{aligned} \tag{3.15}$$

Substituting (3.13) for the rotor currents in (3.15) and re-arranging gives

$$\begin{aligned}
\psi_{ad} &= L''_{ad}\left(i_d + \frac{\psi_{fd}}{L_{fd}} + \frac{\psi_{1d}}{L_{1d}}\right) \\
\psi_{aq} &= L''_{aq}\left(i_q + \frac{\psi_{1q}}{L_{1q}} + \frac{\psi_{2q}}{L_{2q}}\right)
\end{aligned} \tag{3.16}$$

where:

$$\frac{1}{L''_{ad}} = \frac{1}{L_{ad}} + \frac{1}{L_{fd}} + \frac{1}{L_{1d}} \quad \text{and} \quad \frac{1}{L''_{aq}} = \frac{1}{L_{aq}} + \frac{1}{L_{1q}} + \frac{1}{L_{2q}}$$

From (3.12) and (3.14)

$$\begin{aligned}
e_d &= -R_a i_d + \omega_r \psi_q = -R_a i_d + \omega_r \psi_{aq} + \omega_r L_l i_q \\
e_q &= -R_a i_q - \omega_r \psi_d = -R_a i_q - \omega_r \psi_{ad} - \omega_r L_l i_d
\end{aligned} \tag{3.17}$$

Taking the infinite bus as reference, and generator rotor angle δ, the external network is represented in the d-q reference frame as

$$\begin{aligned} e_d &= -X_E i_q + R_E i_d + E_B \sin\delta \\ e_q &= X_E i_d - R_E i_q + E_B \cos\delta \end{aligned} \tag{3.18}$$

Equating (3.17) and (3.18) and re-arranging gives

$$\begin{aligned} i_d &= \frac{-(X_{T_3} E_{qN} + R_T E_{dN})}{D} \\ i_q &= \frac{X_{Td} E_{dN} - R_T E_{qN}}{D} \end{aligned} \tag{3.19}$$

where:

$$\begin{aligned} E_{dN} &= E_B \sin\delta - E''_d & E_{qN} &= E_B \cos\delta + E''_q \\ E''_d &= \omega_r L''_{cq} \left(\frac{\psi_{1q}}{L_{1q}} + \frac{\psi_{2q}}{L_{2q}} \right) & E''_q &= \omega_r L''_{ad} \left(\frac{\psi_{fd}}{L_{fd}} + \frac{\psi_{1d}}{L_{1d}} \right) \\ X_{Td} &= X_E - \omega_r (L''_{ad} + L_l) & X_{Tq} &= X_E + \omega_r (L''_{aq} + L_l) \\ &= X_E + X''_d & &= X_E + X''_q \\ R_T &= R_E + R_a & D &= R_T^2 + X_{Td} X_{Tq} \end{aligned}$$

Linearizing (3.19) yields

$$\begin{aligned} \Delta i_d &= m_1 \Delta\psi_{fd} + m_2 \Delta\psi_{1d} + m_3 \Delta\psi_{1q} + m_4 \Delta\psi_{2q} + m_5 \Delta\omega_r + m_6 \Delta\delta \\ \Delta i_q &= n_1 \Delta\psi_{fd} + n_2 \Delta\psi_{1d} + n_3 \Delta\psi_{1q} + n_4 \Delta\psi_{2q} + n_5 \Delta\omega_r + n_6 \Delta\delta \end{aligned} \tag{3.20}$$

where m_j, n_j are coefficients whose expressions are given in Appendix E, Section A.2. If rotor speed deviation is neglected in speed voltage terms, m_5 and n_5 in (3.20) are equal to zero.

Linearizing (3.16) gives

$$\begin{aligned} \Delta\psi_{ad} &= L''_{ad} \left(\Delta i_d + \frac{\Delta\psi_{fd}}{L_{fd}} + \frac{\Delta\psi_{1d}}{L_{1d}} \right) \\ \Delta\psi_{aq} &= L''_{aq} \left(\Delta i_q + \frac{\Delta\psi_{1q}}{L_{1q}} + \frac{\Delta\psi_{2q}}{L_{2q}} \right) \end{aligned} \tag{3.21}$$

The generator rotor circuit equations are

$$\begin{aligned}
\dot{\psi}_{fd} &= \frac{\omega_0 R_{fd}\psi_{ad}}{L_{fd}} - \frac{\omega_0 R_{fd}\psi_{fd}}{L_{fd}} + \omega_0 e_{fd} \\
\dot{\psi}_{1d} &= \frac{\omega_0 R_{1d}\psi_{ad}}{L_{1d}} - \frac{\omega_0 R_{1d}\psi_{1d}}{L_{1d}} \\
\dot{\psi}_{1q} &= -\omega_0 R_{1q} i_{1q} = -\omega_0 R_{1q}\frac{\psi_{1q} - \psi_{aq}}{L_{1q}} \\
\dot{\psi}_{2q} &= -\omega_0 R_{2q} i_{2q} = -\omega_0 R_{2q}\frac{\psi_{2q} - \psi_{aq}}{L_{2q}}
\end{aligned} \tag{3.22}$$

The equations of motion are

$$\begin{aligned}
\dot{\omega}_r &= \frac{1}{2H}(T_m - T_e - K_D\Delta\omega_r) \\
\dot{\delta} &= \omega_r - \omega_0
\end{aligned} \tag{3.23}$$

where:

H - Inertia constant (s)

K_D - Damping torque coefficient

T_e - Electrical torque

T_m - Mechanical torque

In (3.23), time t is in seconds, the rotor angle δ is in electrical radians, and ω_r and ω_0 are in *rad/s*.

Linearizing (3.22) and (3.23) yields

$$\begin{aligned}
\Delta\dot{\psi}_{fd} &= \frac{\omega_0 R_{fd}}{L_{fd}}\Delta\psi_{ad} - \frac{\omega_0 R_{fd}}{L_{fd}}\Delta\psi_{fd} + \omega_0\Delta e_{fd} \\
\Delta\dot{\psi}_{1d} &= \frac{\omega_0 R_{1d}}{L_{1d}}\Delta\psi_{ad} - \frac{\omega_0 R_{1d}}{L_{1d}}\Delta\psi_{1d} \\
\Delta\dot{\psi}_{1q} &= \frac{-\omega_0 R_{1q}}{L_{1q}}(\Delta\psi_{1q} - \Delta\psi_{aq}) \\
\Delta\dot{\psi}_{2q} &= \frac{-\omega_0 R_{2q}}{L_{2q}}(\Delta\psi_{2q} - \Delta\psi_{aq}) \\
\Delta\dot{\omega}_r &= \frac{1}{2H}(\Delta T_m - \Delta T_e - K_D\Delta\omega_r) \\
\Delta\dot{\delta} &= \omega_0\Delta\omega_r
\end{aligned} \tag{3.24}$$

The electrical torque is given by

$$T_e = \psi_{ad} i_q - \psi_{aq} i_d \tag{3.25}$$

Linearizing (3.25) gives

$$\begin{aligned} \Delta T_e &= \psi_{ad0}\Delta i_q + i_{q0}\Delta\psi_{ad} - \psi_{aq0}\Delta i_d - i_{d0}\Delta\psi_{aq} \\ &= K_1\Delta\psi_{fd} + K_2\Delta\psi_{1d} + K_3\Delta\psi_{1q} + K_4\Delta\psi_{2q} + K_5\Delta\omega_r + K_6\Delta\delta \end{aligned} \tag{3.26}$$

The expressions for the K coefficients are given in Appendix E, Section A.2.

The term $K_5\Delta\omega_r$ represents a damping torque component. The magnitude and sign of K_5 depend on the parameters of the machine, the external network, and the operating condition. The damping of the local modes is expected to be higher for a positive value of K_5 than for a negative value. If rotor speed deviation is neglected in stator voltage calculation, K_5 is zero.

The state-space model for the system (equation (3.24)) has the following form:

$$\begin{pmatrix} \Delta\dot{\psi}_{fd} \\ \Delta\dot{\psi}_{1d} \\ \Delta\dot{\psi}_{1q} \\ \Delta\dot{\psi}_{2q} \\ \Delta\dot{\omega}_r \\ \Delta\dot{\delta} \end{pmatrix} = \begin{pmatrix} a_{11} & a_{12} & a_{13} & a_{14} & a_{15} & a_{16} \\ a_{21} & a_{22} & a_{23} & a_{24} & a_{25} & a_{26} \\ a_{31} & a_{32} & a_{33} & a_{34} & a_{35} & a_{36} \\ a_{41} & a_{42} & a_{43} & a_{44} & a_{45} & a_{46} \\ a_{51} & a_{52} & a_{53} & a_{54} & a_{55} & a_{56} \\ 0 & 0 & 0 & 0 & \omega_0 & 0 \end{pmatrix} \begin{pmatrix} \Delta\psi_{fd} \\ \Delta\psi_{1d} \\ \Delta\psi_{1q} \\ \Delta\psi_{2q} \\ \Delta\omega_r \\ \Delta\delta \end{pmatrix} \tag{3.27}$$

The expressions for the elements a_{ij} are given in Appendix E, Section A.2.

Row 5 in (3.27) corresponds to the linearized swing equation given by

$$\Delta\dot{\omega}_r = \frac{1}{2H}(\Delta T_m - \Delta T_e - K_D\Delta\omega_r) \tag{3.28}$$

Substituting (3.26) in (3.28) for ΔT_e gives

$$\begin{aligned} \Delta\dot{\omega}_r = &\frac{1}{2H}[\Delta T_m - K_1\Delta\psi_{fd} - K_2\Delta\psi_{1d} - K_3\Delta\psi_{1q} - K_4\Delta\psi_{2q} \\ &- (K_5 + K_D)\Delta\omega_r - K_6\Delta\delta] \end{aligned} \tag{3.29}$$

The speed governor is not modeled ($\Delta T_m = 0$). Therefore, comparing row 5 in (3.27) with (3.29), it can be seen that $a_{5i} = -K_i/2H$, for $i = 1, 2, 3, 4,$ and 6, and $a_{55} = -(K_5 + K_D)/2H$.

If $K_D = 0$ then $a_{55} = -K_5/2H$. A negative value of a_{55} is indicative of a positive damping coefficient K_5 whereas a positive value of a_{55} is indicative of a negative value of K_5. Hence, the damping of the local mode is expected to be higher for a negative value of a_{55} than for a positive value.

If rotor speed deviation is neglected in speed voltage terms, elements a_{15}, a_{25}, a_{35}, and a_{45} are all equal to zero and $a_{55} = -K_D/2H$.

A summary of the speed voltage terms modeling by the five industrial-grade tools is given in Chapter 4.

3.3 Turbine output

A turbine converts the kinetic energy of a moving fluid into mechanical energy that is in turn converted into electrical energy by the generator. Under steady state conditions, the mechanical torque input is equal to the electrical torque output and the generator rotates at synchronous speed. An imbalance of the mechanical and electrical torques causes the generator to accelerate if the mechanical torque is greater than the electrical torque, or decelerate if the mechanical torque is less than the electrical torque. The swing equation defines the accelerating torque of the generator caused by the torque imbalance. The swing equation is commonly expressed as (3.23) as was given in Section 3.2 and is repeated here for reference.

$$\dot{\omega}_r = \frac{1}{2H}\left(T_m - T_e - K_D\Delta\omega_r\right) \tag{3.23}$$

From the literature, it is not clear whether the turbine output should be modeled as mechanical power P_m or mechanical torque T_m. For example, Kundur [7] represents turbine output as T_m whereas IEEE Committee Report [78] and Rogers [49] represent it as P_m. Different simulation tools represent the turbine output differently.

The relationship between torque and power is given by

$$T_m = \frac{P_m}{\omega_r} \tag{3.30}$$

If speed deviation is neglected ($\omega_r = 1\ pu$), then $T_m = P_m\ pu$; T_m and P_m can be used interchangeably in the swing equation. Suppose the effect of rotor speed deviation on stator voltage is neglected i.e. the rotor speed deviation is small and has insignificant effect on the stator voltage. Thus the electrical torque T_e is not a function of ω_r; T_e is a function of ψ_{fd}, ψ_{1d}, ψ_{1q}, ψ_{2q}, and δ.

The linearized swing equation is given in Section 3.2 as

$$\Delta\dot{\omega}_r = \frac{1}{2H}(\Delta T_m - \Delta T_e - K_D\Delta\omega_r) \tag{3.28}$$

where ΔT_e is given by (3.26).

Assuming constant turbine output ($\Delta T_m = 0$), and neglecting speed deviation in speed voltage terms i.e. $K_5 = 0$ in (3.26), 3.28 may be re-written as

$$\begin{aligned}\Delta\dot{\omega}_r =& \frac{1}{2H}[-K_1\Delta\psi_{fd} - K_2\Delta\psi_{1d} - K_3\Delta\psi_{1q} - K_4\Delta\psi_{2q} \\ & - K_D\Delta\omega_r - K_6\Delta\delta]\end{aligned} \tag{3.31}$$

Equation (3.31) corresponds to row 5 in (3.27) where $a_{5i} = -K_i/2H$, for i = 1, 2, 3, 4, and 6, and $a_{55} = -K_D/2H$.

If speed deviation is considered in the mechanical power-torque relationship ($\omega_r \neq 1$), $T_m \neq P_m$ *pu*. Our results [14] and those reported by Johansson *et al.* [76] show that modeling of the turbine output affects the damping of the electromechanical modes.

If the swing equation is expressed as (3.23) and the turbine output is specified as P_m, the corresponding value of T_m is computed using (3.30). Substituting (3.30) for T_m in (3.23) gives

$$\dot{\omega}_r = \frac{1}{2H}\left(\frac{P_m}{\omega_r} - T_e - K_D\Delta\omega_r\right) \tag{3.32}$$

Linearizing (3.32) as shown in Appendix E, Section A.3 yields

$$\Delta\dot{\omega}_r = \frac{1}{2H}\left[\Delta P_m - \Delta T_e - (K_D + P_{m0})\Delta\omega_r\right] \tag{3.33}$$

where ΔT_e is given by (3.26) and P_{m0} is the steady-state mechanical power.

Assuming constant turbine output ($\Delta P_m = 0$), and neglecting speed deviation in speed voltage terms i.e. $K_5 = 0$ in (3.26), (3.33) may be re-written as

$$\begin{aligned}\Delta\dot{\omega}_r = &\frac{1}{2H}[-K_1\Delta\psi_{fd} - K_2\Delta\psi_{1d} - K_3\Delta\psi_{1q} - K_4\Delta\psi_{2q} \\ &- (P_{m0} + K_D)\Delta\omega_r - K_6\Delta\delta]\end{aligned} \tag{3.34}$$

Equation (3.34) corresponds to row 5 in (3.27). Comparing these two equations, it can be seen that $a_{5i} = -K_i/2H$, for $i = 1, 2, 3, 4$, and 6, and $a_{55} = -(P_{m0} + K_D)/2H$.

From a theoretical viewpoint, if the turbine output is P_m and rotor speed deviation is considered in the mechanical power-torque relationship, the damping of the electromechanical modes is expected to be higher than the damping obtained with T_m turbine output. The damping increases due to the additional term $P_{m0}/2H$ in (3.34) associated with the power-torque relationship.

Our results [14] and those reported by Johansson *et al.* [76] affirm this view. It should be noted that the amount of additional damping depends on the size of the generator (H) and its loading i.e. P_{m0} is the generator loading at steady-state. The smaller the generator and the more heavily it is loaded, the higher the additional damping, and vice versa.

If a machine is not equipped with a speed governor or if a governor is not modeled, constant turbine output is assumed. Reference [45] observes that it is likely for a steam or hydraulic turbine without governor response to provide constant power. In such a case, if the turbine output is assumed to be constant torque, an error is introduced. The authors note that the error can be avoided by calculating T_m from P_m and using the true value of P_m, as in (3.32).

A summary of the turbine output used by the five industrial-grade tools is given in Chapter 4.

3.4 Summary

Previous research shows that different tools can give different results for the same benchmark network. In this chapter, the variations among the five tools in some aspects of turbo-generator modeling that cause discrepancies in eigenvalue results have been investigated. The modeling aspects investigated include modeling of generator saturation, speed voltage terms, and turbine output. Different methods of representing generator saturation have been presented. From the literature, incremental saturation representation is favored for small-signal stability studies. However, only one out of the five simulation tools investigated in this research allows incremental satura-

tion representation. The theoretical investigation presented in this chapter shows that the modeling of the speed voltage terms affects the damping of the electromechanical modes. The additional damping can be negative or positive depending on the system operating condition and the generator parameters. From the theoretical investigation, it has been shown that P_m turbine output is expected to give results with higher damping than those obtained with T_m turbine output.

ω_0 - base angular velocity
H - inertia constant
T_m - mechanical torque
T_e - electrical "
K_D - damping torque coefficient
L_{fd} — field winding leakage inductance
ψ_{ad} — mutual flux linkages
e_{fd} - field voltage
R_{1d} - d-axis amortisseur resistance
L_{1d} - d " " reactance
ψ_{1d} - d-axis amortisseur flux linkage
ψ_{1q} - q-axis " "
R_{1q} - 2 q-axis amortisseur resistances
L_{2q}, L_{1q} - 3 " " reactance
ψ_{aq} - 1
R_{2q} - 4
R_{2q} - 2
~~L_{2q}~~ - 3

HVDC
Gen
AVR
PSS
line
bus
Transf
loads

Chapter 4

Comparison of features and capabilities of the tools

As discussed in Chapter 1, the quality of a simulation mainly depends on the components modeling, numerical methodology, and input data. For most tools, the user only has control of the input data. It is therefore important that the user understands the capabilities and limitations of the tool selected to be used for a particular study.

In this chapter, five industrial-grade tools are compared based on their components modeling and numerical methodology. The tools' flexibility is also compared based on the method of data input and the available data output. The comparison pertains to small-signal stability application.

4.1 Components modeling

4.1.1 Synchronous generator

(i) Model availability

In power system dynamic studies, models of varying degrees of complexity are used to represent the generator. The simplest is the 2^{nd} order[1] (classical) model that assumes a constant voltage behind a transient reactance. Higher order models use the dq-axes representation. The models available in power system analysis tools range from 2^{nd} to 8^{th} order. The most complex models suggested for usage in power system stability studies are of 7^{th} and 8^{th} order. These models are used to better fit data derived from standstill frequency response tests [11, 70]. For 3^{rd} and higher order models, rotor characteristics are represented by a field winding and amortisseur on the d-axis and/or q-axis. Table 4.1 gives a summary of the number of rotor circuits in each model.

Table 4.1: Number of rotor circuits in generator models of varying degrees of complexity

Degree of complexity	No. of windings	
	d-axis	q-axis
3^{rd}	1	0
4^{th}	1	1
5^{th}	2	1
6^{th}	2	2
7^{th}	3	2
8^{th}	3	3

[1]Model order defines the number of state variables

For stability studies, the 5^{th} and 6^{th} order models have been found to be adequate for representing salient pole and round rotor generators, respectively [7, 27, 68, 79]. In the analysis of local oscillations, lower order models can be used to represent machines that are remote from the area under study. However, for the study of inter-area oscillations, all the machines in the system should be represented using detailed machine models [27].

A summary of the generator models available in the built-in libraries of the five tools is presented in Table 4.2, given at the end of the chapter.

(ii) Model representation

In power system analysis, synchronous machine models are commonly represented using operational-impedance and coupled-circuit methods [17]. Figures 4.1 and 4.2 show the representation of a 6^{th} order model by operational impedance and coupled-circuit methods, respectively. PSS/E represents the generator models using the operational-impedance method whereas PowerFactory, EUROSTAG, SSAT, and MatNetEig use the coupled-circuit method. The 7^{th} and 8^{th} order models in PSS/E are represented using the coupled-circuit method.

Synchronous machine data are usually specified in terms of standard parameters, also known as derived parameters (transient and sub-transient inductances and time constants), and may be obtained from manufacturer's data or field tests. Models represented by the operational-impedance method use data specified in standard-parameter format whereas models represented by the coupled-circuit method use data specified in basic-parameter format, also known as fundamental-parameter format (resistances and inductances). Hence, if the machine model is represented using the coupled-circuit method, standard parameters are converted to basic parameters. The two methods of

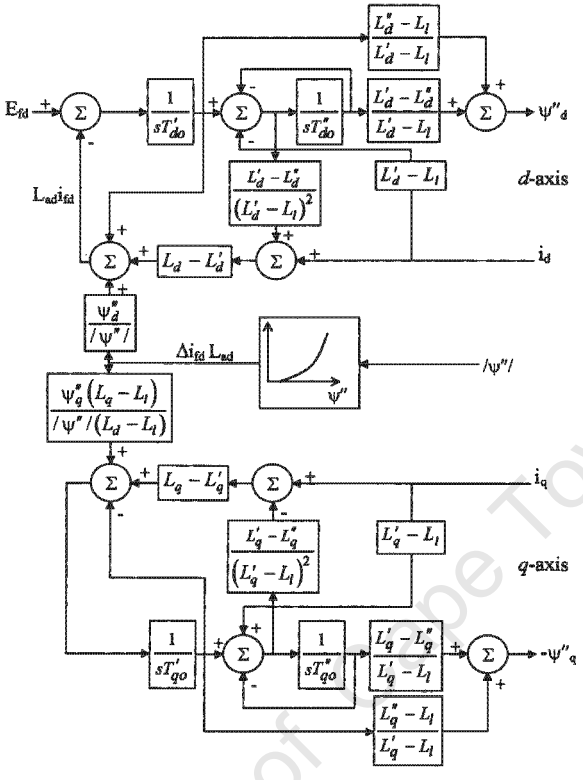

Figure 4.1: Representation of 6^{th} order generator model using operational impedance method

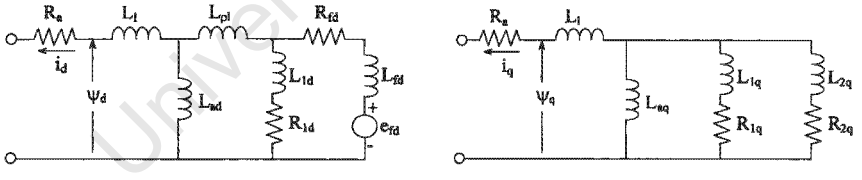

(a) d-axis (b) q-axis

Figure 4.2: Representation of 6^{th} order generator model using coupled-circuit method

representing the synchronous machine give identical results if generator saturation is neglected, and the conversion from standard to basic parameters is correctly performed [17].

4.1.2 Infinite bus

In power systems, an infinite bus is defined as a voltage source with constant magnitude, phase, and frequency [7, 60, 77]. The five tools investigated in this thesis represent the infinite bus using different components as follows:

- PSS/E represents the infinite bus using the classical generator model with inertia constant set to zero [11]. The value of the generator's effective dynamic impedance (ZSORCE) specified in load flow input data, is the short circuit impedance at the infinite bus.
- PowerFactory represents the infinite bus using either the *AC voltage source* or the *external grid*, available in the built-in library. The positive sequence impedance of the *AC voltage source* represents the short circuit impedance at the infinite bus. The *external grid* may be used to represent an infinite bus "by specifying an appropriate value of short-circuit power" [80].
- EUROSTAG has an *infinite node* in the standard library. In dynamic simulation the user specifies the node impedance which represents the short circuit impedance at the infinite bus.
- SSAT - reduces any generator model (any order) to an infinite bus. The reduction criteria may be by area, zone or bus. All the generators in a specified area, zone, or bus are reduced to an infinite bus.
- MatNetEig - the user specifies the generator to be reduced to infinite bus.

To ensure electrical stiffness, a low value of short circuit reactance should be specified at the infinite bus. If the same value of short circuit reactance is

used, the different representations of the infinite bus employed by the tools are equivalent and they do not cause discrepancies in results.

4.1.3 Load

Load models are broadly classified as static and dynamic. A static load model expresses the active and reactive powers at any instant of time as functions of the bus voltage magnitude and frequency at that instant. A dynamic load model expresses the active and reactive powers at any instant of time as functions of the bus voltage magnitude and frequency at past instants of time and, usually, including the present instant [81]. In this research, the loads were represented using static models and thus the discussion is limited to these models.

The static load at a bus may be modeled either as an exponential function (4.1) or as a polynomial function (4.2) also known as a ZIP model [7, 81, 82]. These models account for both voltage and frequency dependency of loads.

$$\begin{aligned} P &= P_0(\bar{V})^a(1 + K_{pf}\Delta f) \\ Q &= Q_0(\bar{V})^b(1 + K_{qf}\Delta f) \end{aligned} \tag{4.1}$$

$$\begin{aligned} P &= P_0[p_1\bar{V}^2 + p_2\bar{V} + p_3](1 + K_{pf}\Delta f) \\ Q &= Q_0[q_1\bar{V}^2 + q_2\bar{V} + q_3](1 + K_{qf}\Delta f) \end{aligned} \tag{4.2}$$

where:

$\bar{V} = V/V_0$ and $\Delta f = f - f_0$

P, Q	- active, reactive components of load corresponding to bus voltage magnitude V
P_0, Q_0	- initial values of active, reactive power
a, b,	- parameters of the exponential function
p_1, p_2, p_3	- coefficients of active power, ZIP model
q_1, q_2, q_3	- coefficients of reactive power, ZIP model
f	- frequency
V_0, f_0	- initial values of bus voltage magnitude and frequency
K_{pf}, K_{qf}	- active power, reactive power frequency dependency

If the parameters a and b are equal to 0, 1, or 2, the model represents constant power, constant current, or constant impedance characteristics, respectively. The coefficients p_1, p_2, and p_3 (q_1, q_2, and q_3) in the ZIP model define the proportion of constant impedance (Z), constant current (I), and constant power (P) components respectively. For example, for an active load composed of 50% constant Z, 20% constant I, and 30% constant P, p_1, p_2, and p_3 would be equal to 0.5, 0.2, and 0.3 respectively.

The load models available in MatNetEig ignore the effects of frequency deviation but the other four tools consider them. The static load models available in each tool are given in Table 4.2.

4.2 Rotor angle reference

If the system matrix is defined in terms of absolute rotor speed and angle deviations, one or two zero eigenvalues result if the system has no infinite bus model. One of the zero eigenvalues appears due to lack of uniqueness of absolute rotor angles. The second zero eigenvalue appears if all generator torques are assumed to be independent of speed deviations [7,49,83]. Due to round-off errors in the calculation of the $\boldsymbol{A}$ matrix and mismatches in the load flow solution, the zero eigenvalues may not be computed exactly and they appear as modes near the origin with a positive real part whose magnitude is small. To eliminate the zero eigenvalues, one of the generators can be chosen as a reference and the angle and speed deviations of all the other machines are measured with respect to this reference. The relative values become the new state variables replacing the absolute ones. The system order reduces by one.

4.3 Numerical methodology

4.3.1 Construction of the A matrix

As discussed in Chapter 2, the methods used by the tools for constructing the $\boldsymbol{A}$ matrix are numerical differentiation and analytical differentiation. PSS/E and PowerFactory use numerical differentiation whereas EUROSTAG, SSAT, and MatNetEig use analytical differentiation.

PSS/E employs the one-sided difference method. The program requires, from the user, to specify the perturbation size, h. The magnitude of h should be small enough to ensure correct linear approximation but it should not be too

small to cause numerical instability. A typical value of h is 10^{-4}.

PowerFactory employs the central difference scheme and the perturbation is fixed at 10^{-3} by the vendor.

4.3.2 Computation of eigenvalues

The five tools investigated in this thesis use the QR algorithm for computing the eigenvalues of the $\boldsymbol{A}$ matrix [9, 52].

SSAT uses the implicitly restarting Arnoldi method (IRAM) to compute eigenvalues of the system within specified frequency and damping ranges [9]. Furthermore, this tool uses enhanced AESOPS algorithm to compute a mode(s) that are most dominant in a specified generator.

4.4 Software flexibility

4.4.1 Data input

The five tools have graphical user interface (GUI). Through this interface, system data are entered using data-input windows. In PSS/E, SSAT, and MatNetEig, the user can also introduce data in text format.

4.4.2 Data output

The five tools give eigenvalue results. In addition, PSS/E, SSAT, and MatNetEig give the frequency of oscillatory modes and the damping ratio.

Accessibility to the system matrices is important for controller design and parameter setting e.g. PSS and AVR. The $\boldsymbol{B}$ and $\boldsymbol{C}$ matrices are of interest

in the formulation of the mode controllability and observability matrices. PSS/E, SSAT, and MatNetEig allow the user access to $\boldsymbol{A}$, $\boldsymbol{B}$, $\boldsymbol{C}$, and $\boldsymbol{D}$ matrices, EUROSTAG only allows access to the $\boldsymbol{A}$ matrix and PowerFactory does not allow access to any of the matrices.

The eigenvectors and participation factors are important for placement of power system support devices. PSS/E, SSAT, and MatNetEig give the normalized complex right eigenvectors from which the user can deduce local area and inter-area electromechanical modes of oscillations. These tools also give the normalized participation factors (magnitude only) for all the system modes. In addition, MatNetEig gives the left eigenvectors and the normalized complex participation factors. PowerFactory gives the participation factors of generator state variables only i.e. the tool does not give the participation factors of state variables associated with controllers and other system equipment. EUROSTAG gives neither eigenvectors nor participation factors; users have to determine the electromechanical modes using other programs.

Table 4.2 summarizes the comparison of the features and capabilities of the five simulation tools.

Table 4.2: Summary of software comparison

FEATURE		TOOL				
		PSS/E	**PowerFactory**	**EUROSTAG**	**SSAT**	**MatNetEig**
Components models	***Available generator models, order of complexity***	2^{nd}, 3^{rd}, 5^{th}, 6^{th}, 7^{th}, 8^{th}	5^{th},6^{th}	3^{rd},5^{th},6^{th}	2^{nd}, 5^{th},6^{th}, 8^{th}	2^{nd},5^{th},6^{th}
	Generator model representation	Operational impedance [2]	Coupled-circuit	Coupled-circuit	Coupled-circuit	Coupled-circuit
	Saturation representation	Effective excitation	Total saturation	Total saturation	Total or incremental saturation	Total saturation
	Turbine output	P_m	P_m	T_m	P_m or T_m	T_m
	Speed voltage terms	$\omega_r = 1$ [3]	$\omega_r \neq 1$	$\omega_r \neq 1$	$\omega_r = 1$	$\omega_r = 1$
	Infinite bus	Classical generator, H = 0	*AC voltage source* or *external grid*	Constant voltage source	Classical generator, H = 0	Classical generator
	Static load models	Exponential and *ZIP*	Exponential	Exponential	Exponential and *ZIP*	Exponential
Numerical methodology	***Construction of A matrix***	Numerical differentiation, one-sided difference	Numerical differentiation, central difference	Analytical differentiation	Analytical differentiation	Analytical differentiation
	Perturbation size	User specified	10^{-3}	*N/A*	*N/A*	*N/A*
	Eigenvalues computation	*QR*	*QR*	*QR*	*QR*	*QR*
Tool flexibility	***Data input***	GUI with data input windows or text	GUI with data input windows	GUI with data input windows	GUI with data input windows and text	GUI with data input windows or text
	Accessible system matrices	*A, B, C, D*	None	*A*	*A, B, C, D*	*A, B, C, D*
	Eigenvectors	Right only	Not available	Not available	Right only	Right and left
	Participation factors	Available	Available	Not available	Available	Available

[2] 7^{th} and 8^{th} order models are represented using coupled–circuit method

[3] $\omega_r \neq 1$ for 7^{th} and 8^{th} order models

4.5 Summary

The features and capabilities of the five industrial-grade simulation tools have been compared. The main criteria used for comparison are components modeling, numerical methodology, and tool flexibility. PSS/E has the widest variety of generator models ranging from 2^{nd} (classical) to 8^{th} order. This tool represents generator saturation using effective excitation method whereas the other four tools use total saturation method. In addition, SSAT has incremental saturation method. PSS/E, PowerFactory, and SSAT model the turbine output as P_m whereas EUROSTAG and MatNetEig model it as T_m. Additionally, SSAT models the turbine output as T_m. EUROSTAG and PowerFactory consider rotor speed deviation in the speed voltage terms whereas PSS/E, SSAT, and MatNetEig neglect it. Both PSS/E and PowerFactory use numerical differentiation for constructing the $\boldsymbol{A}$ matrix whereas EUROSTAG, SSAT, and MatNetEig use analytical differentiation. A PSS/E user has to specify the perturbation size whereas in PowerFactory, the perturbation size is fixed by the vendor at 10^{-3}. All the five tools have graphical user interface and data entry is by data input windows. MatNetEig gives the most data output.

Chapter 5

Investigation methods and procedure

Components modeling and numerical methodology used by the five tools were first studied and variations in modeling of generator saturation, speed voltage terms, and turbine output were identified. It was also found that the tools use different techniques for constructing the $\boldsymbol{A}$ matrix. The impact of these variations on the electromechanical modes were investigated using two power systems.

To be able to closely monitor the impact of the variations on local modes, the single machine infinite bus (SMIB) system was chosen, for its simplicity, as the first power system. The two-area four-generator (2A4G) system was chosen as the second power system. This system was used to investigate the impact of the identified factors on the inter-area modes.

Each power system was developed from a simple case with the generator(s) on manual control to full model representation with the excitation system(s) controlled by automatic voltage regulator (AVR) with power system stabilizer (PSS), and speed governor control. The effect of each controller on the

electromechanical modes was analyzed.

In this chapter, the procedure for investigating the impact of the variations in modeling and numerical methodology used by the five industrial-grade tools is outlined.

5.1 Simulation tools

As mentioned in Chapter 1, the simulation tools investigated in this thesis are as shown in Table 5.1. The academic/research institutions versions of the programs were used for the research. The investigation pertains to small-signal stability application.

Table 5.1: The investigated industrial-grade simulation tools

Tool	Company
PSS/E	Power Technologies International
PowerFactory	DIgSILENT GmbH
EUROSTAG	Tractebel Energy Engineering
SSAT	PowerTech Labs Inc
MatNetEig	Cherry Tree Scientific Software

5.2 Description of the power systems

5.2.1 SMIB system

Figure 5.1 shows the SMIB system given in [7]. Generator G1 was represented using a 6^{th} order model. System data are given in Appendix B, Section B.1.

Owing to its simplicity, the SMIB system was used to study the impact of

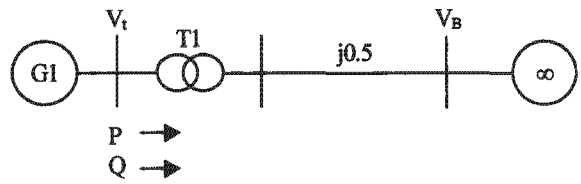

Figure 5.1: SMIB system

variations among the tools in generator modeling on the local modes.

5.2.2 2A4G system

Figure 5.2 shows the 2A4G system. The system consists of two similar areas, connected by a weak tie-line. Each area has two generators; G1 and G2 in area 1, and G3 and G4 in area 2. All four generators were represented using 6^{th} order models. Power transfer from area 1 to area 2 of 400 MW was considered.

The loads were represented using static models. The active components of the loads were modeled as constant current and the reactive components as constant impedance.

System data are given in Appendix B, Section B.2. The lengths of the transmission lines are shown in Fig.5.2.

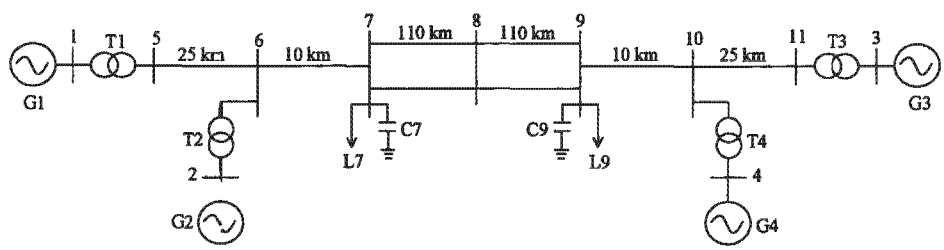

Figure 5.2: 2A4G system

The system has three electromechanical modes; two local plant modes, and

one inter-area modes. In reference [84], the authors note that although small, the parameters and structure of the 2A4G system are realistic. From their experience with large interconnected systems, the authors of [84] express confidence that the general conclusions drawn from the work on the two-area system could be applied to large systems.

5.3 Turbo-generator controllers

The following excitation system and prime mover control configurations were used.

(i) Excitation system control and constant prime mover output

  (a) Manual excitation control

  (b) AVR without PSS

  (c) AVR with PSS

(ii) Excitation system control and speed governor control

  (a) Manual excitation control and speed governor

  (b) AVR without PSS, and speed governor

  (c) AVR with PSS, and speed governor.

The 1981 IEEE type AC4 excitation system model, and an IEEE PSS model responding to the shaft speed of its designated generator as its only input, were used with the five tools. The simplified block diagram of this generator excitation system is shown in Fig. B.1 in Appendix B, Section B.1. The PSS model used for the SMIB system had one lead-lag block as in [7]. The

excitation system input data are given in Appendix B, sections B.1 and B.2 for the SMIB and 2A4G system, respectively.

The IEEEG1 model — the IEEE recommended general model for steam turbine speed governing systems [11,85,86] — was used for the investigation. The simplified block diagram of the turbine-governor set is shown in Fig. B.2 in Appendix B, Section B.1. The input data for the turbine-governor set, used for the two power systems, are given in the same section.

5.4 Investigation of variations among the tools

The following modeling and algorithmic factors were identified as possible causes of the discrepancies in results:

(i) Turbo-generator modeling

  (a) generator saturation

  (b) speed voltage terms

  (c) turbine output

(ii) Method used for constructing the $\boldsymbol{A}$ matrix.

The impact of the above factors on the electromechanical modes were investigated as described in the following sections.

5.4.1 Effect of generator saturation

The effect on the electromechanical modes of the three methods of representing the effect of saturation – total saturation, incremental saturation, and

effective excitation – used by simulation tools was investigated. Total saturation and incremental saturation methods are applicable to machine models represented using coupled-circuit method, and effective excitation method is for machine models represented using the operational-impedance method. As mentioned in Chapter 3, the coupled-circuit method assumes that only the mutual inductances are affected by saturation, whereas the operational-impedance method assumes that both mutual and leakage inductances are affected. The effect of the assumptions made by the two methods of machine model representation was also investigated.

Out of the five tools investigated in this thesis, only SSAT allows representation of saturation effects using either total or incremental saturation method; only PSS/E represents the generator using the operational-impedance method. Therefore, SSAT was chosen to investigate the effect on electromechanical modes of total and incremental saturation methods and PSS/E for effective excitation method. For each of the three excitation system configurations given in Section 5.3, simulations were run both with saturation neglected and with saturation included.

PSS/E allows the user to represent the 6^{th} order model using either coupled-circuit or operational-impedance methods. This tool was used to investigate the discrepancies in results caused by variations in the two methods. GENROU model (6^{th} order) was used to investigate the operational-impedance method and CGEN1 model (8^{th} order) for the coupled-circuit method. In PSS/E, saturation is modeled using total saturation method for the coupled-circuit method, whereas for operational-impedance method, saturation is modeled using effective excitation method. For the purpose of this study, CGEN1 model was reduced to an equivalent 6^{th} order model as described

in [11]. The basic parameters used with CGEN1 were calculated using the equations given in [11]. The data are given in Appendix B, sections B.1 and B.2 for the SMIB and the 2A4G systems, respectively.

5.4.2 Effect of speed voltage terms

In Chapter 3, it was highlighted that rotor speed deviation is neglected in speed voltage terms to counterbalance the effect of neglecting stator transients. The five tools investigated in this thesis neglect stator transients but only three tools – PSS/E, SSAT, and MatNetEig – neglect the effect of speed deviation on stator voltage. EUROSTAG and PowerFactory consider speed deviation and do not allow the user the flexibility to neglect it. Therefore, a technique that utilizes the $\boldsymbol{A}$ matrix was developed for neglecting the effect of speed deviation. Since the $\boldsymbol{A}$ matrix in PowerFactory is not accessible, EUROSTAG was chosen for this purpose.

A software for eliminating the effect of speed deviation was developed using MATLAB. The $\boldsymbol{A}$ matrix obtained with EUROSTAG was modified and the eigenvalues of the resultant matrix were computed. The following illustration shows the modification of the $\boldsymbol{A}$ matrix obtained for the SMIB system with the generator on manual excitation control and constant prime mover output.

The $\boldsymbol{A}$ matrix obtained from EUROSTAG (with the effect of speed deviation considered) is in the form given in Chapter 3 as

$$\begin{pmatrix} \Delta\dot{\psi}_{fd} \\ \Delta\dot{\psi}_{1d} \\ \Delta\dot{\psi}_{1q} \\ \Delta\dot{\psi}_{2q} \\ \Delta\dot{\omega}_r \\ \Delta\dot{\delta} \end{pmatrix} = \begin{pmatrix} a_{11} & a_{12} & a_{13} & a_{14} & a_{15} & a_{16} \\ a_{21} & a_{22} & a_{23} & a_{24} & a_{25} & a_{26} \\ a_{31} & a_{32} & a_{33} & a_{34} & a_{35} & a_{36} \\ a_{41} & a_{42} & a_{43} & a_{44} & a_{45} & a_{46} \\ a_{51} & a_{52} & a_{53} & a_{54} & a_{55} & a_{56} \\ 0 & 0 & 0 & 0 & \omega_0 & 0 \end{pmatrix} \begin{pmatrix} \Delta\psi_{fd} \\ \Delta\psi_{1d} \\ \Delta\psi_{1q} \\ \Delta\psi_{2q} \\ \Delta\omega_r \\ \Delta\delta \end{pmatrix}$$

To neglect the effect of speed deviation, elements $a_{15} - a_{45}$ in column 5 were set to zero as explained in Chapter 3. Element a_{55} was set to $-K_D/2H$.

Similar modifications were done for the matrix obtained with excitation system controlled by AVR without PSS. The same alterations were performed for the 2A4G system.

The $\boldsymbol{A}$ matrix obtained from EUROSTAG for excitation system controlled by AVR with PSS is in the form (5.1).

$$\begin{pmatrix} \Delta\dot{\psi}_{fd} \\ \Delta\dot{\psi}_{1d} \\ \Delta\dot{\psi}_{1q} \\ \Delta\dot{\psi}_{2q} \\ \Delta\dot{\omega}_r \\ \Delta\dot{\delta} \\ \Delta\dot{v}_1 \\ \Delta\dot{v}_2 \\ \Delta\dot{v}_s \end{pmatrix} = \begin{pmatrix} a_{11} & a_{12} & a_{13} & a_{14} & a_{15} & a_{16} & a_{17} & a_{18} & a_{19} \\ a_{21} & a_{22} & a_{23} & a_{24} & a_{25} & a_{26} & a_{27} & a_{28} & a_{29} \\ a_{31} & a_{32} & a_{33} & a_{34} & a_{35} & a_{36} & a_{37} & a_{38} & a_{39} \\ a_{41} & a_{42} & a_{43} & a_{44} & a_{45} & a_{46} & a_{47} & a_{48} & a_{49} \\ a_{51} & a_{52} & a_{53} & a_{54} & a_{55} & a_{56} & a_{57} & a_{58} & a_{59} \\ 0 & 0 & 0 & 0 & \omega_0 & 0 & 0 & 0 & 0 \\ a_{71} & a_{72} & a_{73} & a_{74} & a_{75} & a_{76} & a_{77} & a_{78} & a_{79} \\ a_{81} & a_{82} & a_{83} & a_{84} & a_{85} & a_{86} & a_{87} & a_{88} & a_{89} \\ a_{91} & a_{92} & a_{93} & a_{94} & a_{95} & a_{96} & a_{97} & a_{98} & a_{99} \end{pmatrix} \begin{pmatrix} \Delta\psi_{fd} \\ \Delta\psi_{1d} \\ \Delta\psi_{1q} \\ \Delta\psi_{2q} \\ \Delta\omega_r \\ \Delta\delta \\ \Delta v_1 \\ \Delta v_2 \\ \Delta v_s \end{pmatrix} \quad (5.1)$$

The simplified block diagram of the excitation system that was used for the research is shown in Fig. B.1 in Appendix B, Section B.1. The input signal to the PSS is shaft speed deviation. The output of the signal washout block and the phase compensation block (one lead-lag block was used for the SMIB power system) are functions of speed; the perturbed outputs of these blocks (Δv_2 and Δv_s) are state variables. This means that the field voltage and hence the field flux linkage is also a function of speed. Thus, it was not possible to isolate the effect of considering rotor speed deviation in the stator voltage calculation in element a_{15} in (5.1).

5.4.3 Effect of turbine output

The turbine output is modeled differently by the five tools investigated in this thesis. Only SSAT allows the user to choose between the two turbine outputs i.e. mechanical torque T_m, and mechanical power P_m. Thus, this tool was found suitable for the investigation.

A SSAT user chooses the *Solution Option for Generator Swing Equation* as either *Torque* or *Power*. For the two solution options, the swing equation is expressed as shown in (3.23) given in Chapter 3 and it is repeated here for reference.

$$\dot{\omega}_r = \frac{1}{2H}\left(T_m - T_e - K_D\Delta\omega_r\right)$$

For the two solution options, the turbine output is P_m. For the *Torque* option, speed deviation is considered in the mechanical power-torque relationship ($T_m = P_m/\omega_r \ pu$) whereas for *Power* option, speed deviation is neglected ($T_m = P_m \ pu$). With the swing equation expressed as (3.23), it follows that the *Torque* and *Power* options correspond to P_m and T_m turbine output, as discussed in Chapter 3, Section 3.3.

For each of the three excitation control configurations, two cases were simulated; with P_m turbine output and with T_m turbine output. For each case, two sets of results were obtained: (i) with constant prime mover output and (ii) with speed governor control.

5.4.4 Effect of method used for constructing the A matrix

As discussed in Chapter 2, numerical differentiation introduces truncation errors in the computation of the $\boldsymbol{A}$ matrix. Thus an investigation was done to establish the discrepancy in electromechanical modes results caused by the method used for constructing the $\boldsymbol{A}$ matrix.

SSAT and PSS/E which employ analytical differentiation and numerical differentiation, respectively were used for the investigation. For both tools, the 8^{th} order generator model CGEN1 was used; the two tools represent this model using coupled-circuit method (the two tools represent other models using different methods) and the input data are in basic-parameter format i.e. the programs do not have to compute the basic parameters (resistances and inductances) from standard parameters (transient and sub-transient inductances and time constants). The generator was modeled with manual excitation control and saturation was neglected. For both tools, the turbine output was P_m.

A perturbation of 10^{-4} was used with PSS/E. The effect of speed deviation on stator voltage is considered for the CGEN1 model in PSS/E. This effect was eliminated from the $\boldsymbol{A}$ matrix obtained with PSS/E as described in Section 5.4.2.

It should be noted that it was not possible to investigate the impact of the linearization schemes used in PSS/E (one-sided difference) and PowerFactory (central difference) since there are modeling differences between the two tools which could not be isolated.

Perturbation size

As shown in Chapter 2, the accuracy to which the $\boldsymbol{A}$ matrix is computed using numerical differentiation depends on the perturbation size. The effect of perturbation size on the electromechanical modes was investigated using PSS/E with the generator on manual excitation control. The perturbation size was varied from 10^{-6} to 10^{-1}.

5.5 Cases simulated for comparison of results

The two power systems were simulated for the three excitation control configurations using the five tools and the results compared. For each power system, two sets of results were obtained using EUROSTAG and SSAT; one set for T_m turbine output and the other set for P_m turbine output. This was done to improve the qualitative analysis of the results. For example, out of the five tools, only EUROSTAG and PowerFactory consider the effect of speed deviation in stator voltage calculation. However, EUROSTAG employs T_m turbine output whereas PowerFactory employs P_m turbine output and considers speed deviation in the mechanical power-torque relationship i.e. $P_m \neq T_m\ pu$. Thus, the results obtained with the two tools cannot be effectively compared unless the modeling of the turbine output is the same. Therefore, a turbine model was defined in EUROSTAG for realizing $T_m = P_m/\omega_r$ output. The macroblock for this user defined model is shown in Fig. B.3, Appendix B.

To assess the discrepancies in results for different excitation control configurations, each power system was simulated with manual excitation control, automatic excitation control without PSS and with PSS. To investigate the

effect on the results of the saturation model used by each tool, two sets of simulations were run with each of the three excitation system configurations: (i) with saturation included and (ii) with saturation neglected. Saturation parameters $S_{1.0}$ and $S_{1.2}$ were computed as described in Section 3.1. All the cases were simulated with constant prime mover output. Each simulation was run using the five tools. A total of sixty simulations were run.

More cases were simulated to assess the effect of speed governor control on the results. Each power system was simulated for the three excitation control configurations with saturation neglected, using the four tools – PSS/E, PowerFactory, EUROSTAG, and SSAT. MatNetEig does not have in its standard library, the IEEEG1 turbine-governor model used in the study. Hence this tool was excluded from these investigations. A total of twenty four simulations were run.

5.6 Electromechanical modes sensitivity

In Chapter 2, the need to verify the robustness of eigenvalues in relation to system parameters was highlighted. To ascertain that the discrepancies in results obtained in the investigation of the impact of tools variations were not due to ill-conditioning of the $\boldsymbol{A}$ matrix, the sensitivity of the electromechanical modes in relation to the elements of the $\boldsymbol{A}$ matrix were evaluated. To accomplish this task, a software was developed using MATLAB for evaluating the relative (logarithmic) sensitivity of the electromechanical modes.

For all the investigated cases, the relative sensitivities were less than 1. Thus it was confirmed that for all the investigated cases, the $\boldsymbol{A}$ matrix was well conditioned. Some eigenvalue sensitivities are given in Appendix D.

5.7 Summary

The techniques and procedure for investigating the impact of variations in components modeling and numerical methodology have been described. The factors that were investigated include generator saturation and machine model representation, speed voltage terms, turbine output, construction of the $\boldsymbol{A}$ matrix, and perturbation size. Eighty four simulations were run for comparison of the five tools with different controller configurations.

The simulation results are presented in Chapter 6.

Chapter 6

Simulation results and discussion

The investigation of the variations among the five industrial-grade tools was carried out using two power systems:

- The single machine infinite bus (SMIB) system
- The two-area four-generator (2A4G) system.

In this chapter, eigenvalue results obtained using PSS/E, PowerFactory, EUROSTAG, SSAT, and MatNetEig are presented. The chapter has two main sections divided according to the power system models. Each power system model was simulated with three excitation control configurations:

- manual excitation control
- automatic excitation control without PSS
- automatic excitation control with PSS.

Each excitation control configuration was simulated with generator saturation included and with saturation neglected. All the cases were simulated

with constant prime mover output i.e. mechanical torque T_m or mechanical power P_m, is constant. Each simulation was run using the five tools. In total, sixty simulations were run.

In addition to the above simulations that were all run with constant prime mover output, more cases were simulated with speed governor control. Each power system was simulated for the three excitation control configurations with saturation neglected, and using four tools. MatNetEig was excluded from these investigations because it does not have the IEEEG1 turbine-governor model used in the study in its standard library. A total of twenty four simulations were run. Figure 6.1 gives a summary of the simulated cases.

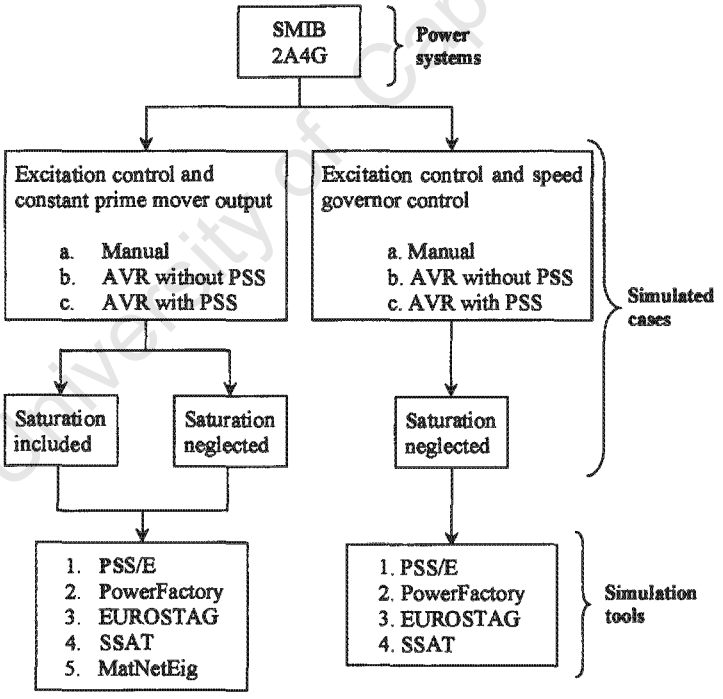

Figure 6.1: Summary of the simulated cases

The results obtained using EUROSTAG are labeled EURO(T) or EURO(P) for results obtained with T_m or P_m turbine output, respectively. The results

obtained using SSAT are labeled in parenthesis T or P for T_m or P_m turbine output and t or i for total or incremental saturation representation, respectively. Results obtained using PowerFactory and MatNetEig are labeled PF and MNE, respectively.

For ease of reference, Table 6.1 gives a summary of the components modeling and numerical methodologies used by the five tools investigated in this thesis.

Table 6.1: Summary of components modeling and numerical methodologies used by five industrial-grade tools

Tool	Saturation	Speed voltage terms	Turbine output	Construction of $\boldsymbol{A}$ matrix
PSS/E	Effective excitation	ψ	P_m	Numerical differentiation
PowerFactory	Total	$\omega_r\psi$	P_m	Numerical differentiation
EUROSTAG	Total	$\omega_r\psi$	T_m or P_m[1]	Analytical differentiation
SSAT	Total or incremental	ψ	T_m or P_m	Analytical differentiation
MatNetEig	Total	ψ	T_m	Analytical differentiation

The amount of output data for all the investigated cases is quite voluminous. Since the local modes and inter-area modes are of prime interest in small-signal stability studies, only the results of these modes are presented.

6.1 SMIB system

6.1.1 Impact of tools' variations on local modes

After critical review of the five tools' user manuals [9–13], variations in the following components modeling and algorithmic factors were identified:

[1]User defined for comparison

- generator saturation
- speed voltage terms
- turbine output
- the techniques used by the tools for the construction of the state matrix.

The information from the manuals was supplemented by direct communication with the vendors. Thus, some of the information presented in this thesis is not documented in the tools' user manuals.

Results showing the effect on the local modes, of variations in the modeling and algorithmic factors mentioned above are presented and discussed in the following subsections.

6.1.1.1 Effect of saturation

SSAT and PSS/E were used to investigate the effect of saturation modeling on the local modes. The results are given in Table 6.2.

Table 6.2: Effect of saturation on local modes

Excitation control	Saturation representation				
	SSAT			PSS/E	
	Neglected	Total	Incremental	Neglected	Effective excitation
Manual	$-0.268 \pm j6.421$ f = 1.022 Hz $\zeta = 4.17$ %	$-0.272 \pm j6.414$ f = 1.021 Hz $\zeta = 4.24$ %	$-0.241 \pm j6.461$ f = 1.028 Hz $\zeta = 3.73$ %	$-0.269 \pm j6.418$ f = 1.021 Hz $\zeta = 4.18$ %	$-0.276 \pm j6.396$ f = 1.018 Hz $\zeta = 4.31$ %
AVR without PSS	$+0.507 \pm j7.444$ f = 1.185 Hz $\zeta = -6.79$ %	$+0.426 \pm j7.393$ f = 1.177 Hz $\zeta = -5.75$ %	$+0.459 \pm j7.384$ f = 1.175 Hz $\zeta = -6.21$ %	$+0.505 \pm j7.437$ f = 1.184 Hz $\zeta = -6.78$ %	$+0.424 \pm j7.337$ f = 1.168 Hz $\zeta = -5.77$ %
AVR with PSS	$-1.198 \pm j6.745$ f = 1.073 Hz $\zeta = 17.5$ %	$-1.188 \pm j6.695$ f = 1.066 Hz $\zeta = 17.5$ %	$-1.146 \pm j6.752$ f = 1.075 Hz $\zeta = 16.7$ %	$-1.193 \pm j6.745$ f = 1.073 Hz $\zeta = 17.4$ %	$-1.149 \pm j6.719$ f = 1.069 Hz $\zeta = 16.9$ %

Table 6.3 shows the percentage change in damping ($\Delta\sigma$), frequency (Δf), and damping ratio ($\Delta\zeta$) of the local modes caused by saturation. The percentage change is evaluated according to (6.1).

$$\Delta k = \frac{k_s - k_u}{k_u} \times 100 \tag{6.1}$$

where k is σ, f, or ζ and subscripts s and u denote results obtained with saturation included and with saturation neglected, respectively. A positive value of Δk signifies an increase, and a negative value signifies a decrease. The local modes are unstable for excitation controlled by AVR without PSS (positive real part and negative damping ratio). Thus, a decrease in the magnitude of the real part and damping ratio signifies an increase in damping and damping ratio, respectively.

Table 6.3: Percentage (%) change in local modes caused by saturation

Excitation control	SSAT						PSS/E		
	Total			Incremental			Effective excitation		
	$\Delta\sigma$	Δf	$\Delta\zeta$	$\Delta\sigma$	Δf	$\Delta\zeta$	$\Delta\sigma$	Δf	$\Delta\zeta$
Manual	1.5	-0.1	1.7	-10.0	0.6	-10.6	2.6	-0.3	3.1
AVR without PSS	16.0	-0.7	15.3	9.5	-0.8	8.5	16.0	-1.3	14.9
AVR with PSS	-0.8	-0.7	0.0	-4.3	0.1	-4.6	-3.7	-0.4	-2.9

Tables 6.2 and 6.3 show that the three methods of representing generator saturation have little effect on the frequency for the three excitation control configurations. The following discussion focuses on the damping ratio since it captures both damping and frequency.

Manual excitation control

For manual excitation control, the damping ratio obtained with total saturation and effective excitation methods is higher than that obtained with

saturation neglected; the damping ratio obtained with the incremental saturation method is lower than that obtained with the saturation neglected. However, for total saturation and effective excitation methods, the effect of saturation on the local modes can be considered to be negligible.

Excitation controlled by AVR without PSS

For excitation controlled by AVR without PSS, the damping ratio obtained with each of the three methods of representing saturation is higher than that obtained with the saturation neglected. The increase in damping ratios obtained with total saturation and effective excitation methods are very similar. The incremental saturation method has less impact on the damping ratio than the other two methods.

Excitation controlled by AVR with PSS

For excitation controlled by AVR with PSS, the damping ratio obtained with incremental saturation and effective excitation methods is lower than that obtained with saturation neglected. However, for the total saturation method, the damping ratio is not affected by saturation; both the damping and frequency decrease by similar percentages, thus effectively leaving the damping ratio unchanged.

It is not clear why the saturation modeled using the three methods has different effects on the local modes for different excitation control configurations. For instance, saturation modeled using the incremental saturation method causes the damping ratio to decrease for manual excitation control and for excitation controlled by AVR with PSS, whereas it has the opposite effect for excitation controlled by AVR without PSS.

It is also not clear why, for manual excitation control, saturation modeled using the incremental saturation method causes the damping ratio to decrease, whereas other methods cause the damping ratio to increase. For all excitation control configurations, generator saturation reduces the values of both d and q axes inductances of round-rotor machines. Therefore, the general effect of saturation on the local modes is expected to be similar for the three excitation control configurations.

The effect of the method used for representing the generator model cannot be deduced by comparing the results obtained with SSAT (coupled-circuit) and PSS/E (operational-impedance), since there are other differences between the two tools. Therefore, PSS/E was used to investigate the effect of variations in the two methods of representing the generator model on the local modes. The results are given in Table 6.4. These results were obtained with the generator on manual excitation control.

Table 6.4: Effect of generator model representation on local modes

Model representation	Coupled–circuit method	Operational impedance method
Saturation neglected	$-0.269 \pm j6.407$ f = 1.020 Hz $\zeta = 4.19$ %	$-0.269 \pm j6.418$ f = 1.021 Hz $\zeta = 4.18$ %
Saturation included	$-0.270 \pm j6.459$ f = 1.028 Hz $\zeta = 4.18$ %	$-0.277 \pm j6.394$ f = 1.018 Hz $\zeta = 4.34$ %

The discrepancies in damping $\Delta\sigma$, frequency Δf, and damping ratio $\Delta\zeta$ are quantified according to (6.2), as shown in Table 6.5.

$$\Delta k = \frac{k_{oi} - k_{cc}}{k_{cc}} \times 100 \tag{6.2}$$

where k is σ, f, or ζ and subscripts oi and cc denote results obtained with

operational-impedance and coupled-circuit methods, respectively.

Table 6.5: Percentage (%) change in local modes caused by variations in model representation

Saturation	$\Delta\sigma$	Δf	$\Delta\zeta$
Neglected	0.0	0.2	-0.2
Included	2.6	-1.0	3.8

The two methods give similar results with saturation neglected, as can be seen from tables 6.4 and 6.5. However, with saturation included, some discrepancies are observed. These observations agree with the literature [17]. The discrepancies in results obtained with the two methods of representing the generator model are due to variation in the representation of saturation; i.e. the coupled-circuit method assumes saturation affects only the mutual inductance, whereas the operational-impedance method assumes saturation affects both mutual and leakage inductances.

For practical purposes, the discrepancies in results caused by variation in model representation can be considered to be negligible. Therefore, it can be concluded that saturation modeled using the total saturation method and the effective excitation method give similar results.

Since the effect of saturation has been investigated in the previous section, for the following investigations saturation will be neglected.

6.1.1.2 Effect of speed voltage terms

The MATLAB code that was developed for modifying the $\boldsymbol{A}$ matrix does not introduce significant discrepancies in the eigenvalue results; therefore the results agree. This conclusion was drawn after comparing the eigenvalues

obtained directly from EUROSTAG (with rotor speed deviation considered in speed voltage terms) with those obtained using the MATLAB code from the raw $\boldsymbol{A}$ matrix extracted from EUROSTAG.

Table 6.6 gives the results obtained using EUROSTAG with speed deviation considered in speed voltage terms and with speed deviation neglected, for two excitation control configurations. For the excitation system controlled by AVR with PSS, the effect of speed voltage terms on the local modes was not investigated. This investigation could not be carried out using the technique employed for the other two excitation control configurations, due to the limitation, explained in Chapter 5, of isolating the effect of rotor speed deviation from the $\boldsymbol{A}$ matrix.

Table 6.6: Effect of speed voltage terms on local modes

Excitation control	Rotor speed deviation	
	Considered	Neglected
Manual	$-0.192 \pm j6.398$ f = 1.018 Hz $\zeta = 3.00$ %	$-0.210 \pm j6.399$ f = 1.018 Hz $\zeta = 3.28$ %
AVR without PSS	$+0.641 \pm j7.384$ f = 1.175 Hz $\zeta = -8.65$ %	$+0.558 \pm j7.428$ f = 1.182 Hz $\zeta = -7.48$ %

Table 6.7 gives the percentage increase in damping ($\Delta\sigma$), frequency (Δf), and damping ratio ($\Delta\zeta$) of the local modes caused by neglecting speed deviation in speed voltage terms, computed using (6.3).

$$\Delta k = \frac{k_{devn} - k_{devc}}{k_{devc}} \times 100 \tag{6.3}$$

where k is σ, f, or ζ and subscripts *devn* and *devc* denote results obtained with rotor speed deviation neglected and with rotor speed deviation considered, respectively.

Table 6.7: Percentage (%) increase in local modes caused by neglecting rotor speed deviation

Excitation control	$\Delta\sigma$	Δf	$\Delta\zeta$
Manual	9.4	0.02	9.3
AVR without PSS	12.9	0.6	13.5

Tables 6.6 and 6.7 show that for each of the two excitation control configurations, the modeling of speed voltage terms has an insignificant effect on the frequency, and both the damping and the damping ratio increase by about the same percentage. Thus, although the following discussion refers to the damping ratio, it also applies to the damping.

The damping ratio obtained with speed deviation neglected is higher than that obtained with the speed deviation considered as observed from Table 6.6. It can also be observed from Table 6.7 that the increase in the damping ratio is higher with excitation controlled by AVR without PSS than with manual excitation control. These results agree with [45], where it is stated that significant error in the excitation system output could result if the speed effect is neglected.

In Chapter 3, it was stated that if rotor speed deviation is considered, the damping torque coefficient K_5 in (3.26) can be either negative or positive depending on the parameters of the machine, the external network, and the operating condition. The damping of the local modes obtained with a negative value of K_5 is lower than that obtained with the speed deviation neglected (i.e. $K_5 = 0$), whereas that obtained with a positive value is higher. Therefore, it can be deduced from the results of Table 6.6 that for the operating condition considered, K_5 is negative since the damping obtained with speed deviation considered is lower than that obtained with speed deviation

neglected.

For the SMIB system studied, a positive value of K_5 can be obtained if the generator is lightly loaded and the network resistance is considered. An example of such a scenario with the generator operating at 0.1 *pu* active power, is given in Appendix C, Section C.1. For this operating condition, K_5 is negative if the network resistance is neglected and positive if included. It is observed from these results that for negative K_5, the damping of the local modes is lower than that obtained for positive K_5.

Since the input to the excitation system is the generator terminal voltage, the effect of speed voltage terms for excitation controlled by AVR with PSS is expected to be similar to that observed for excitation controlled by AVR without PSS i.e. higher damping and damping ratio are obtained with speed deviation neglected than with speed deviation considered.

6.1.1.3 Effect of turbine output

Table 6.8 gives results obtained using SSAT with T_m and P_m turbine output, with different controller configurations.

Table 6.8: Effect of turbine output on the local modes

Controllers		Turbine output	
		T_m	P_m
Constant prime mover output	Manual	$-0.203 \pm j6.421$ f = 1.022 Hz $\zeta = 3.17$ %	$-0.268 \pm j6.421$ f = 1.022 Hz $\zeta = 4.17$ %
	AVR without PSS	$+0.567 \pm j7.440$ f = 1.184 Hz $\zeta = -7.60$ %	$+0.507 \pm j7.444$ f = 1.185 Hz $\zeta = -6.79$ %
	AVR with PSS	$-1.146 \pm j6.763$ f = 1.076 Hz $\zeta = 16.7$ %	$-1.198 \pm j6.745$ f = 1.073 Hz $\zeta = 17.5$ %
Speed governor control	Manual	$-0.129 \pm j6.443$ f = 1.026 Hz $\zeta = 2.00$ %	$-0.192 \pm j6.444$ f = 1.026 Hz $\zeta = 2.98$ %
	AVR without PSS	$+0.614 \pm j7.452$ f = 1.186 Hz $\zeta = -8.21$ %	$+0.554 \pm j7.456$ f = 1.187 Hz $\zeta = -7.41$ %
	AVR with PSS	$-1.078 \pm j6.782$ f = 1.080 Hz $\zeta = 15.7$ %	$-1.129 \pm j6.764$ f = 1.077 Hz $\zeta = 16.5$ %

Table 6.9 shows the percentage change in damping ($\Delta\sigma$), frequency (Δf), and damping ratio ($\Delta\zeta$) of the local modes caused by variation in modeling of turbine output. The percentage change is computed using (6.4).

$$\Delta k = \frac{k_{Pm} - k_{Tm}}{k_{Tm}} \times 100 \tag{6.4}$$

where k is σ, f, or ζ and subscripts Pm and Tm denote results obtained with P_m and T_m turbine output, respectively.

Table 6.9: Percentage (%) change in local modes caused by variation in turbine output

Controllers		$\Delta\sigma$	Δf	$\Delta\zeta$
Constant prime mover output	Manual	32.0	0.0	31.5
	AVR without PSS	10.6	0.1	10.7
	AVR with PSS	4.5	-0.3	4.8
Speed governor control	Manual	48.8	0.0	49.0
	AVR without PSS	9.8	0.1	9.7
	AVR with PSS	4.7	-0.3	5.1

In Chapter 3, it was shown analytically that P_m turbine output "adds" damping to the system. The results given in Table 6.8 corroborate this finding; the damping obtained with P_m turbine output is higher than that obtained with T_m turbine output. This observation is true both for constant prime mover output and for speed governor control.

It can be seen from Table 6.9 that for all the three excitation control configurations, the frequency is marginally affected by the modeling of the turbine output and both the damping and the damping ratio increase by almost the same percentage. Therefore, in the following discussion reference is made to the damping ratio but the discussion also applies to the damping.

For both the constant prime mover output and the speed governor control, the increase in damping ratio is highest for manual excitation control and lowest for excitation controlled by AVR with PSS, as can be observed from Table 6.9. This observation can be attributed to the fact that the damping due to the excitation system is much higher than the damping "added" by P_m turbine output.

6.1.1.4 Effect of method used for constructing the A matrix

Table 6.10 gives the results obtained using analytical (SSAT) and numerical (PSS/E) differentiation techniques for constructing the A matrix. These results show that the method used for constructing the A matrix has little effect on the local modes. The discrepancies in damping, frequency, and damping ratio obtained with the two techniques are less than 1%.

Table 6.10: Effect of method used for constructing the A matrix on local modes

Analytical differentiation	Numerical differentiation
$-0.268 \pm j6.421$	$-0.269 \pm j6.407$
f = 1.022 Hz	f = 1.020 Hz
$\zeta = 4.16$	$\zeta = 4.19$

Figures 6.2 and 6.3 show the loci and the damping ratio of the local modes, respectively for perturbation varied from 10^{-6} to 10^{-1}.

It can be seen from figures 6.2 and 6.3 that there is numerical instability if the perturbation size is too small i.e. less than about 5×10^{-5}. The system is numerically stable for perturbation ranging between 5×10^{-5} and 10^{-2} . The results obtained with perturbation chosen within this range are close to those obtained with tools employing analytical differentiation.

For large perturbation (greater than 10^{-2}), the frequency is arbitrarily low, whereas the damping is marginally affected, thus causing the damping ratio to increase as seen in Fig. 6.3. As explained in Chapter 2, large perturbation gives inaccurate results because the truncation error is high.

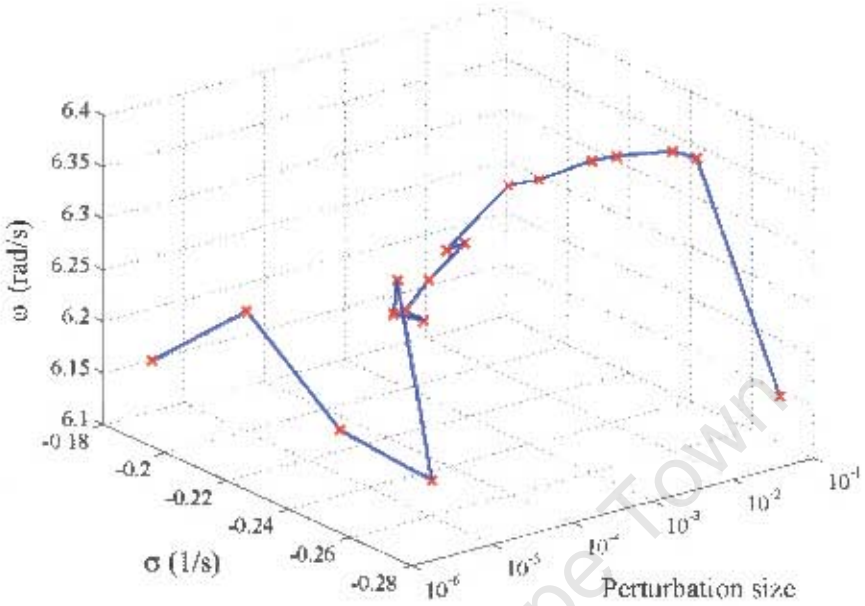

Figure 6.2: Effect of perturbation size on the loci of the local modes in the upper complex plane

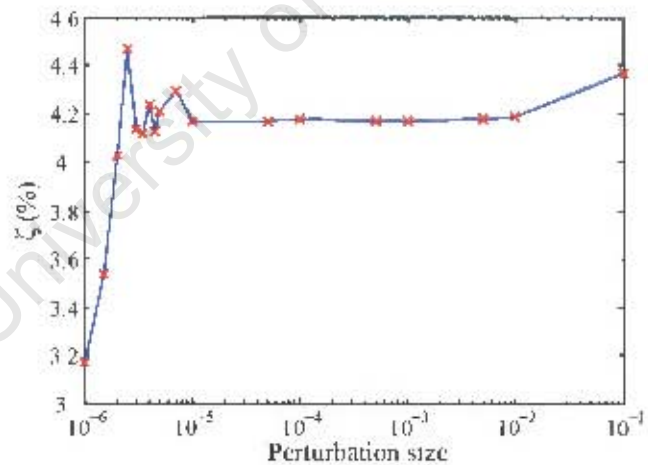

Figure 6.3: Effect of perturbation size on the damping ratio of the local modes

6.1.2 Comparison of results

6.1.2.1 Excitation control

In this subsection, the results obtained with the five tools – PSS/E, PowerFactory, EUROSTAG, SSAT, and MatNetEig – are presented. These results were obtained with three excitation control configurations i.e. manual, AVR without PSS, and AVR with PSS, and constant prime mover output. For each excitation control configuration, two sets of results were obtained; one set with saturation included and the other set with saturation neglected. The results are given in Table 6.11.

Table 6.11: Local modes results obtained with five industrial-grade tools

Tool	Saturation neglected			Saturation included		
	Manual	AVR without PSS	AVR with PSS	Manual	AVR without PSS	AVR with PSS
PSS/E	$-0.269 \pm j6.418$ f = 1.021 Hz $\zeta = 4.18$ %	$+0.505 \pm j7.437$ f = 1.184 Hz $\zeta = -6.78$ %	$-1.198 \pm j6.745$ f = 1.073 Hz $\zeta = 17.4$ %	$-0.276 \pm j6.396$ f = 1.018 Hz $\zeta = 4.31$ %	$+0.424 \pm j7.337$ f = 1.168 Hz $\zeta = -5.77$ %	$-1.149 \pm j6.719$ f = 1.069 Hz $\zeta = 16.9$ %
SSAT(P-i)	$-0.268 \pm j6.421$ f = 1.022 Hz $\zeta = 4.17$ %	$+0.507 \pm j7.444$ f = 1.185 Hz $\zeta = -6.79$ %	$-1.198 \pm j6.745$ f = 1.073 Hz $\zeta = 17.5$ %	$-0.272 \pm j6.414$ f = 1.021 Hz $\zeta = 4.24$ %	$+0.426 \pm j7.393$ f = 1.177 Hz $\zeta = 5.75$ %	$-1.188 \pm j6.695$ f = 1.066 Hz $\zeta = 17.5$ %
PF	$-0.271 \pm j6.405$ f = 1.019 Hz $\zeta = 4.23$ %	$+0.579 \pm j7.391$ f = 1.176 Hz $\zeta = -7.81$ %	$-1.107 \pm j6.714$ f = 1.069Hz $\zeta = 16.3$ %	$-0.265 \pm j6.415$ f = 1.021 Hz $\zeta = 4.13$ %	$+0.562 \pm j7.292$ f = 1.161 Hz $\zeta = -7.68$ %	$-1.201 \pm j6.752$ f = 1.075Hz $\zeta = 17.5$ %
EURO(P)	$-0.257 \pm j6.398$ f = 1.018 Hz $\zeta = 4.02$ %	$+0.581 \pm j7.389$ f = 1.175 Hz $\zeta = -7.84$ %	$-1.111 \pm j6.708$ f = 1.068 Hz $\zeta = 16.3$ %	$-0.258 \pm j6.404$ f = 1.019 Hz $\zeta = 4.02$ %	$+0.567 \pm j7.282$ f = 1.159 Hz $\zeta = -7.76$ %	$-1.195 \pm j6.726$ f = 1.070 Hz $\zeta = 17.5$ %
SSAT(P-i)	$-0.268 \pm j6.421$ f = 1.022 Hz $\zeta = 4.17$ %	$+0.507 \pm j7.444$ f = 1.185 Hz $\zeta = -6.79$ %	$-1.198 \pm j6.745$ f = 1.073 Hz $\zeta = 17.5$ %	$-0.241 \pm j6.461$ f = 1.028Hz $\zeta = 3.73$ %	$-0.459 \pm j7.384$ f = 1.175 Hz $\zeta = -6.21$ %	$-1.146 \pm j6.752$ f = 1.075 Hz $\zeta = 16.7$ %
SSAT(T-i)	$-0.203 \pm j6.421$ f = 1.022 Hz $\zeta = 3.17$ %	$+0.567 \pm j7.440$ f = 1.184 Hz $\zeta = -7.60$ %	$-1.146 \pm j6.763$ f = 1.076 Hz $\zeta = 16.7$ %	$0.207 \pm j6.414$ f = 1.021 Hz $\zeta = 3.23$ %	$+0.487 \pm j7.380$ f = 1.176 Hz $\zeta = -6.57$ %	$-1.135 \pm j6.712$ f = 1.068 Hz $\zeta = 16.7$ %
MNE	$-0.203 \pm j6.425$ f = 1.022 Hz $\zeta = 3.16$ %	$+0.570 \pm j7.871$ f = 1.173 Hz $\zeta = -7.72$ %	$-1.138 \pm j6.744$ f = 1.073 Hz $\zeta = 16.6$ %	$0.201 \pm j6.432$ f = 1.024 Hz $\zeta = 3.13$ %	$+0.541 \pm j7.278$ f = 1.158 Hz $\zeta = -7.41$ %	$-1.204 \pm j6.793$ f = 1.081 Hz $\zeta = 17.5$ %
EURO(T)	$-0.192 \pm j6.398$ f = 1.018 Hz $\zeta = 3.00$ %	$+0.611 \pm j7.384$ f = 1.175 Hz $\zeta = -8.65$ %	$-1.059 \pm j6.725$ f = 1.070 Hz $\zeta = 15.6$ %	$-0.193 \pm j6.403$ f = 1.019 Hz $\zeta = 3.01$ %	$+0.627 \pm j7.279$ f = 1.158 Hz $\zeta = -8.58$ %	$-1.142 \pm j6.744$ f = 1.073 Hz $\zeta = 16.7$ %
SSAT(T-i)	$-0.203 \pm j6.421$ f = 1.022 Hz $\zeta = 3.17$ %	$+0.567 \pm j7.440$ f = 1.184 Hz $\zeta = -7.60$ %	$-1.146 \pm j6.763$ f = 1.076 Hz $\zeta = 16.7$ %	$-0.177 \pm j6.461$ f = 1.028 Hz $\zeta = 2.74$ %	$+0.529 \pm j7.381$ f = 1.175 Hz $\zeta = -7.03$ %	$-1.092 \pm j6.769$ f = 1.077Hz $\zeta = 15.9$ %

Table 6.12 gives the percentage change in damping $\Delta\sigma$, frequency Δf, and damping ratio $\Delta\zeta$ of the local modes caused by saturation. The percentage change Δk (where k is σ, f or ζ) is evaluated using (6.1) with results obtained with saturation neglected taken as reference. A positive value of Δk signifies an increase and a negative value signifies a decrease.

The results given in tables 6.11 and 6.12 are discussed below.

Table 6.12: Percentage (%) change in local modes caused by saturation; results obtained with five industrial-grade tools

Tool	manual excitation control			AVR without PSS			AVR with PSS		
	$\Delta\sigma$	Δf	$\Delta\zeta$	$\Delta\sigma$	Δf	$\Delta\zeta$	$\Delta\sigma$	Δf	$\Delta\zeta$
PSS/E	2.6	-0.3	3.1	16.0	-1.3	14.9	-3.7	-0.4	-2.9
SSAT(P-t)	1.5	-0.1	1.7	16.0	-0.7	15.3	-0.8	-0.7	0.0
PF	-2.2	0.2	-2.4	2.9	-1.3	1.7	8.5	0.6	7.4
EURO(P)	0.4	0.1	0.0	2.4	-1.4	1.0	7.6	0.3	7.4
SSAT(P-i)	-10.1	0.6	-10.6	9.5	-0.8	8.5	-4.3	0.1	-4.6
SSAT(T-t)	2.0	-0.1	1.9	14.1	-0.7	13.6	-1.0	-0.8	0.0
MNE	-1.0	0.1	-0.9	5.1	-1.3	4.0	5.8	0.7	5.4
EURO(T)	0.5	0.1	0.3	2.2	-1.4	0.8	7.8	0.3	7.1
SSAT(T-i)	-12.8	0.6	-13.6	8.3	-0.8	7.5	-4.7	0.1	-4.8

A. Manual excitation control

Figure 6.4 shows the loci of the local modes in the upper complex plane for manual excitation control, with saturation included and with saturation neglected. Figure 6.5 shows the corresponding damping ratios.

The results obtained with the five tools show that the local modes are stable, both with saturation included and with saturation neglected, as seen from figures 6.4 and 6.5. It can also be observed, from Table 6.12 column 3, that saturation has very little effect on the frequency.

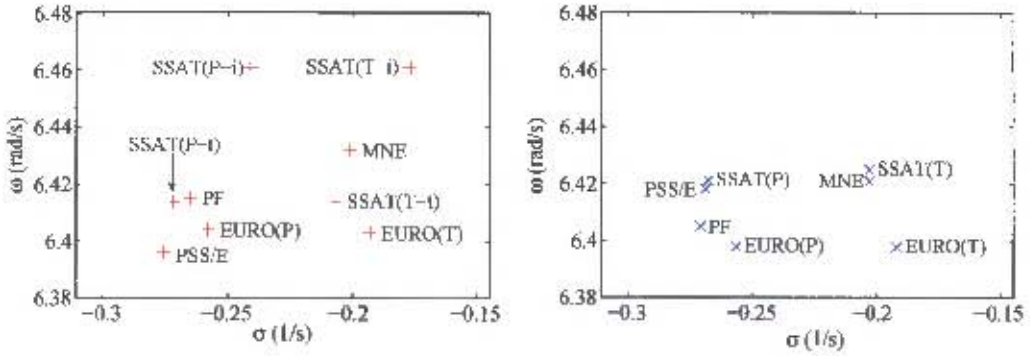

(a) Saturation included (b) Saturation neglected

Figure 6.4: Loci of the local modes in the upper complex plane; manual excitation control

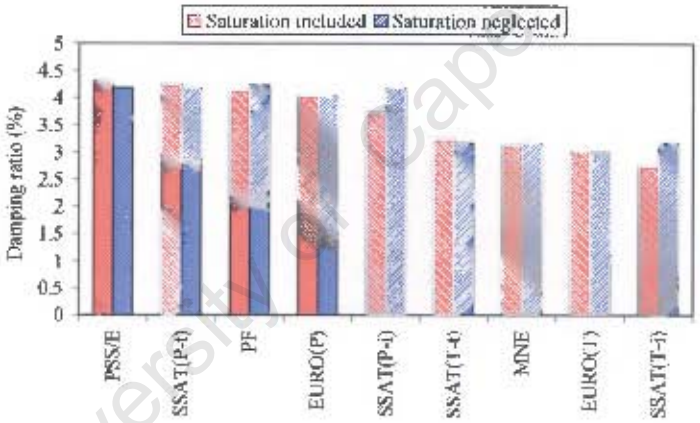

Figure 6.5: Effect of saturation on the damping ratio of local modes; manual excitation control

It can be seen from Table 6.12 column 2- 4 that total saturation (PowerFactory, EUROSTAG, SSAT(t), and MatNetEig) and effective excitation (PSS/E) methods have little effect on the results. It can also be seen that compared with other methods of representing saturation, incremental saturation (SSAT(i)) has the greatest impact on the local modes. The results obtained with saturation modeled using this method have a lower damping ratio than those obtained with saturation neglected. Indeed, it can be seen

from Fig. 6.5 that with saturation included, the damping ratio obtained with SSAT(T-i) is below 3 %. As mentioned in Chapter 2, damping is often considered adequate if the damping ratio of the electromechanical modes is in the range 3 to 5%. Therefore, the results obtained with SSAT(T-i) predict an unsatisfactory damping ratio, whereas those obtained with all the other tools predict a satisfactory damping ratio. These results underscore the fact that different conclusions can be drawn for the same power system from results obtained with different tools.

The damping ratio obtained with tools that employ P_m turbine output (SSAT(P), PowerFactory, EUROSTAG(P), and PSS/E) is higher than that obtained with tools that employ T_m turbine output (SSAT(T), MatNetEig, and EUROSTAG(T)) both with saturation included and with saturation neglected, as seen from Fig. 6.5. In addition, it can be seen from Fig. 6.4 that with saturation neglected, the results obtained using EUROSTAG with P_m and T_m turbine output are more conservative[2] than those obtained using the other tools that employ similar turbine output i.e. SSAT(P), PowerFactory, EUROSTAG(P), and PSS/E for P_m and SSAT(T), MatNetEig, and EUROSTAG(T) for T_m. This observation may be attributed to the fact that EUROSTAG considers rotor speed deviation in the stator voltage calculation, which reduces damping as illustrated in Section 6.1.1. However, the results obtained using PowerFactory with saturation neglected contradict this observation; indeed these results are the most optimistic[3]. One possible cause is the fact that PowerFactory considers the change in system frequency in network equations [52] whereas all the other tools neglect it. For a better understanding of these results, there is a need for further investigation into

[2]The real part is closer to the imaginary axis
[3]Real part furthest from the imaginary axis

the effect of considering change in system frequency on local modes.

B. AVR without PSS

Figure 6.6 shows the loci of the local modes in the upper complex plane for excitation controlled by AVR without PSS, with saturation included and with saturation neglected. Figure 6.7 shows the corresponding damping ratios.

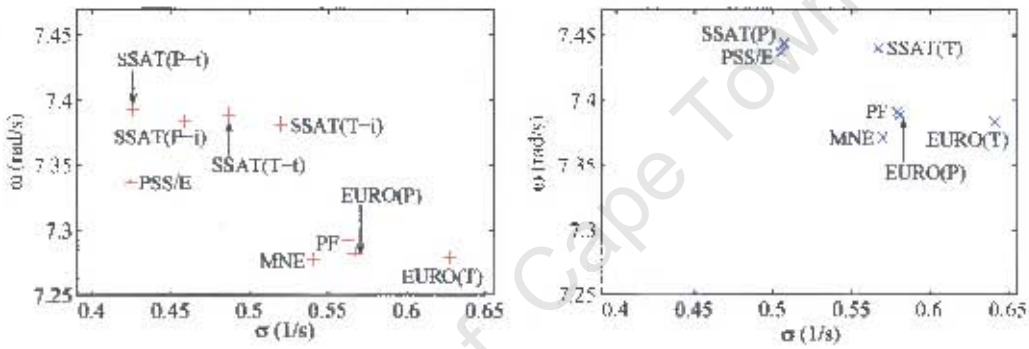

(a) Saturation included (b) Saturation neglected

Figure 6.6: Loci of the local modes in the upper complex plane; AVR without PSS

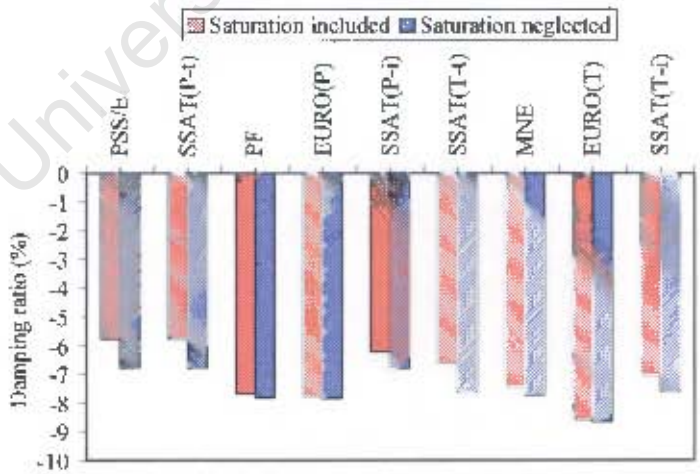

Figure 6.7: Effect of saturation on the damping ratio of local modes; AVR without PSS

The AVR introduces negative damping and hence the local modes are unstable (the loci of the local modes are on the right hand side of the complex plane and the damping ratio is negative), as can be seen from figures 6.6 and 6.7. Since the modes are unstable, a decrease in the real part signifies an increase in damping. Similarly, a decrease in the magnitude of the damping ratio signifies improved damping.

For all the five tools, the results obtained with saturation included have higher damping (and damping ratio) and lower frequency than those obtained with saturation neglected, as seen from Table 6.12 column 5–7. However, the decrease in the frequency is marginal. It can be observed from Table 6.12 and Fig. 6.7 that saturation has least impact (least percentage change in damping) on results obtained with the tools that consider speed deviation in stator voltage calculation – EUROSTAG and PowerFactory. Moreover, the highest impact of saturation is observed for results obtained with PSS/E and SSAT(t). The impact of saturation on results obtained with MatNetEig is moderate.

It can be seen from Fig. 6.6(b) that with saturation neglected, the results obtained with the tools that consider rotor speed deviation in speed voltage terms (EUROSTAG and PowerFactory) are the most conservative. These results agree with those presented in Section 6.1.1 i.e. for the operating condition considered, the inclusion of speed deviation reduces damping.

The results obtained with the tools that employ P_m turbine output are more optimistic than those obtained with tools that employ T_m turbine output, and with similar modeling of speed voltage terms. For example, results obtained with SSAT(P) and PSS/E (these two tools employ P_m turbine output and neglect speed deviation) are more optimistic than those obtained

with SSAT(T) and MatNetEig (these two tools employ T_m turbine output and neglect speed deviation). This observation confirms the finding of the investigation in Section 6.1.1 that P_m turbine output "adds" damping to the system.

C. AVR with PSS

Figure 6.8 shows the loci of the local modes in the upper complex plane for excitation controlled by AVR with PSS, with saturation included and with saturation neglected. Figure 6.9 shows the corresponding damping ratios.

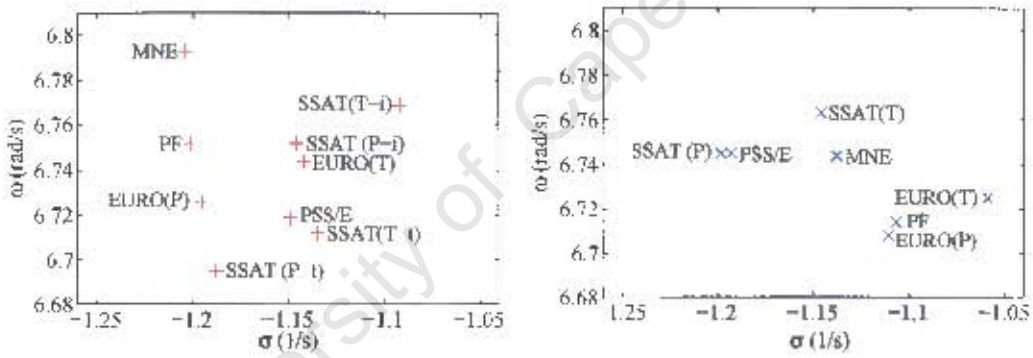

(a) Saturation included

(b) Saturation neglected

Figure 6.8: Loci of the local modes in the upper complex plane; AVR with PSS

Comparing with the results obtained for excitation controlled by AVR without PSS, the addition of PSS results in increased damping and thus the stabilization of the local modes. Saturation affects the results obtained with different tools differently, as can be seen from figures 6.8 and 6.9. The results obtained with EUROSTAG, PowerFactory, and MatNetEig have a higher damping ratio with saturation included than with saturation neglected. On the contrary, the results obtained with PSS/E and SSAT(i) have a lower damping ratio with saturation included than with saturation neglected. In

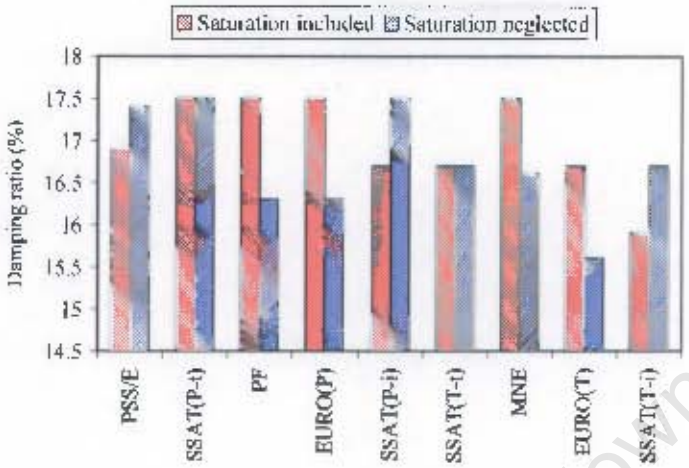

Figure 6.9: Effect of saturation on the damping ratio of local modes; AVR with PSS

addition, SSAT's total saturation model has no effect on the damping ratio. For all the five tools, saturation has little effect on the frequency as seen from Table 6.12 column 9.

Comparing figures 6.8(a) and 6.8(b), with saturation included, the effect of speed voltage terms on EUROSTAG and PowerFactory results is not apparent. In contrast, with saturation neglected, it is clear from Fig. 6.8(b) that the results obtained using EUROSTAG and PowerFactory are the most conservative. It is also clear that the results obtained with tools that employ P_m turbine output are more optimistic than those obtained with tools that employ T_m turbine output, and with similar modeling of speed voltage terms. For example, results obtained with EUROSTAG(P) and PowerFactory (these two tools employ P_m turbine output and consider speed deviation) are more optimistic than those obtained with EUROSTAG(T) (this tool employs T_m turbine output and considers speed deviation).

6.1.2.2 Excitation and prime mover control

The results presented in this subsection were obtained with different excitation control configurations and speed governor control, with saturation neglected. The results obtained for constant prime mover output are included for comparison purposes. The results obtained with the four tools – PSS/E, PowerFactory, EUROSTAG, and SSAT – are given in Table 6.13.

Table 6.13: Effect of speed governor on local mode

Tool	Speed governor control			Constant prime mover output		
	Manual	AVR without PSS	AVR with PSS	Manual	AVR without PSS	AVR with PSS
PF	$-0.195 \pm j6.428$ f = 1.023 Hz $\zeta = 3.03$ %	$-0.626 \pm j7.404$ f = 1.178 Hz $\zeta = -8.42$ %	$-1.040 \pm j6.735$ f = 1.072Hz $\zeta = 15.3$ %	$-0.271 \pm j6.405$ f = 1.019 Hz $\zeta = 4.23$ %	$+0.579 \pm j7.391$ f = 1.176 Hz $\zeta = -7.81$ %	$-1.107 + j6.714$ f = 1.069Hz $\zeta = 16.3$ %
PSS/E	$-0.193 \pm j6.440$ f = 1.025 Hz $\zeta = 2.99$ %	$+0.557 \pm j7.454$ f = 1.186 Hz $\zeta = -7.45$ %	$-1.125 \pm j6.764$ f = 1.077 Hz $\zeta = 16.4$ %	$-0.269 \pm j6.418$ f = 1.021 Hz $\zeta = 4.18$ %	$+0.505 \pm j7.437$ f = 1.184 Hz $\zeta = -6.78$ %	$-1.193 \pm j6.745$ f = 1.073 Hz $\zeta = 17.4$ %
SSAT(P)	$-0.192 + j6.444$ f = 1.026 Hz $\zeta = 2.98$ %	$+0.554 \pm j7.456$ f = 1.187 Hz $\zeta = -7.41$ %	$-1.129 \pm j6.764$ f = 1.077 Hz $\zeta = 16.5$ %	$-0.268 + j6.421$ f = 1.022 Hz $\zeta = 4.17$ %	$+0.507 \pm j7.444$ f = 1.185 Hz $\zeta = -6.79$ %	$-1.198 \pm j6.745$ f = 1.073 Hz $\zeta = 17.5$ %
EURO(P)	$-0.181 \pm j6.421$ f = 1.022 Hz $\zeta = 2.82$ %	$+0.628 \pm j7.402$ f = 1.178 Hz $\zeta = -8.45$ %	$-1.044 + j6.729$ f = 1.071 Hz $\zeta = 15.3$ %	$-0.257 \pm j6.398$ f = 1.018 Hz $\zeta = 4.02$ %	$+0.581 \pm j7.389$ f = 1.175 Hz $\zeta = -7.84$ %	$-1.111 + j6.708$ f = 1.068 Hz $\zeta = 16.3$ %
SSAT(T)	$-0.129 + j6.443$ f = 1.026 Hz $\zeta = 2.00$ %	$+0.614 \pm j7.452$ f = 1.186 Hz $\zeta = -8.21$ %	$-1.078 + j6.782$ f = 1.080 Hz $\zeta = 15.7$ %	$-0.203 \pm j6.421$ f = 1.022 Hz $\zeta = 3.17$ %	$+0.567 \pm j7.440$ f = 1.184 Hz $\zeta = -7.60$ %	$-1.146 \pm j6.763$ f = 1.076 Hz $\zeta = 16.7$ %
EURO(T)	$-0.117 + j6.421$ f = 1.022 Hz $\zeta = 1.83$ %	$+0.687 \pm j7.398$ f = 1.177 Hz $\zeta = -9.25$ %	$-0.993 \pm j6.746$ f = 1.074 Hz $\zeta = 14.6$ %	$-0.192 + j6.398$ f = 1.018 Hz $\zeta = 3.00$ %	$+0.641 \pm j7.384$ f = 1.175 Hz $\zeta = -8.65$ %	$-1.059 \pm j6.725$ f = 1.070 Hz $\zeta = 15.6$ %

The percentage change in damping ($\Delta\sigma$), frequency (Δf), and damping ratio ($\Delta\zeta$) of the local modes caused by the speed governor, evaluated according to (6.5), is given in Table 6.14.

$$\Delta k = \frac{k_{gov} - k_{const}}{k_{const}} \times 100 \tag{6.5}$$

where k is σ, f, or ζ and subscripts *gov* and *const* denote results obtained with speed governor control and constant prime mover output, respectively. A positive value of Δk signifies an increase and a negative value signifies a decrease.

The discussion of tables 6.14 and 6.13 is given below.

Table 6.14: Percentage (%) change in local modes caused by speed governor

Tool	Manual excitation control			AVR without PSS			AVR with PSS		
	$\Delta\sigma$	Δf	$\Delta\zeta$	$\Delta\sigma$	Δf	$\Delta\zeta$	$\Delta\sigma$	Δf	$\Delta\zeta$
PF	-28.0	0.4	-28.4	-8.1	0.2	-7.8	-6.1	0.3	-6.1
PSS/E	-28.3	0.3	-28.5	-10.3	0.2	-9.9	-5.7	0.3	-5.7
SSAT(P)	-28.4	0.4	-28.5	-9.3	0.2	-9.1	-5.8	0.3	-5.7
EURO(P)	-29.6	0.4	-29.9	-8.1	0.2	-7.8	-6.0	0.3	-6.1
SSAT(T)	-36.5	0.3	-36.9	-8.3	0.2	-8.0	-5.9	0.3	-6.0
EURO(T)	-39.1	0.4	-39.0	-7.2	0.2	-6.9	-6.2	0.3	-6.4

A. Manual excitation control and governor

It can be seen from Table 6.13 column 2, that with manual excitation and speed governor control, the results obtained using the four tools predict that the local modes are stable. These results agree on the frequency of the oscillations; the difference between the highest (SSAT(P)) and the lowest (EUROSTAG(P)) value is less than 0.5%. However, results obtained with PowerFactory, EUROSTAG(P), PSS/E, and SSAT(P), rounded-off to the nearest whole number, predict a satisfactory damping ratio ($\zeta \geq 3\%$), whereas

those obtained with EUROSTAG(T) and SSAT(T) predict an unsatisfactory damping ratio. These results emphasize the fact that different conclusions can be drawn for the same power system from results obtained with different tools. The difference in damping between the highest (PowerFactory) and the lowest (EUROSTAG(T)) value is over 40%.

Figure 6.10 shows the loci of the local modes in the upper complex plane for manual excitation control, with constant prime mover output and with speed governor control. Figure 6.11 shows the corresponding damping ratios.

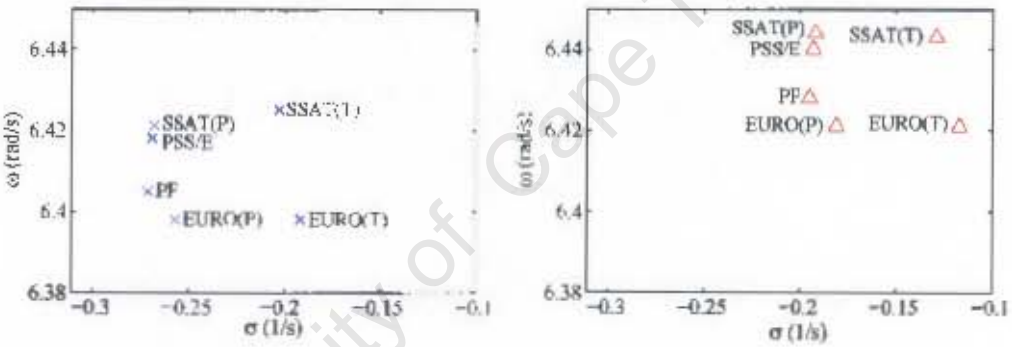

(a) Constant prime mover output (b) Speed governor control

Figure 6.10: Loci of the local modes in the upper complex plane; manual excitation control

The addition of the speed governor results in increased frequency and decreased damping as can be seen from Table 6.14 column 2–4 and Fig. 6.10. The net effect of these changes is a decrease in the damping ratio as can be observed from Fig. 6.11. The speed governor adds negative damping to the system, thus reducing the damping of the local modes. For all the tools, the damping ratio decreases by at least 28 % and the increase in frequency is marginal (less than 1%).

It can be observed from Fig. 6.10 that the results obtained with the tools

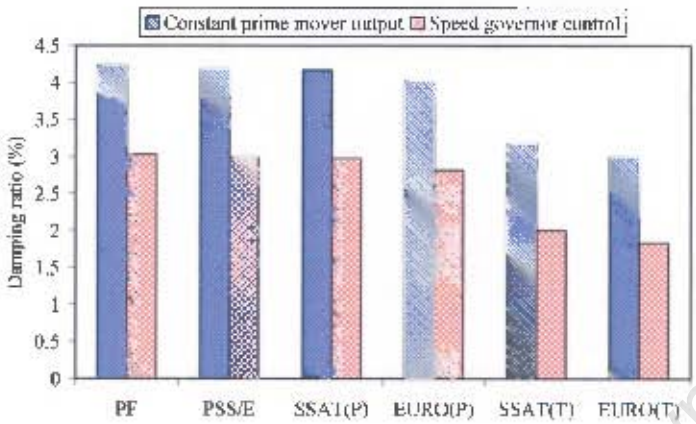

Figure 6.11: Effect of governor on the damping ratio of local modes; manual excitation control

that employ P_m turbine output (SSAT(P), PSS/E, PowerFactory, and EUROSTAG(P)) are more optimistic than those obtained with tools that employ T_m turbine output (SSAT(T) and EUROSTAG(T)), for both constant prime mover output and speed governor control. These results confirm that P_m turbine output "adds" damping to the system.

B. AVR without PSS, and governor

It can be seen from Table 6.13 column 3 that for excitation controlled by AVR without PSS, and with speed governor control, the results obtained using the four tools predict the local modes are unstable. Both the AVR and the governor introduce negative damping thus rendering the modes unstable. These results agree on the frequency of the oscillations; the difference between the highest (SSAT(P)) and the lowest (EUROSTAG(T)) values is less than 1%. The difference in damping between the highest (SSAT(P)) and the lowest (EUROSTAG(T)) value is over 19%.

Figure 6.12 shows the loci of the local modes in the upper complex plane

with excitation controlled by AVR without PSS, with constant prime mover output and with speed governor control. Figure 6.13 shows the corresponding damping ratios.

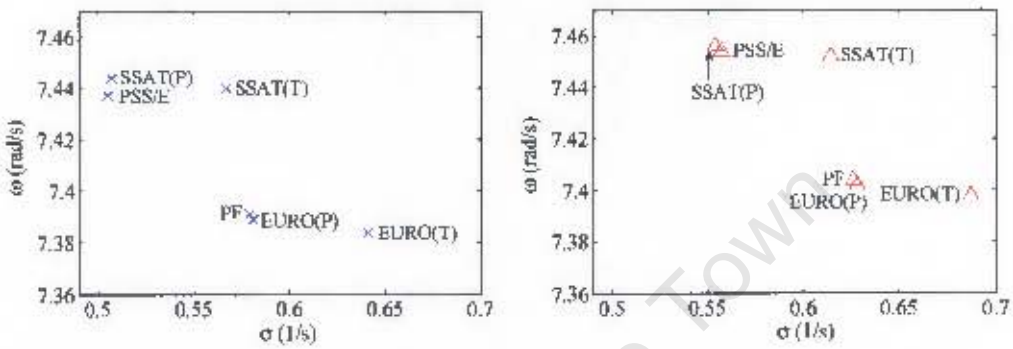

(a) Constant prime mover output (b) Speed governor control

Figure 6.12: Loci of the local modes in the upper complex plane; AVR without PSS

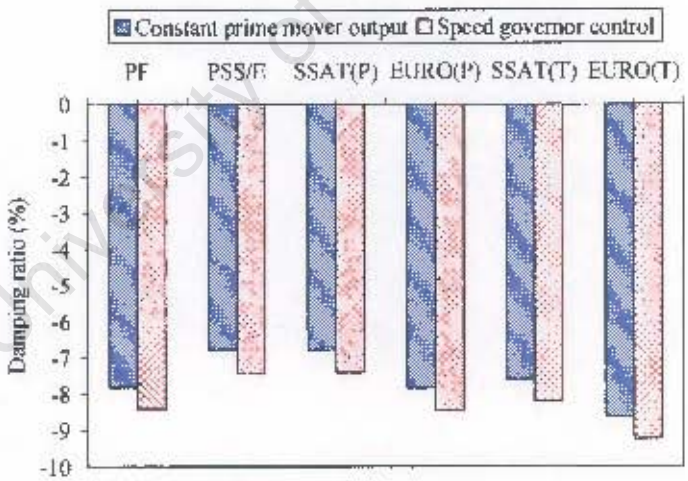

Figure 6.13: Effect of governor on the damping ratio of local modes; AVR without PSS

When figures 6.12(a) and 6.12(b) are compared, it can be seen that the addition of the speed governor causes an increase in frequency and a decrease in the damping of the local modes. However, for all the tools, the increase

in frequency is marginal (0.2%), as can be seen from Table 6.14 column 6.

It can be observed from Fig. 6.12 that the effect of the speed governor is to shift the loci of the local modes to the right and it does not affect the characteristics related to the modeling of speed voltage terms and turbine output observed and discussed earlier for constant prime mover output.

C. AVR with PSS, and governor

It can be seen from Table 6.13 column 4 that for excitation controlled by AVR with PSS, and with speed governor control, the results obtained using the four tools predict the local modes are stable. These results agree on the frequency of the oscillations; the difference between the highest (SSAT(P)) and the lowest (EUROSTAG(P)) value is less than 1%. The difference in damping between the highest (SSAT(P)) and the lowest (EUROSTAG(T)) value is over 12%.

Figure 6.14 shows the loci of the local modes in the upper complex plane for excitation controlled by AVR with PSS, with constant prime mover output and with speed governor control. Figure 6.15 shows the corresponding damping ratios.

As observed for the other excitation control configurations, the speed governor introduces negative damping as can be seen from figures 6.14 and 6.15. It can be observed from Table 6.14 column 8, that the percentage decrease in damping caused by the addition of the speed governor is almost uniform for all the tools and the frequency increases by 0.3%. The characteristics related to the modeling of speed voltage terms and turbine output are the same for speed governor control as for constant prime mover output.

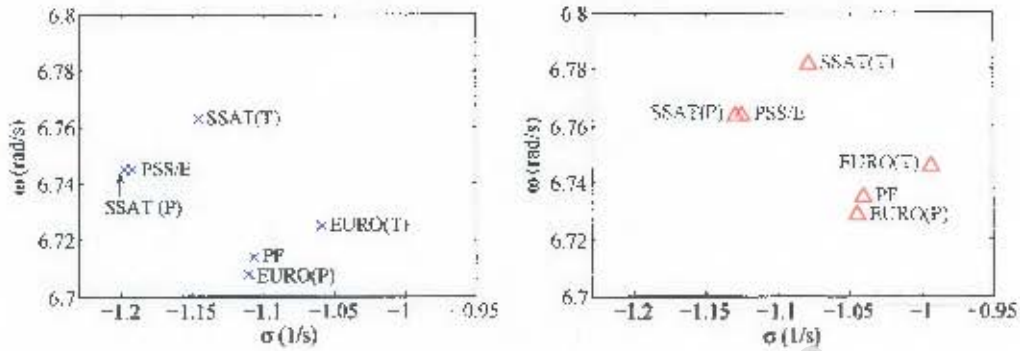

(a) Constant prime mover output (b) Speed governor control

Figure 6.14: Loci of the local modes in the upper complex plane; AVR with PSS

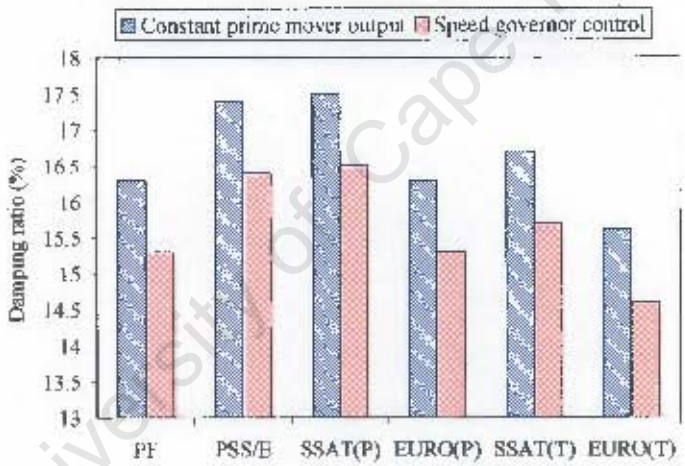

Figure 6.15: Effect of governor on the damping ratio of local modes; AVR with PSS

6.2 2A4G system

6.2.1 Identification of inter-area modes

For the single machine infinite bus system, identification of the local modes is obvious since the system has only one pair of oscillatory modes. For the two-area system, there are at least three pairs of oscillatory modes; two local area

modes and one inter-area mode. Speed components of the right eigenvectors (modes shape) and participation factors were used to identify the inter-area modes from the eigenvalue results obtained with each tools.

In Chapter 4, the flexibility of the five tools with regard to data output is presented. It is noted that PowerFactory does not give eigenvectors. Therefore, for this tool the inter-area modes were identified from the participation factors. A sample of the participation factor representation by this tool is shown in Fig. 6.16(a). Both SSAT and MatNetEig give participation factors and right eigenvectors. Figures 6.16(b) and 6.16(c) show the graphical representation of the right eigenvector components associated with speed for the inter-area mode, obtained using SSAT and MatNetEig, respectively. It can be seen from Fig. 6.16 that the mode with generators G1 and G2 (connected at bus 1 and bus 2) of area 1 swinging against generators G3 and G4 (connected at bus 3 and bus 4) of area 2 is the inter-area mode.

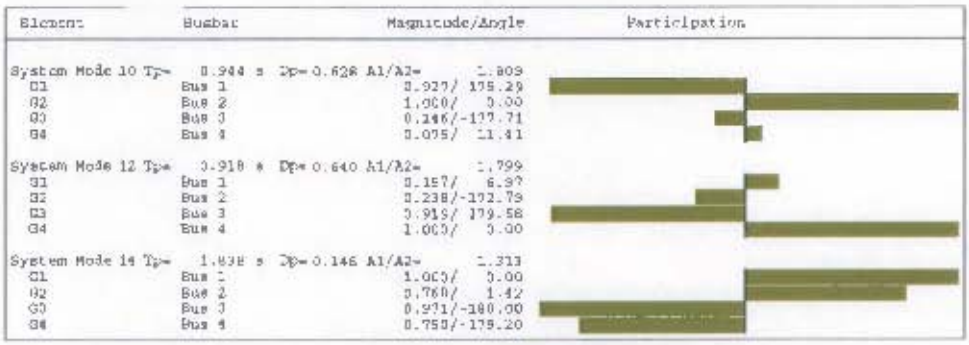

(a) PowerFactory; Participation factor

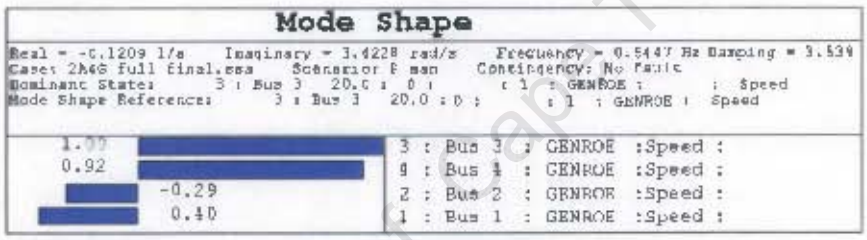

(b) SSA1; mode shape

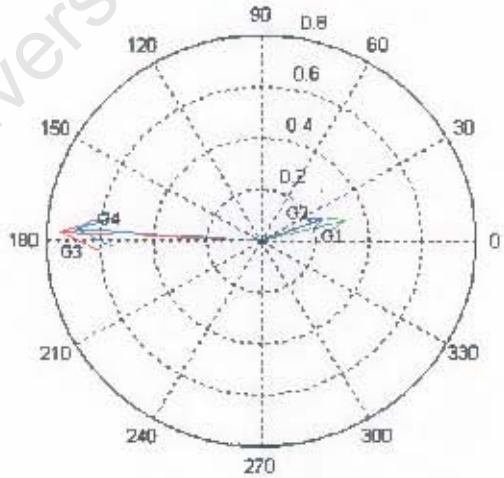

(c) MatNetEig; Compass plot of speed eigenvector components

Figure 6.16: Identification of the inter-area mode

PSS/E gives the right eigenvectors and they can be represented graphically. EUROSTAG computes neither the eigenvectors nor the participation factors. Thus, a code was developed in MATLAB for computing the normalized eigenvectors from the $\boldsymbol{A}$ matrix. A sample of right eigenvector components associated with the speed and rotor angle deviations for the inter-area mode are given in Table 6.15. It can be seen that the right eigenvector components associated with speed deviations of generators G1 and G2 of area 1 are about 180° out of phase with those of generators G3 and G4 of area 2.

Table 6.15: Eigenvectors for inter-area mode

State variable	PSS/E $\lambda = -0.156 + j3.404$	EUROSTAG $\lambda = -0.124 + j3.411$
$\Delta\omega_1$	$0.0038\angle -70°$	$0.0050\angle 109°$
$\Delta\delta_1$	$0.4229\angle -162°$	$0.9882\angle -1°$
$\Delta\omega_2$	$0.0028\angle -63°$	$0.0036\angle 119°$
$\Delta\delta_2$	$0.3110\angle -155°$	$0.8177\angle -0.1°$
$\Delta\omega_3$	$0.0090\angle 93°$	$0.0133\angle -95°$
$\Delta\delta_3$	$1.0000\angle 0°$	$1.0000\angle 180°$
$\Delta\omega_4$	$0.0083\angle 91°$	$0.0125\angle -96°$
$\Delta\delta_4$	$0.9188\angle -1°$	$0.9010\angle 179°$

6.2.2 Impact of tools' variations on inter-area modes

The investigations done for the SMIB system were repeated for the 2A4G system to establish the impact of the variations in components modeling and algorithmic factors among the five tools, on the inter-area modes. This section presents the investigation results. For each investigation, the tool(s) and technique used are similar to the ones used for SMIB system.

6.2.2.1 Effect of saturation

The effect of saturation modeling, on the inter-area modes was investigated using SSAT and PSS/E. The results are given in Table 6.16. It can be observed that the three saturation methods have different effects on the inter-area modes for different excitation control configurations.

Table 6.16: Effect of saturation on inter-area modes

Excitation control	Saturation representation				
	SSAT			PSS/E	
	Neglected	Total	Incremental	Neglected	Effective excitation
Manual	$-0.154 \pm j3.424$ f = 0.545 Hz ζ = 4.49 %	$-0.152 \pm j3.424$ f = 0.545 Hz ζ = 4.44 %	$-0.144 \pm j3.427$ f = 0.546 Hz ζ = 4.18 %	$-0.155 \pm j3.420$ f = 0.547 Hz ζ = 4.57 %	$-0.152 \pm j3.416$ f = 0.544 Hz ζ = 4.44 %
AVR without PSS	$-0.025 \pm j3.845$ f = 0.612 Hz ζ = 0.65 %	$-0.032 \pm j3.833$ f = 0.610 Hz ζ = 0.83 %	$-0.005 \pm j3.839$ f = 0.611 Hz ζ = 0.12 %	$-0.024 \pm j3.842$ f = 0.612 Hz ζ = 0.63 %	$-0.007 \pm j3.832$ f = 0.610 Hz ζ = 0.19 %
AVR with PSS	$-0.579 \pm j3.822$ f = 0.608 Hz ζ = 15.0 %	$-0.579 \pm j3.812$ f = 0.607 Hz ζ = 15.0 %	$-0.548 \pm j3.829$ f = 0.609 Hz ζ = 14.2 %	$-0.579 \pm j3.819$ f = 0.608 Hz ζ = 15.0 %	$-0.563 \pm j3.849$ f = 0.613 Hz ζ = 14.5 %

Table 6.17 gives the percentage change in the damping $\Delta\sigma$, frequency Δf, and damping ratio $\Delta\zeta$ of the inter-area modes caused by saturation. The percentage change Δk (where k is σ, f or ζ) is evaluated using (6.1) with results obtained with saturation neglected taken as reference. A positive value of Δk signifies an increase and a negative value signifies a decrease.

Table 6.17: Percentage (%) change in inter-area modes caused by saturation

Excitation control	Total			Incremental			Effective excitation		
	$\Delta\sigma$	Δf	$\Delta\zeta$	$\Delta\sigma$	Δf	$\Delta\zeta$	$\Delta\sigma$	Δf	$\Delta\zeta$
Manual	-1.3	0.0	-1.1	-6.5	0.1	-6.9	-1.9	-0.1	-2.8
AVR without PSS	28.0	-0.3	27.7	-80.0	-0.2	-81.5	-70.8	-0.3	-69.8
AVR with PSS	0.0	-0.3	0.0	-5.4	0.2	-5.3	-2.8	0.8	-3.3

It can be observed from Table 6.17 that the three methods of representing generator saturation have little effect on the frequency of the inter-area modes for the three excitation control configurations. The following discussion focuses on the damping ratio but is also applicable to the damping.

Manual excitation control

For manual excitation control, the damping ratio obtained with saturation represented using the three methods is lower than that obtained with saturation neglected. The highest decrease is observed for results obtained with incremental saturation method. Both total and effective excitation methods have little effect on the damping ratio.

Excitation controlled by AVR without PSS

For excitation controlled by AVR without PSS, the damping ratio obtained with saturation represented using the total saturation method is higher than that obtained with saturation neglected whereas the damping ratio obtained with incremental and effective excitation methods is lower than that obtained with saturation neglected.

For excitation controlled by AVR without PSS, the inter-area modes are marginally stable (the damping is close to zero) as seen from Table 6.16. Hence even a small change in damping translates to a high percentage change as observed in Table 6.17. For instance, if the damping obtained with saturation neglected is -0.025 and that obtained with saturation included is -0.005, the absolute decrease is only 0.02 but the percentage decrease is 80%.

Excitation controlled by AVR with PSS

For excitation controlled by AVR with PSS, total saturation representation has no effect on the damping ratio; saturation represented using incremental saturation and effective excitation methods causes the damping ratio to decrease.

It can be seen from Table 6.17 that for the three excitation control configurations, saturation represented using incremental and effective excitation methods causes the damping ratio to decrease. However, it is not clear why saturation modeled using the total saturation method has different effects on the inter-area modes for different excitation control configurations. That is, for manual excitation control, saturation causes the damping ratio to decrease whereas for excitation controlled by AVR without PSS, saturation causes the damping ratio to increase. For all excitation control configurations, generator saturation reduces the values of both d and q axes inductances of round-rotor machines and therefore the general effect of saturation on the inter-area modes is expected to be similar.

Further investigations were carried out to establish the effect of variations in the methods used for representing the generator model. Table 6.18 gives the results obtained with the generators on manual excitation control.

Table 6.18: Effect of generator model representation on inter-area modes

Model representation	Coupled–circuit method	Operational impedance method
Saturation neglected	$-0.154 \pm j3.420$ f = 0.544 Hz $\zeta = 4.48$ %	$-0.155 \pm j3.420$ f = 0.544 Hz $\zeta = 4.52$ %
Saturation included	$-0.147 \pm j3.460$ f = 0.551 Hz $\zeta = 4.24$ %	$-0.150 \pm j3.424$ f = 0.545 Hz $\zeta = 4.37$ %

The percentage change in damping $\Delta\sigma$, frequency Δf, and damping ratio $\Delta\zeta$ of the inter-area modes computed using (6.2) and taking the results obtained with coupled-circuit method as reference, is given in Table 6.19.

Table 6.19: Percentage (%) change in inter-area modes caused by variations in model representation

Saturation	$\Delta\sigma$	Δf	$\Delta\zeta$
Neglected	0.6	0.0	0.9
Included	2.0	-1.0	3.1

Tables 6.18 and 6.19 show that, with saturation neglected, the method used for representing the generator model has little effect on the inter-area modes. However, with saturation included, some discrepancies are observed and again these results agree with the literature [17]. The discrepancies in the results obtained with the two methods of representing the generator model are due to variation in the representation of saturation as explained in section 6.1.1.

For practical purposes, the discrepancies in results caused by variations in model representation can be considered to be insignificant. Therefore, it can be concluded that saturation modeled using total saturation method and

effective excitation method give similar results.

6.2.2.2 Effect of speed voltage terms

The effect of variation in modeling of speed voltage terms on the inter-area modes was investigated using EUROSTAG and MATLAB, as explained in Chapter 5. The results obtained with the speed deviation considered and speed deviation neglected are given in Table 6.20.

Table 6.20: Effect of speed voltage terms on the inter-area modes

Excitation control	Rotor speed deviation	
	Considered	Neglected
Manual	$-0.124 \pm j3.411$ f = 0.543 Hz $\zeta = 3.65$ %	$-0.128 \pm j3.413$ f = 0.543 Hz $\zeta = 3.75$ %
AVR without PSS	$+0.049 \pm j3.807$ f = 0.606 Hz $\zeta = -1.28$ %	$+0.008 \pm j3.813$ f = 0.607 Hz $\zeta = -0.2$ %

Table 6.21 gives the percentage increase in damping $\Delta\sigma$, frequency Δf, and damping ratio $\Delta\zeta$ of the inter-area modes caused by variation in modeling of speed voltage terms. These percentages are computed using (6.3), taking the results obtained with speed deviation considered as reference.

Table 6.21: Percentage (%) increase in inter-area modes caused by neglecting rotor speed deviation

Excitation control	$\Delta\sigma$	Δf	$\Delta\zeta$
Manual	3.2	0.1	2.7
AVR without PSS	83.7	0.2	84.4

It can be seen from tables 6.20 and 6.21 that variation in the modeling of speed voltage terms has a marginal effect on the frequency of the inter-area modes. However, the damping (and damping ratio) obtained with speed deviation neglected is higher than that obtained with speed deviation considered. Therefore, it can be concluded that for the operating condition considered, inclusion of speed deviation in speed voltage terms "adds" negative damping to the system (K_5 is negative). The high percentage increase in damping (and damping ratio) observed for excitation controlled by AVR without PSS is due to the fact that the damping of the inter-area modes is small. Thus, even for small changes in damping, the percentage change is large.

6.2.2.3 Effect of turbine output

The effect of variation in modeling of turbine output on the inter-area modes was investigated using SSAT. Table 6.22 gives results obtained with T_m and P_m turbine output, with different controller configurations.

Table 6.22: Effect of turbine output on the inter-area modes

Controllers		Turbine output	
		T_m	P_m
Constant prime mover output	Manual	$-0.123 \pm j3.423$ f = 0.545 Hz $\zeta = 3.58$ %	$-0.154 \pm j3.424$ f = 0.545 Hz $\zeta = 4.49$ %
	AVR without PSS	$+0.007 \pm j3.844$ f = 0.612 Hz $\zeta = -0.18$ %	$-0.025 \pm j3.845$ f = 0.612 Hz $\zeta = 0.65$ %
	AVR with PSS	$-0.547 \pm j3.826$ f = 0.609 Hz $\zeta = 14.2$ %	$-0.579 \pm j3.822$ f = 0.608 Hz $\zeta = 15.0$ %
Speed governor control	Manual	$-0.068 \pm j3.518$ f = 0.560 Hz $\zeta = 1.93$ %	$-0.098 \pm j3.519$ f = 0.560 Hz $\zeta = 2.80$ %
	AVR without PSS	$+0.060 \pm j3.920$ f = 0.624 Hz $\zeta = -1.52$ %	$+0.029 \pm j3.921$ f = 0.624 Hz $\zeta = -0.73$ %
	AVR with PSS	$-0.479 \pm j3.916$ f = 0.623 Hz $\zeta = 12.2$ %	$-0.511 \pm j3.913$ f = 0.623 Hz $\zeta = 12.9$ %

Table 6.23 gives the percentage increase in the damping $\Delta\sigma$, frequency Δf, and damping ratio $\Delta\zeta$ of the inter-area modes caused by variation in modeling of turbine output. These percentages are computed using (6.4), taking the results obtained with T_m turbine output as reference.

Table 6.23: Percentage (%) increase in inter-area modes caused by variation in turbine output

Controllers		$\Delta\sigma$	Δf	$\Delta\zeta$
Constant prime mover output	Manual	25.2	0.0	25.4
	AVR without PSS	457.1	0.0	461.1
	AVR with PSS	5.9	-0.1	5.6
Speed governor control	Manual	44.1	0.0	45.1
	AVR without PSS	51.7	0.0	52.0
	AVR with PSS	6.7	-0.1	5.7

It can be seen from Table 6.23 that for all controller configurations, the frequency is insignificantly affected by variation in turbine output. Therefore, the following discussion refers to the damping ratio, but it is also applicable to the damping.

As observed from Table 6.22, the damping ratio obtained with P_m turbine output is higher than that obtained with T_m turbine output for the three excitation control configurations, both with constant prime mover output and with speed governor control. This observation can be attributed to the fact that a turbine with P_m output "adds" damping to electromechanical modes as discussed in Chapter 3. For excitation controlled by AVR without PSS, and constant prime mover output, the damping ratio obtained with T_m turbine output shows that the inter-area modes are unstable, whereas that obtained with P_m turbine output shows the modes are stable. For this excitation control configuration with speed governor control, the damping ratio obtained with the two turbine outputs shows that the modes are unstable. The speed governor adds negative damping to the system and thus, even for P_m turbine output, the inter-area modes are unstable.

For manual excitation control and AVR with PSS, the percentage increase in damping is higher with speed governor control than with constant prime mover output. However, the increase in damping ratio for the two prime mover control configurations, with excitation controlled by AVR with PSS, are comparable. The high percentage increase observed for excitation controlled by AVR without PSS and constant prime mover output is due to the small value of damping, as earlier discussed in subsection 6.2.2.1.

6.2.2.4 Effect of method used for constructing the A matrix

The effect of variations in the methods used for constructing the $\boldsymbol{A}$ matrix was investigated using SSAT (analytical differentiation) and PSS/E (numerical differentiation), with the generator on manual excitation control. The results are given in Table 6.24. A perturbation of 10^{-3} was used with PSS/E.

Table 6.24: Effect of method used for constructing the $\boldsymbol{A}$ matrix on inter-area modes

Analytical differentiation	Numerical differentiation
$-0.154 \pm j3.424$	$-0.154 \pm j3.420$
f = 0.545 Hz	f = 0.544 Hz
$\zeta = 4.49$ %	$\zeta = 4.48$ %

The results of Table 6.24 show that for the perturbation size chosen, the method used for constructing the $\boldsymbol{A}$ matrix has little effect on the inter-area modes.

6.2.3 Comparison of results

6.2.3.1 Excitation control

In this subsection, the results obtained with the five tools – PSS/E, PowerFactory, EUROSTAG, SSAT, and MatNetEig – are presented. The results were obtained with different excitation control configurations and constant prime mover output.

A. Manual excitation control

The eigenvalue analysis results obtained using PSS/E, PowerFactory, EUROSTAG, SSAT, and MatNetEig are shown in Table 6.25. The first three oscillatory pairs represent: (i) area 1 local modes, (ii) area 2 local modes, and (iii) inter-area modes, respectively.

Table 6.25: Eigenvalues for the 2A4G system with the generators on manual excitation control

PSS/E	PF	EURO(P)	EURO(T)	SSAT(T-t)	SSAT(T-i)	SSAT(P-t)	SSAT(P-i)	MNE
$-0.613 \pm j6.754$	$-0.628 \pm j6.656$	$-0.590 \pm j6.577$	$-0.558 \pm j6.577$	$-0.594 \pm j6.765$	$-0.503 \pm j6.823$	$-0.626 \pm j6.766$	$-0.534 \pm j6.823$	$-0.588 \pm j6.765$
$f = 1.075Hz$;	$f = 1.059Hz$;	$f = 1.047Hz$;	$f = 1.047Hz$;	$f = 1.077Hz$;	$f = 1.086Hz$;	$f = 1.077Hz$;	$f = 1.086Hz$;	$f = 1.077Hz$;
$\zeta = 9.05$ %	$\zeta = 9.39$ %	$\zeta = 8.93$ %	$\zeta = 8.46$ %	$\zeta = 8.75$ %	$\zeta = 7.35$ %	$\zeta = 9.21$ %	$\zeta = 7.81$ %	$\zeta = 8.66$ %
$-0.625 \pm j6.948$	$-0.640 \pm j6.848$	$-0.603 \pm j6.767$	$-0.570 \pm j6.767$	$-0.603 \pm j6.958$	$-0.516 \pm j7.013$	$-0.637 \pm j6.959$	$-0.549 \pm j7.014$	$-0.596 \pm j6.958$
$f = 1.106Hz$;	$f = 1.090Hz$;	$f = 1.077Hz$;	$f = 1.077Hz$;	$f = 1.107Hz$;	$f = 1.116Hz$;	$f = 1.108Hz$;	$f = 1.116Hz$;	$f = 1.107Hz$;
$\zeta = 8.96$ %	$\zeta = 9.31$ %	$\zeta = 8.88$ %	$\zeta = 8.39$ %	$\zeta = 8.64$ %	$\zeta = 7.34$ %	$\zeta = 9.12$ %	$\zeta = 7.81$ %	$\zeta = 8.54$ %
$-0.152 \pm j3.416$	$-0.148 \pm j3.418$	$-0.146 \pm j3.417$	$-0.115 \pm j3.416$	$-0.121 \pm j3.423$	$-0.112 \pm j3.426$	$-0.152 \pm j3.424$	$-0.144 \pm j3.427$	$-0.114 \pm j3.426$
$f = 0.544Hz$;	$f = 0.544Hz$;	$f = 0.544Hz$;	$f = 0.544Hz$;	$f = 0.545Hz$;	$f = 0.545Hz$;	$f = 0.545Hz$;	$f = 0.546Hz$;	$f = 0.545Hz$;
$\zeta = 4.44$ %	$\zeta = 4.33$ %	$\zeta = 4.28$ %	$\zeta = 3.36$ %	$\zeta = 3.53$ %	$\zeta = 3.27$ %	$\zeta = 4.44$ %	$\zeta = 4.18$ %	$\zeta = 3.33$ %
$+0.010 \pm j0.142$	$-0.204 \pm j0.015$	$-0.124 \pm j0.049$	$-0.100 \pm j0.030$	$+0.005 \pm j0.008$	$-37.75 \pm j0.172$	$+0.004 \pm j0.001$	$-37.75 \pm j0.172$	-38.00
$f = 0.023Hz$;	$f = 0.002Hz$;	$f = 0.008Hz$;	$f = 0.005Hz$;	$f = 0.001Hz$;	$f = 0.027Hz$;	$f = 0.0001Hz$;	$f = 0.027Hz$;	-37.90
$\zeta = -7.07$ %	$\zeta = 99.7$ %	$\zeta = 93.0$ %	$\zeta = 61.5$ %	$\zeta = -56.7$ %	$\zeta \approx 100.0$ %	$\zeta = -97.7$ %	$\zeta \approx 100.0$ %	-36.67
								-36.54
$-0.120 \pm j0.093$	-37.31	-37.10	-37.10	-37.29	$-37.87 \pm j0.126$	$-0.061 \pm j0.024$	$-37.87 \pm j0.125$	-35.36
$f = 0.015Hz$;	-37.23	-37.01	-37.01	-37.21	$f = 0.020Hz$;	$f = 0.004Hz$;	$f = 0.020Hz$;	-33.85
$\zeta = 79.0$ %	-34.86	-34.61	-34.61	-36.39	$\zeta \approx 100.0$ %	$\zeta = 93.1$ %	$\zeta \approx 100.0$ %	-31.20
	-33.55	-33.13	-33.13	-36.22				-29.82
-37.16	-33.03	-31.37	-31.37	-34.87	-35.45	-37.29	$-0.106 \pm j0.022$	-4.895
-37.08	-32.81	-31.20	-31.20	-33.45	-34.00	-37.21	$f = 0.004Hz$;	-4.858
-35.86	-27.00	-24.22	-24.22	-30.61	-32.23	-36.39	$\zeta = 97.9$ %	-3.645
-35.67	-25.42	-22.35	-22.35	-29.15	-30.80	-36.22		-2.831
-34.72	-5.582	-5.989	-5.992	-4.716	-5.238	-34.87	-35.45	-0.212
-33.33	-5.547	-5.962	-5.964	-4.679	-5.221	-33.45	-34.00	-0.200
-29.94	-4.274	-4.706	-4.706	-3.380	-4.057	-30.61	-32.23	-0.132
-28.47	-3.406	-3.811	-3.812	-2.508	-3.330	-29.15	-30.80	-0.056
-5.210	-0.226	-0.218	-0.218	-0.189	-0.267	-4.713	-5.236	0
-5.177	-0.081	-0.203	-0.204	-0.180	-0.256	-4.676	-5.218	0
-3.861	-0.040	-0.039	-0.026	-0.043	-0.108	-3.380	-4.057	
-2.985	0	0	0	-0.021	-0.088	-2.508	-3.329	
-0.274					-0.002	-0.189	-0.267	
-0.231					+0.002	-0.180	-0.256	
							-0.045	
							0	

It can be seen from Table 6.25 that some of the eigenvalues obtained with PSS/E and SSAT have positive real parts. This may due to the fact that these tools use absolute deviations of rotor speed and angle as state variables, in the construction of the $\boldsymbol{A}$ matrix [7,49,83]. The eigenvalues with a positive real part should be zero, but they were not computed exactly, due to round-off errors in the calculation of the $\boldsymbol{A}$ matrix and mismatches in the load flow solution.

To confirm system stability, time domain simulations were run using PSS/E and DSA-TSAT[4]. A small disturbance was simulated in the system by disconnecting one of the tie-lines interconnecting the two areas, for 5 *ms*. The results for the generator speeds are shown in Fig. 6.17.

It can be observed from Fig. 6.17 that the oscillations initiated by the temporary line outage are damped, hence the system is stable.

Table 6.26 gives results obtained with the five simulation tools for three excitation control configurations – manual, AVR without PSS, and AVR with PSS – and constant prime mover output. For each excitation control configuration, two sets of results are given; one set was obtained with saturation neglected and the other set with saturation included.

[4]Module for transient stability analysis in DSA PowerTools

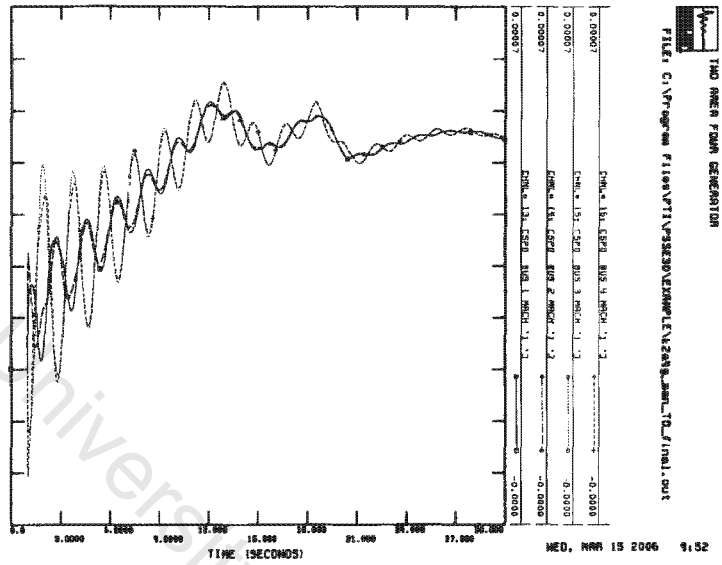

(a) PSS/E

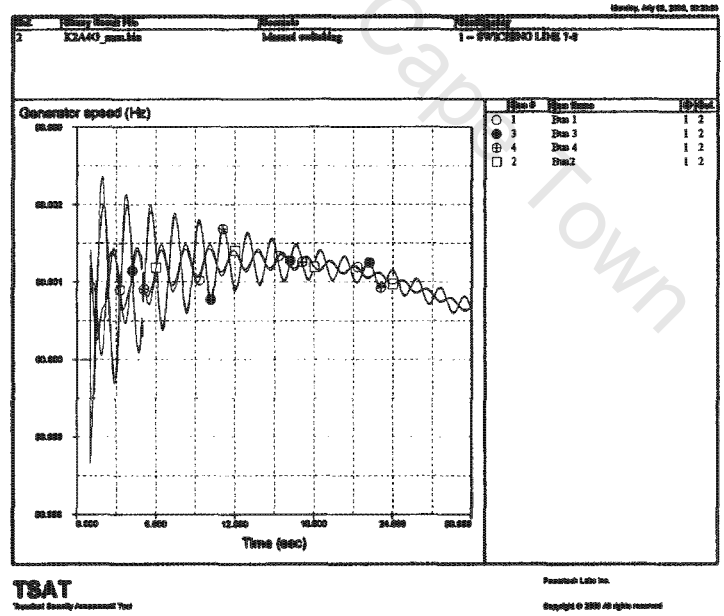

(b) DSA-TSAT

Figure 6.17: Time domain simulation results

Table 6.26: Inter-area modes results obtained with five industrial-grade tools

Tool	Saturation neglected			Saturation included		
	Manual	AVR without PSS	AVR with PSS	Manual	AVR without PSS	AVR with PSS
PSS/E	$-0.155 \pm j3.420$ f = 0.547 Hz $\zeta = 4.57$ %	$-0.024 \pm j3.842$ f = 0.612 Hz $\zeta = 0.63$ %	$-0.579 \pm j3.819$ f = 0.608 Hz $\zeta = 15.0$ %	$-0.152 \pm j3.416$ f =0.544 Hz $\zeta = 4.44$ %	$-0.007 \pm j3.832$ f = 0.610 Hz $\zeta = 0.19$ %	$-0.563 \pm j3.849$ f = 0.613 Hz $\zeta = 14.5$ %
SSAT(P-t)	$-0.154 \pm j3.424$ f = 0.545 Hz $f\zeta = 4.49$ %	$-0.025 \pm j3.845$ f = 0.612 Hz $\zeta = 0.65$ %	$-0.579 \pm j3.822$ f = 0.608 Hz $\zeta = 15.0$ %	$-0.152 \pm j3.424$ f = 0.545 Hz $\zeta = 4.44$ %	$-0.032 \pm j3.833$ f = 0.610 Hz $\zeta = 0.83$ %	$-0.579 \pm j3.812$ f = 0.607 Hz $\zeta = 15.0$ %
PF	$-0.161 \pm j3.414$ f = 0.543 Hz $\zeta = 4.71$ %	$+0.014 \pm j3.821$ f = 0.608 Hz $\zeta = -0.37$ %	$-0.530 \pm j3.799$ f = 0.605 Hz $\zeta = 13.8$ %	$-0.148 \pm j3.418$ f = 0.544 Hz $\zeta = 4.33$ %	$+0.028 \pm j3.817$ f = 0.607 Hz $\zeta = -0.73$ %	$-0.541 \pm j3.837$ f = 0.611 Hz $\zeta = 14.0$ %
EURO(P)	$-0.156 \pm j3.412$ f = 0.543 Hz $\zeta = 4.57$ %	$+0.017 \pm j3.808$ f = 0.606 Hz $\zeta = -0.45$ %	$-0.520 \pm j3.785$ f = 0.602 Hz $\zeta = 13.6$ %	$-0.146 \pm j3.417$ f = 0.544 Hz $\zeta = 4.28$ %	$+0.033 \pm j3.804$ f = 0.605 Hz $\zeta = -0.86$ %	$-0.533 \pm j3.818$ f = 0.608Hz $\zeta = 13.8$ %
SSAT(P-i)	$-0.154 \pm j3.424$ f = 0.545 Hz $\zeta = 4.49$ %	$-0.025 \pm j3.845$ f = 0.612 Hz $\zeta = 0.65$ %	$-0.579 \pm j3.822$ f = 0.608 Hz $\zeta = 15.0$ %	$-0.144 \pm j3.427$ f = 0.546 Hz $\zeta = 4.18$ %	$-0.005 \pm j3.839$ f = 0.611 Hz $\zeta = 0.12$ %	$-0.548 \pm j3.829$ f = 0.609 Hz $\zeta = 14.2$ %
SSAT(T-t)	$-0.123 \pm j3.423$ f = 0.545 Hz $\zeta = 3.58$ %	$+0.007 \pm j3.844$ f = 0.612 Hz $\zeta = -0.18$ %	$-0.547 \pm j3.826$ f = 0.609 Hz $\zeta = 14.2$ %	$-0.121 \pm j3.423$ f = 0.545 Hz $\zeta = 3.53$ %	$+0.0001 \pm j3.832$ f = 0.610 Hz $\zeta \approx 0$ %	$-0.547 \pm j3.816$ f = 0.607 Hz $\zeta = 14.2$ %
EURO(T)	$-0.124 \pm j3.411$ f = 0.543 Hz $\zeta = 3.65$ %	$+0.049 \pm j3.807$ f = 0.606 Hz $\zeta = -1.28$ %	$-0.488 \pm j3.789$ f = 0.603 Hz $\zeta = 12.8$ %	$-0.115 \pm j3.416$ f = 0.544 Hz $\zeta = 3.36$ %	$+0.064 \pm j3.803$ f = 0.605 Hz $\zeta = -1.69$ %	$-0.500 \pm j3.822$ f = 0.608Hz $\zeta = 13.0$ %
MNE	$-0.123 \pm j3.423$ f = 0.545 Hz $\zeta = 3.58$ %	$+0.020 \pm j3.827$ f = 0.609 Hz $\zeta = -0.52$ %	$-0.547 \pm j3.861$ f = 0.614 Hz $\zeta = 14.0$ %	$-0.114 \pm j3.426$ f = 0.550 Hz $\zeta = 3.33$ %	$+0.035 \pm j3.783$ f = 0.600 Hz $\zeta = -0.92$ %	$-0.557 \pm j3.886$ f = 0.620 Hz $\zeta = 14.2$ %
SSAT(T-i)	$-0.123 \pm j3.423$ f = 0.545 Hz $\zeta = 3.58$ %	$+0.007 \pm j3.844$ f = 0.612 Hz $\zeta = -0.18$ %	$-0.547 \pm j3.826$ f = 0.609 Hz $\zeta = 14.2$ %	$-0.112 \pm j3.426$ f = 0.545 Hz $\zeta = 3.27$ %	$+0.027 \pm j3.838$ f = 0.611 Hz $\zeta = -0.70$ %	$-0.516 \pm j3.833$ f = 0.610 Hz $\zeta = 13.3$ %

It can be seen from Table 6.26 column 2 and 5, that the results obtained using the five tools show that the inter-area modes are stable. These results agree on the frequency of the oscillations; the difference between the highest and the lowest value is less than 0.5%. However, discrepancies are noted in the damping (and damping ratio) results. For each set of results, the difference in damping between the highest and the lowest value is over 30%.

Table 6.27 gives the percentage change in damping $\Delta\sigma$, frequency Δf, and damping ratio $\Delta\zeta$ of the inter-area modes caused by saturation. These percentages are computed according to (6.1), taking the results obtained with saturation neglected as reference.

Table 6.27: Percentage (%) change in inter-area modes caused by saturation; results obtained with five industrial-grade tools

Tool	manual excitation control			AVR without PSS			AVR with PSS		
	$\Delta\sigma$	Δf	$\Delta\zeta$	$\Delta\sigma$	Δf	$\Delta\zeta$	$\Delta\sigma$	Δf	$\Delta\zeta$
PSS/E	-1.9	-0.1	-2.8	-70.8	-0.3	-69.8	-2.8	0.8	-3.3
SSAT(P-t)	-1.3	0.0	-1.1	28.0	-0.3	27.7	0.0	-0.3	0.0
PF	-8.1	0.1	-8.1	100.0	-0.1	97.3	2.1	1.0	1.4
EURO(P)	-6.4	0.1	-6.3	-94.1	-0.1	-91.1	2.5	0.9	1.5
SSAT(P-i)	-6.5	0.1	-6.9	-80.0	-0.2	-81.5	-5.4	0.2	-5.3
SSAT(T-t)	-1.6	0.0	-1.4	98.6	-0.3	100.0	0.0	-0.3	0.0
EURO(T)	-7.3	0.1	-7.9	-30.6	-0.1	-32.0	2.5	0.9	1.6
MNE	-7.3	0.1	-7.0	-75.0	-1.1	-76.9	1.8	0.6	1.4
SSAT(T-i)	-8.9	0.1	-8.7	-285.7	-0.2	-288.9	-5.7	0.2	-6.3

Figure 6.18 shows the loci of the inter-area modes on the upper complex plane for manual excitation control, with saturation included and with saturation neglected. Figure 6.19 shows the corresponding damping ratios.

It can be seen from Table 6.27 column 3, that for manual excitation control, saturation has very little effect on the frequency obtained with the five tools.

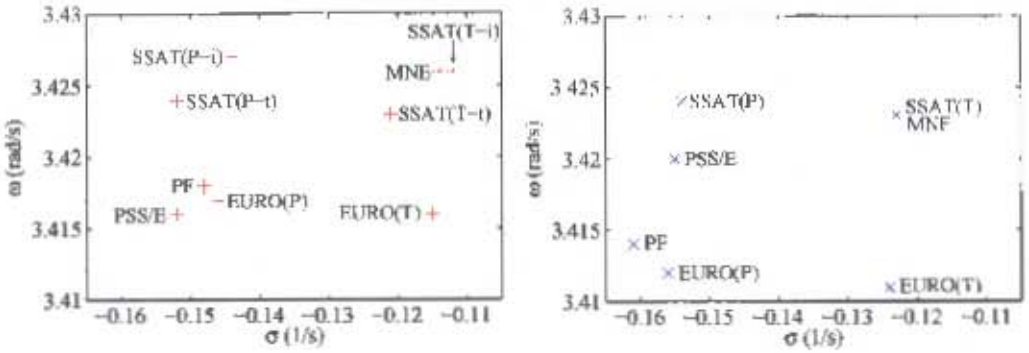

(a) Saturation included (b) Saturation neglected

Figure 6.18: Loci of the inter-area modes in the upper complex plane; manual excitation control

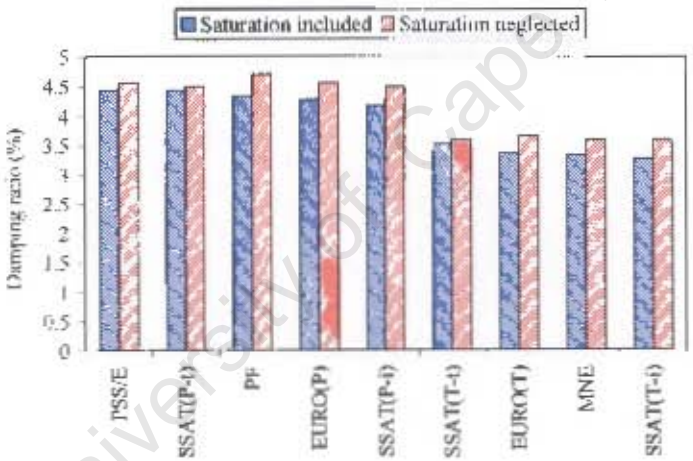

Figure 6.19: Effect of saturation on the damping ratio of inter-area modes; manual excitation control

Therefore, the following discussion focuses on the damping ratio, which captures changes in both frequency and damping.

For the five tools, with manual excitation control, saturation reduces the damping ratio as can be seen from Fig. 6.19 and Table 6.27 column 4. It can also be noted that saturation has little effect on the results obtained with PSS/E and SSAT(t).

It can be seen from Fig. 6.18 that the results obtained with tools that employ T_m turbine output (SSAT(T), MatNetEig, and EUROSTAG(T)) are more conservative than those obtained with tools that employ P_m turbine output (SSAT(P), PowerFactory, EUROSTAG(P), and PSS/E), both with saturation included and with saturation neglected. These results corroborate the theoretical framework given in Chapter 3, that the P_m turbine output "adds" damping to the system.

With manual excitation control, the effect of speed voltage terms on the inter-area modes is not apparent.

B. AVR without PSS

The AVR adds negative damping to the system. Thus for each tool, comparing the results obtained with manual excitation control, with results obtained from excitation controlled by AVR without PSS exhibit lower damping of the inter-area modes, as can be seen from Table 6.26. It can be seen from column 3 and 6 that the results obtained with the five tools agree on the frequency. The difference between the highest and the lowest value is less than 1.5%. However, discrepancies are noted in the damping (and damping ratio) results. The difference in damping between the highest and the lowest value is about 150%, both with saturation neglected and with saturation included.

It can be seen from Table 6.27 column 5–7 that for each of the five tools, saturation marginally reduces the frequency of the inter-area mode, and both the damping and damping ratio change by similar percentages. It should be noted that if the real part of the eigenvalue is positive, an increase in this value signifies decreased damping. Similarly, if the damping ratio is negative, an increase in this value signifies decreased damping ratio. The

high percentage changes in the damping (and damping ratio) is due to the fact that the damping is very close to zero. Therefore, a small change is seen as a high percentage change. For instance, if the damping obtained with saturation neglected is 0.007 and that obtained with saturation included is 0.027, the absolute decrease is only 0.02 but the percentage decrease is 286%.

It can be observed from Table 6.27 column 5-7 that for SSAT(t) and PowerFactory, saturation improves the damping (and damping ratio) whereas for PSS/E, EUROSTAG, SSAT(i), and MatNetEig it reduces the damping (and damping ratio). This erratic effect of saturation was also observed and discussed in Section 6.2.2.

Figure 6.20 shows the loci of the inter-area modes on the upper complex plane for excitation controlled by AVR without PSS, with saturation included and with saturation neglected. Figure 6.21 shows the corresponding damping ratios.

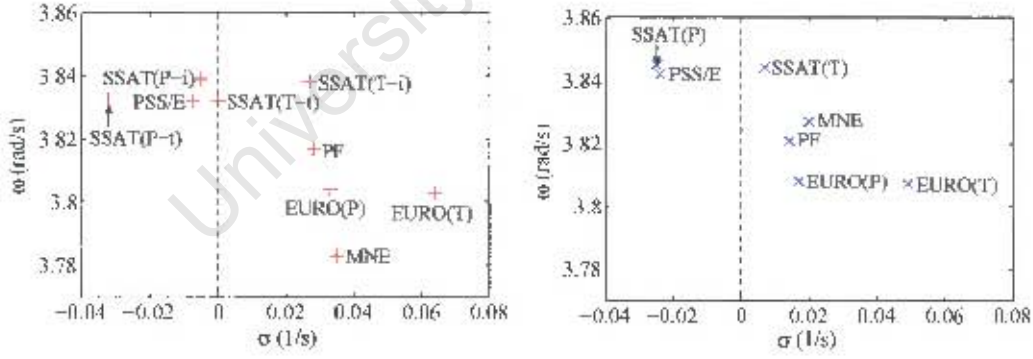

(a) Saturation included

(b) Saturation neglected

Figure 6.20: Loci of the inter-area modes in the upper complex plane; AVR without PSS

It can be seen from figures 6.20 and 6.21 that the results obtained with SSAT(P) and PSS/E show the inter-area modes are stable, whereas those

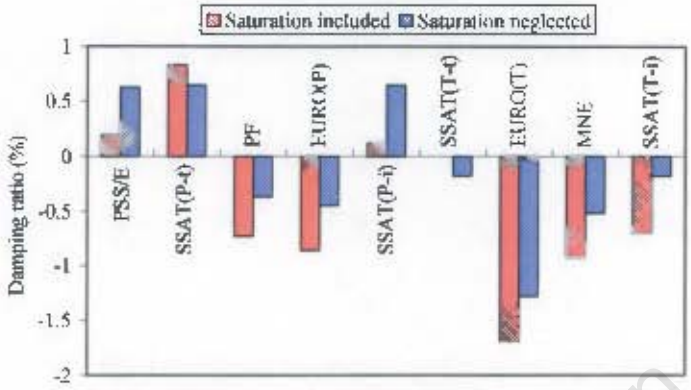

Figure 6.21: Effect of saturation on the damping ratio of inter-area modes; AVR without PSS

obtained with SSAT(T), EUROSTAG, PowerFactory, and MatNetEig show they are unstable. The eigenvalue results obtained using PSS/E and SSAT(P) were validated using time domain simulations. The oscillations were initiated by disconnecting one of the tie-lines for 5 *ms*. The results are shown in Fig. C.1, Appendix C. For comparison purposes, time domain simulation results obtained with PowerFactory (this tool was chosen arbitrarily) are also shown. These contradictory results emphasize the fact that different conclusions can be drawn from results obtained from different simulation tools for the same power system.

It can be observed from figures 6.20 and 6.21 that the results obtained with PowerFactory and EUROSTAG are more conservative than the results obtained with other tools that employ similar turbine output. That is, the results obtained with PowerFactory and EUROSTAG(P) are more conservative than those obtained with SSAT(P) and PSS/E (P_m turbine output) and those obtained with EUROSTAG(T) are more conservative than the ones obtained with SSAT(T) and MatNetEig (T_m turbine output). This observation can be attributed to the fact that both PowerFactory and EUROSTAG

consider speed deviation in the speed voltage terms and this reduces the damping as illustrated in Section 6.2.2.

The results that predict stable system operation were obtained with tools that employ P_m turbine output. This observation confirms that P_m turbine output "provides" additional damping to the system.

C. AVR with PSS

For all the tools, the results obtained with excitation controlled by AVR with PSS exhibit higher damping than those obtained with excitation controlled by AVR without PSS, both with saturation included and with saturation neglected, as can be observed from Table 6.26 column 4 and 7. This is due to the damping added to the system by the PSS. The results obtained with the five tools agree on the frequency. The difference between the highest and the lowest value is about 2%. However, some discrepancies are observed in the damping (and damping ratio). The difference in damping between the highest and the lowest value is over 13%, both with saturation neglected and with saturation included.

It can be seen from Table 6.27 column 9, that for each of the five tools, saturation marginally affects the frequency of the inter-area modes. For PSS/E and SSAT(i), saturation reduces the damping (and damping ratio) and it has no effect on the damping obtained with SSAT(t). For PowerFactory, EUROSTAG, and MatNetEig, saturation increases the damping. It is not clear why the effect of saturation on the inter-area modes is different for different tools, since for all the tools, saturation reduces the mutual inductance. Therefore, it is expected that, for all the tools, its effect on the inter-area modes would be the same e.g. for all the tools, saturation increases or de-

creases the damping, or has no effect. It can be noted that only incremental saturation has some reasonable impact on the damping of the inter-area modes.

Figure 6.22 shows the loci of the inter-area modes on the upper complex plane for excitation controlled by AVR with PSS, with saturation included and with saturation neglected. Figure 6.23 shows the corresponding damping ratios.

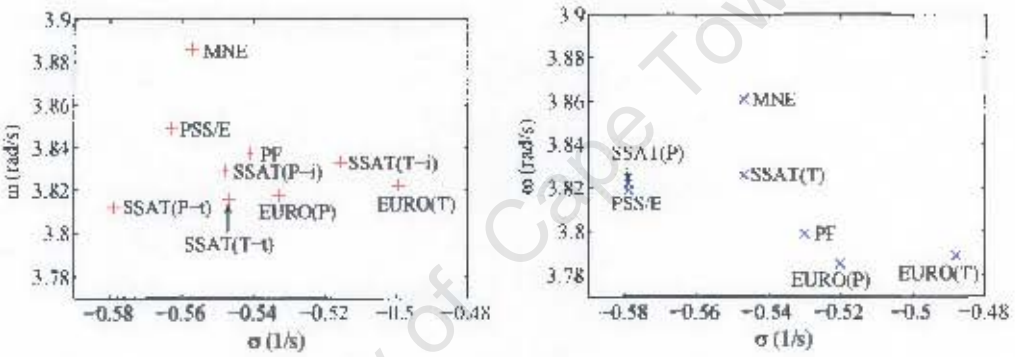

(a) Saturation included (b) Saturation neglected

Figure 6.22: Loci of the inter-area modes in the upper complex plane; AVR with PSS

Comparing figures 6.22(a) and 6.22(b), it can be observed that with saturation included the effect of speed voltage terms and turbine output is not apparent. However, with saturation neglected, it is clear that the most conservative results are those obtained with tools that consider speed deviation in the speed voltage terms (EUROSTAG and PowerFactory). Results obtained with tools that employ T_m turbine output are more conservative than those obtained with tools that employ P_m turbine output with similar modeling of speed voltage terms.

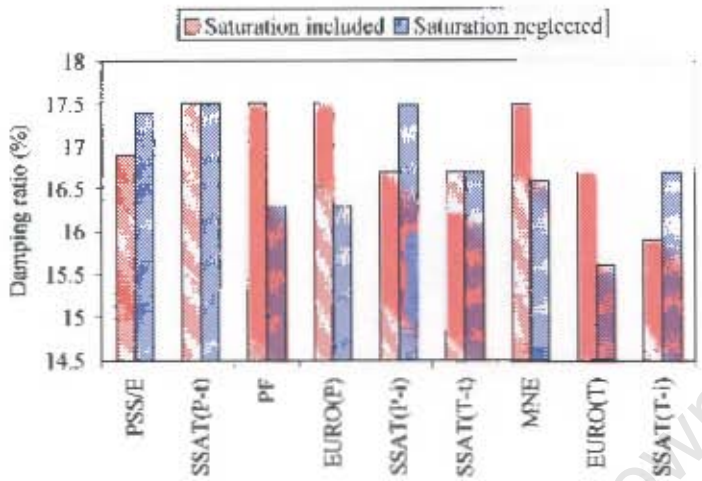

Figure 6.23: Effect of saturation on the damping ratio of inter-area modes; AVR with PSS

6.2.3.2 Excitation and prime mover control

The results presented in this subsection were obtained with different excitation control configurations and speed governor control, with saturation neglected. The results obtained with constant prime mover output are included for comparison purposes. The results obtained with the four tools – PSS/E, PowerFactory, EUROSTAG, and SSAT – are given in Table 6.28.

Table 6.28: Effect of speed governor on inter-area mode

Tool	Speed governor control			Constant prime mover output		
	Manual	AVR without PSS	AVR with PSS	Manual	AVR without PSS	AVR with PSS
PF	$-0.105 \pm j3.508$ f = 0.558 Hz $\zeta = 2.99$ %	$+0.064 \pm j3.895$ f = 0.620 Hz $\zeta = -1.64$ %	$-0.467 \pm j3.887$ f = 0.619 Hz $\zeta = 11.9$ %	$-0.161 + j3.414$ f = 0.543 Hz $\zeta = 4.71$ %	$+0.014 \pm j3.821$ f = 0.608 Hz $\zeta = -0.37$ %	$-0.530 \pm j3.799$ f = 0.605 Hz $\zeta = 13.8$ %
EURO(P)	$-0.100 \pm j3.508$ f = 0.558 Hz $\zeta = 2.86$ %	$+0.069 \pm j3.886$ f = 0.618 Hz $\zeta = -1.76$ %	$0.455 + j3.877$ f = 0.617 Hz $\zeta = 11.7$ %	$-0.156 \pm j3.412$ f = 0.543 Hz $\zeta = 4.57$ %	$+0.017 \pm j3.808$ f = 0.606 Hz $\zeta = -0.45$ %	$-0.520 \pm j3.785$ f = 0.602 Hz $\zeta = 13.6$ %
PSS/E	$-0.099 + j3.516$ f =0.560 Hz $\zeta = 2.82$ %	$+0.029 \pm j3.919$ f = 0.624 Hz $\zeta = -0.75$ %	$-0.510 \pm j3.911$ f = 0.622 Hz $\zeta = 12.9$ %	$-0.155 \pm j3.420$ f = 0.547 Hz $\zeta = 4.57$ %	$-0.024 + j3.842$ f = 0.612 Hz $\zeta = 0.63$ %	$-0.579 \pm j3.819$ f = 0.608 Hz $\zeta = 15.0$ %
SSAT(P)	$-0.098 \pm j3.519$ f = 0.560 Hz $\zeta = 2.80$ %	$+0.029 + j3.921$ f = 0.624 Hz $\zeta = -0.73$ %	$-0.511 \pm j3.913$ f = 0.623 Hz $\zeta = 12.9$ %	$-0.154 \pm j3.424$ f = 0.545 Hz $\zeta = 4.49$ %	$-0.025 \pm j3.845$ f = 0.612 Hz $\zeta = 0.65$ %	$-0.579 \pm j3.822$ f = 0.608 Hz $\zeta = 15.0$ %
EURO(T)	$-0.070 \pm j3.506$ f = 0.558 Hz $\zeta = 1.98$ %	$+0.099 \pm j3.884$ f = 0.618 Hz $\zeta = -2.56$ %	$-0.424 + j3.880$ f = 0.618 Hz $\zeta = 10.9$ %	$-0.124 \pm j3.411$ f = 0.543 Hz $\zeta = 3.65$ %	$+0.049 \pm j3.807$ f = 0.606 Hz $\zeta = -1.28$ %	$-0.488 \pm j3.789$ f = 0.603 Hz $\zeta = 12.8$ %
SSAT(T)	$-0.068 + j3.518$ f = 0.560 Hz $\zeta = 1.93$ %	$+0.060 \pm j3.920$ f = 0.624 Hz $\zeta = -1.52$ %	$0.479 + j3.916$ f = 0.623 Hz $\zeta = 12.2$ %	$-0.123 \pm j3.423$ f = 0.545 Hz $\zeta = 3.58$ %	$+0.007 + j3.844$ f = 0.612 Hz $\zeta = -0.18$ %	$-0.547 \pm j3.826$ f = 0.609 Hz $\zeta = 14.2$ %

Table 6.29 gives the percentage change in the damping $\Delta\sigma$, frequency Δf, and damping ratio $\Delta\zeta$ of the inter-area modes caused by the addition of the speed governor. These percentages are computed according to (6.5), taking the results obtained with constant prime mover output as reference.

Tables 6.28 and 6.29 are discussed below.

Table 6.29: Percentage (%) change in inter-area modes caused by speed governor

Tool	manual excitation control			AVR without PSS			AVR with PSS		
	$\Delta\sigma$	Δf	$\Delta\zeta$	$\Delta\sigma$	Δf	$\Delta\zeta$	$\Delta\sigma$	Δf	$\Delta\zeta$
PF	-34.8	2.8	-36.5	-357.1	1.9	-343.2	-11.9	2.3	-13.8
EURO(P)	-35.9	2.8	-37.4	-305.9	2.0	-291.1	-12.5	2.4	-14.0
PSS/E	-36.1	2.8	-38.3	-220.8	2.0	-219.0	-11.9	2.4	-14.0
SSAT(P)	-36.4	2.8	-37.6	-216.0	2.0	-212.3	-11.7	2.4	-14.0
EURO(T)	-43.5	2.8	-45.8	-102.0	2.0	-100.0	-13.1	2.4	-14.8
SSAT(T)	-44.7	2.8	-46.1	-757.1	2.0	-744.4	-12.4	2.4	-14.1

A. Manual excitation control and governor

It can be seen from Table 6.28, column 2, that with manual excitation and speed governor control, the results obtained using the four tools predict that the inter-area modes are stable. These results agree on the frequency of the oscillations; the difference between the highest (SSAT(P)) and the lowest (EUROSTAG(T)) value is less than 0.5%. However, results obtained with PowerFactory, EUROSTAG(P), PSS/E, and SSAT(P), rounded-off to the nearest whole number, predict a satisfactory damping ratio ($\zeta \geq 3\%$), whereas those obtained with EUROSTAG(T) and SSAT(T) predict an unsatisfactory damping ratio. The difference in damping between the highest (PowerFactory) and the lowest (SSAT(T)) value is over 35%.

Figure 6.24 shows the loci of the inter-area modes on the upper complex

plane for manual excitation control, with constant prime mover output and with speed governor control. Figure 6.25 shows the corresponding damping ratios.

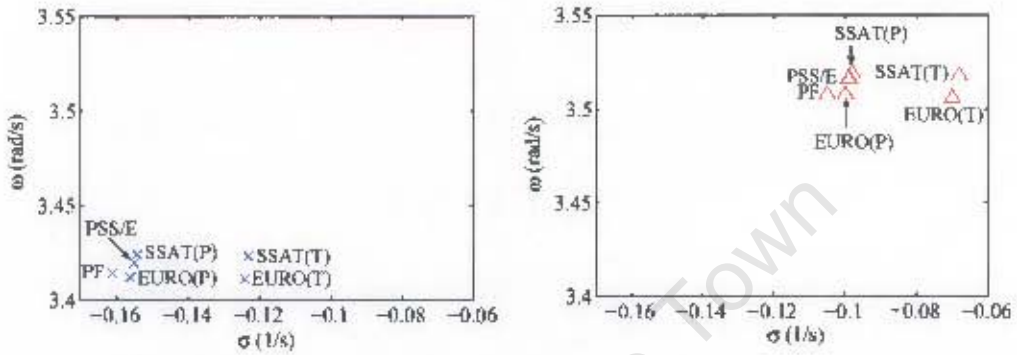

(a) Constant prime mover output (b) Speed governor control

Figure 6.24: Loci of the inter-area modes in the upper complex plane; manual excitation control

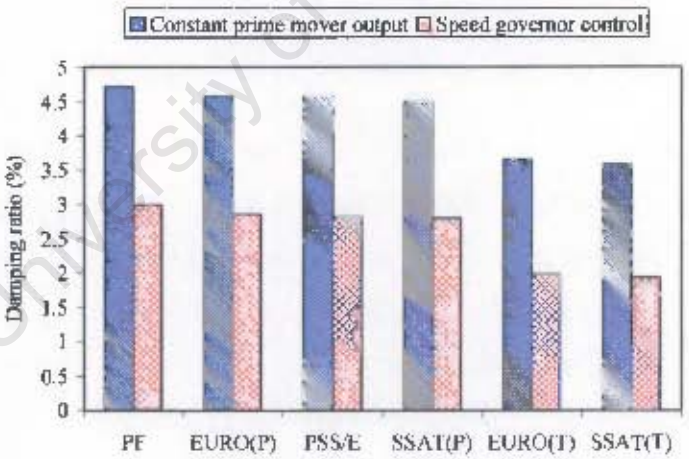

Figure 6.25: Effect of governor on the damping ratio of the inter-area modes; manual excitation control

The addition of the speed governor reduces the damping (and damping ratio) as can be observed from Table 6.29 column 2–4 and figures 6.24 and 6.25. The frequency increases by 2.8% for the four tools.

It can be seen from Fig. 6.24 that for both constant prime mover output and speed governor control, the results obtained with the tools that employ P_m turbine output (EUROSTAG(P), SSAT(P), PSS/E, and PowerFactory) are more optimistic than those obtained with tools that employ T_m turbine output (EUROSTAG(T) and SSAT(T)). This can be attributed to the "additional" damping due to the speed-torque relationship associated with P_m turbine output.

B. AVR without PSS, and governor

The results obtained with the four tools show that the inter-area modes are unstable for excitation controlled by AVR without PSS, and with speed governor control, as seen from Table 6.28 column 3. These results agree on the frequency of the oscillations: the difference between the highest (SSAT(P)) and the lowest (EUROSTAG(T) value is less than 1%.

The damping (and damping ratio) of the inter-area modes decreases due to the addition of the speed governor as can be seen from Table 6.29 column 5 and 7. The percentage decrease is high due to the fact that the damping of these modes is low and therefore even small changes translate to a high percentage change. For example, if the damping obtained with constant prime mover output is 0.007 and that obtained with speed governor control is 0.06, the decrease is only 0.053 but the percentage decrease is 757%. It can be seen from column 6 that for the four tools, the frequency of the oscillations increases by about 2%.

Figure 6.26 shows the loci of the inter-area modes on the upper complex plane for excitation controlled by AVR without PSS, with constant prime mover output and with speed governor control. Figure 6.27 shows the corresponding

damping ratios.

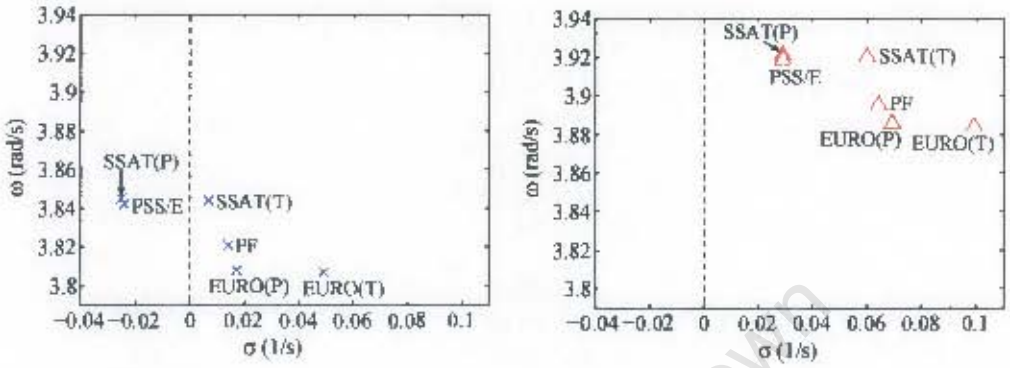

(a) Constant prime mover output (b) Speed governor control

Figure 6.26: Loci of the inter-area modes in the upper complex plane; AVR without PSS

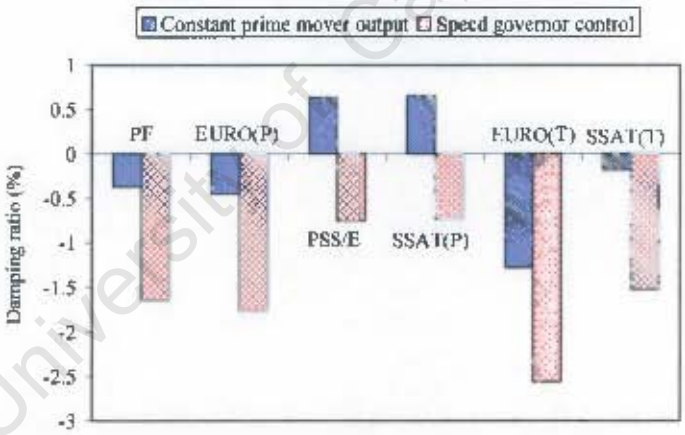

Figure 6.27: Effect of governor on the damping ratio of inter-area modes; AVR without PSS

The results obtained with PSS/E and SSAT(P) are pushed to instability by the speed governor as seen in figures 6.26 and 6.27. That is, the results obtained with these tools are on the left hand plane for constant prime mover output and on the right hand plane for speed governor control. The effect of speed voltage terms and turbine output modeling with speed governor

control is as discussed earlier in subsection 6.2.3.1, for constant prime mover output.

C. AVR with PSS, and governor

It can be seen from Table 6.28 column 4 that for excitation controlled by AVR with PSS, and with speed governor control, the results obtained using the four tools predict that the inter-area modes are stable. These results agree on the frequency of the oscillations; the difference between the highest (SSAT(T)) and the lowest (EUROSTAG(P) value is about 1%. The difference in damping between the highest (SSAT(P)) and the lowest (EUROSTAG(T) value is over 17%.

Figure 6.28 shows the loci of the inter-area modes on the upper complex plane for excitation controlled by AVR with PSS, with constant prime mover output and with speed governor control. Figure 6.29 shows the corresponding damping ratios.

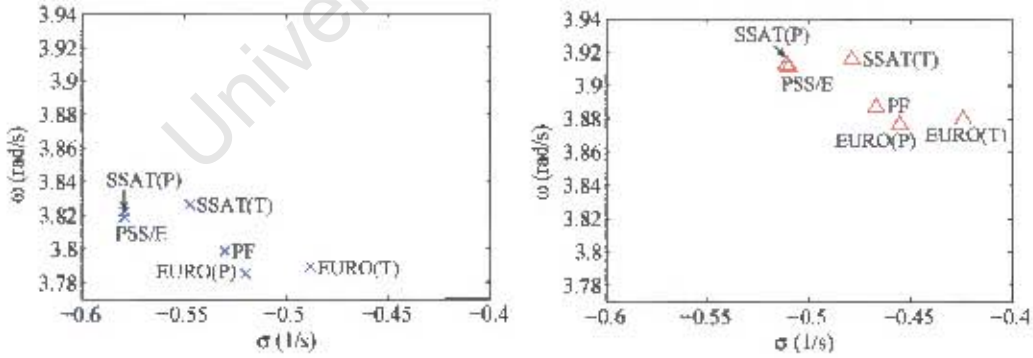

(a) Constant prime mover output

(b) Speed governor control

Figure 6.28: Loci of the inter-area modes in the upper complex plane; AVR with PSS

As with the other two excitation control configurations, the results obtained

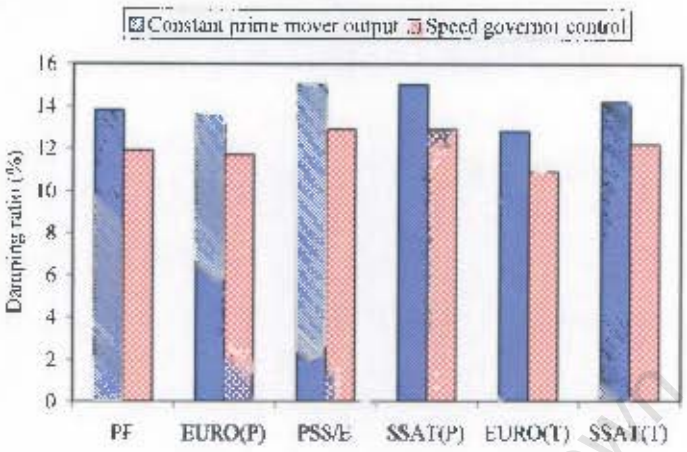

Figure 6.29: Effect of governor on the damping ratio of inter-area modes; AVR with PSS

with excitation controlled by AVR with PSS and speed governor control are more conservative than those obtained with constant prime mover output, as can be observed from figures 6.28 and 6.29. However, the percentage decrease in the damping and damping ratio is much lower than for the other excitation control configurations, as can be seen from Table 6.29. This observation can be attributed to the fact that the damping added by the excitation system is much higher than the negative damping added by the speed governor. For all the tools, the frequency increases by about 2.4% due to the addition of the speed governor.

The effect of speed voltage terms and turbine output modeling with speed governor control is as discussed earlier in subsection 6.2.3.1, for constant prime mover output.

6.3 Summary

Some variations in components modeling and algorithmic factors among the five tools, have been identified as possible causes of discrepancies in eigenvalue results obtained with the tools. These variations include modeling of generator saturation, speed voltage terms, and turbine output, and the techniques used for the construction of the state matrix. The impact of each factor on the local modes and the inter-area modes has been investigated.

For the three excitation control configurations, the effect of the three methods of representing generator saturation – total saturation, incremental saturation, and effective excitation – on the damping of the local modes has been found to be erratic. None of the three methods has a consistent effect on the damping of the local modes e.g. increase or decrease or has no effect on the damping, for the three excitation control configuration. For the inter-area modes, incremental saturation and effective excitation methods reduce the damping for all three excitation control configurations. Furthermore, the incremental saturation method has a higher impact on the damping than the effective excitation method. The effect of the total saturation method is inconsistent for the three excitation control configurations. The three saturation methods have very little effect on the frequency of both the local and inter-area modes, for the three excitation control configurations.

The impact of modeling of speed voltage terms was investigated with manual excitation control and excitation controlled by AVR without PSS. For these two excitation control configurations, consideration of speed deviation in speed voltage terms has been found to decrease the damping of both the local and inter-area modes, for the operating condition considered. However,

it has been shown that consideration of speed deviation enhances damping if the system is lightly loaded. The effect of the speed voltage terms is more significant with excitation controlled by AVR without PSS than with manual excitation control.

It has also been found that for the three excitation control configurations, the results obtained with T_m turbine output are more conservative than those obtained with P_m turbine output both with constant prime mover output and with speed governor control. The largest discrepancies are observed with manual excitation control and the smallest with excitation controlled by AVR with PSS. These observations are true for both the local and inter-area modes.

The method used for constructing the state matrix appears to have little effect on the electromechanical modes. However, this observation should be taken cautiously since the accuracy of numerical differentiation depends on the perturbation size chosen.

The results obtained for the local modes and the inter-area modes of the SMIB and 2A4G systems respectively, using the five tools, have been compared and some discrepancies observed. For all the cases that were simulated, results obtained with the five tools generally agree on the frequency of oscillation but differ on the damping (and damping ratio). It has been found that for the SMIB system with manual excitation control, results obtained with some tools predict a satisfactory damping ratio ($\zeta \geq 3\%$), whereas those obtained with other tools predict an unsatisfactory damping ratio for the local modes. Contradictory results were obtained with different tools for the 2A4G system with excitation controlled by AVR without PSS. For this case, the results obtained with some of the tools show that the inter-area modes

are stable whereas those obtained with other tools show that it is unstable. However, all the damping ratios obtained for this case are unsatisfactory. The discrepancies in results are due to variations in the factors discussed above.

For the three excitation control configurations, results obtained with speed governor control are more conservative than those obtained with constant prime mover output. This is due to the negative damping torque introduced by the speed governor.

Chapter 7

Quantification of discrepancies in results

The results obtained with five industrial-grade simulation tools for the electromechanical modes of the single machine infinite bus (SMIB) system and the two-area four-generator (2A4G) system agree on the frequency of oscillation but differ on the damping (and damping ratio), as seen in Chapter 6. The main factors that cause discrepancies in results obtained with the five tools have been identified as modeling of:

- generator saturation
- speed voltage terms
- turbine output.

Results presented in the same chapter show that the method used for constructing the $\boldsymbol{A}$ matrix does not cause significant discrepancies if the perturbation size used in numerical differentiation is well chosen.

The three methods used by the five tools for representing saturation effects have been identified as total saturation, incremental saturation, and effective

excitation. Comparing the results obtained using the five tools with saturation included and with saturation neglected, the effect of saturation on the electromechanical modes has been found to be erratic. In some cases, for the same excitation control configuration, results obtained with some tools indicate that saturation increases damping whereas those obtained with other tools indicate that saturation decreases damping. Hence, it is difficult to characterize the effect of saturation from the simulation results. Moreover, it has been found that saturation masks the effect of variations in modeling of speed voltage terms and turbine output, in some cases. An example of such a case is the 2A4G system with excitation controlled by AVR with PSS. The results obtained for this case are shown in Chapter 6, Fig. 6.22. It is observed from these results that with saturation included, the effect of speed voltage terms and turbine output on the inter-area modes is not apparent. However, with saturation neglected, the effect of these two modeling aspects is clear. Therefore, the results analyzed in this chapter are those that were obtained with saturation neglected.

In this chapter, quantification results of the impact of variations in modeling of speed voltage terms and turbine output on the damping ratios of the local and inter-area modes obtained for the SMIB and 2A4G systems, respectively are presented. Results obtained for the three excitation control configurations both with constant prime mover output and speed governor control, are analyzed. The results presented in Chapter 6 show that variations in modeling of speed voltage terms and turbine output do affect damping but they have negligible effect on frequency. Therefore, although the quantification analysis focuses on the damping ratio, the findings are also applicable to damping.

7.1 Manual excitation control

Figure 7.1 shows the quantification of discrepancies in the damping ratio of the local and inter-area modes, obtained with the five tools for manual excitation control and constant prime mover output. The information contained in each box includes; (i) the tool used for the simulation, (ii) in parenthesis, the models of speed voltage terms and turbine output used by the tool, and (iii) the damping ratio obtained with the tool ζ, in percentage. The numbers 1 to 7 are used to identify the tools and the associated damping ratios.

The discrepancy in damping ratio ε_{ij}, between results obtained with tool i and tool j is given by

$$\varepsilon_{ij} = \frac{\zeta_j - \zeta_i}{\zeta_i} \times 100 \tag{7.1}$$

where ζ_i and ζ_j are the damping ratios obtained with tools i and j, respectively.

Tool i is in the box where the arrow starts and tool j is in the one where the arrow ends. A positive value of ε_{ij} signifies that the damping ratio obtained with tool j is higher than that obtained with tool i, and vice versa. The cause of the discrepancy ε_{ij}, is deduced by comparing the modeling of speed voltage terms and turbine output by tools i and j. For example, referring to Fig. 7.1(a), the discrepancy between the results obtained using EUROSTAG($\omega_r\psi$, T_m) and SSAT(ψ, T_m), ε_{12} is 5.7%. The difference between the two simulation tools is the modeling of speed voltage terms i.e. EUROSTAG considers speed deviation ($\omega_r \neq 1$) whereas SSAT neglects it ($\omega_r = 1$). Therefore, it can be deduced that for T_m turbine output, neglecting the effect of speed deviation in speed voltage terms causes the damping ratio to increase by 5.7%.

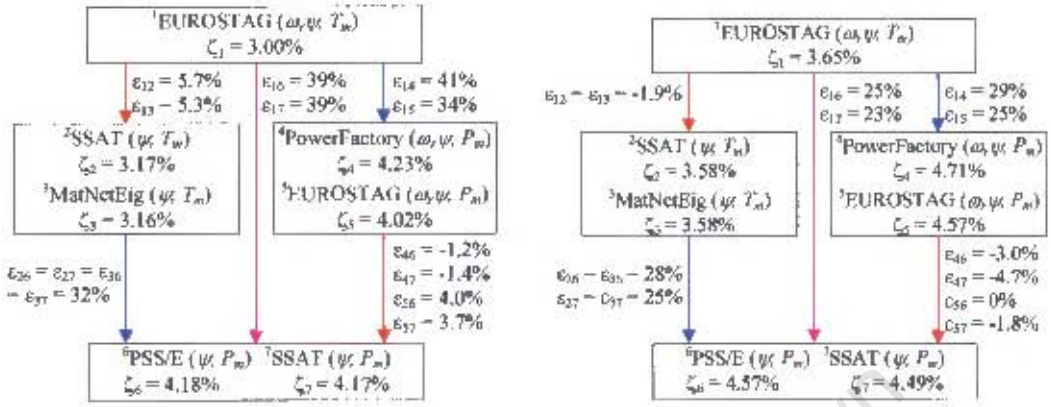

(a) Local modes (b) Inter-area modes

Figure 7.1: Quantification of discrepancies in results obtained with five tools; manual excitation control and constant prime mover output

It can be seen from Fig. 7.1 that for both the local and inter-area modes, the impact on the damping ratio of variation in modeling of speed voltage terms is lower than that of variation in modeling of turbine output. On average, the damping ratio obtained with tools that neglect speed deviation is higher than that obtained with tools that consider it by 2.7% and -2.2% for the local and inter-area modes, respectively. The negative sign signifies that the damping ratio obtained with tools that neglect speed deviation is lower than that obtained with those that do consider it. Additionally, on average, the damping ratio obtained with tools that employ P_m turbine output is higher than that obtained with tools that employ T_m turbine output by 34% and 27% for the local and inter-area modes, respectively.

It can be observed from Fig. 7.1(a) that the damping ratio obtained with PowerFactory (considers speed deviation) is higher than that obtained with PSS/E and SSAT (both tools neglect speed deviation) i.e. ε_{46} and ε_{47} are negative. From the investigations carried out to assess the impact on the local and inter-area modes of variation in modeling speed voltage terms, it has

been found that the damping ratio obtained with speed deviation neglected is higher than that obtained with speed deviation considered. Therefore, there are more variations than the modeling of speed voltage terms between PowerFactory on the one hand, and PSS/E and SSAT on the other hand. It can also be observed from Fig. 7.1(b) that the damping ratio of the inter-area modes obtained with tools that consider speed deviation in speed voltage terms is higher than that obtained with tools that neglect it. These results contradict the earlier finding, thus suggesting that there could be more variations among the tools. However, for the inter-area modes the discrepancies are small except for PowerFactory. Quantification results of the discrepancies in damping ratios of the electromechanical modes obtained using the same tool with different models of speed voltage terms and turbine output are presented later in this section.

It was noted in Chapter 3 that inclusion of rotor speed deviation in the speed voltage terms can "add" either positive or negative damping to the system. The magnitude and the sign of the "additional" damping depend on the parameters of the machine, the external network, and the operating condition i.e. the "additional" damping is system specific. Therefore, the discrepancies in the damping ratio caused by variation in modeling of speed voltage terms are not expected to be the same for the two power systems. However, for the operating condition considered for each power system, it has been found that the additional damping due to the inclusion of speed deviation is negative. Hence, for the same turbine output, the discrepancies in damping ratio due to variation in modeling of speed voltage terms, shown in Fig. 7.1 should be positive.

It was also noted in Chapter 3 that the amount of damping "added" by

the P_m turbine output is directly proportional to the generator loading and inversely proportional to the inertia constant, H. For the SMIB system, the generator is loaded at $P = 0.9\ pu$ and has $H = 3.5\ s$, whereas for the 2A4G system, the generators are loaded at about $P = 0.8\ pu$ and they have $H = 6.5\ s$ for those in area 1 and $H = 6.175\ s$ for those in area 2. Hence, the discrepancy in the damping ratio due to variation in turbine output is higher for the local modes than for the inter-area modes since the generator in the SMIB system is more heavily loaded and it has a lower inertia constant than those in the 2A4G system .

To eliminate the influence of other unidentified variations among the tools, EUROSTAG was used for investigating the impact of variations in modeling speed voltage terms and turbine output. That is, by using one tool for the investigations, it is possible to have control of the factor to vary and to ensure that all other factors – modeling, numerical methodology, accuracy of the solution etc. are identical. The results are shown in Fig. 7.2. EUROMAT denotes a combination of EUROSTAG and MATLAB i.e. the $\boldsymbol{A}$ matrix was obtained using EUROSTAG and then processed further to eliminate the effect of speed deviation as explained in Chapter 5. It was confirmed that the algorithm used by MATLAB for computing eigenvalues does not introduce significant discrepancies in results.

It can be seen from Fig. 7.2 that the damping ratios of both the local and the inter-area modes increase if speed deviation is neglected in speed voltage terms. For the inter-area modes, the percentage increase is small compared to the increase observed for the local modes.

It is possible that there are variations among the tools in other factors that have not been identified in this thesis. These factors have a greater influence

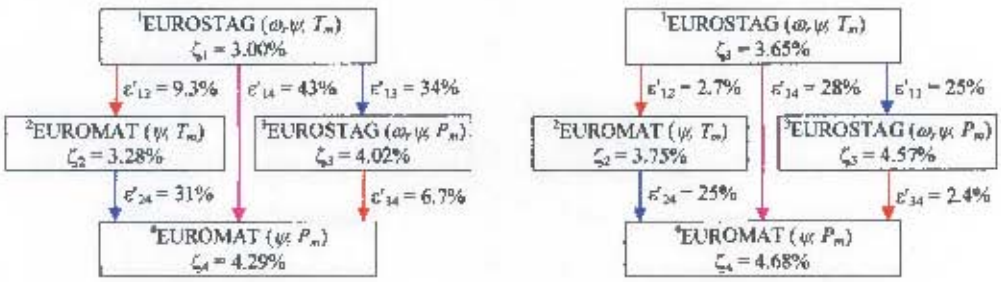

(a) Local modes (b) Inter-area modes

Figure 7.2: Quantification of discrepancies in results obtained with EUROSTAG/MATLAB; manual excitation control and constant prime mover output

on the damping ratio of the inter-area modes than the influence of speed voltage terms. Hence, the quantification results shown in Fig. 7.1(b) show that the damping ratio of the inter-area modes obtained with tools that consider speed deviation in speed voltage terms is higher than that obtained with tools that neglect it.

An example of other variations that were not investigated is the effect of considering the change in system frequency on electromechanical modes. PowerFactory considers the change in system frequency in network equations [52] whereas all the other tools neglect it. This might be the cause of the high damping ratios obtained with this tool for both the local and inter-area modes as observed in Fig. 7.1. For a better understanding of these results, there is a need for further investigations into the effect of variation in this modeling aspect on electromechanical modes.

Figure 7.3 shows the quantification of discrepancies in the damping ratio of the local and inter-area modes obtained with the five tools for manual excitation control and speed governor control.

The discrepancies in results obtained with speed governor control follow a

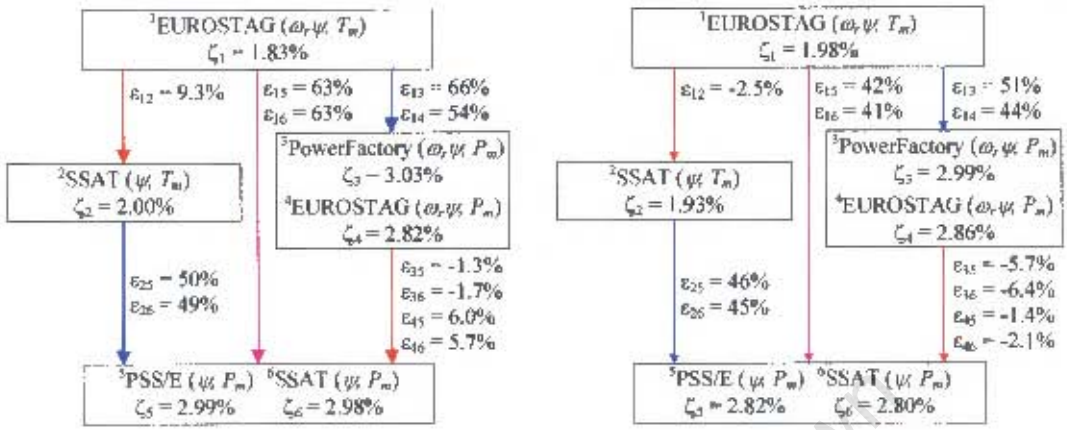

(a) Local modes (b) Inter-area modes

Figure 7.3: Quantification of discrepancies in results obtained with four tools; manual excitation control and speed governor control

trend similar to the one for constant prime mover control, as can be seen from Fig. 7.3. Comparing the results given in Fig. 7.3 with those of Fig. 7.1, it can be observed that for the same model of speed voltage terms, the discrepancies in the damping ratios of the local and inter-area modes obtained with tools that employ P_m turbine output and those obtained with tools that employ T_m turbine output are higher with speed governor control than with constant prime mover output.

It should be noted that for manual excitation control and speed governor control, the damping ratios of both local and inter-area modes obtained with the tools that employ T_m turbine output is unsatisfactory ($\zeta < 3\%$), whereas that obtained with tools that employ P_m turbine output is satisfactory (all values rounded-off to the nearest whole number). These results emphasize the fact that different conclusions can be drawn for the same power system from results obtained with different tools.

7.2 AVR without PSS

Figure 7.4 shows the quantification of discrepancies in the damping ratio of the local and inter-area modes obtained with the five tools, for excitation controlled by AVR without PSS and constant prime mover output. The negative damping ratios signify that the modes are unstable and in such cases the smaller the values, the higher the damping ratio.

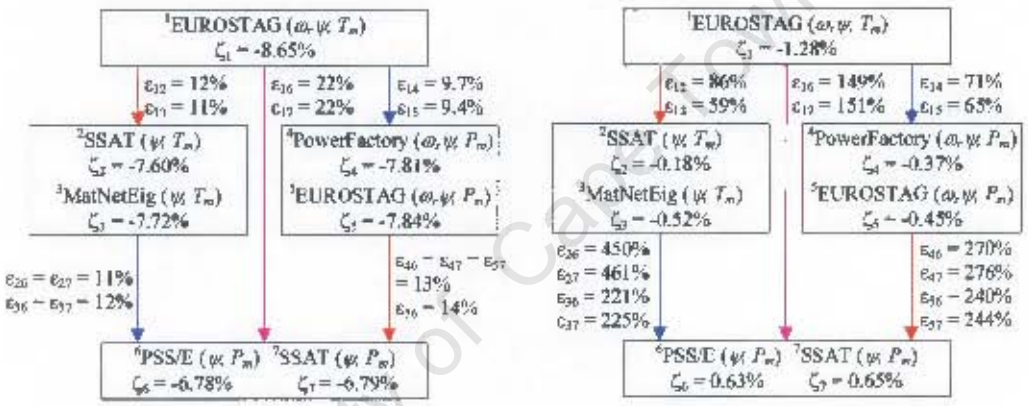

(a) Local modes (b) Inter-area modes

Figure 7.4: Quantification of discrepancies in results obtained with five tools; AVR without PSS and constant prime mover output

Comparing figures 7.1(a) and 7.4(a), it can be observed that the discrepancy due to the cumulative effect of variations in speed voltage terms and in turbine output is higher for manual excitation control than for excitation controlled by AVR without PSS. This may be due to the fact that, the negative damping that is introduced by the AVR is larger than the positive damping "added" by the inclusion of speed deviation and P_m turbine output.

For the inter-area modes, very high percentages are obtained for the impact of variations in modeling of speed voltage terms and turbine output, as seen from Fig. 7.4(b). The damping ratio of the inter-area modes with excitation

controlled by AVR without PSS is close to zero and thus any small deviations translate to large percentage changes. For example, the damping ratio obtained with SSAT(T) is -0.18% and that obtained with PSS/E is 0.63%. The difference between the two values is 0.81 but the percentage difference is 450%. However, it can be observed that the calculated discrepancies are all positive. Thus, these results agree with the findings that the damping ratio obtained with speed deviation neglected is higher than that obtained with speed deviation considered and the damping ratio obtained with P_m turbine output is higher than that obtained with T_m turbine output.

It should be noted that the damping ratio of the inter-area modes obtained with tools that neglect speed deviation in speed voltage terms and employ P_m turbine output (PSS/E and SSAT(P)) is positive, whereas that obtained with all the other tools is negative. This means that both PSS/E and SSAT(P) predict that the inter-area modes are stable and all the other tools predict that they are unstable. These contradictory results imply that different conclusions can be drawn on the stability of the same power system from results obtained using different tools. Thus, it is important that the variations among simulation tools are known and the impact of these variations on the damping of electromechanical modes is well understood.

For comparison purposes, the impact of variations in modeling of speed voltage terms and turbine output on the damping ratios of the local and inter-area modes was investigated using one tool. Figure 7.5 shows the quantification of discrepancies in the results that were obtained using EUROSTAG/MATLAB.

Comparing figures 7.4 and 7.5, it can be seen that the discrepancies in the damping ratio of local and inter-area modes obtained with the five tools

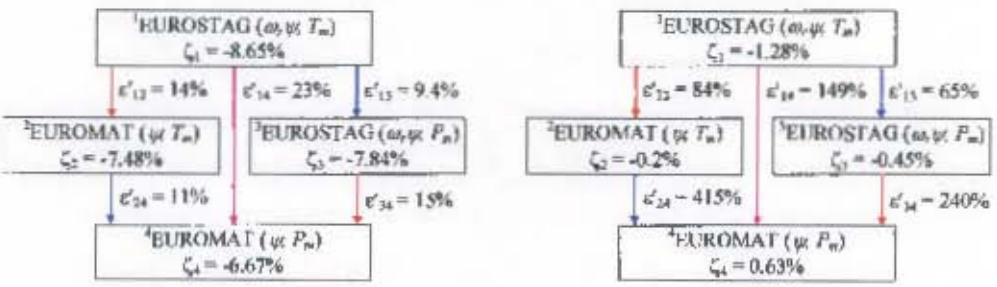

(a) Local modes (b) Inter-area modes

Figure 7.5: Quantification of discrepancies in results obtained with EUROSTAG/MATLAB; AVR without PSS and constant prime mover output

agree with those obtained with EUROSTAG/EUROMAT. In both cases, the results were obtained with excitation controlled by AVR without PSS and constant prime mover output.

Figure 7.6 shows the quantification of discrepancies in the damping ratio of the local and inter-area modes obtained with the five tools, for excitation controlled by AVR without PSS and speed governor control.

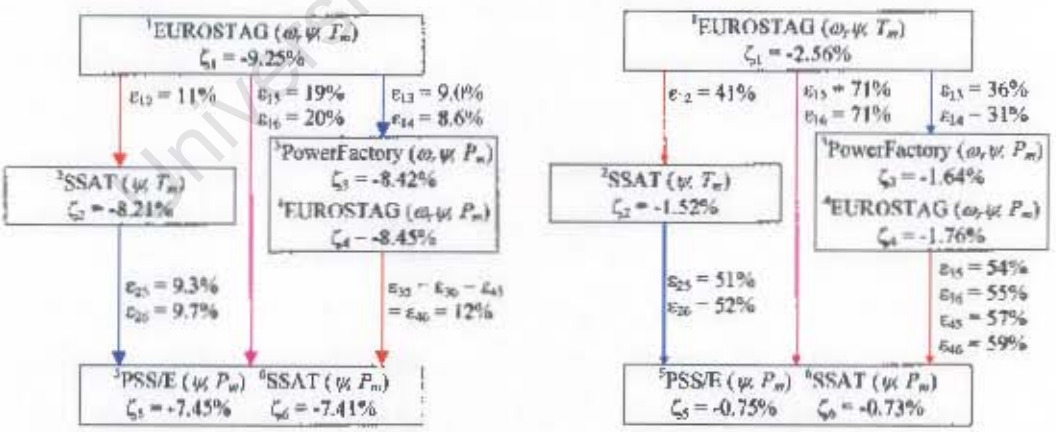

(a) Local modes (b) Inter-area modes

Figure 7.6: Quantification of discrepancies in results obtained with four tools; AVR without PSS and speed governor control

It can be seen from Fig. 7.6 that the discrepancies in results obtained with

speed governor control follow a trend similar to the one for constant prime mover control. On average, the damping ratio obtained with tools that neglect speed deviation is higher than that obtained with tools that consider it, by 11.8% and 53% for the local modes and inter-area modes, respectively. Additionally, on average, the damping ratio obtained with tools that employ P_m turbine output is higher than that obtained with tools that employ T_m turbine output by 9.2% and 42.5% for the local and inter-area modes, respectively.

7.3 AVR with PSS

Figure 7.7 shows the quantification of discrepancies in damping ratio of the local and inter-area modes obtained with the five tools, for excitation controlled by AVR with PSS and constant prime mover output.

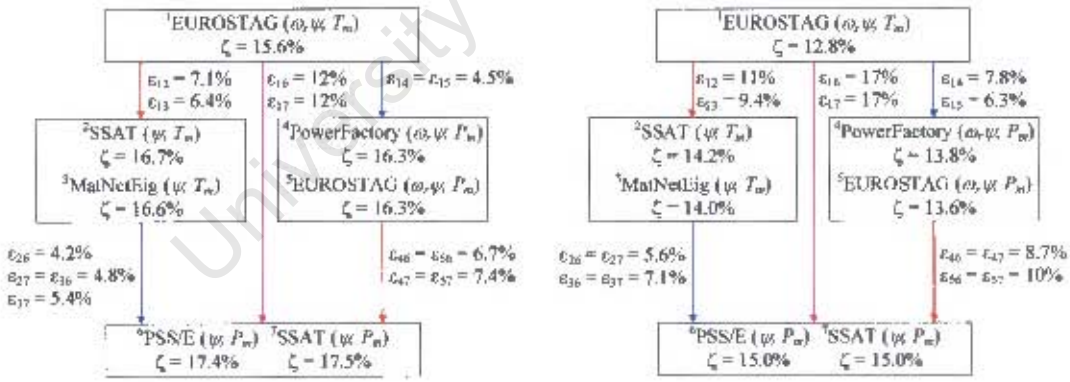

Figure 7.7: Quantification of discrepancies in results obtained with five tools; AVR with PSS and constant prime mover output

It can be observed from Fig. 7.7 that for both the local and inter-area modes, the impact on the damping ratio of variation in modeling of speed voltage

terms is higher than that of variation in modeling of turbine output. On average, the damping ratio obtained with tools that neglect speed deviation is higher than that obtained with tools that consider it by 6.9% and 9.7% for the local modes and inter-area modes, respectively. Additionally, on average, the damping ratio obtained with tools that employ P_m turbine output is higher than that obtained with tools that employ T_m turbine output by 4.7% and 6.6% for the local and inter-area modes, respectively.

Comparing figures 7.1(a), 7.4(a) and 7.7(a), it can be observed that the discrepancy due to the cumulative effect of variations in speed voltage terms and in turbine output is highest for manual excitation control, excitation controlled by AVR without PSS and AVR with PSS, in descending order. This may be due to the fact that, the AVR and PSS add damping to the system that is larger than the damping "added" by the inclusion of speed deviation and P_m turbine output, thus reducing the impact of these two modeling aspects.

Figure 7.8 shows the quantification of discrepancies in the damping ratio of the local and inter-area modes obtained with the five tools, for excitation controlled by AVR with PSS and speed governor control.

The discrepancies in results obtained with speed governor control follow a trend similar to the one for constant prime mover control as can be seen from Fig. 7.8. On average, the damping ratio obtained with tools that neglect speed deviation is higher than that obtained with tools that consider it by 7.5% and 9.8% for the local modes and inter-area modes, respectively. Moreover, on average, the damping ratio obtained with tools that employ P_m turbine output is higher than that obtained with tools that employ T_m turbine output by 4.8% and 7.0% for the local and inter-area modes, re-

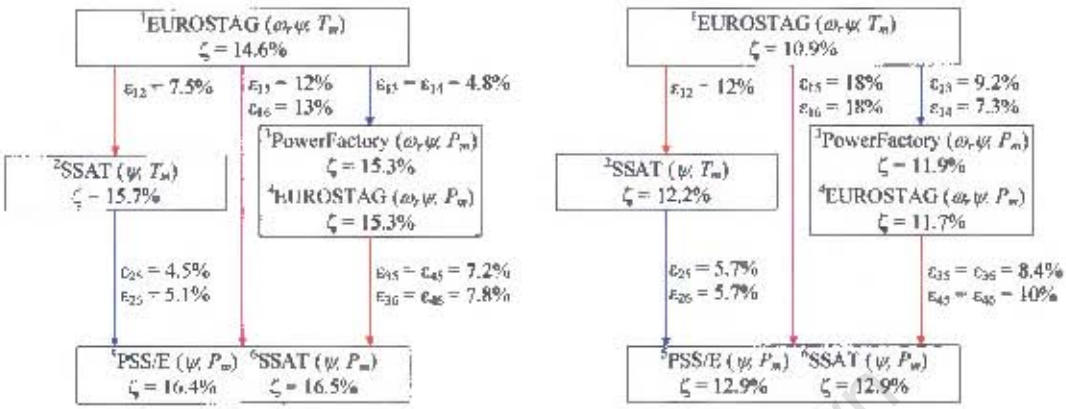

(a) Local modes (b) Inter-area modes

Figure 7.8: Quantification of discrepancies in results obtained with four tools; AVR with PSS and speed governor control

spectively. The discrepancy in the damping ratio obtained with tools that neglect speed deviation and employ P_m turbine output, and those that consider speed deviation and employ T_m turbine output is 12.5% and 18% for the local and inter-area modes, respectively.

7.4 Summary

The impact of variations in modeling of speed voltage terms and turbine output on the damping ratio of electromechanical modes has been quantified. The quantification results show that the impact of variation in turbine output is greater than that of variation in speed voltage terms, if the generator is on manual excitation control. Moreover, for this excitation control configuration, the disparities are wider with speed governor control than with constant prime mover output. That is, the percentage difference between results obtained with tools that employ P_m turbine output and those obtained with tools that employ T_m turbine output is higher with speed governor con-

trol than with constant prime mover output. However, with the excitation system on automatic control, the damping ratio is affected more by variation in speed voltage terms than the variation in turbine output.

The percentage increase in the damping ratio of the local modes due to the damping "added" by P_m turbine output is highest for manual excitation control and smallest for excitation controlled by AVR with PSS. This observation may be due to the fact that the damping added by the excitation system is much higher than the damping "added" by P_m turbine output. Thus, the differences in results are less with the excitation system on automatic control.

Chapter 8

Conclusions and Recommendations

8.1 Conclusions

In this thesis, the features and capabilities of five industrial-grade simulation tools – PSS/E, PowerFactory, EUROSTAG, SSAT, and MatNetEig – have been compared. The comparison is based on components modeling, numerical methodology, and tool flexibility in terms of data input and output. PSS/E was found to have the widest variety of generator models ranging from 2^{nd} (classical) to 8^{th} order. In addition, the five tools have 5^{th} and 6^{th} order models that are the required minimum representation, in stability studies, for round-rotor and salient pole machines, respectively. It has also been found that EUROSTAG, SSAT, and MatNetEig use analytical differentiation for constructing the $\boldsymbol{A}$ matrix, whereas PSS/E and PowerFactory use numerical differentiation. Unlike PowerFactory, for which the perturbation size is fixed at 10^{-3} by the vendor, PSS/E allows the user flexibility to choose the perturbation size. However, to make a good choice of perturbation size, some experience working with the tool is necessary. If the perturbation is

too small, the system becomes numerically unstable, whereas a large perturbation gives inaccurate results because the truncation error is high. All the five tools give eigenvalues. In addition, all the tools except PowerFactory give the $\boldsymbol{A}$ matrix.

The main objective of this thesis, was to investigate the five industrial-grade simulation tools with regard to small-signal stability application and this has been achieved. In the thesis, variations have been identified among the tools in components modeling and solution methodology. These variations include modeling of generator saturation, speed voltage terms, turbine output, and the method used for constructing the $\boldsymbol{A}$ matrix. The variations cause discrepancies in the results obtained with the five tools .

The five tools use either analytical or numerical differentiation for constructing the $\boldsymbol{A}$ matrix. This research has established that variations in the two methods do not introduce significant discrepancies in results i.e. analytical differentiation applies standard rules of differentiation on the system equations, whereas numerical differentiation approximates the derivatives of these equations using the finite difference method. However, it should be noted that the two differentiation methods give similar results if, and only if, the perturbation size used in numerical differentiation is well chosen. The five tools use the QR algorithm for computing eigenvalues. Therefore, it is considered that the discrepancies in the eigenvalue results are not related to the mathematical routines used by these programs.

Two power systems, the single machine infinite bus (SMIB) system and the two-area four-generator (2A4G) system, were used to investigate the impact of the variations in modeling and algorithmic factors on electromechanical modes. The SMIB system was used to study local modes and the 2A4G sys-

tem was used to study inter-area modes. The generators in the two systems were represented using 6^{th} order models. The complexity of the models was progressively increased from simple, manual excitation control and constant prime mover output, to full model with excitation system controlled by automatic voltage regulator (AVR) with power system stabilizer (PSS), and speed governor control.

The methods used by the five tools for representing saturation include total saturation, incremental saturation, and effective excitation. For the three excitation control configurations, saturation was found to have negligible effect on the frequency of both the local and the inter-area modes, using the three methods. However, for different excitation control configurations, the three methods of representing saturation have different effects on the damping of the electromechanical modes as follows:

Total saturation

For total saturation, the damping of the local modes increases marginally for manual excitation control. The damping also increases for excitation controlled by AVR only, and decreases marginally for excitation controlled by AVR with PSS. Additionally, the damping of the inter-area modes decreases marginally for manual excitation control, increases for excitation controlled by AVR only, and is unaffected for excitation controlled by AVR with PSS.

Incremental saturation

For incremental saturation, the damping of the local modes decreases for manual excitation control and for excitation controlled by AVR with PSS, and it increases for excitation controlled by AVR only. Furthermore, the

damping of the inter-area modes decreases for the three excitation control configurations.

Effective excitation

For effective excitation, the damping of the local modes increases for manual excitation control and for excitation controlled by AVR only. The damping of these modes decreases for excitation controlled by AVR with PSS. Additionally, the damping of the inter-area modes decreases for the three excitation control configurations.

It is evident that the impact of saturation on the damping of electromechanical modes is erratic. Thus, it is difficult to draw conclusions from the simulation results about the effect of saturation on damping.

For the three excitation control configurations, the damping of the local and inter-area modes, obtained with rotor speed deviation neglected in speed voltage terms, is higher than that obtained with speed deviation considered. It has been found in this thesis that consideration of rotor speed deviation in speed voltage terms can"add" either positive or negative damping to the system. The magnitude and the sign of the "additional" damping depend on the parameters of the machine, the external network, and the operating condition i.e. the "additional" damping is system specific. The additional damping is negative for a heavily loaded system and positive for a lightly loaded one.

Heavily loaded systems are the main concern in power system stability studies, since they can be a threat to system security as they are more likely to be unstable after a disturbance, than lightly loaded ones. Therefore, for these

systems, consideration of speed deviation in speed voltage terms reduces the damping of both the local and the inter-area modes. The discrepancy in damping caused by the variation in modeling of speed voltage terms is higher with excitation controlled by AVR than with manual excitation control. However, the effect of variation in modeling of speed voltage terms on the frequency is insignificant i.e. the change is less than 1%.

The damping of both the local and the inter-area modes, obtained with P_m turbine output, is higher than that obtained with T_m turbine output. This is due to the "additional" damping (positive) associated with the mechanical power-torque relationship of the turbine. The "additional" damping is directly proportional to the generator loading and inversely proportional to its inertia constant. Thus, with heavy loading, the "additional" damping is higher for a small generator (low inertia constant) than for a large one (high inertia constant). This observation has been found to be true for both constant prime mover output and speed governor control.

The results obtained for the local modes and the inter-area modes of the SMIB and 2A4G system respectively, using the five tools, have been compared. It has been found that for all the cases that were simulated, the results obtained with the five tools agree on the frequency but differ in damping. The largest discrepancies are observed with manual excitation control and the smallest with excitation controlled by AVR with PSS.

Comparing the results obtained using each of the five tools with saturation included and with saturation neglected, the effect of saturation on the damping of the local and the inter-area modes has been found to be erratic, for the three excitation control configurations. Moreover, for the same excitation control configuration, different effects of saturation were observed for tools

that employ the same method of representing saturation (total saturation). Thus, it is difficult to draw conclusions on the effect of saturation on the damping of local and inter-area modes from the results obtained with the five tools.

By comparing the results obtained with the five tools, it has been found that with manual excitation control, the damping of the local and the inter-area modes obtained with tools that employ P_m turbine output is higher than that obtained with tools that employ T_m turbine output. This is due to the "additional" damping associated with the mechanical power-torque relationship of the turbine. For this excitation control configuration, the impact on the damping of variation in the modeling of turbine output predominates over that of variation in the modeling of speed voltage terms.

It has also been found that with excitation controlled by AVR only and with PSS, the highest damping of both the local and the inter-area modes is obtained with tools that neglect speed deviation in speed voltage terms and employ P_m turbine output. Moreover, the lowest damping is obtained with tools that consider speed deviation in speed voltage terms and employ T_m turbine output. For these excitation control configurations, the impact on damping of variation in the modeling of turbine output is comparable to that of variation in the modeling of speed voltage terms. Furthermore, inclusion of speed deviation in speed voltage terms "adds" negative damping and the use of P_m turbine output "adds" positive damping i.e. the two have opposite effects on the damping. Hence, the highest damping is obtained if only positive damping is added (neglect speed deviation and consider P_m turbine output) and the lowest is obtained if only negative damping is added (consider speed deviation and T_m turbine output).

The five tools gave contradictory results for some of the simulated cases. The following discussion highlights only the cases that gave contradictory results.

- **SMIB system**
  - **Manual excitation control, saturation included, and constant prime mover output**: The damping ratio of the local modes obtained using SSAT with incremental saturation and turbine output modeled as mechanical torque (SSAT(T-i)) is unsatisfactory (less than 3 %) whereas that obtained with all the other tools is satisfactory.
  - **Manual excitation control, saturation neglected, and with speed governor control**: The damping ratio of the local modes obtained with PowerFactory, EUROSTAG(P), PSS/E, and SSAT(P) is satisfactory, whereas that obtained with EUROSTAG(T) and SSAT(T) is unsatisfactory.
- **2A4G system**
  - **Manual excitation control, saturation neglected, and with speed governor control**: The damping ratio of the inter-area modes obtained with PowerFactory, EUROSTAG(P), PSS/E, and SSAT(P) is satisfactory, whereas that obtained with EUROSTAG(T) and SSAT(T) is unsatisfactory.
  - **Excitation controlled by AVR only, both with saturation included and with saturation neglected, and constant prime mover output**: The damping ratio of the inter-area modes obtained with PSS/E and SSAT(P) is positive (predicting the modes are stable) whereas that obtained with PowerFactory,

EUROSTAG, SSAT(T), and MatNetEig is negative (predicting instability).

The discrepancies in the results are caused by variations among the tools in the turbo-generator modeling aspects discussed in this thesis. These contradictory results imply that different conclusions can be drawn regarding the stability of the same power system, from results obtained using different tools. Therefore, it is important that the variations among simulation tools are taken into consideration and the impact of these variations on the damping of electromechanical modes is well understood.

For all the tools, the damping ratio of both the local and the inter-area modes obtained with speed governor control are lower than those obtained with constant prime mover output. This is due to the negative damping added by the speed governor. Therefore, for accurate representation of the power system, the governor should be modeled.

Although small benchmark power systems were studied, with different industrial-grade and state-of-the-art tools, different eigenvalue results were obtained that were contradictory for some cases. For a large and more complex system (real power system), the disparities in results may be wider and thus more prominent. It is difficult to deduce from this study which modeling approach most accurately represents the behavior of a real power system. Such a conclusion can only be made after comparing field measurements with the softwares' output results.

8.2 Recommendations

In this thesis, it has been found that for different excitation control configurations, the three methods of representing saturation have different effects on the damping of the electromechanical modes. However, for all three excitation control configurations, generator saturation reduces both the d-axis and q-axis inductances for round-rotor machines. Therefore, for the three excitation control configurations, it is expected that the general effect of saturation on damping should be similar (increase, decrease, or have no effect on damping) for the three methods of representing saturation. It is also expected that for the same excitation control configuration, the effect of saturation on damping should be similar for tools that employ the same method of representing saturation. The results obtained from the investigations carried out in this research are inconclusive. Thus, further work is necessary to determine the cause of the inconsistencies.

For both the local and the inter-area modes, the results obtained with PowerFactory with manual excitation control and with saturation neglected are the most optimistic. This is despite the fact that PowerFactory considers speed deviation in speed voltage terms, which has been found to "add" negative damping, thereby decreasing the damping of the electromechanical modes. In addition, with manual excitation control, the damping of the inter-area modes obtained with the tools that neglect speed deviation in speed voltage terms is lower than that obtained with those that consider it, for the same model of turbine output. These observations suggest that there are more variations in modeling and/or algorithmic factors among the tools than the ones identified in this thesis. One of the factors that may have affected the damping obtained with PowerFactory with manual excitation control is the

consideration of the effect of system frequency in network equations. All the other tools neglect the change in system frequency. There is a need for further investigation into the effect of considering the change in system frequency on electromechanical modes.

The power systems studied in this research are small benchmark systems. Therefore, the findings of this work should be verified for a larger power system (real system).

References

[1] G. Andersson, P. Donalek, R. Farmer, N. Hatziargyriou, I. Kamwa, P. Kundur, N. Martins, J. Paserba, P. Pourbeik, J. Sanchez-Gasca, R. Schulz, A. Stankovic, C. Taylor, and V. Vittal, "Causes of the 2003 major grid blackouts in North America and Europe, and recommended means to improve system dynamic performance," *IEEE Transactions on Power Systems*, vol. 20, pp. 1922–1928, November 2005.

[2] U.S.-Canada Power System Outage Task Force, "Final Report on the August 14th, 2003 blackout in the United States and Canada: Causes and recommendations," tech. rep., April 2004.

[3] V. Vittal, "Consequence and impact of electric power utility industry restructuring on transient stability and small-signal stability analysis," *Proceedings of the IEEE*, vol. 88, pp. 196–207, February 2000.

[4] E. S. Ibrahim, "A comparative study of PC based software packages for power engineering education and research," *International Journal of Electrical Power and Energy Systems*, vol. 24, pp. 799 – 805, December 2002.

[5] J. Persson, J.G. Slootweg, L. Rouco, L. Söder, and W.L. Kling, "A comparison of eigenvalues obtained with two dynamic simulation software packages," in *2003 IEEE Bologna Power Tech Conference*, (Bologna, Italy), 2003.

[6] J.G. Slootweg , J. Persson, A. M. van Voorden, G. C. Paap, and W. L. Kling, "A study of the eigenvalue analysis capabilities of power system dynamics simulation software," in *14th PSCC*, (Sevilla), 2002.

[7] P. Kundur, *Power System Stability and Control*. McGraw-Hill, 1994.

[8] E. Kyriakides and R.G. Farmer, "Modeling of damping for power system stability analysis," *Journal of Electric Power Components and Systems*, vol. 32, no. 8, pp. 827–837, 2004.

[9] *DSATools^{TM} , SSAT User Manual*, April 2006.

[10] *MatNetEig User Manual*, 2005.

[11] Power Technologies International, *PSS/E^{TM} 30.2 Program Application Guide: Volume II*, November 2005.

[12] *DIgSILENT Manuals, DIgSILENT PowerFactory, Version 13*, 2004.

[13] *EUROSTAG Release 4.2 Package Documentation Part I*, October 2002.

[14] K. Kaberere, A. Petroianu, and K. Folly, "Analytical investigation of the effect of generator modelling on electromechanical mode damping," in *IFAC 2006 Symposium on Power Plants and Power Systems Control*, (Kananaskis, Canada), 25-28 June 2006.

[15] K.K. Kaberere, K.A. Folly, M. Ntombela, and A.I. Petroianu, "Comparative analysis and numerical validation of industrial-grade power system simulation tools: Application to small-signal stability," in *15th PSCC*, (Liège, Belgium), 22-26 August 2005.

[16] K.K. Kaberere, M. Ntombela, K.A. Folly, and A.I. Petroianu, "Comparison of industrial-grade analytical tools used in small-signal stability assessment," in *AUPEC 2005*, vol. 1, (Hobart, Tasmania, Australia), pp. 147–152, University of Tasmania, 25-28 September 2005.

[17] CIGRE Task Force 38.01.07 on Power System Oscillations, "Analysis and control of power system oscillations," Final Report CIGRE Technical Brochure 111, December 1996.

[18] C. Taylor, "Improving grid behavior," *IEEE Spectrum*, pp. 40–45, June 1999.

[19] D.N. Kosterev, C.W. Taylor, and W.A. Mittelstadt, "Model validation for the August 10, 1996 WSCC system outage," *IEEE Transactions on Power Systems*, vol. 14, pp. 967–979, August 1999.

[20] E. Kyriakides, G.T. Heydt, and V. Vittal, "Online parameter estimation of round rotor synchronous generators including magnetic saturation," *IEEE Transactions on Energy Conversion*, vol. 20, pp. 529–537, 2005.

[21] J.W. Feltes and L.T.G. Lima, "Validation of dynamic model parameters for stability analysis: Industry need, current practices and future trends," in *IEEE PES General Meeting*, vol. 3, pp. 1295–1301, 13-17 July 2003.

[22] P. Ju, E. Handschin, and D. Karlsson, "Nonlinear dynamic load modelling: model and parameter estimation," *IEEE Transactions on Power Systems*, vol. 11, pp. 1689–1697, November 1996.

[23] V. Knyazkin, C.A. Cañizares, and L.H. Söder, "On the parameter estimation and modelling of aggregate power system loads," *IEEE Transactions on Power Systems*, vol. 19, pp. 1023–1031, May 2004.

[24] J.W. Feltes, S. Orero, B. Fardanesh, E. Uzunovic, S. Zelingher, and N. Abi-Samra, "Deriving model parameters from field test measurements," *IEEE Computer Applications in Power*, pp. 30–36, October 2002.

[25] IEEE/CIGRE Joint Task Force on Stability Terms and Definitions, "Definition and classification of power system stability," *IEEE Transactions on Power Systems*, vol. 19, pp. 1387–1401, May 2004.

[26] M. Pavella, D. Ernst, and D. Ruiz-Vega, *Transient Stability of Power Systems: A Unified Approach to Assessment and Control.* Kluwer Academic Publishers, 2000.

[27] "IEEE Guide for Synchronous Generator Modelling Practices in Stability Analyses," IEEE Std 1110-1991, 1991.

[28] G. Liu, Z. Xu, Y. Huang, and W. Pan, "Analysis of inter-area oscillations in the South China interconnected power system," *Electric Power Systems Research*, vol. 70, pp. 38–45, June 2004.

[29] A. Elices, L. Rouco, H. Bourlès, and T. Margotin, "Design of robust controllers for damping interarea oscillations: Application to the European power system," *IEEE Transactions on Power Systems*, vol. 19, pp. 1058–1067, May 2004.

[30] W. Kao, "The effect of load models on unstable low-frequency oscillation damping in Taipower system system experience w/wo power system stabilizers," *IEEE Transactions on Power Systems*, vol. 16, pp. 463–472, August 2001.

[31] F. Aboytes, F. Sanchez, A.I.M. Cabra, and J.E.G. Castro, "Dynamic stability analysis of the interconnected Colombia-Venezuela power system," *IEEE Transactions on Power Systems*, vol. 15, pp. 376–381, February 2000.

[32] H. Breulmann, E. Grebe, M. Lösing, W. Winter, R. Witzmann, P. Dupuis, M.P. Houry, T. Margotin, J. Zerenyi, J. Dudzik, J. Machowski,

L. Martín, J.M. Rodríguez,and E. Urretavizcaya, "Analysis and damping of inter-area oscillations in the UCTE/CENTREL power system," in *Cigre 38-113 Session 2000.*

[33] J. Hauer, D. Trudnowski, G. Rogers, B. Mittelstadt, W. Litzenberger, and J. Johnson, "Keeping an eye on power system dynamics," *IEEE Computer Applications in Power*, pp. 50–54, 1997.

[34] P. Anderson, "Power system oscillations - summary of utility experience," in *Inter-Area Oscillations in Power systems*, no. IEEE Publication 95 TP 101, pp. 43–54, October 1994.

[35] Y. Hsu, S. Shyue, and C. Su, "Low frequency oscillations in longitudinal power systems: Experience with dynamic stability of Taiwan power system," *IEEE Transactions on Power Systems*, vol. PWRS-2, pp. 92–100, February 1987.

[36] C.Y. Chung, L. Wang, F. Howell, and P. Kundur, "Generation rescheduling methods to improve power transfer capability constrained by small-signal stability," *IEEE Transactions on Power Systems*, vol. 19, pp. 524–530, February 2004.

[37] N. Mithulananthan, C.A. Cañizares, J. Reeve, and G.J. Rogers, "Comparison of PSS, SVC, and STATCOM controllers for damping power system oscillations," *IEEE Transactions on Power Systems*, vol. 18, pp. 786–792, May 2003.

[38] W. Fang and H.W. Ngan, "Enhancing small signal power system stability by coordinating unified power flow controller with power system stabilizer," *Electric Power Systems Research*, vol. 65, pp. 91–99, May 2003.

[39] M.M. Farsangi, Y.H. Song, and K.Y. Lee, "Choice of FACTS device control inputs for damping interarea oscillations," *IEEE Transactions on Power Systems*, vol. 19, pp. 1135–1143, May 2004.

[40] A.D. Del Rosso, C.A. Cañizares, and V.M. Dona, "A study of TCSC controller design for power system stability improvement," *IEEE Transactions on Power Systems*, vol. 18, pp. 1487–1496, November 2003.

[41] X. Yu, M. Khammash, and V. Vittal, "Robust design of a damping controller for Static Var Compensators in power ystems," *IEEE Transactions on Power Systems*, vol. 16, pp. 456–462, August 2001.

[42] D. Povh, "Use of HVDC and FACTS," *Proceedings of the IEEE*, vol. 88, pp. 235–245, February 2000.

[43] H.F. Wang and F.J. Swift, "A unified model for the analysis of FACTS devices in damping power system oscillations part I: Single-machine infinite-bus power systems," *IEEE Transactions on Power Delivery*, vol. 12, pp. 941–946, April 1997.

[44] J.J. Paserba, E.V. Larsen, C.E. Grund, and A. Murdoch, "Mitigation of inter-area oscillations by control," in *Inter-Area Oscillations in Power systems*, no. IEEE Publication 95 TP 101, pp. 103–117, October 1994.

[45] Power System Damping Ad Hoc Task Force of the Power System Dynamic Performance Committee, "Damping representation for power system stability studies," *IEEE Transactions on Power Systems*, vol. 14, no. No. 1, pp. 151–157, 1999.

[46] J.H. Mathews and K.K. Fink, *Numerical Methods Using MATLAB.* Prentice-Hall Inc., 4th ed., 2004.

[47] A. Ostermann, "Sensitivity analysis," in *Analyzing Uncertainty in Civil Engineering*, pp. 100–114, Berlin: Springer, 2004.

[48] P. Kundur, G.J. Rogers, D.Y. Wong, L. Wang, and M.G. Lauby, "A comprehensive computer program package for small signal stability analysis of power systems," in *Inter-area Oscillations in Power Systems*, no. IEEE Publication 95 TP 101, pp. 60–67, October 1994.

[49] G. Rogers, *Power System Oscillations.* Kluwer Academic, 2000.

[50] U. Bachmann, F. Berger, R. Reinisch, I. Erlich, M. Hausler, M. Losing, D. Quadflieg, U. Radtke, J. Rittiger, N. Schnurr, and W.H. Wellssow, "Possibilities of multifunctional FACTS application in the European electric power system under the changing conditions of the liberalized electricity market," Available: http://www.uni-duisburg.de/FB9/EAUN/downloads/papers/cigre2002.pdf.

[51] G. Strang, *Linear Algebra and its Applications.* Harcourt Brace Jovanovich College Publishers, 3rd ed., 1988.

[52] "Personal communication."

[53] E.E.S. Lima and L.F.J. Fernandes, "Assessing eigenvalue sensitivities," *IEEE Transactions on Power Systems*, vol. 15, pp. 299–306, February 2000.

[54] E.E.S. Lima, "A sensitivity analysis of eigenstructures," *IEEE Transactions on Power Systems*, vol. 12, pp. 1393–1399, August 1997.

[55] P. Frank, *Introduction to System Sensitivity Theory.* Academic Press, 1978.

[56] E.D. Smith, F. Szidarovszky, W.J. Karnavas, and A.T. Bahill, "Sensitivity analysis, a powerful system validation tool," Available: http://www.sie.arizona.edu/sysengr/sie442/sensit.doc.

[57] A.M. El-Serafi and N.C. Kar, "Methods for determining the intermediate-axis saturation characteristics of salient-pole synchronous machines from the measured d-axis characteristics," *IEEE Transactions on Energy Conversion*, vol. 20, no. 1, pp. 88–97, 2005.

[58] D.C. Aliprantis, S.D. Sudhoff, and B.T. Kuhn, "Experimental characterization procedure for a synchronous machine model with saturation and arbitrary rotor network representation," *IEEE Transactions on Energy Conversion*, vol. 20, pp. 595–603, September 2005.

[59] D.C. Aliprantis, S.D. Sudhoff, and B.T. Kuhn, "A synchronous machine model with saturation and arbitrary rotor network representation," *IEEE Transactions on Energy Conversion*, vol. 20, pp. 584–594, September 2005.

[60] P. M. Anderson and A. A. Fouad, *Power System Control and Stability.* IEEE Press, 2nd ed., 2003.

[61] N.C. Kar, T. Murata, and J. Tamura, "Effects of synchronous machine saturation, circuit parameters, and control systems on transient stability," *Journal of Electric Machines and Power Systems*, vol. 28, pp. 663–675, 2000.

[62] N.C. Kar and J. Tamura, "Effects of synchronous machine saturation, circuit parameters, and control systems on steady state stability," *Journal of Electric Machines and Power Systems*, vol. 27, pp. 327–342, 1999.

[63] K.A. Corzine, B.T. Kuhn, S.D. Sudhoff, and H.J. Hegner, "An improved method for incorporating magnetic saturation in the Q-D synchronous machine model," *IEEE Transactions on Energy Conversion*, vol. 13, pp. 270–274, September 1998.

[64] S.H. Minnich, R.P. Schulz, D.H. Baker, R.G. Farmer, D.K. Sharma, and J.H. Fish, "Saturation functions for synchronous generators from

finite elements," *IEEE Transactions on Energy Conversion*, vol. EC-2, pp. 680–692, December 1987.

[65] F.P. de Mello and L.N.Hannett, "Representation of saturation in synchronous machines," *IEEE Transactions on Power Systems*, vol. PWRS-1, pp. 8–18, November 1986.

[66] S. Minnich, "Small signals, large signals, and saturation in generator modeling," *IEEE Transactions on Energy Conversion*, vol. EC-1, pp. 94–102, March 1986.

[67] P. Vas, K.E. Hallenius, and J.E. Brown, "Cross-saturation in smooth-air-gap electrical machines," *IEEE Transactions on Energy Conversion*, vol. EC-1, pp. 103–112, March 1986.

[68] IEEE Task Force on Definitions and Procedures, "Current usage & suggested practices in power system stability simulations for synchronous machines," *IEEE Transactions on Energy Conversion*, vol. EC-1, no. 1, pp. 77–93, 1986.

[69] J.C. Flores, G.W. Buckley, and G. McPherson, Jr., "The effects of saturation on the armature leakage reactance of large synchronous machines," *IEEE Transactions on Power Apparatus and Systems*, vol. PAS-103, pp. 593–600, March 1984.

[70] P. Kundur and P.L. Dandeno, "Implementation of advanced generator models into power system stability programs," *IEEE Transactions on Power Apparatus and Systems*, vol. PAS-102, no. 7, pp. 2047–2054, 1983.

[71] R.G. Harley, D.J.N. Limebeer, and E. Chirricozzi, "Comparative study of saturation methods in synchronous machine models," *IEE Proceeding B*, vol. 127, pp. 1–7, January 1980.

[72] G. Shackshaft and P. B. Henser, "Model of generator saturation for use in power system studies," *Proc. IEE*, vol. 126, pp. 759–763, August 1979.

[73] P.L. Dandeno, P. Kundur, and R.P. Schulz, "Recent trends and progress in synchronous machine modeling in the electric utility industry," *Proceeding of the IEEE*, vol. 62, no. 7, pp. 941–950, 1974.

[74] A.R. Bergen and V. Vittal, *Power Systems Analysis*. Prentice-Hall Inc., 2nd ed., 2004.

[75] P.C. Krause, F. Nozari, T.L. Skvarenina, and D.W. Olive, "The theory of neglecting stator transients," *IEEE Transactions on Power Apparatus and Systems*, vol. PAS-98, no. 1, pp. 141–148, 1979.

[76] E. Johansson, J. Persson, L. Lindkvist, and L. Söder, "Location of eigenvalues influenced by different models of synchronous machines," in *sixth IASTED International Conference Power and Energy Systems*, (Marina del Rey, California, USA), 2002.

[77] P.W. Sauer and M.A. Pai, *Power system dynamics and stability.* Prentice-Hall, 1998.

[78] IEEE Committee Report, "Dynamic models for steam and hydro turbines in power system studies," *IEEE Transactions on Power Apparatus and Systems*, vol. PAS-92, pp. 1904–1915, 1973.

[79] J.M. Undrill and T.F. Laskowski, "Model selection and data assembly for power system simulations," *IEEE Transactions on Power Apparatus and Systems*, vol. PAS-101, no. No. 9, pp. 3333–3341, 1982.

[80] *DIgSILENT Manuals, DIgSILENT PowerFactory, Version 12*, 2002.

[81] IEEE Task Force on Load Representation for Dynamic Performance, "Load representation for dynamic performance analysis," *IEEE Transactions on Power Systems*, vol. 8, pp. 472–482, May 1993.

[82] M. Sanaye-Pasand, H. Seyedi, H. Lesani, and M.R. Dadashzadeh, "Simulation and analysis of load modelling effects on power system transient stability," in *AUPEC 2005*, vol. 2, (Hobart, Tasmania, Australia), pp. 426–430, University of Tasmania, 25-28 September 2005.

[83] N. Martins and L.T.G. Lima, "Eigenvalue and frequency domain analysis of small-signal electromechanical stability problems," in *IEEE Symposium on Application of Eigenanalysis and Frequency Domain Methods for System Dynamic Performance*, 90 TH 0292-3 PWR, pp. 17–33, 1989.

[84] M. Klein, G. J. Rogers, and P. Kundur , "A fundamental study of inter-area oscillations in power systems," *IEEE Transactions on Power Systems*, vol. 6, pp. 914–921, August 1991.

[85] J. Arrillaga and C.P. Arnold, *Computer analysis of power systems.* John Wiley & Sons Ltd., 1990.

[86] Y. Yu, *Electric Power System Dynamics.* Academic Press, 1983.

Appendices

Appendix A

Generator modeling

This appendix is divided into three sections. In the first section, expressions for saturation constants A_{sat} and B_{sat} are derived. In the second section, expressions for elements a_{ij} of the $\boldsymbol{A}$ matrix for a SMIB system are given. The generator is represented using a 6^{th} order model and is on manual control. Rotor speed deviation is considered in the calculation of the stator voltage and saturation is neglected. In the third section, the step-by-step linearization of the swing equation is presented.

A.1 Expressions for saturation constants, A_{sat} and B_{sat}

Figure A.1 refers.

$$\begin{aligned} S_{1.0} &= \frac{I_{A1.0} - I_{B1.0}}{I_{B1.0}} \\ S_{1.2} &= \frac{I_{A1.2} - I_{B1.2}}{I_{B1.2}} = \frac{I_{A1.2} - 1.2I_{B1.0}}{1.2I_{B1.0}} \end{aligned} \tag{A.1}$$

$$\begin{aligned} \psi_{I1.0} &= 1.0S_{1.0} = A_{sat}e^{B_{sat}(1.0-\psi_{T1})} \\ \psi_{I1.2} &= 1.2S_{1.2} = A_{sat}e^{B_{sat}(1.2-\psi_{T1})} \end{aligned} \tag{A.2}$$

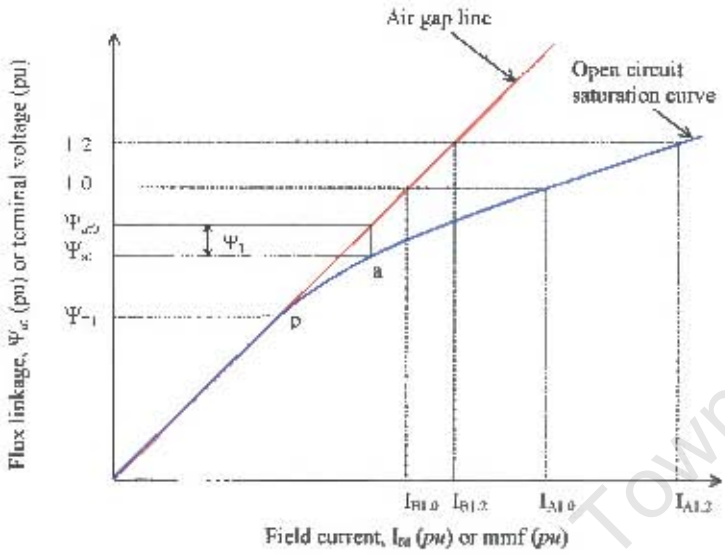

Figure A.1: Typical open-circuit saturation curve

From A.2

$$\ln\left(\frac{S_{1.0}}{A_{sat}}\right) = B_{sat}(1.0 - \psi_{T1})$$
$$\ln\left(\frac{1.2S_{1.2}}{A_{sat}}\right) = B_{sat}(1.2 - \psi_{T1}) \tag{A.3}$$

From A.3

$$B_{sat} = \frac{1}{1.0 - \psi_{T1}} \ln\left(\frac{S_{1.0}}{A_{sat}}\right) = \frac{1}{1.2 - \psi_{T1}} \ln\left(\frac{1.2S_{1.2}}{A_{sat}}\right) \tag{A.4}$$

Re-arranging A.4

$$\left(\frac{S_{1.0}}{A_{sat}}\right)^{(1.2-\psi_{T1})} = \left(\frac{1.2S_{1.2}}{A_{sat}}\right)^{(1.0-\psi_{T1})} \tag{A.5}$$

Making A_{sat} the subject

$$A_{sat}^{\frac{1}{5}} = \frac{S_{1.0}^{1.2-\psi_{T1}}}{(1.2S_{1.2})^{1.0-\psi_{T1}}} \tag{A.6}$$

Hence

$$A_{sat} = \frac{S_{1.0}^{1+5(1-\psi_{T1})}}{(1.2S_{1.2})^{5(1-\psi_{T1})}} \tag{A.7}$$

Substituting A.7 in A.3

$$B_{sat}(1.0-\psi_{T1}) = \ln\left[S_{1.0}\left(\frac{(1.2S_{1.2})^{1.0-\psi_{T1}}}{S_{1.0}^{1.2-\psi_{T1}}}\right)^{5}\right] \tag{A.8}$$

Expanding A.8

$$B_{sat}(1.0-\psi_{T1}) = \ln S_{1.0} + 5\ln\frac{(1.2S_{1.2})^{1.0-\psi_{T1}}}{S_{1.0}^{1.2-\psi_{T1}}} \tag{A.9}$$

Giving

$$B_{sat} = \ln S_{1.0}^{\frac{1}{1.0-\psi_{T1}}} + \ln\left(\frac{(1.2S_{1.2})^{1.0-\psi_{T1}}}{S_{1.0}^{1.2-\psi_{T1}}}\right)^{\frac{5}{1.0-\psi_{T1}}} \tag{A.10}$$

Simplifying A.10 gives

$$\boxed{B_{sat} = 5\ln\left(\frac{1.2S_{1.2}}{S_{1.0}}\right)} \tag{A.11}$$

A.2 Coefficients for the 6^{th} order system – rotor speed deviation considered

$$m_1 = -\frac{X_{Tq0}L''_{ad}}{L_{fd}D_0} \qquad m_2 = -\frac{X_{Tq0}L''_{ad}}{L_{1d}D_0}$$

$$m_3 = \frac{R_T L''_{aq}}{L_{1q}D_0} \qquad m_4 = \frac{R_T L''_{aq}}{L_{2q}D_0}$$

$$m_5 = -\frac{L''_{ad}X_{Tq0}\psi_{fd0}}{D_0L_{fd}} - \frac{L''_{ad}X_{Tq0}\psi_{1d0}}{L_{1d}D_0} + \frac{L''_{aq}R_T\psi_{1q0}}{L_{1q}D_0} + \frac{L''_{aq}R_T\psi_{2q0}}{L_{2q}D_0} - \frac{E_{qN0}L''_q}{D_0} + \left(\frac{X_{Tq0}E_{qN0}+R_TE_{dN0}}{D_0^2}\right)\left(X_{Td0}L''_q + X_{Tq0}L''_d\right)$$

$$m_6 = \frac{(X_{Tq0}E_{B0}\sin\delta_0 - R_TE_{B0}\cos\delta_0)}{D_0}$$

$$n_1 = -\frac{R_TL''_{ad}}{L_{fd}D_0} \qquad n_2 = -\frac{R_TL''_{ad}}{L_{1d}D_0}$$

$$n_3 = -\frac{X_{Td0}L''_{aq}}{L_{1q}D_0} \qquad n_4 = -\frac{X_{Td0}L''_{aq}}{L_{2q}D_0}$$

A.2. COEFFICIENTS FOR THE 6^{th} ORDER SYSTEM – ROTOR SPEED DEVIATION CONSIDERED

$$n_5 = -\frac{L''_{ad}R_T\psi_{fd0}}{D_0L_{fd}} - \frac{L''_{ad}R_T\psi_{1d0}}{L_{1d}D_0} - \frac{L''_{aq}X_{Td0}\psi_{1q0}}{L_{1q}D_0} - \frac{L''_{aq}X_{Td0}\psi_{2q0}}{L_{2q}D_0} + \frac{E_{dN0}L''_d}{D_0} - \left(\frac{X_{Td0}E_{dN0} - R_TE_{qN0}}{D_0^2}\right)\left(X_{Td0}L''_q + X_{Tq0}L''_d\right)$$

$$n_6 = \frac{(X_{Td0}E_{B0}\cos\delta_0 + R_TE_{B0}\sin\delta_0)}{D_0}$$

$$K_1 = \left[\psi_{ad0}n_1 + i_{q0}L''_{ad}\left(m_1 + \frac{1}{L_{fd}}\right) - \psi_{aq0}m_1 - i_{d0}L''_{aq}n_1\right]$$

$$K_2 = \left[\psi_{ad0}n_2 + i_{q0}L''_{ad}\left(m_2 + \frac{1}{L_{1d}}\right) - \psi_{aq0}m_2 - i_{d0}L''_{aq}n_2\right]$$

$$K_3 = \left[\psi_{ad0}n_3 - i_{d0}L''_{aq}\left(n_3 + \frac{1}{L_{1q}}\right) - \psi_{aq0}m_3 + i_{q0}L''_{ad}m_3\right]$$

$$K_4 = \left[\psi_{ad0}n_4 - i_{d0}L''_{aq}\left(n_4 + \frac{1}{L_{2q}}\right) - \psi_{aq0}m_4 + i_{q0}L''_{ad}m_4\right]$$

$$K_5 = \left[\psi_{ad0}n_5 + i_{q0}L''_{ad}m_5 - \psi_{aq0}m_5 - i_{d0}L''_{aq}n_5\right]$$

$$K_6 = \left[\psi_{ad0}n_6 + i_{q0}L''_{ad}m_6 - \psi_{aq0}m_6 - i_{d0}L''_{aq}n_6\right]$$

$$a_{11} = \frac{\omega_0R_{fd}}{L_{fd}}\left[L''_{ad}\left(m_1 + \frac{1}{L_{fd}}\right) - 1\right] \qquad a_{12} = \frac{\omega_0R_{fd}}{L_{fd}}L''_{ad}\left(m_2 + \frac{1}{L_{1d}}\right)$$

$$a_{13} = \frac{\omega_0R_{fd}}{L_{fd}}L''_{ad}m_3 \qquad a_{14} = \frac{\omega_0R_{fd}}{L_{fd}}L''_{ad}m_4$$

$$a_{15} = \frac{\omega_0R_{fd}}{L_{fd}}L''_{ad}m_5 \qquad a_{16} = \frac{\omega_0R_{fd}}{L_{fd}}L''_{ad}m_6$$

$$a_{21} = \frac{\omega_0R_{1d}}{L_{1d}}L''_{ad}\left(m_1 + \frac{1}{L_{fd}}\right) \qquad a_{22} = \frac{\omega_0R_{1d}}{L_{1d}}\left[L''_{ad}\left(m_2 + \frac{1}{L_{1d}}\right) - 1\right]$$

$$a_{23} = \frac{\omega_0R_{1d}}{L_{1d}}L''_{ad}m_3 \qquad a_{24} = \frac{\omega_0R_{1d}}{L_{1d}}L''_{ad}m_4$$

$$a_{25} = \frac{\omega_0R_{1d}}{L_{1d}}L''_{ad}m_5 \qquad a_{26} = \frac{\omega_0R_{1d}}{L_{1d}}L''_{ad}m_6$$

$$a_{31} = \frac{\omega_0R_{1q}}{L_{1q}}L''_{aq}n_1 \qquad a_{32} = \frac{\omega_0R_{1q}}{L_{1q}}L''_{aq}n_2$$

$$a_{33} = \frac{\omega_0R_{1q}}{L_{1q}}\left[L''_{aq}\left(n_3 + \frac{1}{L_{1q}}\right) - 1\right] \qquad a_{34} = \frac{\omega_0R_{1q}}{L_{1q}}L''_{aq}\left(n_4 + \frac{1}{L_{2q}}\right)$$

$$a_{35} = \frac{\omega_0R_{1q}}{L_{1q}}L''_{aq}n_5 \qquad a_{36} = \frac{\omega_0R_{1q}}{L_{1q}}L''_{aq}n_6$$

$$a_{41} = \frac{\omega_0 R_{2q}}{L_{2q}} L''_{aq} n_1 \qquad a_{42} = \frac{\omega_0 R_{2q}}{L_{2q}} L''_{aq} n_2$$

$$a_{43} = \frac{\omega_0 R_{2q}}{L_{2q}} L''_{aq} \left(n_3 + \frac{1}{L_{1q}} \right) \qquad a_{44} = \frac{\omega_0 R_{2q}}{L_{2q}} \left[L''_{aq} \left(n_4 + \frac{1}{L_{2q}} \right) \quad 1 \right]$$

$$a_{45} = \frac{\omega_0 R_{2q}}{L_{2q}} L''_{aq} n_5 \qquad a_{46} = \frac{\omega_0 R_{2q}}{L_{2q}} L''_{aq} n_6$$

$$a_{51} = -K_1/2H \qquad a_{52} = -K_2/2H \qquad a_{53} = -K_3/2H$$

$$a_{54} = -K_4/2H \qquad a_{55} = -(K_5 + K_D)/2H \qquad a_{56} = -K_6/2H$$

A.3 Linearization of swing equation

The swing equation assuming P_m turbine output is given by

$$\dot{\omega}_r = \frac{1}{2H} \left(\frac{P_m}{\omega_r} - T_e - K_D \Delta\omega_r \right) \tag{A.12}$$

where $\Delta\omega_r = \omega_r - \omega_0$
Perturbing each variable by a small amount Δ gives

$$\dot{\omega}_r + \Delta\dot{\omega}_r = \frac{1}{2H} \left[\frac{P_m + \Delta P_m}{\omega_r + \Delta\omega_r} - (T_e + \Delta T_e) - K_D(\omega_r + \Delta\omega_r - \omega_0) \right] \tag{A.13}$$

Using Taylor's expansion and ignoring 2^{nd} and higher order terms yields

$$\begin{aligned} \dot{\omega}_r + \Delta\dot{\omega}_r = & \frac{1}{2H} \left[\frac{P_m}{\omega_r} - \frac{P_m}{\omega_r^2} \Delta\omega_r + \frac{\Delta P_m}{\omega_r} - (T_e + \Delta T_e) - \right. \\ & \left. K_D(\omega_r + \Delta\omega_r - \omega_0) \right] \end{aligned} \tag{A.14}$$

Re-arranging (A.14)

$$\begin{aligned} \dot{\omega}_r + \Delta\dot{\omega}_r = & \frac{1}{2H} \left[\frac{P_m}{\omega_r} - T_e - K_D(\omega_r - \omega_0) \right] + \\ & \frac{1}{2H} \left[\frac{\Delta P_m}{\omega_r} - \Delta T_e - \left(K_D + \frac{P_m}{\omega_r^2} \right) \Delta\omega_r \right] \end{aligned} \tag{A.15}$$

It can be deduced from (A.15) that

$$\Delta\dot{\omega}_r = \frac{1}{2H} \left[\frac{\Delta P_m}{\omega_r} - \Delta T_e - \left(K_D + \frac{P_m}{\omega_r^2} \right) \Delta\omega_r \right] \tag{A.16}$$

Evaluating (A.16) at the equilibrium point where $\omega_r = \omega_0 = 1\ p.u.$ and $P_m = P_{m0}$ yields

$$\Delta\dot{\omega}_r = \frac{1}{2H}\left[\Delta P_m - \Delta T_e - (K_D + P_{m0})\Delta\omega_r\right] \tag{A.17}$$

Appendix B

System data

B.1 SMIB system

The network reactance is in per unit on 2220 MVA, 24 kV base. Transmission line and transformer resistances, and charging capacitance are neglected. Transformer reactance = j0.15 *pu*.

Generator data
Rating: 2220 MVA, 24 kV, 60 Hz

$X_d = 1.81$	$X'_d = 0.30$	$X''_d = 0.23$	$T'_{do} = 8.0$ s	$T''_{do} = 0.03$ s
$X_q = 1.76$	$X'_q = 0.65$	$X''_q = 0.25$	$T'_{qo} = 1.0$ s	$T''_{qo} = 0.07$ s
$X_l = 0.16$	$R_a = 0.003$	$H = 3.5$	$K_D = 0$	$A_{sat} = 0.031$
$B_{sat} = 6.93$	$\psi_{T1} = 0.8$	$\psi_{T2} = \infty$	$S_{1.0} = 0.124$	$S_{1.2} = 0.413$

Basic parameters calculated for use with PSS/E's CGEN1 model

$L_{ad} = 1.65$	$r_{fd} = 0.000598$	$L_{fd} = 0.15298$	$r_{1d} = 0.024757$
$L_{1d} = 0.14$	$L_{aq} = 1.60$	$r_{1q} = 0.006118$	$L_{1q} = 0.706306$
$r_{2q} = 0.022746$	$L_{2q} = 0.11025$		

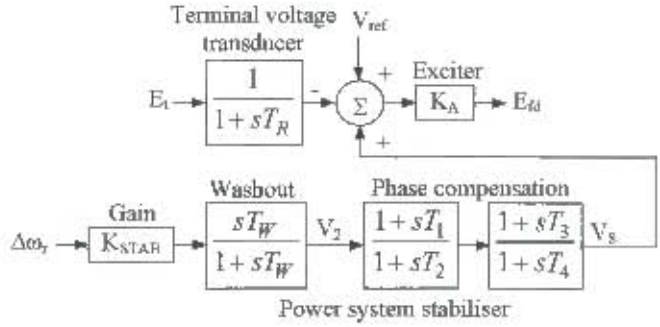

Figure B.1: Block diagram of the thyristor excitation system with AVR and PSS

where:

E_{fd}	- exciter output voltage
E_t	- generator terminal voltage
K_A, K_{STAB}	- voltage regulator gain, PSS gain
T_1, T_3	- PSS lead compensating time constants
T_2, T_4	- PSS lag compensating time constants
T_r	- terminal voltage transducer time constant
T_W	- PSS washout time constant
V_2	- signal washout output
V_{ref}	- voltage regulator reference voltage
V_S	- PSS output
$\Delta\omega_r$	- speed deviation

Excitation system data

$K_A = 200$ $T_R = 0.02$ s $K_{STAB} = 9.5$
$T_W = 1.4$ s $T_1 = 0.154$ s $T_2 = 0.033$ s

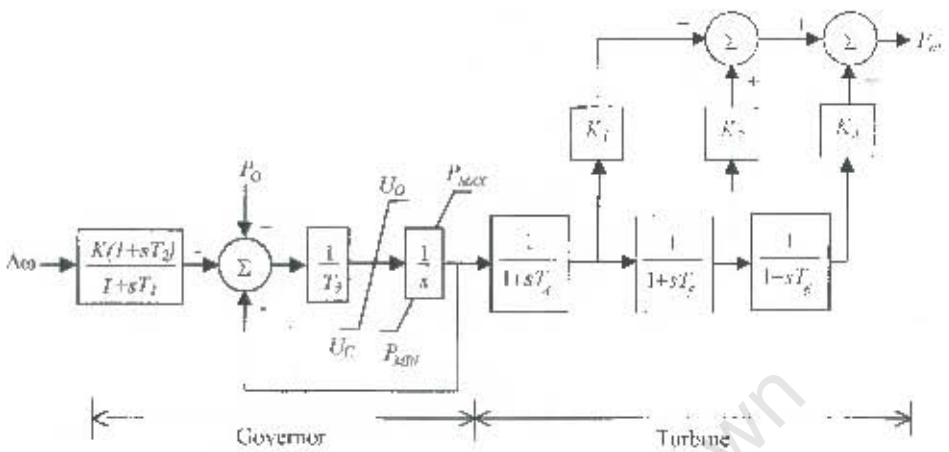

Figure B.2: Block diagram of the turbine-governor set

where:

K	- total effective speed-governing system gain (reciprocal of droop)
T_1	- phase compensation circuit lag time constant
T_2	- phase compensation circuit lead time constant
T_3	- servomotor time constant
T_4	- steam chest time constant
T_5	- reheat time constant
T_6	- crossover time constant
K_1	- fraction of total turbine power generated by high pressure section
K_2	- fraction of total turbine power generated by intermediate pressure section
K_3	- fraction of total turbine power generated by low pressure section
P_O	- initial mechanical power
P_{MAX}, P_{MIN}	- maximum, minimum power limits imposed by valve
U_O, U_C	- limits on rate of change of power imposed by control valve rate limits
P_m	- mechanical power
$\Delta\omega_r$	- speed deviation

Turbine-governor data

K = 20	$T_1 = 0.3$ s	$T_2 = 0$ s	$T_3 = 0.1$ s	$T_4 = 0.3$ s	$T_5 = 7$ s
$T_6 = 0.5$ s	$K_1 = 0.3$	$K_2 = 0.4$	$K_3 = 0.3$	$U_o = 0.1$	U_c = -1
$P_{MAX} = 1$	$P_{MIN} = 0$				

Table B.1 shows the infinite bus model and parameters used in each tool. The impedances are in pu on 2220 MVA, 24 kV base.

Table B.1: Infinite bus data for the five industrial-grade tools

Tool	*Infinite bus model*	*Parameter(s) specification*
PSS/E	Classical generator	$H = 0\ s,\ X'_d = 10^{-8} pu$
PowerFactory	AC voltage source	$Z_1 = 0 + j10^{-8} pu$
EUROSTAG	Infinite node	$Z_{\infty} = 0 + j10^{-7} pu$
SSAT	Classical generator	$H = 0\ s,\ X'_d = 10^{-8} pu$
MatNetEig	Classical generator	$H = 0\ s,\ X'_d = 10^{-8} pu$

System operating condition

P = 1998 MW	Q = 666 MVAr
$V_t = 1.0\angle 36°$	$V_B = 0.995\angle 0°$

Figure B.3 shows the user defined turbine model for realizing the power-torque relationship $T_m = P_m/\omega_r$, in EUROSTAG.

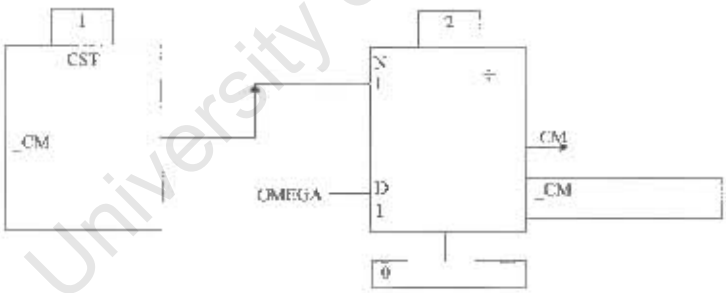

Figure B.3: Constant-power turbine model used with EUROSTAG

where:

_CM	- steady-state mechanical torque
CM	- mechanical torque
OMEGA	- rotor speed

Blocks 1 and 2 are CONSTANT and DIVIDER elementary blocks. The output of Block 1 is the steady-state torque _CM and the output of Block 2 is CM computed as _CM/OMEGA.

B.2 2A4C system

Transmission line data (base: 100 MVA, 230 kV)
$r = 0.0001$ *pu/km* $x_L = 0.001$ *pu/km* $b_C = 0.00175$ *pu/km*

Transformer data
Rating: 900 MVA, 20/230 kV
X = j0.15 *pu* Off-nominal ratio = 1.0

Generator data
Rating: 900 MVA, 20 kV, 60 Hz

$X_d = 1.8$	$X'_d = 0.30$	$X''_d = 0.25$	$T'_{do} = 8.0$ s	$T''_{do} = 0.03$ s
$X_q = 1.7$	$X'_q = 0.55$	$X''_q = 0.25$	$T'_{qo} = 0.4$ s	$T''_{qo} = 0.05$ s
$X_l = 0.2$	$R_a = 0.0025$	$K_D = 0$	$A_{sat} = 0.015$	$B_{sat} = 9.6$
$\psi_{T1} = 0.9$	$\psi_{T2} = \infty$	$S_{1.0} = 0.039$	$S_{1.2} = 0.223$	

H = 6.5 s (for G1 and G2) H = 6.175 s (for G3 and G4)

Basic parameters calculated for use with PSS/E's CGEN1 model

$L_{ad} = 1.6$	$r_{fd} = 0.000566$	$L_{fd} = 0.10667$	$r_{1d} = 0.01768$
$L_{1d} = 0.1$	$L_{aq} = 1.5$	$r_{1q} = 0.01297$	$L_{1q} = 0.45652$
$r_{2q} = 0.02166$	$L_{2q} = 0.05833$		

Excitation system data

$K_A = 200$	$T_R = 0.01$ s	$K_{STAB} = 20.0$	$T_W = 10.0$ s
$T_1 = 0.05$ s	$T_2 = 0.02$ s	$T_3 = 3.0$ s	$T_4 = 5.4$ s

Operating condition

G1	P = 700 MW	Q = 185 MVAr	$V_t = 1.03\angle 20.2°$
G2	P = 700 MW	Q = 235 MVAr	$V_t = 1.01\angle 10.5°$
G3	P = 719 MW	Q = 176 MVAr	$V_t = 1.03\angle -6.8°$
G4	P = 700 MW	Q = 202 MVAr	$V_t = 1.01\angle -17.0°$
Bus 7	P_L = 967 MW	Q_L = 100 MVAr	Q_C = 200 MVAr
Bus 9	P_L = 1767 MW	Q_L = 100 MVAr	Q_C = 350 MVAr

Appendix C

Results

C.1 Effect of speed voltage terms

The SMIB system was simulated using EUROSTAG with the generator lightly loaded at $P = 0.1$ pu and on manual excitation control. The generator terminal voltage $V_t = 1.0$ pu, infinite bus voltage $V_B = 0.995\angle 0°$ pu, and $K_D = 0$. Simulations were ran with the transmission line resistance $R_E = 0$ and with $R_E = 0.05$ pu. The line reactance $X_E = 0.5$ pu in both cases.

The following $\boldsymbol{A}$ matrices and local modes $\lambda_{1,2}$, were obtained for the two cases.

Case I: $P = 0.1$ pu, $R_E = 0.05$

$$\mathbf{A} = \begin{pmatrix} -0.8643 & 0.6918 & 0.0007 & 0.0057 & 0.1150 & 0.0206 \\ 27.4247 & -35.4001 & 0.0310 & 0.2660 & 5.3184 & 0.9511 \\ -0.0084 & -0.0098 & -2.8800 & 2.4051 & -0.0356 & 0.3089 \\ -0.2131 & -0.2487 & 7.1276 & -19.2051 & -0.9052 & 7.8556 \\ 0.0211 & 0.0246 & 0.0150 & 0.1287 & \boxed{-0.0064} & -0.1580 \\ 0 & 0 & 0 & 0 & 376.991 & 0 \end{pmatrix}$$

$\lambda_{1,2} = -0.816 \pm j6.559$
$f = 1.044$ Hz
$\zeta = 12.4\ \%$

Case 11: $P = 0.1$ *pu*, $K_D = 0$

$$\mathbf{A} = \begin{pmatrix} -0.8644 & 0.6916 & 0.0000 & 0.0003 & 0.1143 & 0.0266 \\ 27.4164 & -35.4098 & 0.0018 & 0.0151 & 5.2879 & 1.2315 \\ -0.0005 & -0.0006 & -2.8802 & 2.4041 & -0.0527 & 0.3060 \\ -0.0121 & -0.0141 & 7.1248 & -19.2290 & -1.3404 & 7.7800 \\ 0.0170 & 0.0198 & 0.0151 & 0.1298 & \boxed{0.0026} & -0.1581 \\ 0 & 0 & 0 & 0 & 376.991 & 0 \end{pmatrix}$$

$\lambda_{1,2} = -0.809 \pm j6.564$
$f = 1.045\ Hz$
$\zeta = 12.2\ \%$

The element a_{55} in row 5, column 5 is marked. With $K_D = 0$, $a_{55} = -K_5/2H$. A negative value of a_{55} is indicative of a positive damping coefficient K_5 whereas a positive value of a_{55} is indicative of a negative value of K_5.

It can be seen that the damping of the local modes obtained for a positive value of K_5 (negative a_{55}) is higher than that obtained with a negative value of K_5 (positive a_{55}).

C.2 Effect of perturbation size

Table C.1 gives the detailed results for the local mode of the SMIB system obtained using PSS/E by varying the perturbation size between 10^{-6} and 10^{-1}.

Table C.1: Effect of perturbation size on the electromechanical mode; PSS/E results

Perturbation	$\lambda_{1,2} = \sigma \pm j\omega$	ζ (%)	f (Hz)
0.1	$-0.269 \pm j6.145$	4.37	0.978
0.01	$-0.268 \pm j6.395$	4.19	1.018
0.005	$-0.268 \pm j6.408$	4.18	1.020
0.001	$-0.268 \pm j6.418$	4.17	1.022
0.0005	$-0.268 \pm j6.420$	4.17	1.022
0.0001	$-0.269 \pm j6.418$	4.18	1.021
0.00005	$-0.267 \pm j6.416$	4.17	1.021
0.00001	$-0.265 \pm j6.365$	4.17	1.013
0.000007	$-0.275 \pm j6.389$	4.30	1.017
0.000005	$-0.267 \pm j6.345$	4.21	1.010
0.0000045	$-0.261 \pm j6.308$	4.13	1.004
0.000004	$-0.268 \pm j6.309$	4.24	1.004
0.0000035	$-0.260 \pm j6.306$	4.12	1.004
0.000003	$-0.263 \pm j6.344$	4.14	1.010
0.0000025	$-0.276 \pm j6.169$	4.47	0.982
0.000002	$-0.249 \pm j6.183$	4.03	0.984
0.0000015	$-0.222 \pm j6.264$	3.54	0.997
0.000001	$-0.186 \pm j6.184$	3.17	0.984

C.3 Time-domain simulation results

Figures C.1(a), C.1(b), and C.1(c) show time-domain results for the 2A4G system obtained using PSS/E, DSA-TSAT, and PowerFactory, respectively. The oscillations were initiated by disconnecting one of the tie-lines 7-8 for 5 *ms*. The results show that the system is stable.

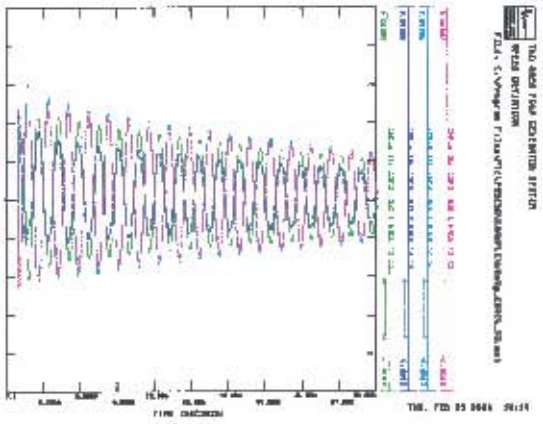

(a) PSS/E

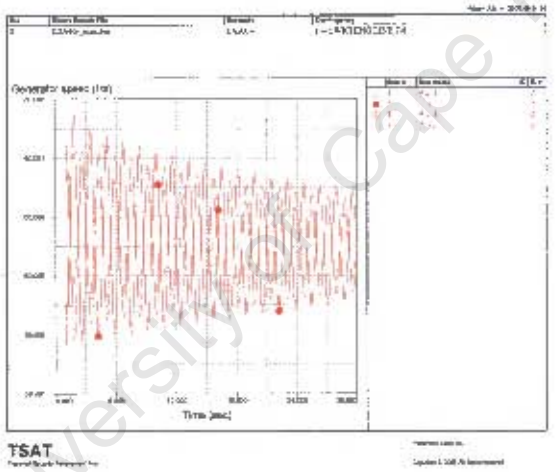

(b) DSA-TSAT

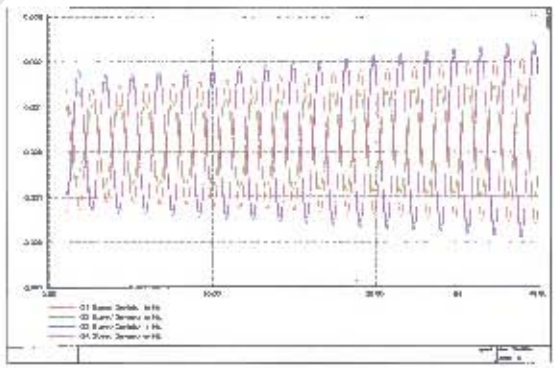

(c) PowerFactory

Figure C.1: Time domain simulation results; AVR without PSS

Appendix D

Eigenvalue sensitivities

D.1 SMIB system

D.1.1 Manual excitation control

```
Sensitivity of the local mode to model uncertainty

SSAT(Pm) ; manual excitation control without saturation

Eigenvalues
 -3.6408e+001
 -2.2304e+001
 -2.6797e-001 +6.4213e+000i
 -2.6797e-001 -6.4213e+000i
 -5.0478e-002
 -1.7383e+000

Mode 3 is the local mode
 -2.6797e-001 +6.4213e+000i

Magnitude of Relative (logarithmic) sensitivity of mode 3 to
elements of the [A] matrix
  1.0046e-002  5.5412e-001  1.0987e-002  5.3207e-002  2.4827e-004  4.6622e-003
  5.0187e-001            0            0            0            0            0
            0  1.0984e-002  2.6432e-003  9.3146e-003  9.1888e-008  1.7231e-006
            0  5.3193e-002  9.3146e-003  5.2907e-002  4.4451e-007  8.3576e-006
            0  2.4919e-004  8.8830e-008  4.3064e-007  4.8722e-004  9.1844e-004
            0  4.6774e-003  1.6679e-006  8.1076e-006  9.1854e-004  4.6139e-003

SSAT(Pm) ; manual excitation control - Full saturation
```

```
Eigenvalues
 -3.6620e+001
 -2.2820e+001
 -2.7200e-001 +6.4144e+000i
 -2.7200e-001 -6.4144e+000i
 -7.4108e-002
 -1.7790e+000

Mode 3 is the local mode
 -2.7200e-001 +6.4144e+000i

Magnitude of Relative (logarithmic) sensitivity of mode 3 to
elements of the [A] matrix
  1.0065e-002  5.5619e-001  1.0633e-002  5.1438e-002  4.4189e-004  8.2889e-003
  5.0227e-001            0            0            0            0            0
            0  1.0629e-002  2.5599e-003  8.9016e-003  1.1667e-007  2.1931e-006
            0  5.1420e-002  8.9016e-003  5.1174e-002  5.6609e-007  1.0613e-005
            0  4.4319e-004  1.1380e-007  5.5052e-007  8.4836e-004  1.5846e-003
            0  8.3082e-003  2.1315e-006  1.0365e-005  1.5848e-003  8.2289e-003

SSAT(Pm) ; manual excitation control - Incremental saturation

Eigenvalues
 -3.7669e+001
 -2.5492e+001
 -2.4143e-001 +6.4609e+000i
 -2.4143e-001 -6.4609e+000i
 -1.8243e-001
 -2.0081e+000

Mode 3 is the local mode
 -2.4143e-001 +6.4609e+000i

Magnitude of Relative (logarithmic) sensitivity of mode 3 to
elements of the [A] matrix
  9.9912e-003  5.5048e-001  9.4091e-003  4.5853e-002  3.5778e-004  6.7637e-003
  5.0215e-001            0            0            0            0            0
            0  9.4062e-003  2.2431e-003  7.3876e-003  8.4988e-008  1.6069e-006
            0  4.5839e-002  7.3876e-003  4.5696e-002  4.1350e-007  7.8258e-006
            0  3.5830e-004  8.2808e-008  4.0315e-007  6.1041e-004  1.1028e-003
            0  6.7782e-003  1.5704e-006  7.6178e-006  1.1026e-003  6.7845e-003
```

D.1.2 AVR without PSS

```
SSAT(Pm) ; AVR without PSS - without saturation

Eigenvalues
```

```
 -1.0000e+006
 -5.4199e+001
  5.0694e-001 +7.4436e+000i
  5.0694e-001 -7.4436e+000i
 -1.6461e+000
 -2.2113e+001
 -1.7046e+001 +1.2164e+001i
 -1.7046e+001 -1.2164e+001i

Mode 3 is the local mode
  5.0694e-001 +7.4436e+000i

Magnitude of Relative (logarithmic) sensitivity of mode 3 to
elements of the [A] matrix
  Columns 1 through 6
  8.1005e-003  3.8487e-001  7.8849e-002  3.7840e-002  1.4169e-004  3.1075e-003
  4.7068e-001           0           0           0           0           0
            0  3.8114e-003  9.4776e-003  3.3096e-003  2.6195e-008  5.7449e-007
            0  2.1479e-002  3.8864e-002  2.1875e-002  1.4762e-007  3.2376e-006
            0  1.0487e-003  3.8666e-006  1.8556e-006  1.6859e-003  3.7114e-003
            0  2.3000e-002  8.4800e-005  4.0696e-005  3.7114e-003  2.1772e-002
            0  1.3690e-001  6.9623e-002  3.3413e-002  9.3454e-004  2.0496e-002
            0           0           0           0           0           0
  Columns 7 through 8
            0           0
            0           0
            0  8.8107e-002
            0           0
            0           0
            0           0
  8.6291e-002           0
  8.8107e-002  8.8107e-002

SSAT(Pm) ; AVR without PSS - Full saturation

Eigenvalues
 -1.0000e+006
 -5.4340e+001
  4.2562e-001 +7.3928e+000i
  4.2562e-001 -7.3928e+000i
 -1.6725e+000
 -2.2601e+001
 -1.7037e+001 +1.2710e+001i
 -1.7037e+001 -1.2710e+001i

Mode 3 is the local mode
  4.2562e-001 +7.3928e+000i

Magnitude of Relative (logarithmic) sensitivity of mode 3 to
```

```
elements of the [A] matrix
  Columns 1 through 6
  8.2464e-003  3.9508e-001  7.5852e-002  3.4144e-002  2.6060e-004  5.6639e-003
  4.7550e-001            0             0            0            0            0
            0  3.6817e-003  8.9050e-003  2.8813e-003  3.3552e-008  7.2969e-007
            0  2.0586e-002  3.5791e-002  1.9145e-002  1.8773e-007  4.0801e-006
            0  1.3670e-003  3.5306e-006  1.5893e-006  2.1740e-003  4.7050e-003
            0  2.9709e-002  7.6735e-005  3.4542e-005  4.7050e-003  2.8306e-002
            0  1.3435e-001  6.8072e-002  3.0642e-002  1.1479e-003  2.4948e-002
            0            0             0            0            0            0
  Columns 7 through 8
            0            0
            0            0
            0  8.1586e-002
            0            0
            0            0
            0            0
  8.0041e-002            0
  8.1586e-002  8.1586e-002

SSAT(Pm) ; AVR without PSS - Incremental saturation

Eigenvalues
 -1.0000e+006
 -5.4406e+001
  4.5943e-001 +7.3844e+000i
  4.5943e-001 -7.3844e+000i
 -1.9315e+000
 -2.5332e+001
 -1.7541e+001 +1.1550e+001i
 -1.7541e+001 -1.1550e+001i

Mode 3 is the local mode
  4.5943e-001 +7.3844e+000i

Magnitude of Relative (logarithmic) sensitivity of mode 3 to
elements of the [A] matrix
  Columns 1 through 6
  8.1996e-003  3.9479e-001  7.5161e-002  3.3650e-002  2.1566e-004  4.6910e-003
  4.7243e-001            0             0            0            0            0
            0  3.4381e-003  9.1321e-003  2.7631e-003  2.6109e-008  5.6802e-007
            0  1.9216e-002  3.4495e-002  1.9602e-002  1.4569e-007  3.1727e-006
            0  1.1019e-003  2.8365e-006  1.2687e-006  1.5778e-003  3.2799e-003
            0  2.3985e-002  6.1893e-005  2.7583e-005  3.2791e-003  2.3217e-002
            0  1.2893e-001  6.5593e-002  2.9366e-002  9.2382e-004  2.0095e-002
            0            0             0            0            0            0
  Columns 7 through 8
            0            0
            0            0
```

```
            0  8.1514e-002
            0            0
            0            0
            0            0
  7.9920e-002            0
  8.1514e-002  8.1514e-002
```

D.1.3 AVR with PSS

```
SSAT(Pm) ; AVR with PSS - without saturation

Eigenvalues
 -1.0000e+006
 -5.4309e+001
 -3.4197e+001
 -1.3271e+001 +1.6370e+001i
 -1.3271e+001 -1.6370e+001i
 -2.2235e+001
 -1.1983e+000 +6.7451e+000i
 -1.1983e+000 -6.7451e+000i
 -7.4198e-001
 -1.6323e+000

Mode 7 is the local mode
 -1.1983e+000 +6.7451e+000i

Magnitude of Relative (logarithmic) sensitivity of mode 7 to
elements of the [A] matrix
  Columns 1 through 6
  8.0136e-003  4.1466e-001  7.1642e-002  6.9168e-002  1.8594e-004  3.5079e-003
  5.3405e-001            0            0            0            0            0
            0  4.6460e-003  9.7429e-003  6.8446e-003  3.8900e-008  7.3285e-007
            0  2.3564e-002  3.5957e-002  4.0715e-002  1.9708e-007  3.7226e-006
            0  1.5972e-003  4.9615e-006  4.7950e-006  3.1254e-003  5.9189e-003
            0  3.0119e-002  9.3590e-005  9.0694e-005  5.9196e-003  2.9873e-002
            0  1.7293e-001  7.4169e-002  7.1607e-002  1.4378e-003  2.7126e-002
  2.6796e-002            0            0            0            0            0
  7.0613e-001            0            0            0            0            0
  8.8605e-001            0            0            0            0            0
  Columns 7 through 10
            0            0            0            0
            0            0            0            0
            0            0            0  7.0264e-002
            0            0            0            0
            0            0            0            0
            0            0            0            0
  2.0691e-001            0            0            0
```

```
           0  2.8304e-003           0           0
           0  7.4400e-002  7.2554e-001           0
  2.0387e-001  9.3357e-002  7.1531e-001  7.0264e-002

SSAT(Pm) ; AVR with PSS - Full saturation

Eigenvalues
 -1.0000e+006
 -5.4448e+001
 -3.4053e+001
 -1.3418e+001 +1.6730e+001i
 -1.3418e+001 -1.6730e+001i
 -2.2743e+001
 -1.1881e+000 +6.6953e+000i
 -1.1881e+000 -6.6953e+000i
 -7.4167e-001
 -1.6561e+000

Mode 7 is the local mode
 -1.1881e+000 +6.6953e+000i

Magnitude of Relative (logarithmic) sensitivity of mode 7 to
elements of the [A] matrix
  Columns 1 through 6
  8.1187e-003  4.2358e-001  7.1158e-002  6.8998e-002  3.3890e-004  6.3526e-003
  5.3356e-001           0           0           0           0           0
           0  4.4142e-003  9.3424e-003  6.5114e-003  4.8797e-008  9.1659e-007
           0  2.2224e-002  3.3808e-002  3.8955e-002  2.4639e-007  4.6160e-006
           0  2.0237e-003  4.5662e-006  4.4277e-006  3.9012e-003  7.2816e-003
           0  3.7911e-002  8.5470e-005  8.3303e-005  7.2827e-003  3.7788e-002
           0  1.6663e-001  7.3874e-002  7.1631e-002  1.7269e-003  3.2369e-002
  2.5768e-002           0           0           0           0           0
  6.7656e-001           0           0           0           0           0
  8.4890e-001           0           0           0           0           0
  Columns 7 through 10
           0           0           0           0
           0           0           0           0
           0           0           0  6.6524e-002
           0           0           0           0
           0           0           0           0
           0           0           0           0
  1.9961e-001           0           0           0
           0  2.7422e-003           0           0
           0  7.1820e-002  6.9521e-001           0
  1.9669e-001  9.0115e-002  6.8538e-001  6.6524e-002

SSAT(Pm) ; AVR with PSS - Incremental saturation

Eigenvalues
```

```
 -1.0000e+006
 -5.4515e+001
 -3.4229e+001
 -1.3852e+001 +1.5745e+001i
 -1.3852e+001 -1.5745e+001i
 -2.5451e+001
 -1.1459e+000 +6.7524e+000i
 -1.1459e+000 -6.7524e+000i
 -7.3971e-001
 -1.9199e+000

Mode 7 is the local mode
 -1.1459e+000 +6.7524e+000i

Magnitude of Relative (logarithmic) sensitivity of mode 7 to
elements of the [A] matrix
  Columns 1 through 6
  8.1826e-003  4.2559e-001  7.2302e-002  6.3964e-002  2.7863e-004  5.2723e-003
  5.3211e-001            0            0            0            0            0
            0  4.1701e-003  9.8840e-003  5.9096e-003  3.7953e-008  7.1829e-007
            0  2.1164e-002  3.3901e-002  3.8068e-002  1.9231e-007  3.6430e-006
            0  1.6254e-003  3.7338e-006  3.3000e-006  2.7894e-003  5.0442e-003
            0  3.0779e-002  7.0874e-005  6.2414e-005  5.0431e-003  3.1062e-002
            0  1.6170e-001  7.3410e-002  6.4945e-002  1.3886e-003  2.6276e-002
  2.5386e-002            0            0            0            0            0
  6.6637e-001            0            0            0            0            0
  8.3763e-001            0            0            0            0            0
  Columns 7 through 10
            0            0            0            0
            0            0            0            0
            0            0            0  6.9883e-002
            0            0            0            0
            0            0            0            0
            0            0            0            0
  1.9343e-001            0            0            0
            0  2.6799e-003            0            0
            0  7.0171e-002  6.8292e-001            0
  1.9079e-001  8.8206e-002  6.7449e-001  6.9883e-002
```

D.2 2A4G system

D.2.1 Manual excitation control

```
EUROSTAG(Tm) ; with speed deviation and without saturation
```

```
Eigenvalues
 -3.6503e+001
 -3.6426e+001
 -3.4012e+001
 -3.2567e+001
 -3.0241e+001
 -3.0426e+001
 -2.3160e+001
 -2.1254e+001
 -5.5783e-001 +6.6048e+000i
 -5.5783e-001 -6.6048e+000i
 -5.7023e-001 +6.7940e+000i
 -5.7023e-001 -6.7940e+000i
 -1.2451e-001 +3.4106e+000i
 -1.2451e-001 -3.4106e+000i
 -5.7759e+000
 -5.8095e+000
 -4.2894e+000
 -3.2202e+000
 -1.8020e-001
 -1.6812e-001
 -5.5506e-002 +7.1107e-002i
 -5.5506e-002 -7.1107e-002i
  2.9560e-002
  3.6723e-007

Mode 13 is the local mode
 -1.2451e-001 +3.4106e+000i

Magnitude of relative (logarithmic) sensitivity of mode 13 to
elements of the [A] matrix
  Columns 1 through 5

  3.6420e-003  6.2011e-003  4.3576e-005  2.3480e-006  3.6145e-005
  6.1980e-003  1.4570e-002  1.0127e-004  5.4630e-006  8.3981e-005
  7.4178e-005  1.7250e-004  8.1034e-003  2.8007e-003  9.9379e-005
  4.0038e-006  9.3091e-006  2.8004e-003  2.9272e-003  5.3587e-006
  6.8518e-003  1.5919e-002  1.0425e-002  5.6248e-004  2.2370e-004
            0            0            0            0  6.2825e-002
  1.3191e-004  3.0674e-004  1.1411e-004  6.1542e-006  3.6624e-005
  3.0645e-004  7.1265e-004  2.6499e-004  1.4266e-005  8.5049e-005
  5.0115e-007  1.1676e-006  3.4378e-003  1.8539e-004  1.3528e-004
  2.7008e-008  6.2986e-008  1.8535e-004  1.0016e-005  7.2934e-006
  2.3747e-003  5.5057e-003  1.6491e-002  8.8914e-004  7.0765e-005
            0            0            0            0  1.6208e-002
  1.5838e-005  3.6802e-005  3.2530e-005  1.7564e-006  5.1466e-006
  3.6772e-005  8.5513e-005  7.5638e-005  4.0771e-006  1.1929e-005
  6.2408e-006  1.4507e-005  1.1176e-004  6.0251e-006  5.9130e-006
  3.3598e-007  7.8082e-007  6.0222e-006  3.2480e-007  3.1856e-007
```

```
3.5177e-004  8.1665e-004  1.6866e-003  9.0879e-005  1.9274e-005
          0            0            0            0  2.0889e-002
2.4796e-005  5.7599e-005  6.3548e-005  3.4299e-006  8.5389e-006
5.7664e-005  1.3410e-004  1.4786e-004  7.9746e-006  1.9856e-005
3.4748e-006  8.0674e-006  2.7427e-004  1.4778e-005  1.1629e-005
1.8732e-007  4.3595e-007  1.4815e-005  8.0036e-007  6.2770e-007
5.8619e-004  1.3628e-003  1.4809e-003  7.9951e-005  8.4377e-005
          0            0            0            0  1.6891e-002

Columns 6 through 10

8.7413e-003  1.3897e-004  3.2243e-004  2.3063e-004  1.2405e-005
2.0322e-002  3.2273e-004  7.4997e-004  5.3471e-004  2.8825e-005
1.3093e-002  1.6428e-004  3.8176e-004  3.0729e-003  1.6572e-004
7.0599e-004  8.8553e-006  2.0594e-005  1.6569e-004  8.9391e-006
3.6987e-001  1.6235e-003  3.7856e-003  4.0889e-002  2.2039e-003
          0            0            0            0            0
3.9291e-003  4.0104e-003  6.8106e-003  1.5506e-004  8.3509e-006
9.1309e-003  6.8091e-003  1.6030e-002  3.6001e-004  1.9432e-005
3.4856e-002  2.3745e-004  5.5180e-004  2.0881e-002  6.6456e-003
1.8793e-003  1.2799e-005  2.9732e-005  6.6439e-003  7.0297e-003
2.5890e-001  6.0536e-003  1.4065e-002  1.6508e-002  8.9106e-004
          0            0            0            0            0
2.8031e-004  2.8546e-005  6.6400e-005  2.6979e-005  1.4537e-006
6.5089e-004  6.6266e-005  1.5399e-004  6.2645e-005  3.3762e-006
8.9319e-004  1.7679e-005  4.1083e-005  2.3735e-004  1.2797e-005
4.8088e-005  9.5359e-007  2.2057e-006  1.2776e-005  6.8956e-007
3.0626e-002  4.7569e-004  1.1045e-003  4.9158e-003  2.6519e-004
          0            0            0            0            0
3.1101e-004  4.5552e-005  1.0572e-004  7.1009e-005  3.8328e-006
7.2401e-004  1.0582e-004  2.4590e-004  1.6525e-004  8.8850e-006
2.6485e-003  2.3641e-005  5.4937e-005  6.1813e-004  3.3345e-005
1.4308e-004  1.2783e-006  2.9602e-006  3.3385e-005  1.8006e-006
3.7617e-002  8.8067e-004  2.0468e-003  5.1583e-003  2.7827e-004
          0            0            0            0            0

Columns 11 through 15

1.8120e-005  5.1926e-003  9.2317e-006  2.1432e-005  7.9101e-005
4.2112e-005  1.2068e-002  2.1448e-005  4.9827e-005  1.8397e-004
8.2302e-005  1.2732e-002  3.2823e-005  7.6255e-005  3.6921e-004
4.4379e-006  6.8651e-004  1.7707e-006  4.1182e-006  1.9881e-005
4.8299e-004  2.7612e-001  1.4214e-004  3.3112e-004  6.2030e-003
1.5678e-002            0            0            0            0
2.8324e-005  6.5649e-003  1.6705e-005  3.8808e-005  9.6374e-005
6.5779e-005  1.5250e-002  3.8790e-005  9.0118e-005  2.2373e-004
1.1836e-004  2.6832e-002  6.8945e-005  1.6017e-004  1.0135e-003
6.3812e-006  1.4466e-003  3.7193e-006  8.6345e-006  5.4632e-005
1.2890e-004  2.6307e-001  7.1388e-005  1.6555e-004  7.2015e-003
```

```
3.4016e-002           0           0           0           0
5.0765e-006  6.5035e-004  1.9358e-003  3.3101e-003  1.0774e-004
1.1785e-005  1.5049e-003  3.3092e-003  7.7243e-003  2.5013e-004
7.1588e-006  8.4348e-004  3.5481e-005  8.2429e-005  8.8849e-003
3.8523e-007  4.5350e-005  1.9095e-006  4.4367e-006  3.0374e-003
1.3015e-005  4.1136e-002  4.7535e-003  1.1039e-002  2.3111e-002
1.5118e-002           0           0           0           0
8.5919e-006  8.7235e-004  7.6894e-005  1.7842e-004  1.7104e-004
2.0005e-005  2.0352e-003  1.7874e-004  4.1524e-004  3.9869e-004
1.5045e-005  2.8248e-003  2.9911e-005  6.9490e-005  3.9322e-003
8.1306e-007  1.5266e-004  1.6152e-006  3.7553e-006  2.1244e-004
4.7510e-005  5.3842e-002  1.5961e-003  3.7170e-003  3.9898e-002
1.2224e-002           0           0           0           0

Columns 16 through 20

4.2780e-006  5.4298e-006  9.1738e-004  9.0411e-006  2.1034e-005
9.9219e-006  1.2634e-005  2.1322e-003  2.1007e-005  4.8861e-005
1.9918e-005  4.9607e-005  3.9536e-004  4.0058e-005  9.3174e-005
1.0770e-006  2.6732e-006  2.1333e-005  2.1619e-006  5.0270e-006
3.3476e-004  4.2939e-004  1.8597e-002  2.2919e-004  5.3436e-004
          0  5.5003e-002           0           0           0
5.2021e-006  1.2014e-005  1.4565e-003  1.6962e-005  3.9418e-005
1.2066e-005  2.7920e-005  3.3759e-003  3.9317e-005  9.1451e-005
5.4638e-005  1.1527e-004  2.1801e-004  8.7033e-005  2.0244e-004
2.9461e-006  6.2115e-006  1.1784e-005  4.6948e-006  1.0908e-005
3.8846e-004  4.0590e-004  2.7357e-002  1.6482e-004  3.8308e-004
          0  4.1151e-002           0           0           0
5.8023e-006  7.5090e-005  7.0750e-003  5.2413e-005  1.2193e-004
1.3520e-005  1.7445e-004  1.6431e-002  1.2181e-004  2.8333e-004
3.0436e-003  1.1931e-004  6.9989e-003  4.6109e-005  1.0725e-004
3.1791e-003  6.4212e-006  3.7668e-004  2.4804e-006  5.7720e-006
1.2528e-003  5.1703e-004  3.9485e-001  5.4372e-004  1.2651e-003
          0  1.6469e-001           0           0           0
9.2426e-006  8.3877e-005  3.9824e-003  1.3491e-003  2.3269e-003
2.1518e-005  1.9515e-004  9.2558e-003  2.3267e-003  5.3912e-003
2.1206e-004  2.1248e-004  1.5485e-002  8.3019e-005  1.9310e-004
1.1468e-005  1.1479e-005  8.3658e-004  4.4867e-006  1.0432e-005
2.1501e-003  2.7453e-004  2.7427e-001  2.9818e-003  6.9446e-003
          0  4.2885e-002           0           0           0

Columns 21 through 24

2.0469e-004  1.1032e-005  3.8040e-006  1.4215e-003
4.7586e-004  2.5601e-005  8.8418e-006  3.3130e-003
3.5112e-004  1.8906e-005  6.5298e-005  1.7311e-003
1.8894e-005  1.0173e-006  3.5230e-006  9.3363e-005
9.1671e-003  4.9430e-004  6.4841e-004  1.6166e-002
          0           0  5.1417e-002           0
```

```
 2.9338e-004  1.5779e-005  1.0615e-005  2.3374e-003
 6.7984e-004  3.6696e-005  2.4662e-005  5.4327e-003
 1.1322e-003  6.1096e-005  1.5608e-004  2.4153e-003
 6.1023e-005  3.2877e-006  8.4153e-006  1.3037e-004
 1.1375e-002  6.1350e-004  6.5086e-004  2.9076e-002
           0            0  3.8468e-002            0
 3.9993e-004  2.1603e-005  5.2384e-005  5.4000e-003
 9.3040e-004  5.0166e-005  1.2166e-004  1.2546e-002
 2.2019e-003  1.1875e-004  1.4435e-004  4.5591e-003
 1.1851e-004  6.3772e-006  7.7690e-006  2.4537e-004
 6.6227e-002  3.5793e-003  1.8498e-003  2.8264e-001
           0            0  4.9579e-002            0
 3.5416e-004  1.9118e-005  7.2233e-005  4.8312e-003
 8.2159e-004  4.4286e-005  1.6796e-004  1.1236e-002
 1.8563e-002  5.7136e-003  1.9877e-004  1.9471e-002
 5.7237e-003  6.0874e-003  1.0738e-005  1.0519e-003
 3.1953e-002  1.7181e-003  4.1485e-004  3.4047e-001
           0            0  1.2449e-001            0
```

D.2.2 AVR without PSS

```
SSAT(P) AVR without PSS; without saturation

Eigenvalues
 -1.0000e+006
 -1.0000e+006
 -1.0000e+006
 -1.0000e+006
 -9.4569e+001
 -9.5702e+001
 -9.7452e+001
 -9.7508e+001
 -1.7851e+001 +2.1591e+001i
 -1.7851e+001 -2.1591e+001i
 -1.8975e+001 +1.5499e+001i
 -1.8975e+001 -1.5499e+001i
 -3.6249e+001
 -3.6179e+001
 -3.1692e+001
 -3.0858e+001
 -2.7068e+001
 -2.7547e+001
 -1.3771e+001
 -1.3302e+001
 -6.9196e-001 +7.1700e+000i
 -6.9196e-001 -7.1700e+000i
 -6.8759e-001 +7.3710e+000i
```

```
 -6.8759e-001 -7.3710e+000i
 -2.4808e-002 +3.8447e+000i
 -2.4808e-002 -3.8447e+000i
 -2.9374e-004
 -6.1263e-002
 -3.6085e+000
 -3.5489e+000
 -3.3521e+000
 -3.3446e+000

Mode 25 is the local mode
 -2.4808e-002 +3.8447e+000i

Magnitude of relative (logarithmic) sensitivity of mode 25 to
elements of the [A] matrix
  Columns 1 through 6

  2.0847e-003  2.5781e-001  2.8216e-002  1.7969e-002  3.1896e-004  2.6461e-003
  1.3395e-001            0            0            0            0            0
            0  1.1076e-003  2.4882e-003  1.2713e-003  2.4250e-007  2.0118e-006
            0  2.5500e-003  4.5962e-003  3.2371e-003  5.5831e-007  4.6317e-006
            0  3.3666e-003  1.1272e-004  7.1785e-005  5.0786e-003  4.8676e-003
            0  2.7929e-002  9.3516e-004  5.9553e-004  4.8676e-003  9.4401e-003
            0  3.2224e-002  1.6001e-002  1.0190e-002  5.9181e-004  4.9096e-003
            0            0            0            0            0            0
            0  2.1433e-001  1.1607e-002  7.3915e-003  6.0013e-004  4.9787e-003
            0            0            0            0            0            0
            0  6.3517e-004  1.2597e-004  8.0222e-005  8.0981e-007  6.7182e-006
            0  1.4624e-003  2.9003e-004  1.8470e-004  1.8645e-006  1.5467e-005
            0  4.8649e-003  4.3002e-007  2.7385e-007  2.1081e-005  1.7489e-004
            0  4.0359e-002  3.5675e-006  2.2718e-006  1.7489e-004  1.4508e-003
            0  1.4733e-002  6.2938e-003  4.0080e-003  2.4170e-004  2.0051e-003
            0            0            0            0            0            0
            0  2.1633e-002  1.4651e-003  9.3298e-004  5.2275e-005  4.3367e-004
            0            0            0            0            0            0
            0  3.6443e-005  1.2167e-005  7.7481e-006  1.8607e-007  1.5436e-006
            0  8.3902e-005  2.8012e-005  1.7839e-005  4.2839e-007  3.5539e-006
            0  4.7719e-004  1.9698e-005  1.2544e-005  2.6233e-006  2.1763e-005
            0  3.9587e-003  1.6342e-004  1.0407e-004  2.1763e-005  1.8055e-004
            0  1.0084e-003  7.0090e-004  4.4635e-004  2.4178e-005  2.0058e-004
            0            0            0            0            0            0
            0  3.0513e-002  2.8069e-003  1.7875e-003  5.2808e-005  4.3810e-004
            0            0            0            0            0            0
            0  4.9955e-005  2.3514e-005  1.4974e-005  4.4826e-007  3.7188e-006
            0  1.1501e-004  5.4136e-005  3.4475e-005  1.0320e-006  8.5618e-006
            0  7.3969e-004  5.7354e-006  3.6524e-006  3.3655e-006  2.7920e-005
            0  6.1365e-003  4.7581e-005  3.0301e-005  2.7920e-005  2.3163e-004
            0  3.1370e-003  1.1948e-003  7.6087e-004  4.7356e-005  3.9286e-004
            0            0            0            0            0            0
```

Columns 7 through 12

0	0	0	1.6313e-001	1.0325e-002	7.9950e-003
0	0	0	0	0	0
0	8.8778e-003	0	5.5729e-004	1.6041e-004	1.2420e-004
0	0	0	1.2831e-003	3.6931e-004	2.8595e-004
0	0	0	2.7737e-003	3.8525e-004	2.9830e-004
0	0	0	2.3011e-002	3.1961e-003	2.4747e-003
8.8735e-003	0	0	9.1035e-003	1.0414e-002	8.0632e-003
8.8778e-003	8.8778e-003	0	0	0	0
0	0	1.2973e-003	1.8450e-001	4.5738e-002	3.5415e-002
0	0	8.3370e-002	0	0	0
0	0	0	8.9882e-004	5.3946e-003	3.3447e-003
0	0	0	2.0694e-003	9.9453e-003	8.5346e-003
0	0	0	3.1732e-003	3.0228e-004	2.3406e-004
0	0	0	2.6325e-002	2.5077e-003	1.9417e-003
0	0	0	1.4581e-002	3.6273e-002	2.8086e-002
0	0	0	0	0	0
0	0	0	2.4593e-002	3.0655e-003	2.3737e-003
0	0	0	0	0	0
0	0	0	7.1394e-005	3.3835e-005	2.6199e-005
0	0	0	1.6437e-004	7.7900e-005	6.0318e-005
0	0	0	3.8178e-004	8.6143e-005	6.6701e-005
0	0	0	3.1672e-003	7.1465e-004	5.5335e-004
0	0	0	1.2300e-003	2.1309e-003	1.6500e-003
0	0	0	0	0	0
0	0	0	3.6976e-002	6.5127e-003	5.0428e-003
0	0	0	0	0	0
0	0	0	1.1898e-004	6.6588e-005	5.1559e-005
0	0	0	2.7394e-004	1.5331e-004	1.1870e-004
0	0	0	6.6842e-004	6.0223e-005	4.6631e-005
0	0	0	5.5452e-003	4.9961e-004	3.8685e-004
0	0	0	7.8149e-004	3.7155e-003	2.8769e-003
0	0	0	0	0	0

Columns 13 through 18

2.0976e-003	1.7402e-002	0	0	0	1.5473e-002
0	0	0	0	0	0
2.1455e-006	1.7799e-005	0	0	0	1.3862e-004
4.9395e-006	4.0978e-005	0	0	0	3.1915e-004
5.8166e-005	4.8254e-004	0	0	0	1.2129e-004
4.8254e-004	4.0032e-003	0	0	0	1.0062e-003
2.7762e-004	2.3032e-003	0	0	0	7.6058e-003
0	0	0	0	0	0
1.0058e-003	8.3441e-003	0	0	0	2.7002e-002
0	0	0	0	0	0
1.8438e-006	1.5296e-005	0	2.0028e-002	0	2.8012e-004
4.2450e-006	3.5217e-005	0	0	0	6.4493e-004

1.1102e-002	1.0505e-002	0	0	0	3.6271e-005
1.0505e-002	2.1620e-002	0	0	0	3.0090e-004
1.6798e-003	1.3935e-002	2.0018e-002	0	0	1.3640e-002
0	0	2.0028e-002	2.0028e-002	0	0
2.5568e-004	2.1211e-003	0	0	2.6635e-003	3.3269e-001
0	0	0	0	1.5832e-001	0
2.5818e-007	2.1419e-006	0	0	0	1.0973e-003
5.9442e-007	4.9313e-006	0	0	0	2.5263e-003
9.3346e-006	7.7440e-005	0	0	0	4.4595e-003
7.7440e-005	6.4244e-004	0	0	0	3.6996e-002
6.6554e-005	5.5213e-004	0	0	0	2.7068e-002
0	0	0	0	0	0
3.0805e-004	2.5556e-003	0	0	0	2.6543e-001
0	0	0	0	0	0
8.3943e-007	6.9639e-006	0	0	0	7.6174e-004
1.9326e-006	1.6033e-005	0	0	0	1.7538e-003
1.2708e-005	1.0543e-004	0	0	0	5.1584e-003
1.0543e-004	8.7463e-004	0	0	0	4.2794e-002
1.3703e-004	1.1368e-003	0	0	0	1.6329e-003
0	0	0	0	0	0

Columns 19 through 24

2.1810e-004	3.7204e-004	3.2374e-004	2.6857e-003	0	0
0	0	0	0	0	0
2.5731e-006	4.3892e-006	7.4991e-007	6.2212e-006	0	0
5.9242e-006	1.0105e-005	1.7265e-006	1.4323e-005	0	0
1.8580e-005	3.1693e-005	7.1001e-006	5.8902e-005	0	0
1.5414e-004	2.6292e-004	5.8902e-005	4.8865e-004	0	0
2.4869e-004	4.2421e-004	9.9238e-006	8.2328e-005	0	0
0	0	0	0	0	0
1.3020e-004	2.2210e-004	4.4601e-004	3.7001e-003	0	0
0	0	0	0	0	0
5.9395e-006	1.0132e-005	1.1639e-006	9.6561e-006	0	0
1.3675e-005	2.3326e-005	2.6798e-006	2.2231e-005	0	0
2.1183e-005	3.6134e-005	1.0578e-005	8.7759e-005	0	0
1.7573e-004	2.9977e-004	8.7759e-005	7.2805e-004	0	0
4.9880e-004	8.5084e-004	4.2881e-005	3.5574e-004	0	0
0	0	0	0	0	0
7.3907e-003	1.2607e-002	1.2224e-003	1.0141e-002	0	0
0	0	0	0	0	0
5.0552e-004	6.9565e-004	1.0472e-006	8.6876e-006	0	8.5198e-004
9.3893e-004	1.7611e-003	2.4110e-006	2.0002e-005	0	0
4.1724e-005	7.1171e-005	1.9543e-002	1.8706e-002	0	0
3.4614e-004	5.9044e-004	1.8706e-002	3.6509e-002	0	0
3.3519e-003	5.7177e-003	1.9774e-003	1.6404e-002	8.5156e-004	0
0	0	0	0	8.5198e-004	8.5198e-004
2.8562e-003	4.8721e-003	2.4195e-003	2.0072e-002	0	0
0	0	0	0	0	0

```
2.7146e-005   4.6305e-005   2.0575e-006   1.7069e-005             0             0
6.2499e-005   1.0661e-004   4.7370e-006   3.9298e-005             0             0
1.8390e-005   3.1369e-005   8.2125e-005   6.8131e-004             0             0
1.5256e-004   2.6024e-004   6.8131e-004   5.6521e-003             0             0
1.4682e-003   2.5044e-003   7.2066e-004   5.9786e-003             0             0
          0             0             0             0             0             0

Columns 25 through 30

          0   1.3722e-002   1.0742e-003   1.4498e-003   5.3514e-004   4.4395e-003
          0             0             0             0             0             0
          0   2.1991e-004   7.6873e-006   1.0375e-005   2.1716e-006   1.8016e-005
          0   5.0629e-004   1.7699e-005   2.3886e-005   4.9998e-006   4.1478e-005
          0   5.4216e-004   6.9164e-005   9.3344e-005   7.5592e-006   6.2711e-005
          0   4.4977e-003   5.7378e-004   7.7438e-004   6.2711e-005   5.2025e-004
          0   1.4369e-002   8.3289e-004   1.1241e-003   5.6869e-005   4.7179e-004
          0             0             0             0             0             0
          0   2.9311e-002   9.1708e-004   1.2377e-003   7.8880e-004   6.5439e-003
          0             0             0             0             0             0
          0   4.6023e-004   1.8363e-005   2.4783e-005   3.9598e-006   3.2850e-005
          0   1.0596e-003   4.2278e-005   5.7059e-005   9.1166e-006   7.5631e-005
          0   4.1061e-004   8.1565e-005   1.1008e-004   1.3230e-005   1.0976e-004
          0   3.4064e-003   6.7666e-004   9.1323e-004   1.0976e-004   9.1055e-004
          0   2.6899e-002   1.6956e-003   2.2884e-003   7.1393e-005   5.9228e-004
          0             0             0             0             0             0
          0   2.4293e-001   2.5788e-003   3.4803e-003   3.9198e-003   3.2518e-002
          0             0             0             0             0             0
          0   8.5539e-004   4.5790e-005   6.1798e-005   4.3613e-006   3.6182e-005
          0   1.9694e-003   1.0542e-004   1.4228e-004   1.0041e-005   8.3302e-005
          0   2.9660e-003   1.6539e-004   2.2321e-004   9.8489e-005   8.1706e-004
          0   2.4606e-002   1.3721e-003   1.8518e-003   8.1706e-004   6.7783e-003
          0   2.4059e-002   3.1668e-003   4.2739e-003   3.6052e-004   2.9909e-003
          0             0             0             0             0             0
2.2136e-003   3.3645e-001   1.6252e-002   2.1934e-002   2.1675e-003   1.7982e-002
1.3514e-001             0             0             0             0             0
          0   9.4417e-004   1.3259e-003   1.4548e-003   4.7459e-006   3.9372e-005
          0   2.1738e-003   2.4818e-003   3.6531e-003   1.0927e-005   9.0647e-005
          0   6.6220e-003   1.5567e-004   2.1010e-004   2.1842e-002   2.0554e-002
          0   5.4936e-002   1.2915e-003   1.7430e-003   2.0554e-002   4.3351e-002
          0   3.7467e-003   9.7159e-003   1.3113e-002   2.4280e-003   2.0143e-002
          0             0             0             0             0             0

Columns 31 through 32

          0             0
          0             0
          0             0
          0             0
          0             0
```

```
            0             0
            0             0
            0             0
            0             0
            0             0
            0             0
            0             0
            0             0
            0             0
            0             0
            0             0
            0             0
            0             0
            0             0
            0             0
            0             0
            0             0
            0             0
            0             0
            0             0
            0             0
            0             0
            0  4.2684e-003
            0             0
            0             0
            0             0
  4.2663e-003             0
  4.2684e-003  4.2684e-003

SSAT(T) AVR without PSS; without saturation

Eigenvalues
 -1.0000e+006
 -1.0000e+006
 -1.0000e+006
 -1.0000e+006
 -9.4569e+001
 -9.5702e+001
 -9.7452e+001
 -9.7508e+001
 -1.7851e+001 +2.1591e+001i
 -1.7851e+001 -2.1591e+001i
 -1.8975e+001 +1.5499e+001i
 -1.8975e+001 -1.5499e+001i
 -3.6249e+001
 -3.6179e+001
 -3.1692e+001
 -3.0858e+001
 -2.7068e+001
 -2.7547e+001
```

```
 -1.3767e+001
 -1.3299e+001
 -6.6008e-001 +7.1667e+000i
 -6.6008e-001 -7.1667e+000i
 -6.5394e-001 +7.3675e+000i
 -6.5394e-001 -7.3675e+000i
  6.8486e-003 +3.8440e+000i
  6.8486e-003 -3.8440e+000i
 -4.4431e-008 +4.2420e-003i
 -4.4431e-008 -4.2420e-003i
 -3.6089e+000
 -3.5519e+000
 -3.3581e+000
 -3.3502e+000

Mode 25 is the local mode
   6.8486e-003 +3.8440e+000i

Magnitude of relative (logarithmic) sensitivity of mode 25 to
elements of the [A] matrix
  Columns 1 through 6

  2.0841e-003  2.5779e-001  2.8170e-002  1.7902e-002  3.1599e-004  2.6276e-003
  1.3388e-001           0           0           0           0           0
            0  1.1057e-003  2.4801e-003  1.2645e-003  2.3985e-007  1.9945e-006
            0  2.5527e-003  4.5938e-003  3.2287e-003  5.5372e-007  4.6045e-006
            0  3.3430e-003  1.1176e-004  7.1023e-005  4.9964e-003  4.8002e-003
            0  2.7799e-002  9.2938e-004  5.9060e-004  4.8002e-003  9.3315e-003
            0  3.2159e-002  1.5944e-002  1.0132e-002  5.8515e-004  4.8659e-003
            0           0           0           0           0           0
            0  2.1429e-001  1.1587e-002  7.3634e-003  5.9448e-004  4.9435e-003
            0           0           0           0           0           0
            0  6.3405e-004  1.2555e-004  7.9788e-005  8.0090e-007  6.6601e-006
            0  1.4638e-003  2.8986e-004  1.8420e-004  1.8490e-006  1.5376e-005
            0  4.8278e-003  4.2608e-007  2.7077e-007  2.0726e-005  1.7235e-004
            0  4.0147e-002  3.5432e-006  2.2516e-006  1.7235e-004  1.4332e-003
            0  1.4703e-002  6.2709e-003  3.9851e-003  2.3896e-004  1.9871e-003
            0           0           0           0           0           0
            0  2.1631e-002  1.4627e-003  9.2951e-004  5.1788e-005  4.3065e-004
            0           0           0           0           0           0
            0  3.6386e-005  1.2129e-005  7.7078e-006  1.8406e-007  1.5306e-006
            0  8.4002e-005  2.8002e-005  1.7795e-005  4.2493e-007  3.5336e-006
            0  4.7389e-004  1.9532e-005  1.2412e-005  2.5811e-006  2.1464e-005
            0  3.9407e-003  1.6242e-004  1.0321e-004  2.1464e-005  1.7848e-004
            0  1.0065e-003  6.9850e-004  4.4389e-004  2.3909e-005  1.9882e-004
            0           0           0           0           0           0
            0  3.0509e-002  2.8022e-003  1.7807e-003  5.2313e-005  4.3502e-004
            0           0           0           0           0           0
            0  4.9868e-005  2.3436e-005  1.4893e-005  4.4335e-007  3.6867e-006
```

```
         0  1.1513e-004  5.4106e-005  3.4384e-005  1.0235e-006  8.5113e-006
         0  7.3425e-004  5.6844e-006  3.6123e-006  3.3098e-006  2.7524e-005
         0  6.1058e-003  4.7270e-005  3.0039e-005  2.7524e-005  2.2888e-004
         0  3.1306e-003  1.1905e-003  7.5654e-004  4.6822e-005  3.8935e-004
         0            0            0            0            0            0

Columns 7 through 12

         0            0            0  1.6310e-001  1.0314e-002  7.9747e-003
         0            0            0            0            0            0
         0  8.8639e-003            0  5.5627e-004  1.5997e-004  1.2369e-004
         0            0            0  1.2842e-003  3.6931e-004  2.8555e-004
         0            0            0  2.7540e-003  3.8216e-004  2.9549e-004
         0            0            0  2.2901e-002  3.1779e-003  2.4572e-003
 8.8567e-003            0            0  9.0839e-003  1.0382e-002  8.0272e-003
 8.8639e-003  8.8639e-003            0            0            0            0
         0            0  1.2966e-003  1.8444e-001  4.5683e-002  3.5322e-002
         0            0  8.3309e-002            0            0            0
         0            0            0  8.9711e-004  5.3795e-003  3.3306e-003
         0            0            0  2.0711e-003  9.9446e-003  8.5219e-003
         0            0            0  3.1486e-003  2.9967e-004  2.3170e-004
         0            0            0  2.6183e-002  2.4919e-003  1.9268e-003
         0            0            0  1.4549e-002  3.6160e-002  2.7958e-002
         0            0            0            0            0            0
         0            0            0  2.4588e-002  3.0622e-003  2.3677e-003
         0            0            0            0            0            0
         0            0            0  7.1273e-005  3.3748e-005  2.6094e-005
         0            0            0  1.6454e-004  7.7911e-005  6.0241e-005
         0            0            0  3.7909e-004  8.5459e-005  6.6077e-005
         0            0            0  3.1524e-003  7.1065e-004  5.4948e-004
         0            0            0  1.2276e-003  2.1248e-003  1.6429e-003
         0            0            0            0            0            0
         0            0            0  3.6966e-002  6.5051e-003  5.0297e-003
         0            0            0            0            0            0
         0            0            0  1.1876e-004  6.6403e-005  5.1343e-005
         0            0            0  2.7418e-004  1.5330e-004  1.1853e-004
         0            0            0  6.6341e-004  5.9718e-005  4.6174e-005
         0            0            0  5.5167e-003  4.9660e-004  3.8397e-004
         0            0            0  7.7979e-004  3.7040e-003  2.8640e-003
         0            0            0            0            0            0

Columns 13 through 18

 2.0883e-003  1.7365e-002            0            0            0  1.5479e-002
         0            0            0            0            0            0
 2.1324e-006  1.7733e-005            0            0            0  1.3845e-004
 4.9230e-006  4.0938e-005            0            0            0  3.1964e-004
 5.7506e-005  4.7820e-004            0            0            0  1.2050e-004
 4.7820e-004  3.9766e-003            0            0            0  1.0021e-003
```

2.7585e-004	2.2939e-003	0	0	0	7.5942e-003
0	0	0	0	0	0
1.0012e-003	8.3260e-003	0	0	0	2.7011e-002
0	0	0	0	0	0
1.8325e-006	1.5238e-005	0	1.9986e-002	0	2.7976e-004
4.2306e-006	3.5180e-005	0	0	0	6.4588e-004
1.0969e-002	1.0404e-002	0	0	0	3.6012e-005
1.0404e-002	2.1463e-002	0	0	0	2.9946e-004
1.6689e-003	1.3878e-002	1.9970e-002	0	0	1.3618e-002
0	0	1.9986e-002	1.9986e-002	0	0
2.5454e-004	2.1167e-003	0	0	2.6641e-003	3.3283e-001
0	0	0	0	1.5831e-001	0
2.5665e-007	2.1342e-006	0	0	0	1.0961e-003
5.9252e-007	4.9272e-006	0	0	0	2.5306e-003
9.2296e-006	7.6750e-005	0	0	0	4.4309e-003
7.6750e-005	6.3823e-004	0	0	0	3.6846e-002
6.6139e-005	5.4999e-004	0	0	0	2.7031e-002
0	0	0	0	0	0
3.0666e-004	2.5501e-003	0	0	0	2.6552e-001
0	0	0	0	0	0
8.3431e-007	6.9379e-006	0	0	0	7.6079e-004
1.9261e-006	1.6017e-005	0	0	0	1.7564e-003
1.2560e-005	1.0444e-004	0	0	0	5.1230e-003
1.0444e-004	8.6850e-004	0	0	0	4.2601e-002
1.3615e-004	1.1322e-003	0	0	0	1.6304e-003
0	0	0	0	0	0

Columns 19 through 24

2.1623e-004	3.7078e-004	3.2229e-004	2.6800e-003	0	0
0	0	0	0	0	0
2.5469e-006	4.3673e-006	7.4534e-007	6.1980e-006	0	0
5.8799e-006	1.0083e-005	1.7207e-006	1.4309e-005	0	0
1.8293e-005	3.1368e-005	7.0194e-006	5.8371e-005	0	0
1.5212e-004	2.6085e-004	5.8371e-005	4.8540e-004	0	0
2.4608e-004	4.2197e-004	9.8602e-006	8.1995e-005	0	0
0	0	0	0	0	0
1.2907e-004	2.2133e-004	4.4397e-004	3.6920e-003	0	0
0	0	0	0	0	0
5.8786e-006	1.0080e-005	1.1568e-006	9.6194e-006	0	0
1.3571e-005	2.3272e-005	2.6706e-006	2.2208e-005	0	0
2.0843e-005	3.5740e-005	1.0452e-005	8.6912e-005	0	0
1.7332e-004	2.9721e-004	8.6912e-005	7.2274e-004	0	0
4.9352e-004	8.4627e-004	4.2604e-005	3.5428e-004	0	0
0	0	0	0	0	0
7.3274e-003	1.2565e-002	1.2170e-003	1.0120e-002	0	0
0	0	0	0	0	0
5.0044e-004	6.9229e-004	1.0410e-006	8.6564e-006	0	8.3397e-004
9.3205e-004	1.7574e-003	2.4032e-006	1.9985e-005	0	0

```
4.1083e-005  7.0447e-005  1.9323e-002  1.8539e-002           0           0
3.4163e-004  5.8582e-004  1.8539e-002  3.6269e-002           0           0
3.3172e-003  5.6882e-003  1.9650e-003  1.6340e-002  8.3330e-004           0
          0           0           0           0  8.3397e-004  8.3397e-004
2.8316e-003  4.8555e-003  2.4085e-003  2.0029e-002           0           0
          0           0           0           0           0           0
2.6868e-005  4.6073e-005  2.0449e-006  1.7005e-005           0           0
6.2029e-005  1.0637e-004  4.7209e-006  3.9258e-005           0           0
1.8099e-005  3.1036e-005  8.1162e-005  6.7492e-004           0           0
1.5051e-004  2.5809e-004  6.7492e-004  5.6124e-003           0           0
1.4527e-003  2.4911e-003  7.1602e-004  5.9542e-003           0           0
          0           0           0           0           0           0

Columns 25 through 30

          0  1.3728e-002  1.0703e-003  1.4452e-003  5.3268e-004  4.4296e-003
          0           0           0           0           0           0
          0  2.1965e-004  7.6466e-006  1.0326e-005  2.1582e-006  1.7947e-005
          0  5.0709e-004  1.7653e-005  2.3838e-005  4.9824e-006  4.1432e-005
          0  5.3865e-004  6.8433e-005  9.2408e-005  7.4724e-006  6.2139e-005
          0  4.4792e-003  5.6907e-004  7.6843e-004  6.2139e-005  5.1672e-004
          0  1.4347e-002  8.2822e-004  1.1184e-003  5.6498e-005  4.6982e-004
          0           0           0           0           0           0
          0  2.9321e-002  9.1363e-004  1.2337e-003  7.8512e-004  6.5288e-003
          0           0           0           0           0           0
          0  4.5965e-004  1.8265e-005  2.4664e-005  3.9349e-006  3.2721e-005
          0  1.0612e-003  4.2167e-005  5.6940e-005  9.0843e-006  7.5542e-005
          0  4.0769e-004  8.0652e-005  1.0891e-004  1.3070e-005  1.0869e-004
          0  3.3903e-003  6.7068e-004  9.0564e-004  1.0869e-004  9.0380e-004
          0  2.6857e-002  1.6860e-003  2.2766e-003  7.0923e-005  5.8977e-004
          0           0           0           0           0           0
          0  2.4304e-001  2.5693e-003  3.4694e-003  3.9018e-003  3.2446e-002
          0           0           0           0           0           0
          0  8.5451e-004  4.5554e-005  6.1513e-005  4.3349e-006  3.6048e-005
          0  1.9728e-003  1.0517e-004  1.4201e-004  1.0008e-005  8.3221e-005
          0  2.9470e-003  1.6366e-004  2.2099e-004  9.7366e-005  8.0967e-004
          0  2.4506e-002  1.3609e-003  1.8377e-003  8.0967e-004  6.7329e-003
          0  2.4027e-002  3.1495e-003  4.2528e-003  3.5822e-004  2.9789e-003
          0           0           0           0           0           0
2.2140e-003  3.3658e-001  1.6192e-002  2.1864e-002  2.1574e-003  1.7941e-002
1.3514e-001           0           0           0           0           0
          0  9.4303e-004  1.3189e-003  1.4479e-003  4.7163e-006  3.9219e-005
          0  2.1771e-003  2.4754e-003  3.6456e-003  1.0888e-005  9.0543e-005
          0  6.5767e-003  1.5397e-004  2.0791e-004  2.1583e-002  2.0359e-002
          0  5.4690e-002  1.2804e-003  1.7289e-003  2.0359e-002  4.3041e-002
          0  3.7409e-003  9.6611e-003  1.3046e-002  2.4121e-003  2.0058e-002
          0           0           0           0           0           0

Columns 31 through 32
```

```
          0            0
          0            0
          0            0
          0            0
          0            0
          0            0
          0            0
          0            0
          0            0
          0            0
          0            0
          0            0
          0            0
          0            0
          0            0
          0            0
          0            0
          0            0
          0            0
          0            0
          0            0
          0            0
          0            0
          0            0
          0            0
          0            0
          0  4.2407e-003
          0            0
          0            0
          0            0
4.2373e-003            0
4.2407e-003  4.2407e-003
```


D.2.3 AVR with PSS

```
EUROSTAG(P) AVR with PSS; with saturation

Eigenvalues
 -9.4920e+001
 -9.5950e+001
 -9.7583e+001
 -9.7635e+001
 -5.0215e+001 +1.5271e-002i
 -5.0215e+001 -1.5271e-002i
 -5.0476e+001
 -5.0511e+001
 -1.7305e+001 +2.1802e+001i
```

```
 -1.7305e+001 -2.1802e+001i
 -1.8770e+001 +1.5755e+001i
 -1.8770e+001 -1.5755e+001i
 -2.9323e+001 +2.1488e+000i
 -2.9323e+001 -2.1488e+000i
 -2.8784e+001 +2.0368e+000i
 -2.8784e+001 -2.0368e+000i
 -2.4611e+001
 -2.4173e+001
 -2.2633e+000 +7.9191e+000i
 -2.2633e+000 -7.9191e+000i
 -2.3360e+000 +8.2358e+000i
 -2.3360e+000 -8.2358e+000i
 -1.1576e+001
 -1.1181e+001
 -5.3257e-001 +3.8177e+000i
 -5.3257e-001 -3.8177e+000i
 -4.6873e+000
 -4.5641e+000
 -3.6224e+000
 -3.5342e+000
 -5.8293e-001
 -4.6975e-001
 -3.2687e-005
  3.3213e-008
 -1.8017e-001
 -1.7871e-001
 -1.7831e-001
 -1.0237e-001
 -1.0303e-001
 -1.0323e-001

Mode 25 is the local mode
 -5.3257e-001 +3.8177e+000i

Magnitude of relative (logarithmic) sensitivity of mode 25 to
elements of the [A] matrix
  Columns 1 through 6

  4.3397e-003  2.6838e-003  1.6111e-005  8.8717e-007  2.9380e-002  2.5605e-003
  7.5751e-003  6.9168e-003  3.9630e-005  2.1823e-006            0            0
  8.5880e-004  7.4844e-004  1.4006e-002  4.5764e-003            0            0
  4.7290e-005  4.1213e-005  4.5764e-003  4.9401e-003            0            0
  2.6459e-002  2.3059e-002  8.4990e-003  4.6800e-004  2.9516e-002            0
            0            0            0            0            0  2.6573e-005
            0            0            0            0            0  1.5439e-003
            0            0            0            0            0  9.8951e-005
  4.1065e-002  3.5788e-002  4.9199e-003  2.7092e-004            0            0
            0            0            0            0            0            0
```

1.6937e-004	1.4761e-004	8.2701e-006	4.5540e-007	0	0
4.1662e-004	3.6309e-004	2.0343e-005	1.1202e-006	0	0
1.8806e-004	1.6390e-004	2.8796e-003	1.5856e-004	0	0
1.0356e-005	9.0250e-006	1.5856e-004	8.7313e-006	0	0
9.1782e-003	7.9988e-003	3.0673e-003	1.6890e-004	0	0
0	0	0	0	0	0
0	0	0	0	0	0
0	0	0	0	0	0
1.6410e-002	1.4301e-002	8.1938e-003	4.5119e-004	0	0
0	0	0	0	0	0
1.8549e-005	1.6165e-005	2.3839e-006	1.3127e-007	0	0
4.5626e-005	3.9763e-005	5.8640e-006	3.2290e-007	0	0
2.4838e-004	2.1646e-004	3.4986e-004	1.9265e-005	0	0
1.3677e-005	1.1919e-005	1.9265e-005	1.0608e-006	0	0
1.1484e-003	1.0008e-003	3.4345e-004	1.8912e-005	0	0
0	0	0	0	0	0
0	0	0	0	0	0
0	0	0	0	0	0
2.1061e-003	1.8355e-003	7.2849e-004	4.0114e-005	0	0
0	0	0	0	0	0
3.2375e-005	2.8215e-005	5.2518e-006	2.8919e-007	0	0
7.9636e-005	6.9403e-005	1.2918e-005	7.1135e-007	0	0
2.7989e-005	2.4393e-005	4.3953e-004	2.4203e-005	0	0
1.5412e-006	1.3432e-006	2.4203e-005	1.3327e-006	0	0
1.7724e-003	1.5447e-003	6.1218e-004	3.3710e-005	0	0
0	0	0	0	0	0
0	0	0	0	0	0
0	0	0	0	0	0
4.0394e-003	3.5203e-003	7.6377e-004	4.2057e-005	0	0
0	0	0	0	0	0

Columns 7 through 12

5.9679e-002	1.5251e-003	9.8368e-002	1.2932e-003	1.5241e-004	1.2293e-004
0	0	2.4606e-005	3.1810e-003	3.7490e-004	3.0239e-004
0	0	5.2605e-004	4.3356e-002	3.3545e-003	2.7057e-003
0	0	2.8967e-005	2.3874e-003	1.8472e-004	1.4899e-004
0	0	2.7619e-003	4.0658e-002	1.0638e-002	8.5804e-003
0	0	1.0210e-003	0	0	0
5.9977e-002	0	5.9321e-002	0	0	0
2.3063e-003	7.3674e-005	3.8019e-003	0	0	0
0	0	1.8246e-003	2.9302e-001	9.0937e-003	7.3349e-003
0	0	1.0202e-001	0	0	0
0	0	1.1408e-005	6.4691e-004	5.1966e-003	2.9732e-003
0	0	2.8062e-005	1.5913e-003	9.0669e-003	7.6661e-003
0	0	3.8003e-004	5.7521e-002	6.7825e-004	5.4708e-004
0	0	2.0927e-005	3.1674e-003	3.7348e-005	3.0125e-005
0	0	9.7427e-004	1.6446e-002	3.3038e-002	2.6648e-002
0	0	0	0	0	0

0	0	0	0	0	0
0	0	0	0	0	0
0	0	1.1748e-004	2.3955e-001	4.0941e-002	3.3023e-002
0	0	3.0157e-002	0	0	0
0	0	1.4503e-006	4.1778e-005	3.2204e-005	2.5975e-005
0	0	3.5675e-006	1.0276e-004	7.9214e-005	6.3894e-005
0	0	6.2641e-005	5.6923e-003	7.2018e-004	5.8089e-004
0	0	3.4494e-006	3.1345e-004	3.9657e-005	3.1987e-005
0	0	1.1642e-004	1.2647e-003	2.1718e-003	1.7518e-003
0	0	0	0	0	0
0	0	0	0	0	0
0	0	0	0	0	0
0	0	2.8848e-005	2.4391e-002	2.7485e-003	2.2169e-003
0	0	3.4332e-002	0	0	0
0	0	2.6797e-006	5.1471e-005	5.7200e-005	4.6138e-005
0	0	6.5916e-006	1.2661e-004	1.4070e-004	1.1349e-004
0	0	6.1450e-005	8.5090e-003	4.4480e-004	3.5877e-004
0	0	3.3838e-006	4.6855e-004	2.4493e-005	1.9756e-005
0	0	1.9084e-004	3.5661e-003	3.4266e-003	2.7639e-003
0	0	0	0	0	0
0	0	0	0	0	0
0	0	0	0	0	0
0	0	1.4144e-004	3.4325e-002	5.8471e-003	4.7162e-003
0	0	3.0842e-002	0	0	0

Columns 13 through 18

2.3840e-005	1.3127e-006	0	0	0	0
5.8641e-005	3.2291e-006	0	0	0	0
5.9263e-003	3.2633e-004	0	0	0	0
3.2633e-004	1.7969e-005	0	0	0	0
2.7916e-003	1.5372e-004	0	0	0	0
0	0	0	0	0	0
0	0	0	0	0	0
0	0	0	0	0	0
2.0811e-002	1.1460e-003	0	0	0	0
0	0	0	0	0	0
4.1344e-005	2.2766e-006	1.4729e-002	2.0981e-003	4.8903e-002	1.2497e-003
1.0170e-004	5.6000e-006	0	0	0	0
2.3152e-002	7.0535e-003	0	0	0	0
7.0535e-003	7.6977e-003	0	0	0	0
1.5544e-002	8.5591e-004	1.4797e-002	0	0	0
0	0	0	2.1775e-005	0	0
0	0	0	1.2652e-003	4.9147e-002	0
0	0	0	8.1084e-005	1.8899e-003	6.0371e-005
1.0669e-002	5.8747e-004	0	0	0	0
0	0	0	0	0	0
2.0798e-006	1.1452e-007	0	0	0	0
5.1158e-006	2.8170e-007	0	0	0	0

9.1537e-004	5.0405e-005	0	0	0	0
5.0405e-005	2.7756e-006	0	0	0	0
6.7551e-004	3.7197e-005	0	0	0	0
0	0	0	0	0	0
0	0	0	0	0	0
0	0	0	0	0	0
2.5531e-003	1.4059e-004	0	0	0	0
0	0	0	0	0	0
6.6751e-006	3.6757e-007	0	0	0	0
1.6419e-005	9.0414e-007	0	0	0	0
1.2201e-003	6.7183e-005	0	0	0	0
6.7183e-005	3.6995e-006	0	0	0	0
1.2717e-003	7.0029e-005	0	0	0	0
0	0	0	0	0	0
0	0	0	0	0	0
0	0	0	0	0	0
3.1284e-003	1.7227e-004	0	0	0	0
0	0	0	0	0	0

Columns 19 through 24

5.0519e-006	7.1070e-004	1.1861e-005	1.4277e-005	8.7762e-006	4.8326e-007
1.2427e-005	1.7482e-003	2.9176e-005	3.5119e-005	2.1588e-005	1.1887e-006
4.4326e-004	3.7910e-002	8.2352e-004	9.9126e-004	7.4853e-004	4.1218e-005
2.4408e-005	2.0875e-003	4.5347e-005	5.4584e-005	4.1218e-005	2.2697e-006
5.8196e-004	1.2618e-002	1.2163e-003	1.4641e-003	3.7861e-005	2.0848e-006
0	0	0	0	0	0
0	0	0	0	0	0
0	0	0	0	0	0
6.9661e-004	2.0336e-001	9.8279e-004	1.1830e-003	3.3539e-003	1.8468e-004
2.5396e-002	0	0	0	0	0
8.0605e-002	1.0166e-003	2.4144e-005	2.9061e-005	1.2520e-005	6.8944e-007
2.1676e-005	2.5007e-003	5.9388e-005	7.1485e-005	3.0798e-005	1.6959e-006
3.3379e-004	4.2177e-002	9.1642e-004	1.1031e-003	1.0998e-003	6.0562e-005
1.8380e-005	2.3225e-003	5.0463e-005	6.0742e-005	6.0562e-005	3.3349e-006
2.1612e-003	1.7874e-002	2.1635e-003	2.6042e-003	3.0611e-004	1.6856e-005
8.3662e-004	0	0	0	0	0
4.8610e-002	0	0	0	0	0
3.1154e-003	0	0	0	0	0
1.1375e-003	2.2632e-001	5.9786e-004	7.1964e-004	4.5945e-003	2.5300e-004
6.3136e-002	0	0	0	0	0
1.4338e-006	9.1087e-005	2.6555e-003	2.2822e-003	4.5038e-005	2.4801e-006
3.5269e-006	2.2406e-004	4.6638e-003	5.8405e-003	1.1079e-004	6.1004e-006
7.6790e-005	5.1758e-003	5.7725e-005	6.9483e-005	4.2154e-002	1.3626e-002
4.2284e-006	2.8501e-004	3.1786e-006	3.8261e-006	1.3626e-002	1.4733e-002
1.2425e-004	1.6996e-003	1.6697e-002	2.0098e-002	2.2252e-002	1.2253e-003
0	0	0	0	0	0
0	0	0	0	0	0
0	0	0	0	0	0

1.8188e-005	3.0442e-002	3.2211e-002	3.8773e-002	1.4905e-002	8.2073e-004
2.4785e-002	0	0	0	0	0
2.7002e-006	1.3704e-004	1.1247e-004	1.3538e-004	1.5149e-005	8.3416e-007
6.6419e-006	3.3710e-004	2.7665e-004	3.3300e-004	3.7262e-005	2.0519e-006
8.1129e-005	8.6318e-003	6.4247e-004	7.7334e-004	8.5902e-003	4.7302e-004
4.4674e-006	4.7531e-004	3.5378e-005	4.2584e-005	4.7302e-004	2.6047e-005
2.0664e-004	9.7188e-004	6.5643e-003	7.9014e-003	7.2310e-003	3.9817e-004
0	0	0	0	0	0
0	0	0	0	0	0
0	0	0	0	0	0
7.9854e-005	4.5644e-002	1.2254e-002	1.4750e-002	2.6090e-002	1.4367e-003
2.2265e-002	0	0	0	0	0

Columns 25 through 30

0	0	0	0	6.9597e-007	1.3088e-004
0	0	0	0	1.7119e-006	3.2194e-004
0	0	0	0	1.2188e-004	7.8435e-004
0	0	0	0	6.7112e-006	4.3191e-005
0	0	0	0	1.2217e-004	7.6872e-003
0	0	0	0	0	0
0	0	0	0	0	0
0	0	0	0	0	0
0	0	0	0	2.7874e-004	1.4110e-002
0	0	0	0	4.0153e-002	0
0	0	0	0	1.7061e-006	2.3374e-004
0	0	0	0	4.1968e-006	5.7495e-004
0	0	0	0	1.5008e-004	7.5891e-004
0	0	0	0	8.2643e-006	4.1789e-005
0	0	0	0	2.3025e-004	1.2213e-002
0	0	0	0	0	0
0	0	0	0	0	0
0	0	0	0	0	0
0	0	0	0	3.0793e-004	2.4201e-002
0	0	0	0	3.4422e-002	0
4.1946e-002	2.6001e-003	6.0604e-002	1.5487e-003	9.9892e-002	1.0257e-003
0	0	0	0	2.3615e-005	2.5230e-003
0	0	0	0	5.8256e-004	4.4933e-002
0	0	0	0	3.2079e-005	2.4743e-003
4.2139e-002	0	0	0	2.8544e-003	2.7363e-002
0	2.6984e-005	0	0	1.0368e-003	0
0	1.5679e-003	6.0906e-002	0	6.0240e-002	0
0	1.0048e-004	2.3421e-003	7.4815e-005	3.8608e-003	0
0	0	0	0	2.3737e-003	3.0084e-001
0	0	0	0	1.2169e-001	0
0	0	0	0	1.1928e-005	6.3958e-004
0	0	0	0	2.9340e-005	1.5732e-003
0	0	0	0	5.2879e-004	4.8343e-002
0	0	0	0	2.9118e-005	2.6620e-003

0	0	0	0	1.0400e-003	1.4792e-003
0	0	0	0	0	0
0	0	0	0	0	0
0	0	0	0	0	0
0	0	0	0	2.0315e-004	2.3931e-001
0	0	0	0	3.5203e-002	0

Columns 31 through 36

1.9019e-005	2.2917e-005	2.4272e-005	1.3366e-006	0	0
4.6782e-005	5.6372e-005	5.9705e-005	3.2877e-006	0	0
1.6489e-003	1.9869e-003	7.9015e-004	4.3510e-005	0	0
9.0797e-005	1.0941e-004	4.3510e-005	2.3959e-006	0	0
2.1772e-003	2.6235e-003	7.7941e-004	4.2919e-005	0	0
0	0	0	0	0	0
0	0	0	0	0	0
0	0	0	0	0	0
2.5629e-003	3.0883e-003	5.4287e-003	2.9893e-004	0	0
0	0	0	0	0	0
4.0006e-005	4.8207e-005	3.9665e-005	2.1842e-006	0	0
9.8407e-005	1.1858e-004	9.7569e-005	5.3727e-006	0	0
1.8994e-003	2.2888e-003	1.3658e-003	7.5206e-005	0	0
1.0459e-004	1.2603e-004	7.5206e-005	4.1412e-006	0	0
3.9303e-003	4.7360e-003	9.5108e-004	5.2371e-005	0	0
0	0	0	0	0	0
0	0	0	0	0	0
0	0	0	0	0	0
2.1768e-003	2.6230e-003	7.9587e-003	4.3825e-004	0	0
0	0	0	0	0	0
1.1258e-004	1.3565e-004	5.1042e-005	2.8106e-006	0	0
2.7691e-004	3.3368e-004	1.2555e-004	6.9136e-006	0	0
3.7339e-003	4.4993e-003	1.0467e-002	5.7636e-004	0	0
2.0561e-004	2.4776e-004	5.7636e-004	3.1738e-005	0	0
8.3415e-003	1.0051e-002	3.7088e-003	2.0423e-004	0	0
0	0	0	0	0	0
0	0	0	0	0	0
0	0	0	0	0	0
5.7853e-003	6.9712e-003	4.0838e-002	2.2488e-003	0	0
0	0	0	0	0	0
3.3609e-003	2.9212e-003	8.6540e-005	4.7654e-006	4.5445e-002	2.6216e-003
5.9632e-003	7.3891e-003	2.1287e-004	1.1722e-005	0	0
1.9617e-003	2.3638e-003	4.8530e-002	1.4332e-002	0	0
1.0802e-004	1.3016e-004	1.4332e-002	1.5721e-002	0	0
2.3292e-002	2.8066e-002	2.4159e-002	1.3303e-003	4.5655e-002	0
0	0	0	0	0	2.7207e-005
0	0	0	0	0	1.5808e-003
0	0	0	0	0	1.0131e-004
3.7840e-002	4.5597e-002	2.4485e-002	1.3483e-003	0	0
0	0	0	0	0	0

Columns 37 through 40

0	0	4.9817e-007	2.0719e-004
0	0	1.2254e-006	5.0964e-004
0	0	1.5938e-004	4.5150e-003
0	0	8.7761e-006	2.4862e-004
0	0	1.3728e-004	1.4430e-002
0	0	0	0
0	0	0	0
0	0	0	0
0	0	4.1633e-004	1.2498e-002
0	0	3.6988e-002	0
0	0	1.5051e-006	3.8290e-004
0	0	3.7024e-006	9.4185e-004
0	0	2.0188e-004	3.0845e-003
0	0	1.1116e-005	1.6985e-004
0	0	2.6612e-004	2.3931e-002
0	0	0	0
0	0	0	0
0	0	0	0
0	0	4.8800e-004	2.6169e-002
0	0	3.1709e-002	0
0	0	6.6669e-006	7.9603e-004
0	0	1.6399e-005	1.9581e-003
0	0	7.0923e-004	3.0092e-002
0	0	3.9054e-005	1.6570e-003
0	0	7.9468e-004	2.4181e-002
0	0	0	0
0	0	0	0
0	0	0	0
0	0	1.1913e-003	2.1846e-001
0	0	3.6099e-002	0
6.1103e-002	1.5615e-003	1.0071e-001	7.8779e-004
0	0	2.4914e-005	1.9378e-003
0	0	4.8944e-004	6.1646e-002
0	0	2.6951e-005	3.3946e-003
0	0	2.7730e-003	3.3894e-003
0	0	1.0453e-003	0
6.1408e-002	0	6.0736e-002	0
2.3614e-003	7.5432e-005	3.8926e-003	0
0	0	1.9468e-003	3.0162e-001
0	0	1.0070e-001	0

Appendix E

Softwares developed using MATLAB

E.1 Software for computing normalized right eigenvector

```
clc;

load K2A4G_man_Euro_Amat_unsat.txt; %2A4G system, manual control;
% 24th order system

for c = 1:496 % read data
k1(c) = K2A4G_man_Euro_Amat_unsat(c,1); %read column 1, i
k2(c) = K2A4G_man_Euro_Amat_unsat(c,2); %read column 2, j
k3(c) = K2A4G_man_Euro_Amat_unsat(c,3); %read column 3, aij
A(k1(c),k2(c)) = k3(c); % [A]
end

% disp('[A] matrix (Tm - EUROSTAG)');
% disp(A);

disp('Eigenvalues'); disp(eig(A));

[V,D] = eig(A); %calculate right eigenvector V
%disp('Right Eigenvector matrix');
%disp(V);
```

```
for i = 1:24
    for j = 1:24
        Vmag(i,j) = abs(V(i,j)); %return magnitude of right eigenvector
    end
end

%The following loop normalises the right eigenvector
for j = 1:24
    X = Vmag(1,j);
    for i = 2:24
        if Vmag(i,j) > X % check for the largest value in a column
            X = Vmag(i,j);
        end
    end
    for i = 1:24
        Vmag(i,j) = Vmag(i,j)/X; %normalise
    end
end

disp('Participation matrix P (Pij = participation of state i in mode
j)'); disp(P);

VAng = angle(V)*180/pi; %angle of right eigenvector
disp('Angle of eigenvector'); disp(VAng);

% ================================================================
```

E.2 Software for eliminating effect of speed deviation in speed voltage terms

E.2.1 SMIB system

```
%==========================================================================

%Forming [A] matrix from the simulation results of EUROSTAG
clc;
format short e

load EUROSTAG_Amat_smib_TmPm_man_unsat.txt %column 1=i; 2=j; 3=Tm_A(i,j);
% 4=Pm_A(i,j) with speed terms % 6th order system

load EUROSTAG_Amat_smib_TmPm_EXAC4_unsat.txt % 7th order system

for n = 1:31 % read data
t1(n) = EUROSTAG_Amat_smib_TmPm_man_unsat(n,1); %read column 1, i
t2(n) = EUROSTAG_Amat_smib_TmPm_man_unsat(n,2); %read column 2, j
t3(n) = EUROSTAG_Amat_smib_TmPm_man_unsat(n,3); %read column 3, aij
ATmwu(t1(n),t2(n)) = t3(n); % [A] Tm output with speed terms
t4(n) = EUROSTAG_Amat_smib_TmPm_man_unsat(n,4); %read column 3, aij
APmwu(t1(n),t2(n)) = t4(n); % [A] Pm output with speed terms
end

disp('EUROSTAG results - manual excitation control'); disp('Without
saturation'); disp('[A] matrix (Tm: with speed terms)');
% disp(ATmwu);

disp('Eigenvalues'); disp(eig(ATmwu));

disp('[A] matrix (Pm: with speed terms)');
% disp(APmwu);
%
disp('Eigenvalues'); disp(eig(APmwu));

% remove speed elements in column 5 of the [A] matrix
j = 5; for i = 1:4
   APmwu(i,j) = 0;
```

```
end
    APmwu(5,5) = APmwu(5,5)-ATmwu(5,5);
    APmu = APmwu;

j = 5; for i = 1:5
    ATmwu(i,j) = 0;
end ATmu = ATmwu;

disp('[A] matrix (Tm: without speed terms)');
% disp(ATmu);

disp('Eigenvalues'); disp(eig(ATmu));

disp('[A] matrix (Pm: without speed terms)');
% disp(APmu);
%
disp('Eigenvalues'); disp(eig(APmu));


for n = 1:39 % read data
t1(n) = EUROSTAG_Amat_smib_TmPm_EXAC4_unsat(n,1); %read column 1, i
t2(n) = EUROSTAG_Amat_smib_TmPm_EXAC4_unsat(n,2); %read column 2, j
t3(n) = EUROSTAG_Amat_smib_TmPm_EXAC4_unsat(n,3); %read column 3, aij
ATewu(t1(n),t2(n)) = t3(n); % [A] Tm output with speed terms
t4(n) = EUROSTAG_Amat_smib_TmPm_EXAC4_unsat(n,4); %read column 3, aij
APewu(t1(n),t2(n)) = t4(n); % [A] Pm output with speed terms
end

disp('EUROSTAG results - Excitation control with AVR');
disp('Without saturation');

disp('[A] matrix (Tm: with speed terms)');
disp(ATewu);
%
disp('Eigenvalues'); disp(eig(ATewu));

disp('[A] matrix (Pm: with speed terms)'); disp(APewu);
%
disp('Eigenvalues'); disp(eig(APewu));

% remove speed elements in column 6 of the [A] matrix
```

```
j = 6; for i = 1:5
   APewu(i,j) = 0;
end
    APewu(6,6) = APewu(6,6)-ATewu(6,6);
    APeu = APewu;

j = 6; for i = 1:6
    ATewu(i,j) = 0;
end ATeu = ATewu;

disp('[A] matrix (Tm: without speed terms)');
 disp(ATeu);
%
disp('Eigenvalues'); disp(eig(ATeu));

disp('[A] matrix (Pm: without speed terms)'); disp(APeu);
%
disp('Eigenvalues'); disp(eig(APeu));

%Forming [A] matrix from the simulation results of EUROSTAG

clc;

load EUROSTAG_Amat_unsat_SMIB.txt; %column 1 + 2, row + column no. ;
% column 3, Tm with speed terms; column 4, Tm without speed terms;
% column 5, Pm with speed terms; column 6, Pm without speed terms;


for c = 1:31 % read data
    k1(c) = EUROSTAG_Amat_unsat_SMIB(c,1);
    k2(c) = EUROSTAG_Amat_unsat_SMIB(c,2);
    k3(c) = EUROSTAG_Amat_unsat_SMIB(c,3); %Tm speed deviation included
    k4(c) = EUROSTAG_Amat_unsat_SMIB(c,4); %Tm speed deviation neglected
    k5(c) = EUROSTAG_Amat_unsat_SMIB(c,5); %Pm speed deviation included
    k6(c) = EUROSTAG_Amat_unsat_SMIB(c,6); %Pm speed deviation neglected

    EuroTmSp(k1(c),k2(c)) = k3(c); % [A]
    EuroTm(k1(c),k2(c)) = k4(c); % [A]
    EuroPmSp(k1(c),k2(c)) = k5(c); % [A]
    EuroPm(k1(c),k2(c)) = k6(c); % [A]
end
```

```
%disp('EUROSTAG');
disp('[A] matrix - EUROSTAG(Tm); with speed deviation and without
saturation'); disp(EuroTmSp);

disp('Eigenvalues'); disp(eig(EuroTmSp));

[V,D] = eig(EuroTmSp);%calculate right eigenvector
disp('Right Eigenvector matrix'); disp(V);

W = inv(V); % calculate left eigenvector W
%disp('Left Eigenvector matrix');
%disp(W);

%calculate the participation factor from both the left and right
%eigenvectors
for i = 1:6
    for j = 1:6
        P(i,j) = (abs(V(i,j) * W(j,i))); % return the magnitude of P
%         P(i,j) = (V(i,j) * W(j,i)); % return the magnitude of P
end end

%disp(P);

%The following loop normalises the participation factors
for j = 1:6
    X = P(1,j);
    for i = 2:6
        if P(i,j) > X % check for the largest value in a column
            X = P(i,j);
        end
    end
    for i = 1:6
        P(i,j) = P(i,j)/X; %normalise
    end
end

disp('Participation matrix P (Pij = participation of state i in mode
j)'); disp(P);
```

E.2.2 2A4G system

```
for c = 1:496 % read data
    k1(c) = EUROSTAG_Amat_2A4G_unsat(c,1);
    k2(c) = EUROSTAG_Amat_2A4G_unsat(c,2);
    k3(c) = EUROSTAG_Amat_2A4G_unsat(c,3); %read column 1, i
    % (speed variations included)
    AETS(k1(c),k2(c)) = k3(c); % [A]
end

% for c = 1:496 % read data
%     k1(c) = EUROSTAG_Amat_Pm_2A4G_unsat(c,1);
%     k2(c) = EUROSTAG_Amat_Pm_2A4G_unsat(c,2);
%     k3(c) = EUROSTAG_Amat_Pm_2A4G_unsat(c,3); %read column 1, i
% (speed variations included)
%     AETS(k1(c),k2(c)) = k3(c); % [A]
% end

% disp('EUROSTAG(Pm) - speed terms included');
% [V,D] = eig(AETS);%calculate right eigenvector
% W = inv(V);%calculate left eigenvector

disp('EUROSTAG(Tm) - speed terms included');

% disp('[A] matrix');
% disp(AETS);

disp('Eigenvalues'); disp(eig(AETS));

j = 5; for i = 1:5
    AETS(i,j) = 0;
end AETSnew = AETS;

for i = 7:11
    AETS(i,j) = 0;
end AETSnew = AETS;

for i = 13:17
    AETS(i,j) = 0;
end AETSnew = AETS;
```

```
for i = 19:23
    AETS(i,j) = 0;
end AETSnew = AETS;

j = 11; for i = 1:5
    AETS(i,j) = 0;
end AETSnew = AETS;

for i = 7:11
    AETS(i,j) = 0;
end AETSnew = AETS;

for i = 13:17
    AETS(i,j) = 0;
end AETSnew = AETS;

for i = 19:23
    AETS(i,j) = 0;
end AETSnew = AETS;

j = 17; for i = 1:5
    AETS(i,j) = 0;
end

AETSnew = AETS;

for i = 7:11
    AETS(i,j) = 0;
end AETSnew = AETS;

for i = 13:17
    AETS(i,j) = 0;
end AETSnew = AETS;

for i = 19:23
    AETS(i,j) = 0;
end AETSnew = AETS;

j = 23; for i = 1:5
    AETS(i,j) = 0;
```

```
end AETSnew = AETS;

for i = 7:11
    AETS(i,j) = 0;
end AETSnew = AETS;

for i = 13:17
    AETS(i,j) = 0;
end AETSnew = AETS;

for i = 19:23
    AETS(i,j) = 0;
end AETSnew = AETS;

disp('EUROSTAG(Tm) - speed terms neglected');
% [V,D] = eig(AETS);%calculate right eigenvector
% W = inv(V);%calculate left eigenvector

% disp('[A] matrix');
% disp(AETSnew);
disp('Eigenvalues'); disp(eig(AETSnew));
```

E.3 Software for computing sensitivity of eigenvalues to elements of the A matrix

```
==========================================================================
for n = 1:31 % read data
    h1(n) = Eurostag_Amat_Tm_sat_SMIB(n,1);
    h2(n) = Eurostag_Amat_Tm_sat_SMIB(n,2);
    h3(n) = Eurostag_Amat_Tm_sat_SMIB(n,3); %Tm speed deviation included
Euro1(h1(n),h2(n)) =h3(n); end
==========================================================================
disp('[A] matrix - EUROSTAG(Tm) ; with speed deviation and with
saturation ');
 disp(Euro1);
disp('Eigenvalues'); disp(eig(Euro1));
[V,D] = eig(Euro1);%calculate right eigenvector
W = inv(V); % calculate left eigenvector W
sum = zeros(6,6); for i = 1:6
```

```
% i = 1;
for k = 1:6
    for j = 1:6
        sai(k,j) = (abs(W(i, k) * V(j,i))); % return the magnitude of
        %absolute sensitivity
        si(k,j) = W(i, k) * V(j,i); % return complex absolute sensitivity
        %of mode i to element akj of the A matrix
    end
end
%     fprintf('Absolute sensitivity of mode %g to elements of the [A]...
 matrix\n',i);
%     disp(si);
   fprintf('Magnitude of relative (logarithmic) sensitivity of mode %g ...
   to elements of the [A] matrix\n',i);
 %     disp(D(i,i));
    LSi = (1/D(i,i))*si.*Euro1;
    ALSi = abs(LSi);
    disp(ALSi);
%     fprintf('Phase of relative (logarithmic) sensitivity of mode %g to ...
elements of the [A] matrix\n',i);
%     AngleLSi = angle(LSi)*180/pi;
%      disp(AngleLSi);

sum = sum + si; % check numerical calculation
 end
disp('sum of Si is ');
disp(sum); % sum of all Si = I
```

Appendix F

Author's Publications

International conferences

K. Kaberere, A. Petroianu, and K. Folly, "Analytical investigation of the effect of generator modelling on electromechanical mode damping," in *IFAC 2006 Symposium on Power Plants and Power Systems Control*, (Kananaskis, Canada), 25-28 June 2006.

K.K. Kaberere, M. Ntombela, K.A. Folly, and A.I. Petroianu, "Comparison of industrial-grade analytical tools used in small-signal stability assessment," in *AUPEC 2005*, vol. 1, (Hobart, Tasmania, Australia), pp. 147-152, University of Tasmania, 25-28 September 2005.

K.K. Kaberere, K.A. Folly, M. Ntombela, and A.I. Petroianu, "Comparative analysis and numerical validation of industrial-grade power system simulation tools: Application to small-signal stability," in *15th PSCC*, (Liège, Belgium), 22-26 August 2005.

K.K. Kaberere, K.A. Folly, and A.I. Petroianu, "Assessment of commercially available software tools for transient stability: Experience gained in an academic environment," in *IEEE Africon*, vol. 02, (Gaberone, Botswana), pp. 711-716, 15-17 September 2004.

Local conferences

K. Kaberere, K. A. Folly, A. Petroianu, and M. Ntombela, "Comparison of four industrial-grade software packages for small-signal stability studies," in *SAUPEC 2006*, (University of KwaZulu-Natal, Durban), 26-27 January 2006.

M. Ntombela, K.K. Kaberere, K.A. Folly, and A.I. Petroianu, "Investigation into the capabilities of MATLAB Power System Toolbox for small signal stability analysis in power systems," in *IEEE PES 2005 Conference and Exposition in Africa*, (Durban, South Africa), 11-15 July 2005.

M. Ntombela, K.K. Kaberere, and K.A. Folly, "Linear analysis capabilities of MATLAB Power System Toolbox (PST)," in *SAUPEC 2005*, (University of the Witwatersrand, Johannesburg), 27 - 28 January 2005.